Development of inhibitory peptides against the NS2-3 and NS3/4A proteases of the Hepatitis C Virus

Von der Fakultät für Lebenswissenschaften
der Technischen Universität Carolo-Wilhelmina
zu Braunschweig
zur Erlangung des Grades eines
Doktors der Naturwissenschaften
(Dr. rer. nat.)
genehmigte
D i s s e r t a t i o n

von Jonas Kügler
aus Lingen

1. Referent: Professor Dr. John Collins

2. Referent: Professor Dr. Thomas Pietschmann

3. Referent: Professor Dr. Stefan Dübel

eingereicht am: 03.08.2011

mündliche Prüfung (Disputation) am: 08.12.2011

Druckjahr 2011

Vorabveröffentlichungen der Dissertation

Teilergebnisse aus dieser Arbeit wurden mit Genehmigung der Fakultät für Lebenswissenschaften, vertreten durch den Mentor, in folgenden Beiträgen vorab veröffentlicht:

Tagungsbeiträge:

Kügler J., Gentzsch J., Pollmann E., Nieswandt S., Pietschmann T., Collins J.: Development of inhibitory peptides against the NS3/4A protease of the Hepatitis C Virus (Poster). EMBO meeting, Barcelona, Spain (2010)

Acknowledgements

First of all I would like to thank my supervisor Prof. Dr. John Collins (TU Braunschweig and Helmholtz Centre for Infection Research, Braunschweig) for giving me the opportunity to do my PhD under his guidance. It has been a privilege.

I am grateful to Prof. Dr. Thomas Pietschmann (Twincore, Hannover) and Prof. Dr. Carlos Guzman (Helmholtz Centre for Infection Research, Braunschweig) for taking part in my thesis committee and guiding my work with valuable discussions.

I also want to express my thanks to Simone Nieswandt and Dr. Erik Pollmann with whom I shared time in the lab and had some fruitful discussions. Especially I want to thank Erik for kindly providing me the peptide phage display library CPL19YS-2 which I used in this work.

Furthermore I would like to say thank you to Dr. Stefan Schmelz (Helmholtz Centre for Infection Research, Braunschweig) for all the help in crystallisation issues and for an outstanding introduction to structural biology.

I would like to thank Juliane Gentsch (Twincore, Hannover) for testing the peptides in the cell culture replicon assay.

I also want to express my thanks to Dr. Joop van den Heuvel (Helmholtz Centre for Infection Research, Braunschweig) who helped me with the production and purification of the NS3/4A protease for crystallisation studies.

I would like to thank Dr. Raimo Franke and Dr. Werner Tegge (Helmholtz Centre for Infection Research, Braunschweig) for the help with all kinds of peptide related issues and for the synthesis of all peptides I used in this work.

I am grateful to Dr. Giuseppe Battaglia (Department of Biomedical Science, University Sheffield, UK) who kindly assented for me to learn new techniques in his lab.

I would like to say thank you to Juliane Lindner for her skilful assistance during her diploma thesis.

I also want to acknowledge Dr. Ralf Bartenschlager (University of Heidelberg) for kindly providing me the HCV replicons used in this work.

Finally I want to thank my parents for their confidence and encouragement all along my studies.

Table of content

List of figures

List of tables

Abbreviations

aa	Amino acid
ABTS	2,2'-azino-bis(3-ethylbenzthiazoline-6-sulphonic acid)
Ac	Acetylated
Antp	Antennapedia peptide
BSA	Bovine serum albumin
Cfu	Colony forming unit
CMC	Critical micelle concentration
CPP	Cell penetrating peptide
Da	Dalton
DAB	3,3'-diaminobenzidine
dH_2O	Double deionised water
dNTP	Deoxynucleotide triphosphate
DMSO	Dimethylsulfoxide
dsDNA	Double stranded DNA
DTT	Dithiothreitol
EC_{50}	Half maximal effective concentration
E. coli	*Escherichia coli*
EDTA	Ethylenediamine tetraacetate
ELISA	Enzyme-linked immunosorbent assay
EMCV	Encephalomyocarditis virus
ER	Endoplasmatic reticulum
FDA	U.S. Food and Drug Administration
HCV	Hepatitis C Virus
HEPES	4-(2-hydroxyethyl)-1-piperazineethanesulfonic acid
HIV	Human immunodeficiency virus
H	Hour
HRP	Horseradish peroxidase
HZI	Helmholtz Centre for Infection Research, Braunschweig, Germany
IC_{50}	Half maximal inhibitory concentration
IFN	Interferon
IRES	Internal ribosome entry site
IgG	Immunoglobulin G
IMAC	Immobilised metal affinity chromatography
IPTG	Isopropyl-ß-D-thiogalactoside
LD	Lipid droplet
LDAO	Lauryldimethyl amine oxide

Luc	Firefly luciferase gen
M	Molar = mol/L
MBP	Maltose binding protein
MTP	Microtiter plate
Min	Minute
NANBH	Non-A, non-B hepatitis
Neo	Neomycin phosphotransferase gen
NS	Non structural
NTA	Nitrilotriacetic acid
PAGE	Polyacrylamide gel-electrophoresis
PBS	Phosphate buffered saline
PBST	Phosphate buffered saline with added Tween 20
PCR	Polymerase chain reaction
PDB	Protein Data Bank
PEG	Polyethylene glycol
Pfu	Plaque forming unit
Rpm	Rotations per minute
SDS	Sodium dodecylsulfate
STAT-C	Specifically targeted antiviral therapy for Hepatitis C
SVR	Sustained virological response
TEMED	N,N,N'N'tetramethylethylenediamine
TLR	Toll-like receptor
Tris	Tris(hydoxymethyl)aminomethane
Tween 20	Polyoxyethylenesorbitan monolaurate
uPA	Urokinase plasminogen activator
UTR	Untranslated region

Amino acid code

A	Ala	Alanin	**M**	Met	Methionine
C	Cys	Cystein	**N**	Asn	Asparagine
D	Asp	Aspartic acid	**P**	Pro	Proline
E	Glu	Glutamic acid	**Q**	Gln	Glutamine
F	Phe	Phenylalanine	**R**	Arg	Arginine
G	Gly	Glycine	**S**	Ser	Serine
H	His	Histidine	**T**	Thr	Threonine
I	Ile	Isoleucine	**V**	Val	Valine
K	Lys	Lysine	**W**	Trp	Tryptophan
L	Leu	Leucine	**Y**	Tyr	Tyrosine

1. Introduction

1.1 Hepatitis C Virus

Hepatitis C virus (HCV) infection is the leading cause of chronic hepatitis, liver cirrhosis and hepatocellular carcinoma (Shepard, 2005). HCV was first termed non-A, non-B hepatitis (NANBH) and was discovered in post transfusion patients in 1975 (Feinstone, 1975). The etiological agent of HCV was identified over one decade later in 1989 by immunoscreening of serum of a patient with NANBH (Choo *et al*., 1989). It is estimated that worldwide up to 170 million people are chronically infected with HCV and a vaccine is not available yet (Yu and Chiang, 2010). The standard of care, pegylated interferon-α and ribavirin, achieves a sustained viral response in only about half of the treated patients (Manns *et al*, 2001; Fried *et al*, 2002) and is associated with considerable severe side effects (Fried, 2002). Thus there is a huge unmet need for direct anti-HCV drugs for a more effective treatment with fewer side effects.

1.1.1 HCV Epidemiology and Genotypes

To date about 123 - 170 million people worldwide are persistently infected with HCV (2 – 3% of the world population), with 3 to 4 million new infections each year (Shepard, 2005; Bruijne *et al.*, 2009). The initial symptoms of the infection are often absent or asymptomatic, as for example abdominal pain and influenza-like symptoms. In most cases the infection remains undiagnosed (Hoofnagle *et al.*, 1997). Of infected individuals 70 to 80% develop a chronic infection (Freeman, 2001; Patel, 2006). Approximately 10 – 20% of chronically infected patients develop liver cirrhosis over a period of 10 to 30 years and 1 – 5% of patients with liver cirrhosis develop a hepatocellular carcinoma (Alberti, 1999; Lauer, 2001). Liver cirrhosis and hepatocellular carcinoma are conditions requiring surgery and the major cause for liver transplantation in Europe and the USA (Perz, 2006). Chronic HCV infections are often associated with steatosis, defined as increased fat content of the liver, with prevalence of 40 – 80% in patients with chronic HCV (Negro, 2010). Moreover, chronic hepatitis is related to insulin resistance and an increased risk of type 2 diabetes mellitus (Mihm, 2010).

The main route of transmission is direct blood-to-blood contact between humans with high incidence among intravenous drug users, recipients of blood products and renal dialysis patients before implementation of screening regimens. Other risk factors are tattooing and needle stick injuries. Sexual and congenital transmissions appear less frequently (Alter, 1995; Terrault, 2002). Since the development of a screening test for HCV in 1990 for blood or blood products the incidence of new infections has greatly diminished (Cohen, 1999). However, between 20 – 50% of HCV cases are not associated to the classic risk factors (Urbani, 1999). Many patients remain asymptomatic for years and are only detected on health screening or at the time of blood transfer (Contreras, 2010).

There is a large geographic variability in the prevalence of HCV infections. The highest reported prevalence rates are in countries located in Africa (5.3%) and Asia (2.15%) compared to lower prevalence rates in industrialised countries in North America (1.7%) and Europe (1.03%) (see Figure 1-1). The prevalence rate varies from 0.6% in Germany and 1.8% in the USA to 22% in Egypt (Sy and Jamal, 2006; Shepard *et al.*, 2005).

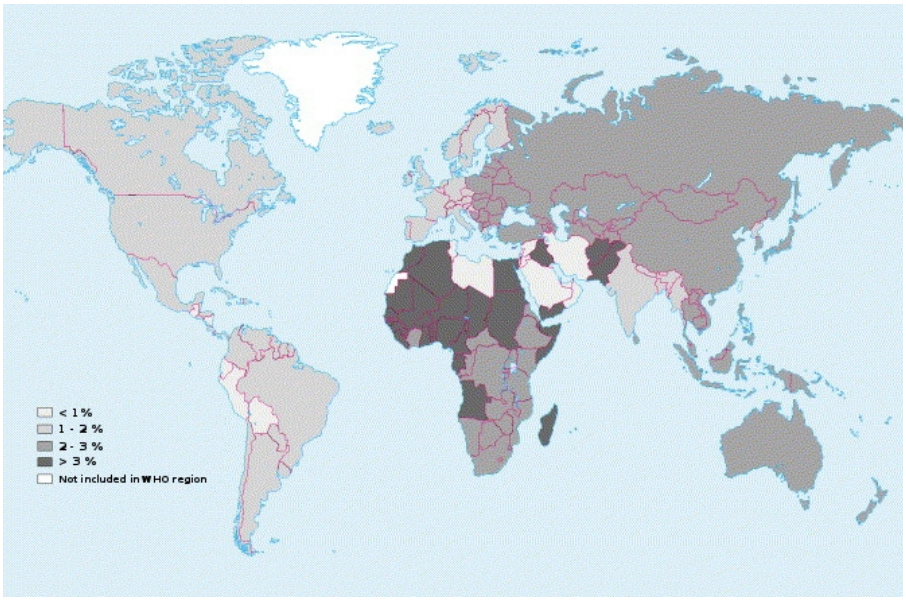

Figure 1-1: Estimated prevalence of HCV infection by WHO region (modified from Shepard, 2005).

At the time of writing six major HCV genotypes and over 100 subgenotypes have been identified (Georgel *et al.*, 2010). The genotypes differ in 31 – 33% of their nucleotide sequence and the subgenotypes differ in 20 – 25% of their sequence (Kuiken and Simmonds, 2009). Mutations of the viral genome due to a low fidelity of the viral polymerase result in a heterogeneous population of virus quasispecies that coexist in an infected patient (Farci *et al.*, 2000; Simmonds *et al.*, 2005). This quasispecies model leads to a significant survival advantage for the virus in its battle with the immune system, because it allows a rapid increase in genomic variability facilitating the emergence of mutants that are better suited to new environmental conditions (Pawlotsky, 2006). This variability also hampers the development of a vaccine against the HCV virus.

The genotypes differ in their geographical prevalence. The genotypes 1, 2 and 3 are distributed worldwide. The other genotypes are found in more distinct geographic areas including Egypt (genotype 4), South Africa (genotype 5) and Southeast Asia (genotype 6). The most common variants in Western Europe and North America are genotype 1a and 1b, followed by the genotypes 2 and 3 (Bartenschlager *et al.*, 2004; Kuiken and Simmonds, 2009).

1.1.2 HCV life cycle and viral proteins

HCV belongs to the *Hepacivirus* genus of the *Flaviridae* family, which includes human and animal pathogens like yellow fever or dengue virus. Viruses within the *Flaviviridae* family have a related genome organisation. They have single stranded RNA genomes, which encode a single polyprotein, and conserved nonstructural protein motifs (Lindenbach and Rice, 2003).

The HCV virion has a size of 55-65 nm in diameter and is enveloped in a lipid bilayer in which two envelope proteins (E1 and E2) are anchored and form a heterodimer. The envelope surrounds the nucleocapsid which is composed of multiple copies of a small basic core protein and contains the RNA genome (see Figure 1-2). The genome is a positive-stranded RNA molecule with a length of about 9.6 kb. It represents a single open reading frame (ORF) encoding a polyprotein of about 3000 amino acids. HCV infects only humans and chimpanzees and targets mainly the hepatocytes (Bartenschlager *et al.*, 2004; Nakamura *et al.*, 2008; Moradpour *et al.*, 2007).

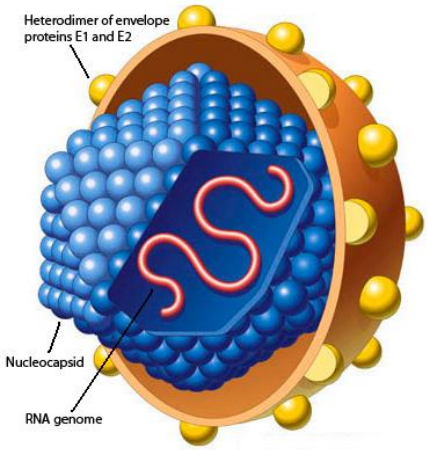

Figure 1-2: Schematic picture of the Hepatitis C Virus. The envelope with heterodimer of the envelope proteins E1 and E2 surrounds the nucleocapsid containing the RNA genome (modified from James A. Perkins, 2001).

The cell entry of the HCV virion is a complex process that involves several viral and cellular factors. In the blood of infected patients, HCV is associated with low density and very low density lipoproteins (LDL and VLDL) (Nielsen *et al.*, 2006). The LDL-receptor (LDL-R) has been proposed as a potential entry factor (Helle and Dubuisson, 2008). Also glycosaminoglycans (GAGs), such as heparin sulfate, and lectins (DC-SIGN and L-SIGN) take part in cell attachment (Barth *et al.*, 2003; Cormier *et al.*, 2004). The LDL-R together with the GAGs and lectins may serve for the first contact with the hepatocytes and direct the virions to the cell surface molecules tetraspin CD81, SR-BI, and the tight junction proteins claudin-1 and occludin for cell entry (Burlone and Budkowska, 2009). CD81 and SR-BI are believed to interact with the viral envelope glycoproteins E1 and E2 (Bartosch and Cosset, 2006). After binding to the hepatocytes, bound virions are internalised by clathrin mediated endocytosis (Meertens *et al.*, 2006). During endocytosis envelope protein E1 and E2 mediate pH dependent fusion with the membrane of early endosomes and the nucleocapsid is released into the cytoplasm (Blanchard *et al.*, 2006; Lavilette *et al.*, 2007).

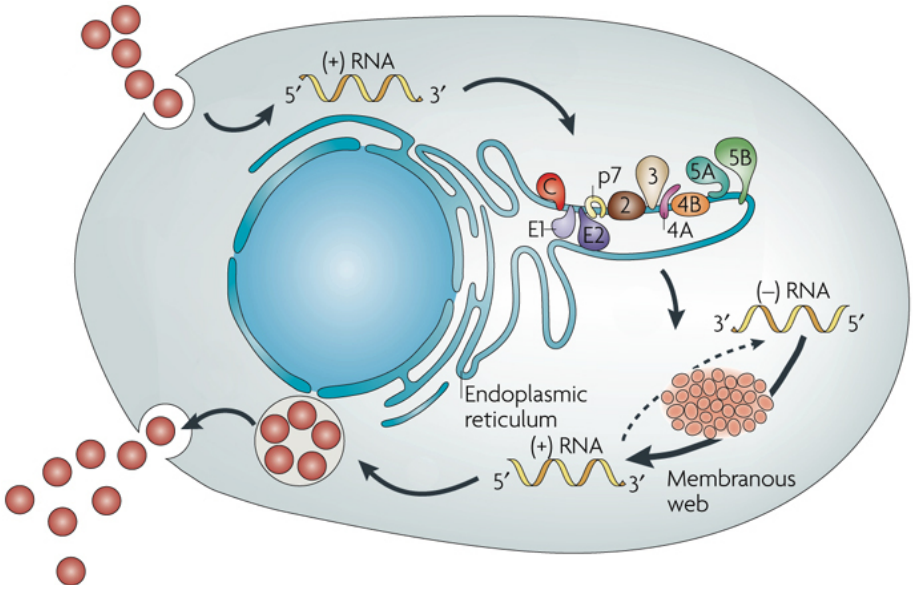

Figure 1-3: HCV life cycle. The HCV virions bind to receptors on the cell surface and enter the cytosol via endocytosis. After fusion of the envelope membrane with the endosomal membrane the viral genome is released. After translation and processing of the polyprotein, the membranous web is formed where the replication of the HCV genome takes place. Virion assembly occurs at the ER membranes surrounding lipid droplets and for maturation and release the pathway for producing very low density lipoproteins is used (modified from Moradpour *et al.*, 2007).

In Figure 1-3 the viral life cycle is shown. Directly after uncoating the translation of the HCV genome starts. The single ORF is flanked by a 5`-untranslated region (UTR) and 3`-UTR that are required for translation and RNA replication (Friebe *et al.*, 2001). An internal ribosome entry site, located in the 5`-UTR, mediates the expression of the polyprotein precursor (Wang *et al.*, 1993). The polyprotein is co- and posttranslationally processed by cellular and viral proteases into 10 mature proteins. The HCV genome also encodes an 11th protein, the F-protein (frame-shift protein), through a ribosomal frame-shift of the RNA encoding the core protein (Xu *et al.*, 2001). The role of the F-protein in the viral life cycle or pathogenesis of HCV is still unclear. The N-terminal located structural proteins core, E1 and E2 and the ion channel protein p7 are cleaved by host signal peptidases. The nonstructural (NS) proteins are processed by viral proteases. The NS2-3 auto-protease is responsible for *cis*-cleavage of NS3 from NS2. The NS3 protein, with protease and helicase function, needs to assemble with its cofactor NS4A to catalyse *cis*-cleavage at the NS3-NS4A junction and *trans*-cleavage at all remaining junctions (Bartenschlager and Lohmann, 2000). All HCV proteins are associated with the ER membrane (see Figure 1-4). The viral replication takes place in a special membrane compartment, called the membranous web. It is induced by the NS4B Protein (Eggert *et al.*, 2005) and contains the replication complex that consists of cellular and viral proteins like the phosphoprotein NS5A and the RNA-dependent RNA polymerase NS5B (Moradpour *et al.*, 2007). The HCV assembly and release is still not fully understood. It is believed that the assembly of virus particles is initiated at lipid droplets and at the surrounding endoplasmatic reticulum (ER) membrane of these organelles. For the maturation and release of HCV virions the pathway for producing very-low density lipoproteins is used (Jones and McLauchan, 2010).

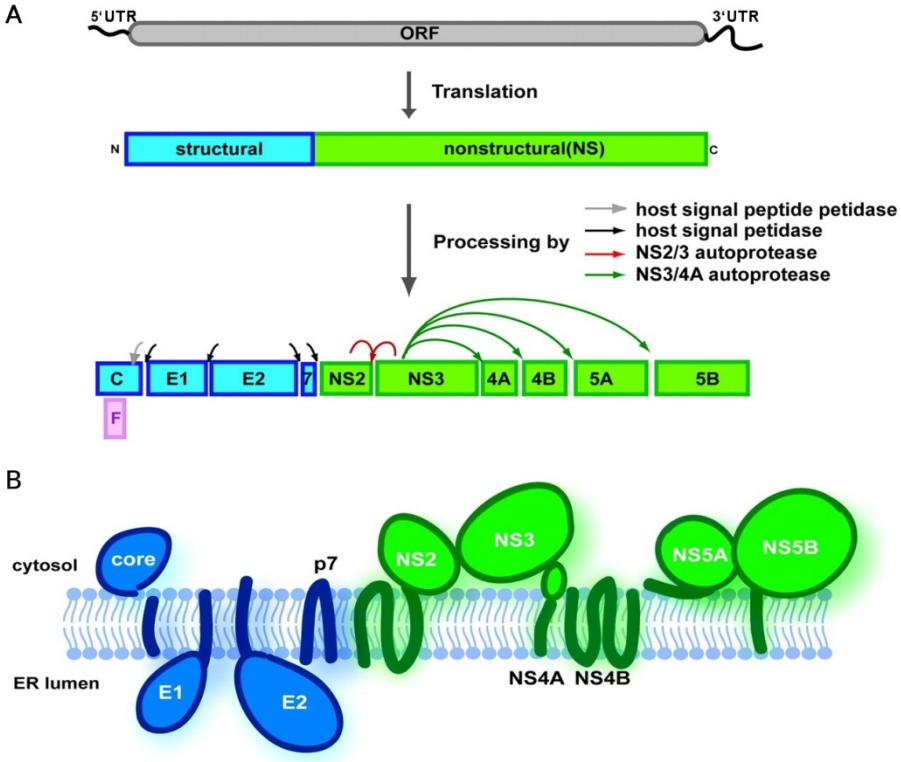

Figure 1-4: HCV genome organisation, polyprotein processing, and protein topology. A: The HCV genome is a single-stranded RNA encoding a single ORF flanked by 5' and 3' UTRs. The translation of the ORF generates a polyprotein. The polyprotein undergoes a series of cleavage events, catalysed by host and viral proteases, to produce 10 individual HCV proteins. **B:** The topology of the HCV proteins relative to the ER membrane (modified from Tellinghuisen, 2007).

Some 80% of infected individuals develop a chronic persistent HCV infection. Viral clearance by the innate and adaptive immune response is required to prevent a chronic infection. The virus has developed various strategies to evade the host immune system. The first innate immune response of infected hepatocytes is the activation of Toll-like receptors (TLR) and RIG-I-like receptors which leads to induction of type I interferon (IFN) production (Rehermann, 2009). The IFN induces an antiviral state that also affects neighboring cells. The NS3/4A protease is important for evading the innate immune response by cleaving not only the viral precursor polypeptide but also the host TRIF and Cardif/MAVS/IPS-1/VISA proteins (Lin *et al.*, 2006). The cleavage of these proteins prevents the TLR-3 and RIG-I dependent virus-sensing and type I IFN production (Li *et al*., 2005; Lemon, 2010). Also the NS2 protein seems to interfere with the RIG-I signaling (Kaukinen *et al.*, 2006) and the signaling downstream of type I IFN is perturbed by several other HCV proteins (Georgel *et al*., 2010).

The adaptive immune system is induced by antigen presenting cells that initiate a virus specific humoral and cell-mediated immune response. The humoral immune response leads to the secretion of HCV specific antibodies by maturated B-lymphocytes, termed plasma cells. Important for maturation of B-lymphocytes is a co-stimulation by activated $CD4^+$ helper T cells. The cell-mediated immune response involves the induction of $CD8^+$ cytotoxic T cells. Cytotoxic T cells kill infected hepatocytes that present viral antigens on their surface (Schmidt *et al*., 2011; Walker, 2010). The HCV virus can stay a step ahead of the adaptive immune response because of the high viral load and the high error rate of the viral RNA polymerase. The high error rate of the polymerase leads to a heterogeneous population of virus quasispecies. These quasispecies have mutations in the viral epitopes which enables them to evade HCV specific antibodies. HCV also induces continued hypermutation of already mature heavy-chain immunoglobin which may lower affinity and specificity of HCV directed antibodies (Machida *et al*., 2008; Georgel *et al*., 2010). In addition HCV proteins, e.g. NS2, interfere with cellular apoptosis mechanism induced by cytotoxic T cells (Machida *et al*., 2001).

1.1.3 Current treatment of HCV

In the late 1980s initial studies indicated that recombinant interferon-α (IFN-α), a type I interferon, based therapy might have an antiviral effect in non-A, non-B hepatitis infections, but the treatment effect was low and severe side effects were reported (Hoofnagle, 1986). Interferons are proteins that induce a direct antiviral effect in the cell. In addition interferon-γ, a type II interferon, is a cytokine that activates the immune system. The pegylation of the interferon improved the half-life of the drug and increased the biological effect. This resulted in longer dosing intervals and higher response rates (Bruijne, 2009). Today the most effective treatment of HCV infection is a combination therapy with pegylated IFN-α 2a or 2b and ribavirin. Ribavirin is a synthetic nucleoside analog with antiviral properties (Reichard, 1991), but the mechanism by which the drug acts is poorly understood. The addition of ribavirin to the pegylated IFN-α therapy significantly decreased relapse rates after termination of the treatment (Feld, 2005). Treatment length varies between 24 – 72 weeks according to the HCV genotype and the viral kinetics of the infected individual (Moradpour, 2009; Lange, 2010). Genotype 1 shows greater resistance to treatment and a 48 week course of pegylated IFN-α and ribavirin is recommended. For patients infected with genotypes 2 or 3, a 24 week course is recommended. Treatment is only moderately effective: A sustained viral response (SVR) is achieved in 40 - 50% of genotype 1 infected patients compared to 70 - 80% of patients with genotypes 2 and 3

(Flamm, 2003). An additional problem is that interferon-ribavirin combination therapy is associated with severe side effects such as fatigue, influenza-like symptoms, hematologic abnormalities, and neuropsychiatric symptoms (Fried, 2002). The side effects lead many patients to prematurely terminate their therapy (Martinot-Peignoux *et al.*, 1998). It is estimated for America that because of a combination of a failure in diagnosis, treatment failure, as well as avoidance and discontinuation of treatment, approximately only 2% of those with HCV are successfully treated with standard of care (Garber, 2007).

Direct-action antiviral drugs are under development in order to improve the treatment of HCV. Two NS3/4A protease inhibitors, telaprevir (Vertex Pharmaceuticals) and boceprevir (Merck) were approved by the FDA in 2011 (Klein and Struble, 2011; Poordad, 2011). Both protease inhibitors appear to be able to improve sustained response while shortening the length of treatment. However, due to a low genetic barrier and high viral mutation rate resistant variants emerge within a few days when used in *monotherapy*. Therefore the inhibitors were combined with pegylated IFN-α and ribavirin in clinical trials. For telaprevir 24 – 48 weeks of total therapy including 12 weeks of triple therapy improved sustained virologic response rates compared with standard of care. The sustained virological response (SVR) rates of HCV genotype 1 patients will be improved by approximately 30%. Also telaprevir can be used for treatment of prior nonresponders or relapsers infected with HCV genotype 1 (Chen and Yu, 2010; Grammatikos and Sarrazin, 2010). The triple therapy with telaprevir improves the treatment outcome but has more side effects than the standard of care, including rash, gastrointestinal disorders and anemia (Gentile *et al.*, 2010).

1.1.4 HCV Proteases

Proteases are proteolytic enzymes that catalyse the cleavage of peptides and proteins through the hydrolysis of peptide bonds. In many infectious diseases proteases play a crucial role and as such are considered as very important drug targets. The classification of proteases is based on the chemical residue in the catalytic center which is responsible for nucleophilic attack of the target peptide bond, e.g., serine, metallo-, aspartyl or cysteine proteases. The subsites of a protease are the surface pockets that bind to a single side chain of a substrate residue and determine the specificity of the protease. Subsites are numbered Sn–S1 from the N terminus of the substrate to the scissile bond and S1`–Sn` towards the C terminus (non-primed sites and primed sites) according to the nomenclature of Schechter and Berger. The substrate residues are numbered P1–Pn and P1`–Pn`, respectively (see Figure 1-5) (Turk, 2006).

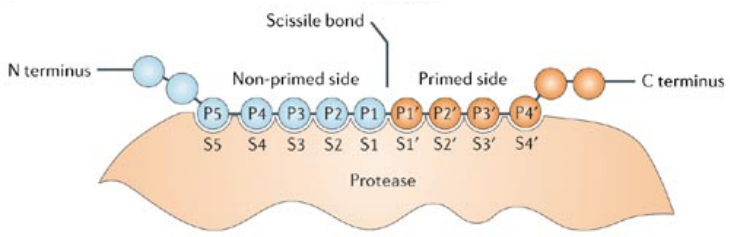

Figure 1-5: Schematic picture of a peptide substrate binding to a protease. The subsites of a protease are the surface pockets that bind to a single side chain of a substrate residue. Subsites are numbered S1–Sn from the N terminus to the scissile bond and S1`–Sn` towards the C terminus (non-primed and primed site). The substrate residues are numbered P1–Pn and P1`–Pn`, respectively (from Turk, 2006).

The HCV virus encodes two proteases for polyprotein processing. The NS2-3 protease is a cysteine protease (Lorenz *et al.*, 2006) and the NS3/4A protease is a serine protease (Lin *et al.*, 1995).

Serine proteases utilise a catalytic triad, formed by a serine, histidine and aspartic acid residue in the active site of the enzyme, for the hydrolysis of a peptide bond. A schematic representation of the hydrolytic mechanism of NS3/4A protease is shown in Figure 1-6.

The aspartic acid positions the histidine residue which acts as a base and abstracts a proton from the serine (see Figure 1-6 A). This facilitates the nucleophilic attack of the serine hydroxyl group on the carbonyl carbon of the peptide bond to be cleaved. The resulting negatively charged tetrahedral intermediate is stabilised through hydrogen bonding of the oxyanion hole. In case of the HCV NS3/4A protease the backbone amide NH groups of Ser139 and Gly137 form the oxyanion hole (see Figure 1-6 B). The C-terminal fragment of the product is released after proton donation of the histidine to the peptide's amide nitrogen which leads to break down of the tetrahedral intermediate. The acyl-enzyme intermediate is attacked by a water molecule forming a second tetrahedral intermediate (see Figure 1-6 C). The histidine is accepting the proton of the attacking water molecule and donating it to the serine residue resulting in a break down of the tetrahedral intermediate. The N-terminal fragment is released with regeneration of the free enzyme (Fersht, 1999; Garrett and Grisham, 2010).

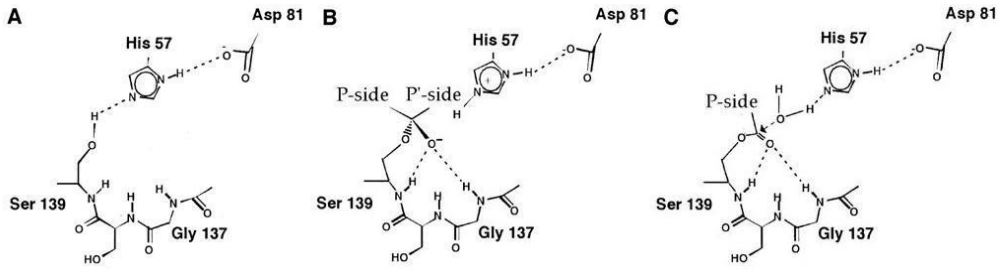

Figure 1-6: Schematic representation of the hydrolytic mechanism of NS3/4A protease (modified from Barbato *et al.*, 2000).

Cysteine proteases contain a catalytic dyad formed by a cysteine and histidine residue in the active site of the enzyme. Additionally a glutamic acid residue is important for orientation of the side chain of the histidine. The thiol group of the cysteine is deprotonated by the histidine and the resulting nucleophilic thiolate anion attacks the carbonyl carbon of the peptide bond to be cleaved. A tetrahedral intermediate is formed and the oxyanion is stabilised by an oxyanion hole similar to serine proteases. The amine of the leaving C-terminal fragment of the cleaved product is protonated by the histidine residue of the protease restoring the deprotonated form. The acyl-enzyme intermediate is hydrolysed and the N-terminal fragment is released with regeneration of the free enzyme (Otto and Schirmeister, 1997; Polaina and MacCabe, 2007).

1.1.4.1 NS2-3 Protease

The NS2-3 protease is responsible for the intramolecular cleavage between the non structural proteins NS2 and NS3 and is one of the two HCV proteases for polyprotein processing (Grakoui, 1993). NS2-

3 is a cysteine autoprotease with the active site residues entirely located in the NS2 protein. NS2 consists of a hydrophobic N-terminal region comprising several transmembrane segments and the C-terminal catalytic domain. Two NS2 monomers form a dimeric cysteine autoprotease with two composite active sites (see Figure 1-7). The active site catalytic triad consists of His143 and Glu163 from one monomer and Cys184 from the second monomer. After intramolecular cleavage between NS2 and NS3 the C-terminal Leu-217 of the NS2 protein remains coordinated in the active site and inactivates the protease. Deletion or mutation of the C-terminal leucine impairs infectious virus production, but not due to inhibition of the protease function. It is suggested that altering the C-terminus could lead to a conformational change of the NS2 protein thus disrupting protein-protein interactions important for viral assembly (Lorenz *et al.*, 2006; Dentzer *et al.*, 2009). For the full activity of NS2-3 protease not only the C-terminal part of NS2 but also the N-terminal part of the NS3 protein that compasses the NS3 serine protease domain with the Zn^{2+} binding site is necessary (Thibeault *et al.*, 2001; Pallaoro *et al.*, 2001). An NS2 protein with two N-terminal NS3 aa has only basal proteolytic activity. NS3 acts as a regulatory cofactor of the NS2 protease and is not involved directly in the catalysis of the cleavage reaction. The NS3 protein promotes the formation of the proteolytic active conformation of the NS2-3 dimer by correct positioning of the cleavage sites (Schregel *et al.*, 2009). For *in vitro* cleavage of NS2-3 the presence of non ionic detergents is necessary, suggesting that a hydrophobic environment is needed for correct folding. However, no cellular cofactors are needed for *in vitro* cleavage of purified NS2-3 protease (Thibeault *et al.*, 2001; Pallaoro *et al.*, 2001).

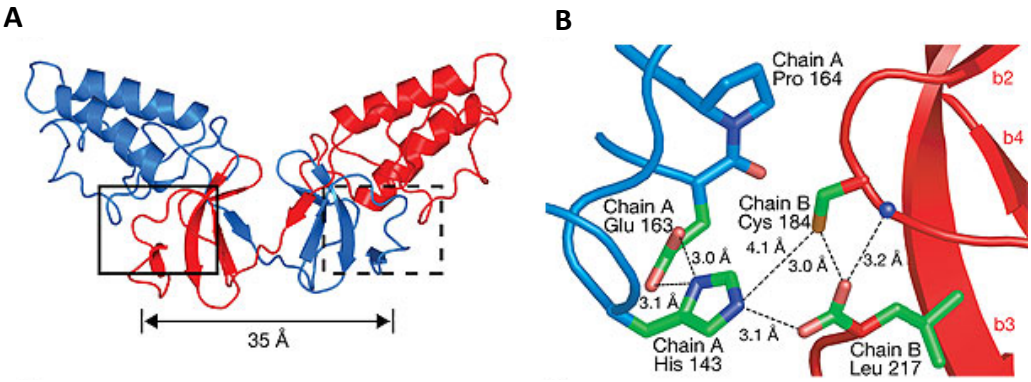

Figure 1-7: NS2 dimer and active site. A: Ribbon diagram showing the NS2 dimer with one catalytic monomer (consisting of aa 94-217 of NS2) in blue, the other in red. The two active sites marked with boxes. **B:** Active site indicated by solid lined box. Residues His 143, Glu 163, Pro 164, Cys 184 and Leu 217 are shown. The active site is composed of His 143 and Glu 163 from one monomer (chain A, drawn in blue), and Cys 184 from the other molecule (chain B, drawn in red). The Leu 217 is the C-terminal residue at the scissile bond (from Lorenz *et al.*, 2006).

The cleavage of the NS2-3 protease is essential for infectious virus production *in vitro* and *in vivo*. The inhibition of the NS2-3 cleavage has a devastating effect on virus production, but it is suggested that it is not due to the interruption of the polyprotein processing. The NS3 serine protease domain is active in the uncleaved NS2-3 and can process the polyprotein, but uncleaved NS2-3 is rapidly degraded. This leads to a decrease in NS3 protein which is also essential for RNA replication (Welbourn *et al.*, 2005). Besides the protease function, the NS2 protein is a key organiser for viral assembly (Jirasko *et al.*, 2010), is important for evasion of the immune system (Kaukinen *et al.*, 2006) and inhibition of apoptosis (Machida *et al.*, 2001). Because of its essential role in the viral life cycle the NS2-3 protease is an interesting target for new specific HCV drugs. Although there are few NS2-3

protease inhibitors the only ones known act indirectly by disrupting the conformation of the uncleaved NS2-3 protease. NS4A cofactor derived peptides change the conformation of the NS3 domain upon binding and inhibit the protease. Also chelating agents that remove the Zn^{2+} from the NS3 zinc binding site lead to a miss folding of the NS3 domain and inhibition of protease activity (Thibeault *et al.*, 2001). Cyclosporine A (CsA) is known to act indirect on the NS2 protein. CsA interacts with cyclophilins (CyP), which are essential cellular cofactors for HCV. CyP catalyse the isomerisation of peptide bonds from the *trans* form to the *cis* form and is it suggested that inhibition of these enzymes leads to missfolding of the NS2 protein due to a *cis*-proline (see Figure 1-7 b), essential for correct folding, in close proximity to the protease active site (Ciesek *et al.*, 2009).

1.1.4.2 NS3 Protease

The HCV NS3 protein is a bifunctional enzyme that consists of two domains, an N-terminal serine protease domain and a C-terminal helicase/ATPase domain. The enzymatic domains are separated and connected by a linker (Yao *et al.*, 1999). The NS3 protease is essential for polyprotein processing and the NS3 helicase/ATPase is required for genome replication and virus assembly (Raney *et al.*, 2010).

The NS3 protease is a chymotrypsin-like serine protease and forms a heterodimeric complex with the NS4A protein. NS4A is a 54 aa long cofactor of the NS3 protease domain enhancing the proteolytic activity (Lin *et al.*, 1995). NS4A forms an additional ß-strand and stabilises the structure of the NS3 protease domain (Kim *et al.*, 1996). It also anchors NS3 to the ER membrane (Wolk *et al.*, 2000). For the activation of the protease *in vitro* only residues 21 to 34 of NS4A are required (Tomei *et al.*, 1996). The crystal structure of NS3/4A revealed the proximity of the C-terminus of NS4A and the N-terminus of NS3 which led to the design of a single chain protease where the NS4A peptide is linked to the NS3 protease domain (Dimasi *et al.*, 1998; Taremi *et al.*, 1998). The NS3 protease domain also contains a Zn^{2+} binding site which is important for stabilisation of the structure (Tedbury and Harris, 2007). After assembly with its cofactor NS4A, NS3/4A catalyses the cis-cleavage at the NS3-NS4A junction and trans-cleavage at all remaining junctions: NS4A-4B, NS4B-5A and NS5A-5B. The active site catalytic triad consists of His57, Asp81 and Ser139.

The NS3/4A protease has the substrate consensus sequence D/EXXXXC-S/A (P6-P1´), with X being any amino acid and the scissile bond being located between C and S/A. The intramolecular cleavage site between NS3 and NS4A was found to differ from this consensus, having a T in the P1 position (Grakoui *et al.*, 1993). The NS3/4A protease has a shallow and solvent exposed substrate binding pocket (Kim *et al.*, 1996). Because of the flat substrate binding pocket the substrate-protease interactions extend over the whole binding region and explain the inability to cleave small substrates. A decapeptide substrate (P6-P4`) was found to be optimal for efficient cleavage by the NS3/4A protease. Further truncation resulted in a significantly decrease in proteolytic activity (Landro *et al.*, 1997). An acidic residue (Asp or Glu) at the P6 position, a cysteine (or threonine) at the P1 position and a small side chain residue (Ala or Ser) at the P1` position are important for substrate binding and cleavage. The crystal structure of the full length NS3 protein revealed that the active site is located at the interface between the protease and the helicase domain and it is suggested that the helicase has influence on the protease domain. The NS3 C-terminus is bound to the active site of the protease and needs to be removed by a conformational change prior to cleavage of a substrate. However, the specific activity of full-length NS3/4A and protease domain NS3/4A are similar or is even enhanced

for the full-length NS3/4A, implying that relatively little energy is required for the conformational change (Yao *et al.*, 1999; Beran and Pyle, 2008).

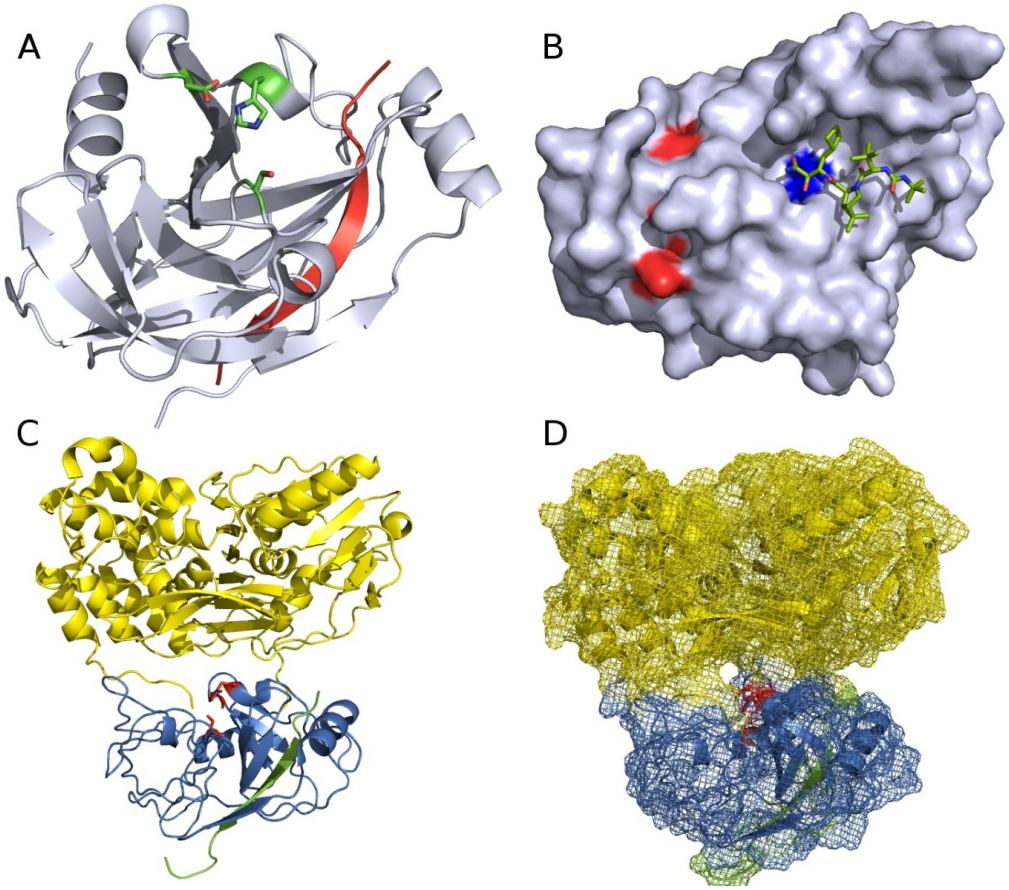

Figure 1-8: Structure of NS3 protein in complex with NS4A peptide. A) Ribbon structure of the NS3/4A complex; NS3 protease domain (aa 4-181) in grey, NS4A peptide (aa 31-34) in red and the side chains of active site residues His-57, Asp-81 and Ser-139 are displayed in stick representation. B) Surface representation of the NS3/4A protease with bound inhibitor boceprevir (PDB code 1W3C); protease domain in grey, NS4A peptide in red and inhibitor boceprevir displayed in stick representation. The active site Ser-139 is highlighted in blue. C) Ribbon structure of the full-length NS3 protein and the protease cofactor NS4A (PDB code 1CU1); the helicase domain is shown in yellow, protease domain in blue and NS4A in green. The active site residues are highlighted in red. D) Surface representation of the full-length NS3 protein and the protease cofactor NS4A (PDB code 1CU1); same coloring as in C.

Beside the essential role in polyprotein processing, the NS3/4A protease is involved in evasion of the immune response by cleaving proteins of the TLR-3 and RIG-I signaling pathways (Li *et al.*, 2005; Lemon, 2010). Inhibition of the NS3/4A protease may not only block viral replication but also restores the host immune response which makes the NS3/4A protease one of the most attractive targets for novel drug development. The shallow and solvent exposed substrate binding pocket makes it relatively difficult to identify specific inhibitors of HCV NS3/4A protease. The finding that the protease is inhibited by peptides corresponding to the C-terminus of the cleavage products led to the development of first potent competitive protease inhibitors. The hexapeptides (P6-P1) from the C-terminus of the NS4A and NS5A cleavage sites act as competitive inhibitors of NS3/4A with K_i values of 0.6 µM (NS4A: Ac-DEMEEC-OH) and 3.1 µM (NS5A: Ac-EDVVCC-OH). It was shown that for optimal binding of the hexapeptide a cysteine residue in position P1 with a free carboxylate is required. Also carboxylic acids in position P5 and P6 have dramatic influence on the binding because of electrostatic interactions with basic amino acids of the NS3/4A protease (Steinkühler *et al.*, 1998; Koch *et al.*, 2001). These interactions are destabilised by increased ionic strength and result in a higher K_i value. Using synthetic peptide analogues sequential substitution of the hexapeptides led to

the optimised inhibitor Ac-Asp-D-Gla-Leu-Ile-Cha-Cys-OH (D-Gla: γ-carboxyglutamic acid; Cha: ß-cyclohexyl-L-alanine) with an IC_{50} value of 40nM (Ingallinella *et al.*, 1998). Further structure-based optimisation led to the design of macrocyclic product-based inhibitors, e.g. BILN-2061 which was the first compound that showed proof-of-concept in clinical studies. It was withdrawn because of cardiac toxicity (Lamarre *et al.*, 2003; Reiser *et al.*, 2005), but other macrocyclic compounds are currently in clinical trials, e.g. TMC-435350 and ITMN-191 (Örtqvist *et al.*, 2010). A second group of NS3/4A drugs are peptidomimetic inhibitors with an electrophilic α-ketoamide group. The α-ketoamide group functions as a trap for the active site serine hydroxyl and forms a covalent bond that is reversible (Lin *et al.*, 2006). In 2011, two α-ketoamide inhibitors, telaprevir (Vertex Pharmaceuticals) and boceprevir (Merck), were approved by the FDA (Klein and Struble, 2011; Poordad, 2011).

The product-based drug design was the most successful method for the development of new specific NS3/4A protease inhibitors so far. Other approaches, e.g. high-throughput screenings (Sudo *et al.*, 2005; Gentzsch *et al.*, 2010), antibody fragments (Martin *et al.*, 1997; Kasai *et al.*, 2001), or aptamers (Kumar *et al.*, 1997) have been explored, but with limited success.

1.1.5 HCV Model systems

HCV research has been hampered both by the lack of a robust, efficient cell culture system and by lack of a small animal model. Such model systems are very important for the evaluation of potential new HCV drugs, e.g., to evaluate cell availability or *in vivo* stability and pharmacokinetics.

First studies were done with primary cell cultures, either with HCV infected hepatocytes or primary cells isolated from tissues of either infected patients or chimpanzees. However, in these systems viral replication and reproducibility were very poor (Iacovacci *et al.*, 1993; Lanford *et al.*, 1994). A milestone was the development of the replicon system (Lohmann *et al.*, 1999). The replicon system is a cell culture model system where the genes coding for the structural proteins were removed from the consensus sequence of a HCV 1b genome (isolate Con1). The HCV non structural proteins are produced and the replicon RNA is replicated, but no virus particles are produced. The neomycin phosphotransferase gene (*neo*) was introduced into the truncated viral replicon for its selection in transfected cells. The translation of *neo* is initiated by the HCV 5´ UTR IRES and translation of the NS proteins is directed by the IRES of the *Encephalomyocarditis virus* (EMCV) (see Figure 1-10). For a luciferase based HCV replication assay a firefly luciferase gen (*luc*) was inserted in the replicon instead of the *neo* gen under the control of poliovirus IRES (PI) for higher translation efficiency (Lohmann *et al.*, 2003) (see Figure 1-9).

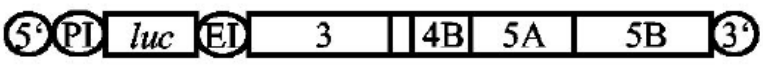

Figure 1-9: Structure of the subgenomic HCV replicon I341 PiLuc/NS3-3´. It is composed of the HCV 5´ UTR, poliovirus IRES (PI), the gene encoding the firefly luciferase (luc), the EMCV IRES (EI), the region encoding HCV 1b NS3-5B and the 3´ UTR (from Lohmann, 2003).

The replication of the replicon was poor in the hepatoma cell line Huh7 but was significantly increased by cell culture adaptive mutations in all NS proteins (Krieger *et al.*, 2001). The discovery of the Huh7.5 subclone that harbors a defect in the RIG-I pathway even enhanced RNA replication

(Blight *et al.*, 2002). In addition Huh7-Lunet cells have a gaussia luciferase gen in their genome that can be used for a cell viability assay.

Also HCV full-length genomes and genomic replicons of other genotypes could be established (Pietschmann *et al.,* 2002; Ikeda *et al.*, 2002; Blight *et al.*, 2003), but the production of infectious virus particles was not possible until the isolation of the HCV genotype 2a strain JFH-1. This HCV isolate could replicate in cell culture without adaptive mutations and release viral particles referred to as HCVcc (HCV cell culture) (Kato *et al.*, 2003; Wakita *et al.*, 2005). Chimeric constructs with the N-terminal regions of a different genotype 2a isolate improved the infectivity considerably (see Figure 1-10) (Lindenbach *et al.*, 2005; Pietschmann *et al.*, 2006). Furthermore the HCVcc are infective in animal models (Lindenbach, 2006).

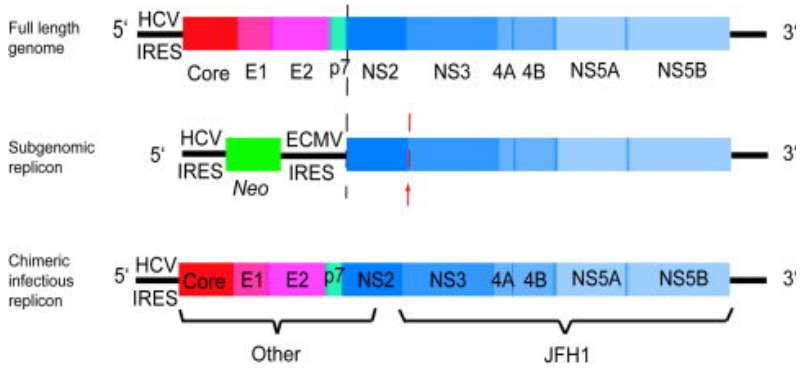

Figure 1-10: Comparison of the genomic structure of HCV replicons. Structure of the full length replicon derived from the JFH1 consensus genome. In the subgenomic replicon the structural sequences were replaced by a neomycin phosphotransferase gene for selection and a EMCV IRES was inserted for translation of the nonstructural proteins. The NS2 region can also be deleted (red arrow). The infectivity of the full length replicons was significantly increased by creating virus chimeras by replacing the core to NS2 region with that of a genotype 2a isolate (from Boonstra *et al.*, 2009).

The only available immunocompetent animal model for HCV is the chimpanzee, the use of which is limited by ethical concerns, limited availability and high costs (Bukh *et al.*, 2004). The most well-established mouse model at the moment is the xenotransplantation model that is based on liver repopulation. In this model immunodeficient uPA/SCID mice are used in which overexpression of a urokinase plasminogen activator (uPA) transgene results in severe liver toxicity (Walters *et al.*, 2006). Mice, with transgene-induced liver disease, are transplanted with primary human hepatocytes. The hepatocytes repopulate the diseased mouse liver and successfully transplanted mice can then be infected with HCV (Meuleman and Leroux-Roels, 2008). Recently a mouse model with humanised mice with human immune system and liver tissue was developed which allows also the study of the specific immune response against HCV (Washburn *et al.*, 2011). These models have several shortcomings, e.g. mice are only available in small numbers and of high variability since the ratio of human/mouse hepatocytes is critical and must exceed 10% (Bissig *et al.*, 2010). Therefore it is being attempted to create a mouse model that is susceptible to HCV infection. Recently HCV was adapted *in vitro* to the mouse CD81 receptor allowing the adapted virus to infect mouse cells (Bitzegeio *et al.*, 2010). However, the need of additional host factors limits the replication of HCV in mouse cells and additional work is needed to overcome the species barrier.

1.1.6 HCV drug discovery and drug resistance

The current standard of care for patients with HCV infection enhances only the anti viral immune response and is associated with severe side effects (Fried, 2002). Therefore a lot of effort is focused on developing novel specifically targeted antiviral therapies for HCV (STAT-C) to improve the treatment. Due to the growing understanding of the HCV life cycle, many targets for new specific drugs have been identified. Besides viral proteins and RNA, several host proteins are being addressed as drug targets, e.g. alpha-glucosidase and cyclophilins. At the time of writing about 30 STAT-C compounds were in clinical trials (Lange *et al.*, 2010). Among the viral proteins the two viral proteases NS2-3 and NS3/4A, which are essential for the viral life cycle, are particularly interesting targets for new specific drugs. The NS2-3 protease turned out to be a difficult drug target (see 1.1.4.1), but for the NS3/4A protease several inhibitors are in clinical trials and two drugs were approved by the FDA (see 1.1.4.2). One problem of the new protease inhibitors is the rapid emergence of resistant variants. In an infected patient 10^{10}-10^{12} virions are produced per day and the HCV RNA polymerase NS5B has a low fidelity with an error rate of approximately 10^{-3}-10^{-5} mutations per nucleotide (Herrmann *et al.*, 2000; Bartenschlager and Lohmann, 2000). Because of this low polymerase fidelity and the high viral yield, huge numbers of novel variants termed quasispecies are produced constantly (Gaudieri *et al.*, 2009). In infected patients variants with resistant mutations often already preexist and can be the dominant quasispecies which will have an effect on the treatment outcome (Bartels *et al.*, 2008). Monotherapy with different protease inhibitors leads to the rapid selection of resistant variants and as such must be avoided at all cost. Chemically related inhibitors share a similar resistance profile with resistance mutations at the same positions (see Figure 1-11). For the linear α-ketoamide inhibitors mutations in NS3 at positions V36A/M, T54A, R155K and A156S confer to a low to medium level of resistance, whereas A156T/V or the double mutants 36/155 or 36/156 all confer high level resistance. A mutation of R155 affects the recognition step of the inhibitor and thereby a selection of a second mutation that affects the covalent binding step will have a resistance synergy effect, as shown by a mutation at V36. It has been shown that, for the macrocyclic inhibitors BILN-2061, ITMN191 and TMC435, mutations at position R155, D168 and A156T/V confer to high level resistance (Zhou *et al.*, 2007; Bae *et al.*, 2010; Lenz *et al.*, 2010). Primary resistance mutations occur at positions where the inhibitors have part of their structure extending outside the consensus volume modelled to be occupied by the normal substrates, the 'substrate envelope', thus the binding of the inhibitors is weakened without severe influence on substrate binding. Notably the residues R155 and A156 interact with the inhibitors where they extend most extensively from the 'substrate envelope'. It is suggested that drugs that fit entirely within the 'substrate envelope' will be less susceptible to resistance as has recently been shown for HIV-1 protease inhibitors (Romano *et al.*, 2010; Nalam *et al.*, 2010). The resistance mutations at position R155 confer resistance to all protease inhibitors which are in clinical trials. Interestingly mutations at R155 exhibit similar replication activity to the wild-type and show a selective advantage (Sarrazin and Zeuzem, 2010; He *et al.*, 2008). The resistance mutation A156V refers to high level resistance for α-ketoamide inhibitors and macrocyclic inhibitors, but was not shown for all inhibitors *in vitro* and *in vivo* (see Figure 1-11).

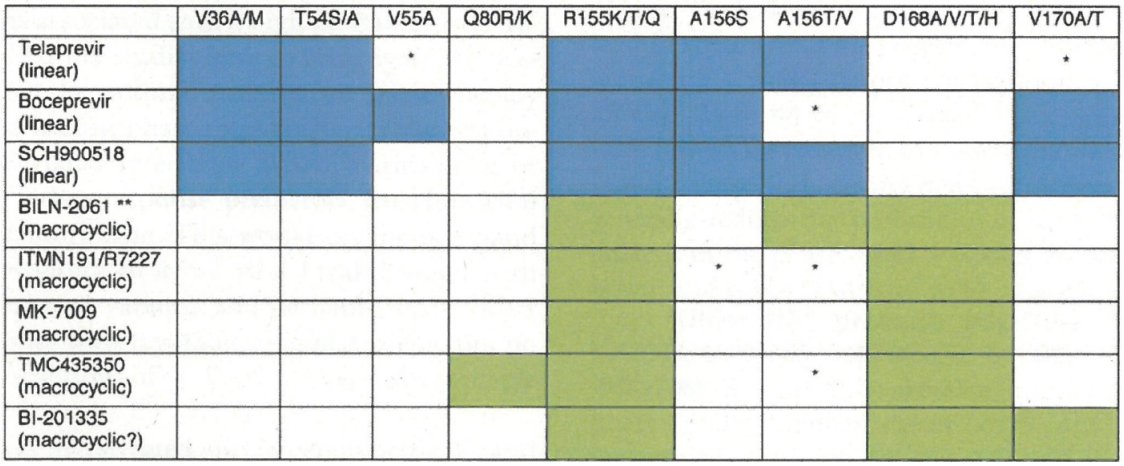

Figure 1-11: Amino acids changes of the NS3/4A protease that are associated with resistance mutations *in vivo* and/or *in vitro* for different inhibitors * Mutations associated with resistance *in vitro* but were not described in patients. ** Mutations associated with resistance *in vitro*. Resistance mutations described for linear α-ketoamide inhibitors are shown in blue and resistance mutations for macrocyclic inhibitors are shown in green (modified from Sarrazin and Zeuzem, 2010).

Because of the heterogeneity between genotypes and subgenotypes in their nucleotide sequence, new STAT-C compounds will not have the same activity in all HCV variants. The protease inhibitors telaprevir and boceprevir show a varying activity in different genotypes. Both inhibitors were designed to inhibit HCV genotype 1 and show reduced efficacy in genotype 2, 3 and 4. Also development of resistant variants occurs more frequently in patients infected with genotype 1a than 1b when treated with telaprevir or boceprevir because of a nucleotide difference in both subtypes that changes the possibility of resistance (Sarrazin and Zeuzem, 2010).

The development of new specific HCV drugs that show a high activity for all HCV variants and a higher barrier to resistance could be achieved by more flexible binding of the inhibitor that allows binding even if resistance mutations occur. This means that more than one amino acid mutation would be needed to prevent proper binding of the inhibitor (McKeage *et al*., 2009; Ghany *et al*., 2009).

1.2 Peptide phage display

Phage display is a powerful technology for the discovery of peptides that can be used as drugs or as lead compounds for drug design. It was first introduced in 1985 by George P. Smith (Smith, 1985) and has become a widely established technique in the last decades (Arap, 2005). The phage display method connects phenotype and genotype of a peptide or protein and mimics the evolutionary process. From the huge diversity of a peptide library single binders are selected under specific selection pressure (Collins, 1997). An advantage of peptide phage display libraries is the enormous number of different peptides presented on phages that can be screened simultaneously. Selected peptides can provide new information about the ligand-target interaction and may be used for development of new drugs or lead compounds. Several phage display systems have been developed and the most common are based on filamentous phage, e.g. the bacteriophage M13 (Lowman, 1997; Molek *et al.*, 2011).

1.2.1 Bacteriophage M13

Bacteriophages are viruses that exclusively infect bacteria. The filamentous phage M13 belongs to the family of *Inoviridae* and has a circular single stranded DNA genome. The genome encodes eleven proteins, five coat proteins, three proteins important for viral assembly and three proteins necessary for viral replication. The genome is packaged into a coat that comprises the 5 coat proteins (see Figure 1-12). The main coat protein is the pVIII protein. About 2700 copies of pVIII form a tube-like capsid which is capped by three to five copies of the proteins pIII and pVI at one end and pVII and pIX at the other (Model and Russel, 1988). The pIII protein is vital for the infectivity of the phage and consists of three domains which are connected by glycine rich linkers. The phage particle has a length of about 700 – 900 nm and a width of about 6.5 nm. The M13 phage infects bacteria after binding to the F-pilus and can therefore only infect bacteria that contain an F-factor (Vieira und Messing, 1987). During production of new phage particles the bacterial cells are not lysed, but the generation time is lengthened. Each generation of bacteria can produce about 100 – 200 phages (Breitling and Dübel, 1997).

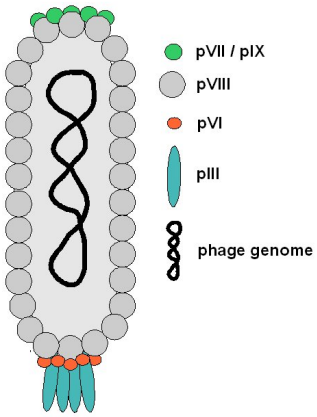

Figure 1-12: Schematic picture of a M13 bacteriophage.

1.2.2 Presentation of peptides using phage display

Phage display is a method for the presentation of recombinant polypeptides on the surface of phage, whereby the genotype and phenotype of the displayed polypeptide are connected (see Figure 1-13). The polypeptide exhibiting a specific phenotype is presented on the surface of the phage and the genetic information, the genotype, is packaged into the phage allowing a direct identification of the coding sequence after an affinity selection (Barbas *et al.*, 1991; Breitling *et al.*, 1991). Peptides can be fused to all capsid proteins for presentation on the phage surface. The fusion to the pIII coat protein is widely used and allows the display of even large proteins (Bratkovic, 2010). The genetic information was first integrated directly into the phage genome (McCafferty *et al.*, 1990), but this resulted in a selection drawback of the phage because of lower infectivity of the pIII and a selective growth advantage of phage with smaller genomes. Therefore display vectors, termed phagemids, have been developed (Breitling *et al.*, 1991; Barbas *et al.*, 1991). Phagemid contain components of plasmids, a bacterial origin of replication and an antibiotic resistance, and elements of phage genomes, a phage origin of replication for packaging of the phagemid DNA into the phage particles. Also phagemid

encode the peptide-pIII fusion protein which is secreted to the periplasm for phage assembly (see Figure 1-13).

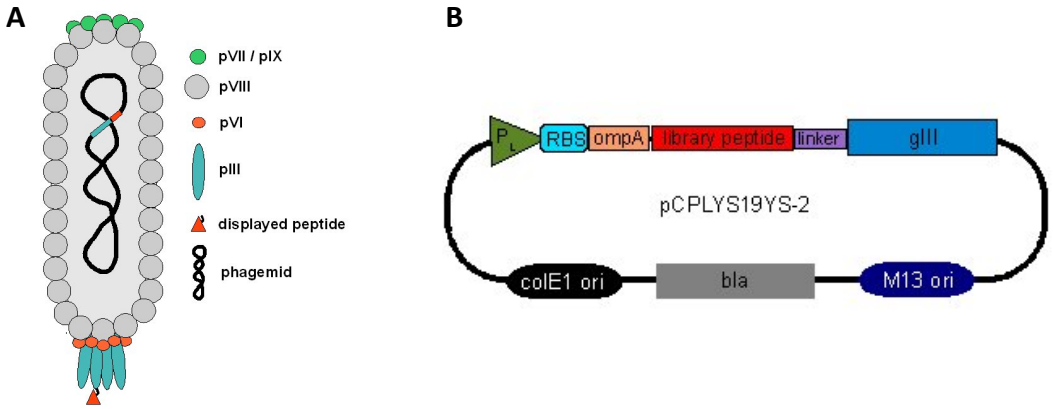

Figure 1-13: Schematic picture of bacteriophage M13 (A) presenting a peptide as a pIII fusion protein and a schematic picture of the phagemid pCPL19YS-2 (B). PL: Lambda promoter, RBS: ribosomal binding site, ompA: ompA periplasm secretion signal peptide, gIII: M13 pIII coat protein gene, bla: ß-lactamase gene, colE1 ori: E. coli origin of replication, M13 ori: M13 phage origin of replication.

The phagemid is present in the cell as a dsDNA replicating plasmid. For production of phage particles a subsequent infection with a helper phage is essential. The helper phage provides all additional components for phage replication and packaging. The helper phage has a mutated origin of replication and the genome of the helper-phage will be packaged less efficiently into new phage particles (Vieira & Messing, 1987) compared to the phagemid. The phagemid will be packed into the phage particle and the peptide-pIII fusion protein will be integrated in the phage coat along with wild type pIII protein. The use of a tightly controlled promoter for weak expression of the pIII-fusion protein, e.g. the lambda P_L promoter under control of the lambda repressor, allows essentially monovalent display. The frequency of multivalent particles can be calculated assuming that there are 5 copies of the pIII/pIII-hybrid protein per particle distributed approximating to a Poisson distribution. The ratio of pIII-hybrid/pIII has been measured by Western-blot analysis (Pollmann, 2010) to be 1:50. According to this estimate about 10% of the phage particle will incorporate one fusion protein and only a very low percent two or more copies of the fusion protein. The majority of the phage display no fusion protein. The monovalent display allows higher differential selection of high affinity binders because of the avoidance of avidity effects that could result in a higher apparent affinity of low affinity ligands (Russel *et al.*, 2004; Röttgen and Collins, 1995).

1.2.3 Panning: Affinity selection of peptide phage

The connection of genotype and phenotype during phage display selection allows the simultaneous screening of an enormous number of different peptides using their affinity to a target protein. Peptide phage display libraries with up to 10^9 different variants have been constructed and displayed peptides with the highest affinity can be enriched from these libraries. Monovalent display allows selection of ligands with affinities ranging from 500 nM to low picomolar binding affinities (Lowmann, 1997). The selection of specific binders from the phage library is called panning (Parmley and Smith, 1988). For an affinity selection the target molecule can be immobilised on a surface or the panning can be done in solution with subsequent capture of the target molecule. For direct immobilisation e.g. plastic

surfaces, coated microtiterplates, resins or beads are used (Russel *et al.*, 2004). The phage displaying the peptides are incubated with the target molecule and unbound particles are removed by several washing steps (see Figure 1-14).

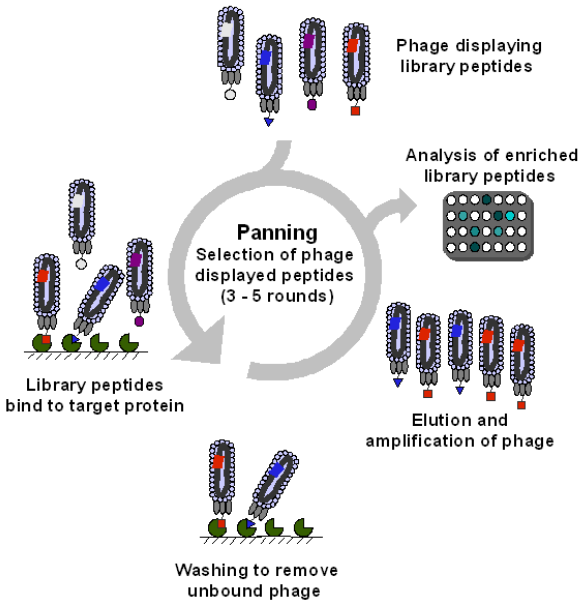

Figure 1-14: Schematic description of an affinity selection procedure with a phage display library.

Bound phage can be eluted through unspecific elution, e.g. lowering the pH, or denaturing the target molecule with DTT or a chaotrope, or through specific elution with a competitive molecule which binds at the desired binding site of the target. The eluted phages are amplified and used for further selection rounds. Usually 3 – 5 panning rounds are enough for enrichment of specific binders which can be identified by sequencing and ELISA tests. This requires enrichment of several hundred- to several thousand-fold per panning round. The outcome of an affinity selection depends on a number of experimental parameters during panning e.g. target immobilisation, buffer conditions, number and duration of washing steps and elution method are very important and have to be adapted for each target.

1.2.4 Library diversity and cosmix-plexing

The library diversity is an important parameter for the selection of peptides with high affinity. Roughly speaking a high library complexity increases the chance of enrichment of variants with high affinity. The practical limitation of the size of a phage display peptide library is about 10^{11} variants, but the complexity of a library normally does not exceed 10^{9} variants (Lowman, 1997). The number of clones required within a library that contains all possible sequences increases exponentially with length of the library peptide. The theoretical complexity of a 20mer peptide library is already about 1 x 10^{26} variants. Therefore only a minute fraction of all possible variants can be covered in peptide libraries. To further extend variability recombination techniques can be used to increase the complexity of a library. This is a central concept of cosmix-plexing libraries. Cosmix-plexing is a technique to increase diversity through DNA recombination and can be used to further increase the diversity of a library before selection and/or to increase the affinity of selected ligands after initial

selection rounds. Restriction enzyme sites located at defined positions allow shuffling of DNA cassettes. The phagemids are cleaved at type IIs restriction enzyme sites inside the library sequence and ligated at high DNA concentration resulting in the formation of long concatemers. After cleavage of these concatemers at a restriction site located outside of the library sequence, the DNA is ligated at low concentration to yield circular phagemid with recombined library sequence. The orientation and order of the fragments is maintained by having non-palindromic sequences where the restiction endonucleases produce cohesive ends (see Figure 1-15). After additional selection rounds the recombination can be repeated with different restriction sites to further increase the affinity of the peptides. The selective enrichment of motifs after recombination and new rounds of selection allows the rapid localisation of important binding motives within the long variable region of the selected peptides (Collins *et al.*, 2001).

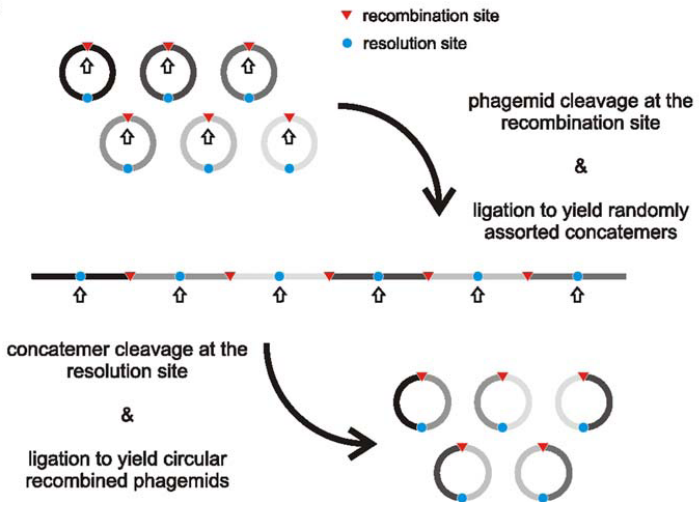

Figure 1-15: Cosmix-plexing procedure. Recombination is achieved by enzyme cleavage and ligation. The circles represent phagemid DNA. The left and right fragments of the phagemids are recombined yielding N2 variants from an initial selected population of N clones. The orientation of the fragments is maintained by using non-palindromic cohesive ends which are generated by cleavage at the recombination and resolution site (from Bratkovic, 2009).

1.2.5 Affinity

The binding strength of a ligand binding to a protein is called affinity. Non-covalent ligand-protein interactions, such as ionic or hydrophobic interactions and hydrogen bonds determine the binding affinity. The formation of the ligand-protein complex can be described by the law of mass action (Eq. 1).

$$[A] + [B] \underset{k_d}{\overset{k_a}{\Leftrightarrow}} [AB] \qquad \textbf{Eq. 1}$$

[A]: protein concentration, [B]: ligand concentration, [AB]: complex concentration, k_a: association rate, k_d: dissociation rate

In an equilibrium state the concentration of the ligand at which half of the protein has a bound ligand is termed equilibrium dissociation constant K_d. The dissociation constant is a dimension for the affinity of the ligand and has molar units. The smaller the dissociation constant K_d the higher the

affinity of the ligand for the protein. K_d is defined by Eq. 2 and can be measured e.g. by isothermal titration calorimetry (Freire, 2004).

$$K_d = \frac{[A][B]}{[AB]} = \frac{k_d}{k_a} \qquad \textbf{Eq. 2}$$

K_d: dissociation constant, [A]: protein concentration, [B]: ligand concentration, [AB]: complex concentration, k_d: dissociation rate, k_a: association rate

In the case of enzyme inhibitors the dissociation constant of the inhibitor is called K_i. Analogue to the K_d the K_i is the concentration of the inhibitor at which half of the enzyme has a bound inhibitor at the binding site at equilibrium. The binding affinity of the inhibitor K_i is related to the IC_{50} value for competitive compounds and can be described through Eq. 3 (Cheng and Prusoff, 1973).

$$K_i = \frac{IC_{50}}{1+\frac{[S]}{K_m}} \qquad \textbf{Eq. 3}$$

K_i: binding affinity of the inhibitor, IC_{50}: half maximal inhibitory concentration, [S]: substrate/ligand concentration, K_m: Michaelis-Menten constant of the substrate/ligand

The IC_{50} value describes the effectiveness of a drug. For an enzyme inhibitor the commonly used relative IC_{50} is the concentration where the compound has the half maximal inhibitory effect. The IC_{50} value of a drug can be determined with a dose-response curve using different concentrations of an inhibitor. The IC_{50} value is dependent on the measurement condition, e.g. substrate affinity and enzyme concentration.

1.2.6 Peptide library CPL19YS-2

The peptide phage display library CPL19YS-2 was constructed by Dr. Erik Pollmann (Pollmannn, 2010). The library peptide coding region is fused via a short linker in the same open reading-frame to the pIII coat protein of the M13 phage. Expression of the fusion protein is under control of the lambda P_L promoter regulated by the CI lambda repressor. This promoter was previously shown to have an appropriate level of expression for monovalent display of the peptide in a host cell with sufficient lambda repressor (Röttgen and Collins, 1995). The library peptide consists of 33 aa from which 26 aa are variable. At degenerate codons not every amino acid is available at each position (see Figure 1-16). The amino acids Glu, Lys, Gln and Trp are absent. To reduce the theoretical complexity only one negatively and positively charged aa is available in the library. The aa Gln is absent to avoid the HPQ motive which binds to streptavidin with high affinity (Devlin *et al.*, 1990). Trp is very hydrophobic, and being a very large amino-acid not easily sequestered within a relatively short peptide. This may make most peptides containing it very hydrophobic and may lead to unspecific interactions especially with plastic sufaces (Adey *et al.*, 1995). Therefore it is not present in the library. The repertoire at some positions is also further limited in order to accommodate restriction sites and avoid stop codons. A fixed cysteine in the middle of the library can form disulfide bridges with further cysteines which may be occur with intermediate frequency at positions convenient for

forming loops. It was considered that fascillitating the formation of such secondary structures would stabilise the peptide structure increasing the likelihood of forming stronger ligands.

Three type IIs restriction sites are integrated in the library peptide sequence: This results in a structure having four cassettes, allowing recombination of the peptide coding region with the cosmix-plexing method (see 1.2.4). The theoretical complexity of the whole library is 1.6 x 10^{25} variants but the highest complexity within a single cassette is 5.5 x 10^{7} variants having a 3-fold coverage in the actual library which comprises approximately 1.8 x 10^{8} independent clones (Pollmann, 2010).

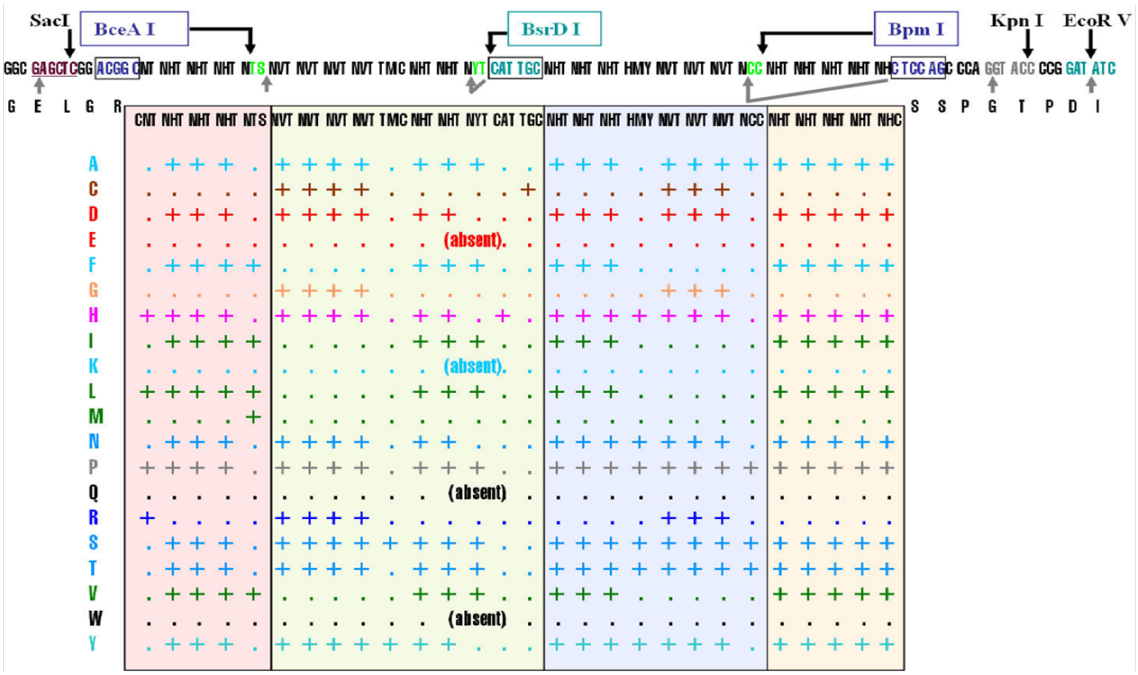

Figure 1-16: CPL19YS-2 library sequence and amino acid availability.The four cassettes of the library are indicated by coloured boxes. ´+´ and ´.´ indicate availability or absence of an amino acid at that position. Glutamic acid, lysine, glutamine and tryptophan are absent in the library (from Pollmann, 2010).

1.3 Peptides as therapeutics

Short chains of amino acids are called peptides, but the transition from peptides to small proteins is fluent and in general polypeptide chains of less than 50 aa are termed peptides. Despite their short length peptides are able to form stable structures, e.g. cyclic, ß-sheet or α-helical structures. (Lien and Lowman, 2003; Sato *et al.*, 2006). Various short peptides have been shown to be structured in solution, e.g. the 18 aa long RTD-1 defensin peptide (Trabi *et al.*, 2001) or the 20 aa long IgE receptor antagonist peptides (Nakamura *et al.*, 2002).

Peptide and protein interactions are essential for biochemical functions of life. They play an important role in modulating all biological processes and are therefore of great interest for the development of new therapeutic products. Over the last decades peptide drugs have become an important field for drug development with about 131 peptides in clinical development and 54 therapeutic peptides on the market (Reichert *et al.*, 2010). Biologics accounted for 25% of FDA approved drugs in 2010 reflecting the increasing importance of this drug class (Mullard, 2011). One prominent peptide drug that showed the potential of therapeutic peptides is enfuvirtide (Roche). The peptide is a 36mer consisting of natural amino acids with an acetylated N-terminus. Enfuvirtide blocks HIV cell entry,

has a high efficacy and a relative long serum half-life (Kazmierski *et al*., 2006). The development of this drug was a breakthrough for peptides as important pharmaceuticals and was accompanied by enormous efforts to dramatically reduce the cost of peptide synthesis and purification (Buchholz and Collins, 2011). Main sources for peptide leads are natural bioactive peptides and combinatorial peptide libraries, e.g. chemical libraries and phage display libraries (Lien and Lowman, 2003; Kay *et al.*, 1998).

The majority of drug targets for small molecules are enzymes, receptors and ion channels that offer substrate binding pockets able to interact with small compounds. The “druggable genome study", was an attempt to indentify all proteins belonging to families whereof one member was already targeted by a drug, assuming that all members of a family are good drug targets. The study revealed for the human genome a much smaller number of possible targets than originally thought (Hopkins and Groom, 2002). Many proteins involved in disease processes are not 'druggable' because of the lack of suitable ('addressable') binding pockets. Peptides in contrast can have a larger surface area that is involved in binding and a synergistic binding effect of many interactions at various sites on the target protein. Therefore peptides and protein therapeutics have the potential to extend the number of ‘druggable’ targets (Groner, 2009). Peptides have other advantages over small molecules, e.g. high activity, target specificity, low side-effects and lower potential toxicity since their natural degradation in the body produces no toxic substances. However, peptides can also have some important drawbacks such as degradation in the stomach preventing oral delivery without extensive confectioning, low *in vivo* stability, short serum half-life, risk of immunogenic effects and inefficient cellular uptake (Sato *et al.*, 2006). These drawbacks hamper the development of peptide therapeutics and have been addressed in the past years. Alternatively if these issues cannot be resolved the peptides can still serve as lead structures for the development of peptide mimetics (Sillerud and Larson, 2005).

1.3.1 Application and stability of peptide therapeutics

Peptides have a low oral bioavailability because they are degraded by proteolytic enzymes and they cannot cross the membrane of the intestinal tract. Peptide therapeutics are mostly administered by injection or infusion which has a low patient compliance. Therefore non invasive application methods are needed. Novel application methods that are in development are intranasal delivery, pulmonary delivery, buccal administration, transdermal delivery and even enhanced oral delivery. The most promising alternatives are the intranasal and pulmonary delivery with a bioavailability of up to 80%, although it should be noted that the variability in uptake from one patient to another has been a major barrier in quantifying delivery and a barrier in getting clinical approval. To increase the bioavailability several formulation approaches, like absorption enhancer, nanoparticles or liposomes have been studied to improve the absorption (Mao *et al.*, 2009). Although non invasive delivery methods are promising, injection devices have become more user-friendly improving the compliance of patients (Nielsen and Jorgensen, 2009).

For all delivery methods the *in vivo* stability of peptides should be improved to reduce the number of medications necessary. Peptides have normally a short serum half-life time of minutes to hours. To avoid fast clearance modifications, including conjugation with polymers, N- and C-terminal modifications and incorporation of unnatural aminoacids, can be used. For protein stabilisation by the addition of hydrophilic polymers conjugation with polyethylene glycol (PEG) has been used

preferentially, even though hydroxyethyl starch (HESylation) has a long history of acceptance in the clinic and is presently a major development program at Fresenius Kabi (Buchholz and Collins, 2011). PEG residues are attached to the peptides at the ends or within the peptide. The PEG-conjugates have a higher molecular weight, better water solubility and are partially protected from degradation by proteases. However, the modification of the peptide can lead to a loss of function. Acetylation and glycosylation of the N-terminus and amidation of the C-terminus prevents degradation of the peptides by proteases and improves the serum half-life time. The incorporation of D-amino acids or other unnatural amino acids can also prevent proteolytic degradation of the peptides. The decrease of degradation of the peptides can reduce the possible immunogenicity of the peptides by limited MHC presentation of the epitopes (Lien and Lowman, 2003; Sato *et al.*, 2006). A recent approach to increase the bioavailability of peptides is the stabilisation of the peptide structure. Bird and co-workers showed that a hydrocarbon crosslink within an α-helical peptide stabilised the structure and led to protease resistance and increased cellular uptake of the peptide (Bird *et al.*, 2010).

1.3.2 Intracellular delivery of peptides

Peptide drugs that target intracellular proteins have to cross the plasma membrane. Because of the highly selective permeability of cell membranes to macromolecules, methods for cell delivery of peptides and proteins have been developed.

Cell penetrating peptides (CPP) are short peptides that can cross cellular membranes and thereby deliver a cargo into cells (Schwarze *et al.*, 2000). CPPs can be classified as cationic or amphipathic peptides. Cationic CPPs, for example the HIV-Tat peptide (Green and Loewenstein, 1988) and the Antennapedia peptide (Joliot *et al.*, 1991), contain segments of positive charged amino acids, whereas amphipathic CPPs contain a balanced number of hydrophilic and hydrophobic amino acids and form an α-helical structure. Although many CPPs are derived from transduction domains of natural proteins artificial CPPs have also been developed (Pooga *et al*, 1998; Morris *et al*, 2001) so that the number of different cell penetrating peptides is constantly increasing. They have been used for the delivery of various cargoes into cells *in vitro* and *in vivo*: peptides, proteins, small molecules and nucleic acids (Heitz *et al*, 2009). For cytoplasmic delivery the first step of CPP internalisation involves interaction with the extracellular matrix. Most CPPs interact with proteoglycans which act as receptors for the initial contact (Pujals *et al.*, 2006). For internalisation direct translocation across the plasma membrane, clathrin and caveolin mediated endocytosis and macropinocytosis have been proposed. It has been suggested that endocytosis and macropinocytosis are the most important pathways for internalisation, but different uptake mechanisms may be exploited in parallel. Internalisation and cellular localisation of CPPs also depends strongly on the delivered cargo, the concentration of the CPP and the used cell type (Richard *et al.*, 2005; Duchardt *et al*., 2007; Patel *et al.*, 2007; Van den Berg and Dowdy, 2011). Intracellular uptake by endocytosis and macropinocytosis requires escape from the endosomal vesicles into the cytoplasm. The mechanism of endosomal escape of CPPs is still not clear, but acidification of early endosomes and retrograde transport is thought to be critical (Fischer *et al.*, 2003; Potocky *et al.*, 2003). The endosomal escape is the rate limiting step of intracellular delivery because only a fraction of the CPP is able to escape from the endosmal vesicles and the remaining peptide will be degraded in the lysosomes (Heitz *et al.*, 2009; Patel *et al.*, 2007).

An alternative method for intracellular delivery of biopharmaceuticals is the use of nanoparticles. Nanoparticles are vesicles with a membrane like structure in which the cargo is encapsulated. Different nanoparticle vectors are in development, for example liposomes, artificial phospholipid vesicles, and polymer nanovesicles. The encapsulation into nanovesicles prevents degradation of the cargo and immune response against the cargo (Torchilin and Lukyanov, 2003). Cellular uptake of nanoparticles is mediated via endocytosis and can be enhanced by modification of the surface, as has been shown for attachment of CPPs to the particle surface (Torchilin, 2008). A limiting factor for the cytosolic delivery can be the low endosomal escape of nanovesicles and CPPs and a resulting degradation of the cargo in the lysosomes (Duchardt *et al*., 2007). To overcome the endosomal entrapment various techniques are in development. One interesting method is the use of pH sensitive polymersomes. Polymersomes are nanoparticles that consist of a pH-sensitive copolymer which self assembles and forms vesicles in nanometer size at a pH higher than 6.5. They have been used to deliver nucleic acids and antibodies and are internalised by cells via endocytosis. Acidification of the early endosomes leads to disaggregation of the polymersomes. Because of the abrupt local change in osmotic pressure caused by this, pores are formed in the endosomal membrane and the cargo is released into the cytosol (Massignani *et al.*, 2009; Massignani *et al.*, 2010).

The lack of tissue specificity reduces the efficacy of intracellular delivery methods or applied biopharmaceuticals in general (Torchilin and Lukyanov, 2003). Cell type specific delivery can be achieved by the use of coupled targeting ligands. As targeting ligands peptides, antibodies or small molecules can be used, which bind to receptors or surface structures that are specific for cell types or tissues (Vasievich and Huang, 2009). For the targeting of hepatocytes coupling of galactosamine or coupling with hepatocyte specific peptides to delivery vectors has been described (Seymour *et al.*, 2002; Gripon *et al.*, 2004; Wakefield, 2005).

1.4 Aim of the project

The aim of this work was the development of inhibitory peptides against the NS2-3 and NS3/4A proteases of the Hepatitis C Virus as leads for drugs for HCV treatment. These proteases are essential for the viral life cycle and therefore the NS2-3 and NS3/4A proteases are interesting targets for the development of new specific antiviral drugs against HCV. Nonetheless, the proteases are difficult drug targets, e.g. the NS3/4A protease has a shallow and solvent exposed binding pocket which makes it difficult to develop small molecule drugs (Kim *et al.*, 1996). A combinatorial phage display peptide library displaying large peptides should be used for iterative affinity enrichment on immobilised HCV protease. Larger peptides have the potential for additive binding interactions at different sites of the protease. The inhibitory effect of the enriched peptides should be characterised and optimised and various methods for cell delivery should be tested.

Specific aims of this work were:

- Production and purification of recombinant proteases NS2-3 and NS3/4A in an active form
- Affinity selection on immobilised HCV proteases with the combinatorial phage display peptide library CPL19YS-2
- Characterisation of enriched peptides and backcrossing recombination of inhibitory peptides to yield variants with increased affinity
- Cell delivery of inhibitory peptides for inhibition of viral replication in a cell culture model

2. Materials and Methods

2.1 Materials

2.1.1 Chemicals

Unless stated otherwise, all used chemicals were commercially available and of analytical grade.

2.1.2 Buffers and solutions

All aqueous solutions were prepared with double deionised water (Millipore, Milli Q ultra-pure). If needed the solutions were sterilised by autoclaving or filtration.

2.1.2.1 Buffers

name	formulation
Buffer A	50 mM TrisHCl (pH 8), 300 mM NaCl, 10 % (v/v) glycerol, 0.05 % Tween 20, 5 mM ß-mercaptoethanol
Buffer D	50 mM TrisHCl (pH 7.5), 300 mM NaCl, 20 % (v/v) glycerol, 0.05 % Tween 20, 5mM DTT
Buffer H	50 mM HEPES (pH7.5)
Buffer M2235	50 mM HEPES (pH 7.8), 100 mM NaCl, 20% glycerol, 5 mM DTT, 0.6 mM LDAO
Buffer (P)	50 mM TrisHCl (pH 7.5), 150 mM NaCl, 10 % (v/v) glycerol, 0.05 % Tween 20
Buffer P	Buffer (P) with 5mM DTT
Cleavage buffer 1 (NS2-3)	50 mM TrisHCl (pH 7.5), 50% glycerol, 1% tritonX, 250 mM NaCl, 50 µM $ZnCl_2$, 3 mM DTT, 3mM cysteine
Cleavage buffer 2 (NS2-3)	50 mM TrisHCl (pH 7.5), 50% glycerol, 1% CHAPS, 250 mM NaCl, 50 µM $ZnCl_2$, 3 mM DTT, 3mM cysteine
Cleavage buffer 3 (NS2-3)	50 mM TrisHCl (pH 7.5), 30% glycerol, 0.2% CHAPS, 50 µM $ZnCl_2$, 3 mM DTT
Elution buffer; pH 2.2	0.1 M glycin in dH_2O
Laemmli sample buffer (6x)	10 % (w/v) SDS; 50 % (v/v) glycerol; 0.02 % (w/v) bromphenolblue; 15 % (v/v) ß-mercaptoethanol in dH_2O
SDS running buffer(10x); pH 8.3	0.25 M Tris; 2 M glycin; 1 % (w/v) SDS in dH_2O
Lysis buffer lysozym	50 mM TrisHCl (pH 8), 0.1% Triton X100; 50 µg/ml DNAseI; 1 mg/ml lysozyme; 500 mM NaCl; 5 mM ß-mercaptoethanol; 5 mM imidazole; 10% glycerol
Lysis buffer homogeniser	50 mM TrisHCl (pH 8), 500 mM NaCl, 5 mM imidazole, 5 mM ß-mercaptoethanol, 0.2% LDAO, 10% glycerol; 25µg/ml DNAseI
Lysis buffer Inclusion Bodies	25 mM Tris-HCl (pH 8.0), 6 M guanidine hydrochloride, 500 mM NaCl
Dialysis Buffer NS2-3	50 mM Tris (pH 7.5), 50 µM ZnCl2, 3 mM DTT, 750 mM guanidine hydrochloride
MPBST	0.05 % (v/v) Tween 20, 2 % milkpowder in PBS
Na-Phosphat buffer (pH 8.1)	0.5 M: 21.15 % (v/v) NaH_2PO_4-solution (1M in water); 28.85 % (v/v) Na_2HPO_4-solution (1M in water)
Neutralisation buffer	2.0 M Tris in dH_2O
PBS (10x)	2.0 g/L KCl; 2.0 g/L KH_2PO_4; 80.0 g/L NaCl; 11.50 g/L Na_2HPO_4 in dH_2O
PBST	0.05 % (v/v) Tween 20 in PBS

name	formulation
Profinia native IMAC Buffers	50 mM TrisHCl (pH 8.0), 500 mM NaCl, 5 mM Imidazol, 5 mM ß-mercaptoethanol, 0.1 % LDAO, 10% glycerol Wash buffer 1: 5 mM imidazole Wash buffer 2: 10 mM imidazole Elution buffer: 250 mM imidazole
Profinia Desalting Buffer 1	50 mM TrisHCl (pH 8.0), 500 mM NaCl, 5 mM imidazol, 5 mM ß-mercaptoethanol, 0.1 % LDAO, 10% glycerol
Profinia Desalting Buffer 2	50 mM Na-acetate (pH6.3), 500 mM NaCl, 5 mM DTT, 0.6mM LDAO, 10% glycerol
TAE (50x); pH 8.5	2 M Tris; 1 M acetic acid; 50 mM Na_2EDTA
Tricine page sample buffer (4x)	6% (w/v) SDS, 30 % (v/v) glycerol; 0.05 % (w/v) coomassie blue G-250; 6 % (v/v) ß-mercaptoethanol, 150 mM Tris HCl (pH 7.0)
Tricine page anode buffer (10x)	1 M TrisHCl (pH 8.9)
Tricine page cathode buffer (10x)	1 M Tris pH (8.25), 1 M tricine, 1% (w/v) SDS
Tricine page fixing solution	50% methanol, 10% acetic acid, 100 mM ammonium acetate
Tricine page gel buffer (3x)	3 M Tris pH (8.45), 0.3% (w/v) SDS
Blotting buffer	6 g/L Tris, 2.9 g/L glycine, 0.037 % (v/v) SDS, 20% methanol

2.1.2.2 Solutions

name	formulation
Acrylamidmix 29:1 (Roth)	30% (w/v) acrylamide, 0,8% (w/v) bisacrylamide
APS	10% (w/v) ammonium persulfate in dH_2O
ABTS substrate solution	4.62 mg ABTS; 21 ml 0.05 M citric acid pH 4.0; 36 µl 30 % H_2O_2
Coomassie discolouration solution	20 % ethanol; 10 % acetic acid
Coomassie staining solution	1 tablet PhastGel BlueR (Pharmacia) in 80 ml dH_2O; 120 ml methanol; before use add 200 ml acetic acid (20 %)
DAB substrate solution	1 mg/ml DAB (3,3'-Diaminobenzidine), 0.07% imidazole, 0.02% $CoCl_2$, 0.01% H_2O_2, 0.1M phosphate buffer (pH 7.3)
Ethidium bromide	50 mg ethidium bromide in 10 ml dH_2O
Loading Dye (6x)	4 g sucrose; 25 mg bromphenolblue; add 10 ml dH_2O
PEG/NaCl	2.5 M NaCl; 20 % PEG 6000 in dH_2O

2.1.3 Kits

name	commercially available
NucleoSpin Extract II (NS II)	Macherey-Nagel, Düren
PureYield Plasmid Miniprep System	Promega, Madison, USA
Qiagen Plasmid Maxi Kit	Quiagen, Venlo, Netherlands
QIAprep Spin Miniprep Kit	Quiagen, Venlo, Netherlands
Roti-Black P silver staining kit	Carl Roth, Karlsruhe

2.1.4 Media and supplements

Media	
2 x YT medium	16 g/L tryptone, 10 g/L yeast extract, 5 g/L NaCl optional: 2 % (w/v) agar
TB medium	12g/L tryptone, 24g/L yeast extract, 0.4% (v/v) glycerol, 17 mM KH_2PO_4, 72 mM K_2HPO_4
SOC medium	20 g/L tryptone, 5 g/L yeast extract, 5 g/L NaCl, pH 7.0, 20 mM Mg^{2+} solution, 20 mM glucose
M9-medium	100 ml/l M9-salt solution (10x), 12.5 ml glucose 40 % (w/v), 100 µl CaCl (1 M), 1 ml/l $MgSO_4$, 100 µl/l thiamine, 100 µg/ml leucine, isoleucine, valine
M9-salt solution (10x)	74.1 g/L Na_2HPO_4 * H_2O, 30 g/L KH_2PO_4, 5 g/L NaCl, 10 g/L NH_4Cl

Antibiotics	
Ampicillin	Stock-solution: 50 mg/ml in dH_2O Final concentration: 100 µg/ml
Kanamycin	Stock-solution: 50 mg/ml in dH_2O Final concentration: 30 µg/ml
Tetracyclin	Stock-solution: 6 mg/ml in 70% Ethanol Final concentration: 6 µg/ml
Chloramphenicol	Stock-solution: 34 mg/ml in 100% Ethanol Final concentration: 34 µg/ml

2.1.5 Bacterial strains and bacteriophage

strain	genotype	commercially available
E. coli TOP 10 F`	F´[lacI^q Tn10 (TetR)] mcrA Δ(mrr-hsdRMS-mcrBC) ϕ80 lacZ$_{ΔM15}$ ΔlacX74 recA1 deoR araD139 Δ(ara-leu)7697 galU galK rpsL (Str^R) end A1 nupG	Invitrogen, Carlsbad, USA
E. coli TOP 10 F` λ$^+$	λ lysogen Top10F' strain	Prof. John Collins, Technical University Braunschweig, Germany
E. coli XL1-blue MRF`	F´ [lacI^{q}Z$_{ΔM15}$ Tn10 (TetR) proAB] Δ (mcrA)183 Δ(mrr-hsdRMS-mcrBC)173 endA1 supE44 thi-1 recA1 gyrA96 relA1 lac	Stratagene Santa Clara, USA
Rosetta 2 (DE3)	F$^-$ *ompT hsdS*$_B$(r$_B^-$ m$_B^-$) *gal dcm* (DE3) pRARE2 (Cam^R)	Merck, Darmstadt
M13K07 Helperphage	mutation Met40Ile in gII; origin of replication from P15A; Kmr from Tn903	NEB, Ipswich, USA

2.1.6 Plasmids

name	description / availability
pEPO8-CPL19YS-2 library phagemid vector	constructed by Dr. Erik Pollmann, kindly provided by HZI, Braunschweig, Germany
pMALc4E plasmid	NEB, Ipswich, USA
pET28c	Novagen (Merck, Darmstadt)
HCV replicon I389/NS2-3'UTR (AJ242653)	kindly provided by Ralf Bartenschlager, University Heidelberg, Germany
HCV replicon I389/NS3-3'UTR (AJ242654)	kindly provided by Ralf Bartenschlager, University Heidelberg, Germany
HCV replicon I341 PiLuc/3-3'/ET (Lohmann *et al*., 2003)	kindly provided by Ralf Bartenschlager, University Heidelberg, Germany

2.1.7 Antibodies, proteins and enzymes

name	description	commercially available
Anti-g3p (pIII) antibody	monoclonal murine IgG; clone 10C3	MoBiTec, Göttingen
Anti-mouse IgG, HRP linked	horse anti-mouse IgG antibody	Cell Signaling, Boston, USA
Anti-MBP antibody	monoclonal murine IgG, isotype IgG2a	NEB, Ipswich, USA
Anti-poly Histidine antibody, HRP linked	monoclonal murine IgG; clone His-1	Sigma-Aldrich, St. Louis, USA
Anti-M13 IgG, HRP linked	monoclonal murine anti-M13 (pVIII) IgG	GE Healthcare, UK
MBP4*	Maltose binding protein with the polylinker encoded by the pMAL-c4E vector	NEB, Ipswich, USA
T4 DNA ligase		NEB, Ipswich, USA
T4 polynucleotide kinase		NEB, Ipswich, USA
T4 DNA polymerase		NEB, Ipswich, USA
Antarctic phosphatase		NEB, Ipswich, USA
Phusion DNA Polymerase		Finnzymes, Vantaa, Finland
Restriction endonucleases		NEB / MBI Fermentas
Neutrophil elastase		MD Biosciences, St. Paul, USA
Trypsin, chymotrypsin		Carl Roth, Karlsruhe
DNAseI		Sigma-Aldrich, St. Louis, USA

2.1.8 Oligonucleotides

name	sequence (5´ – 3´)
malE1	GCCGACATCATAACGGTTCTGGCA
malE2	TGCAAGAACCGTACTTCACCTGGC
malE2-rev	GCCAGGTGAAGTACGGTTCTTGCA
malE3	GGTCGTCAGACTGTCGATGAAGCC
malE3-rev	GGCTTCATCGACAGTCTGACGACC
malE4-rev	CGCCAGGGTTTTCCCAGTCACGAC
primNS3-4A	TTTTGGTACCGGGCTCAGTAGTAATCGTAGGCAGAATCATCCTGTCCGGCAAAGGTGGCCCT ATTACGGCCTACTCCCAAC
primNS3-4A-rev	GCCGGACTGCAGTTTAGTGATGGTGATGGTGATGGGAGCCCCGCATAGTGGTTTCCATAGA
primNS2-3	GTCGGGTACCGACCAAAGTGCCGTACTTCGTG
primNS2-3-rev	TTTACTGCAGTTTAGTGATGGTGATGGTGATGGGAGCCCCGCATAGTGGTTTCCATAGA
primNS3-4A-pET	GCCGGACTCGAGTTTAGTGATGGTGATGGTGATGGGAGCCCCGCATAGTGGTTTCCATAGA
primNS3-4A-pET-rev	ATTTTCCATGGGTTCTGTTGTAATTGTAGGTAGAATCATTCTGTCCGGTAAAGGTGGCCCTAT TACGGCCTACTCCCAAC
Pep-pMAL uni 5`	GGCGAGCTCGGA
Pep-pMAL uni 3`	CGTCCTGCAGTTAGTGATGGTGATGGTGATGGGAGCCACCTGGGCTGGAG
FSQJCO	TTCTACAACTTGCTTGGATT
RSQJCO	TCCAGACGTTAGTAAATGAA
Ant-pET 5`	CATGCGCCAGATTAAAATTTGGTTTCAGAACCGCCGCATGAAATGGAAAAAATC
Ant-pET 3`	CATGGATTTTTTCCATTTCATGCGGCGGTTCTGAAACCAAATTTTAATCTGGCG
Pep-pET uni 5`	TCTTAACCATGGGCGAGCTCGGA
Pep-pET uni 3`	AGAATTCTCGAGACCTGGGCTGGAG
T7	TAATACGACTCACTATAGGG
T7-term	TATGCTAGTTATTGCTCAG
primCP5-46-4D5E 5`	GGCGAGCTCGATGAGCTTGTTTATCTTTTGG
mutA156V 5`	CATCTTTCGGGTTGCCGTGTGC
mutA156V 3`	GCACACGGCAACCCGAAAGATG

2.1.9 Peptides

All peptides were synthesised by Dr. Werner Tegge or Dr. Raimo Franke (Department of Chemical Biology, Helmholtz Centre for Infection Research, Braunschweig, Germany).

name	sequence (N- to- C-terminus)
K5-66-A	GELGRLVYLLDGPGYDPI-amid
K5-66-B	Ac-HCSLAYGDASTLVVF-amid
K6-10-A	GELGRPVYVLGDPGYYAT-amid
K6-10-B	Ac-HCIYATTNDALIFSV
K5-66-R	GELGRIPSDTYDLAVGALHCPFYLVSGLVYLDG-amid
CP5-46-A	GELGRLVYLLDGPGYDPIHCD-amid
CP5-46-P1	Ac-RLVYLLDGPGYDPI-amid
CP5-46-P3	Ac-DGPGYDPIHCD-amid
CP5-46-P4	Ac-DGPGYDPIHCDVVTRGGS-amid
CP5-46-R	GELGRDIGGPLDLYPVDLHCY-amid
CP5-46	GELGRLVYLLDGPGYDPIHCDVVTRGGSHLFNF-amid
CP5-46-A-4D4E	GELDELVYLLDGPGYDPIHS-amid
CP5-46-A-6D	GELGRDVYLLDGPGYDPIHS-amid
CP5-46-A-6E	GELGREVYLLDGPGYDPIHS-amid
CP5-46-A-6Q	GELGRQVYLLDGPGYDPIHS-amid
CP5-46-A-10Q	GELGRLVYLQDGPGYDPIHS-amid
CP5-46-A-10E	GELGRLVYLEDGPGYDPIHS-amid
Ant-K5-66-A	RQIKIWFQNRRMKWKKGELGRLVYLLDGPGYDPI
Tat-K5-66-A	GRKKRRQRRRPPQGELGRLVYLLDGPGYDPI
Nona-arg-K5-66-A	RRRRRRRRRGELGRLVYLLDGPGYDPI
PTD-5-K5-66-A	RRQRRTSKLMKRGELGRLVYLLDGPGYDPI
Ant-CP5-46	RQIKIWFQNRRMKWKKGELGRLVYLLDGPGYDPIHCDVVTRGGSHLFNF
Ant-CP6-4	RQIKIWFQNRRMKWKKGELGRLVYLLDGPGYDPIHCFPIYSRGSYASYV
CPP-Control 1	RLIFAGKQLEDGRGELGRVYLLDGPGYDPI
CPP-Control 2	RQIKIWFQNRRMKWKKYVGIPRDLGLDGYEPLG

2.1.10 DNA and protein ladders

name	company
GeneRuler™ 1kb Plus DNA Ladder	MBI Fermentas, St. Leon-Rot
GeneRuler™ 1kb DNA Ladder	MBI Fermentas, St. Leon-Rot
GeneRuler™ 100bp Plus DNA Ladder	MBI Fermentas, St. Leon-Rot
PageRuler™ Plus Prestained Protein Ladder	MBI Fermentas, St. Leon-Rot
PageRuler™ Low Range Protein Ladder	MBI Fermentas, St. Leon-Rot

2.1.11 Computer software

program	description
ImageJ 1.37	Densitometric analysis http://rsb.info.nih.gov/ij
VectorNTI 11	DNA analysis, primer design Invitrogen, Carlsbad, USA
BioEdit 7.0.9.0	Sequence alignment and editing Ibis Therapeutics, USA
Photoshop CS5	Densitometric analysis and image editing Adobe Systems, San Jose, USA

program	description
PyMol 1.3	Structure visualisation and rendering (DeLano, 2002)
Coot	Building, refining and analysing of structure models (Emsley and Cowtan, 2004)
Gimp 2	Image editing http://www.gimp.org/
Graph Pad Prism	Graphing, nonlinear regression and statistics GraphPad Software, San Diego, USA

2.1.12 Equipment

type	apparatus	manufacturer
Microplate Reader	Tecan Sunrise	Tecan, Crailsheim
	Synergy 2 Multi-Mode	Biotek, Vermont, USA
Spectrophotometer	Genesys 10 uv scanner	Thermo ElectronCorporation, Langenselbold
	ND1000 NanoDrop	Peqlab, Erlangen
Centrifuges	Sorvall RC-5B	Thermo Scientific, Waltham, USA
	Mikro 200	Hettich Zentrifugen, Tuttlingen
	Biofuge primo R	Heraeus, Hanau
Gel documentation	Gel Jet Imager	Intas, Göttingen
Overhead shaker	Rotator SB2	Stuart, Stone, UK
Platform shaker	Duomax 1030	Heidolph, Schwabach
Thermocycler	Primus Evolution 96	Clemens GmbH, Waldbüttelbrunn
Balances	Precisa 120A	PAG Oerlikon AG, Zurich, Switzerland
	Kern 440-43N	Kern & Sohn GmbH, Balingen
Concentrator	miVac DUO concentrator	Genevac, Ipswich, England.
Laminar flow hood	Lamin Air HBB 2472S	Heraeus, Hanau
Water purification unit	Milli-Quf Plus	Millipore, Schwalbach
Thermal shakers	Thermomixer comfort 5355	Eppendorf, Hamburg
Electrophoresis apparatus	Horizon 58	Whatman, Dassel
	Miniprotean 3 cell	Bio-Rad, Munich
Pipettes	Research 10 µL	Eppendorf, Hamburg
	Research 100 µL	Eppendorf, Hamburg
	Research 1000 µL	Eppendorf, Hamburg
	Research pro 8x 5-100 µL	Eppendorf, Hamburg
	Finnpipette 8x 50-300 µl	Thermo Scientific, Waltham, USA
Electrophoretic transfer cell	TransBlot semi-dry	Bio-Rad, Munich
Power supply	E835 Power Supply	Consort, Turnhout, Belgium
Incubator	BE-400	Memmert, Schwabach
	Innova 4400 / 4430 Incubator	New Brunswick Scientific, Edison, USA
	Shaker Type AG 15	Infors AG, Bottmingen, Switzerland
pH-meter	S20 SevenEasy	Mettler-Toledo GmbH, Giessen
Magnetic stirrer	RH digital KT/C IKAMAG	IKAWerke GmbH & Co. KG, Stauffen
Magnetic particle concentrator	Dynal MBC-5	Invitrogen, Karlsruhe
Electroporator	EasyjecT prima	EquiBio, Milford, USA
Protein Purification Instrument	Profinia	Bio-Rad, Munich
Automated dispenser	HoneyBee 961	Zinsser Analytic, Frankfurt
Homogeniser	TS Series Benchtop	Constant Systems Ltd, Daventry, UK

2.1.13 Disposals

type	manufacturer
Adhesive PCR film	Thermo Scientific, Waltham, USA
Amicon Ultra 0.5 ml Centrifugal Filters (3 kDa)	Millipore, Schwalbach
Amicon Ultra 4 ml Centrifugal Filters (3 kDa)	Millipore, Schwalbach
Amicon Ultra 4 ml Centrifugal Filters (10 kDa)	Millipore, Schwalbach
Amicon Ultra 15 ml Centrifugal Filters (10 kDa)	Millipore, Schwalbach
Amicon Ultrafree MC 0.5 ml filter	Millipore, Schwalbach
Amylose Beads	NEB, Ipswich, USA
Anti-MBP Beads	NEB, Ipswich, USA
Bio-Scale Mini Profinity IMAC Cartridge (1 ml / 5 ml)	Bio-Rad, Munich
Bio-Scale Mini Bio-Gel P-6 Desalting Cartridge (10 ml / 50 ml)	Bio-Rad, Munich
Blot paper Protean XL	Bio-Rad, Munich
Cellulose acetat syringe filter (0.22 µm and 0.45 µm)	GE Healthcare, Munich
Dialysis membrane VISKING, type 27/32 14 kDa	Carl Roth, Karlsruhe
EasyXtal 15-Well DG-Tool X-Seal plate	Quiagen, Venlo, Netherlands
Electroporation cuvette (2 mm)	Eurogentec, Belgium
High Performance Crystal Clear tape	Manco Inc, Avon, USA
His Select nickel affinity gel	Sigma-Aldrich, St. Louis, USA
Intelli-Plate 96-3 Crystallisation Plate	Art Robbinsons Instruments, USA
Maxisorp microtiter plates	Nunc, Rochester, USA
Microtiter plate, 96 well, polystyrene, flat bottom	Sarstedt, Nümbrecht
NeXtal 24-6 Well Crystallisation Plate (hanging drop)	Quiagen, Venlo, Netherlands
Nitrocellulose membrane	Carl Roth, Karlsruhe
Parafilm 'M'	Carl Roth, Karlsruhe
PCR plate 96-well (semi-skirted)	Thermo Scientific, Waltham, USA
PCR-sealing mat	Thermo Scientific, Waltham, USA
PCR reaction vial (Mµlti Ultra 0.2 ml)	Carl Roth, Karlsruhe
Petri dishes (145/20 and 120/17)	Greiner bio-one, Frickenhausen
Pipettor tips	Sarstedt, Nümbrecht
Profinia Native IMAC Buffer Kit	Bio-Rad, Munich
Reaction vials (1.5 ml and 2 ml)	Sarstedt, Nümbrecht
Reaction vials (15 ml and 50 ml)	Sarstedt, Nümbrecht
Screw Cap tubes	Sarstedt, Nümbrecht
µclear non-binding MTP 96 well (black)	Greiner bio-one, Frickenhausen

2.2 Methods

2.2.1 Microbiological methods

2.2.1.1 Cultivation of bacteria

E. coli cells were cultivated with either liquid 2xYT media with appropriate antibiotics or on 2xYT agar plates containing antibiotics. Incubation was done at 37°C, in case of liquid culture under shaking with 180 rpm.

2.2.1.2 Storage of bacteria

For long term storage of bacteria cultures, 0.8 ml of bacterial cells were mixed with 0.2 ml of sterile 87% glycerol, frozen in liquid nitrogen and stored at -80°C. For short term storage bacteria were stored on agar plates sealed with parafilm at 4°C for up to two weeks.

2.2.1.3 Preparation of electrocompetent cells

Desired cells were separated by plating on M9 media agar plates supplemented with needed antibiotics. A single colony was picked for inoculation of an overnight culture with 2xYT medium with appropriate antibiotics. 10 ml overnight culture was used for inoculation of 1 L 2xYT medium with antibiotics and cells were grown until OD_{600} 0.9. The culture was cooled for 15 min on ice and centrifuged for 15 min at 4°C and 4000 g. The supernatant was removed and the cell pellet was resuspended in 1 L precooled dH_2O and centrifuged for 15 min at 4°C and 4000 g. The cell pellet was washed again with 500 ml precooled dH_2O. After centrifugation the pellet was resuspended in 20 ml precooled 10% glycerol. After a last centrifugation step of 15 min, 4°C, 4000g cell the pellet was resuspended in 2 ml precooled 10% glycerol. 50 µl aliquots were frozen in liquid nitrogen and stored at -80°C.

2.2.1.4 Transformation of *E. coli* cells

The transformation of *E. coli* cells was done by electroporation. 50 µl electrocompetent cells were mixed with 1–5 µl of DNA in dH_2O and incubated for 1 min on ice. The suspension was pipetted into an ice-cooled 2 mm electroporation cuvette. Electroporation was done with an electric pulse of 2500 V for about 5 ms. After electroporation 1 ml of to 37°C prewarmed SOC medium was added to the cells immediately and transferred into a sterile 15 ml tube. Cells were incubated at 37°C and 160 rpm for 60 min. To determine the number of transformants dilutions were made and plated onto agar plates with appropriate antibiotics. For library preparation the cell suspension was plated onto large selective antibiotic agar plates.

2.2.1.5 Protein production in *E. coli*

2.2.1.5.1 Protein production with the pMAL expression system

For expression of MBP fusion proteins the pMAL expression system was used. The pMALc4E expression vector containing the protein insert was transformed into *E. coli* TOP 10F`cells. For a starter culture 2xYT medium containing ampicillin, tetracycline and 2 g/L glucose was inoculated from a glycerol stock and incubated over night at 37°C and 180 rpm. For later expression in minimal medium the M9 medium was used for the starter culture. The culture was used to inoculate 200 ml of the appropriate medium to an OD_{600} < 0.1 and incubated at 37°C and 180 rpm. For a soluble protein expression in 2xYT medium 0.4 mM IPTG were added at an OD_{600} of about 0.5 and the protein was expressed for 3 h at 30°C. For a protein production in 'inclusion bodies' 1 mM IPTG were added at an OD_{600} of about 1 and the protein was expressed for 5 h at 37°C . The cells were collected by centrifugation at 6000 rpm and 4°C for 20 min and the cell pellets were stored at -20°C for up to four weeks.

2.2.1.5.2 Protein production with the pET expression system

For expression of Antp-fusion proteins and high expression of NS3/4A protease the pET expression system was used. The pET28c expression vector containing the protein insert was transformed into *E. coli* Rosetta2 (DE3) cells. For a starter culture LB medium containing kanamycin, chloramphenicol and 2 g/L glucose was inoculated from a glycerol stock and incubated over night at 37°C and 180 rpm. For production of Antp-fusion peptides the starter culture was used to inoculate 200 ml of 2xYT medium to an OD_{600} < 0.1 and incubated at 37°C and 180 rpm. For Expression 1 mM IPTG were added at an OD_{600} of about 0.5 and the protein was expressed for 3 h at 37°C. For high expression of NS3/4A protease the starter culture was used to inoculate 4x 500 ml of TB medium in Fernbach flasks to an OD_{600} 0.1 and incubated at 37°C and 130 rpm for 3.5 h and at 18°C and 130 rpm for 2 h. After 5.5 h the OD_{600} was 5 – 8. The expression was induced by addition of 0.4 mM IPTG and the culture was incubated at 18°C for 22 h. The cells were collected by centrifugation at 6000 rpm and 4°C for 20 min and the cell pellets were stored at -20°C for up to four weeks.

2.2.2 Molecular biological methods

2.2.2.1 Isolation of plasmid DNA

For the isolation of plasmid DNA commercial kits were used. For small scale preparation (1 - 5 µg plasmid DNA) 'QIAprep Spin Miniprep' kit from Qiagen was used. For large scale preparations (> 50 µg plasmid DNA) the 'NucleoBond PC 500' kit from Macherey-Nagel was used. Isolation was performed according to manufacturer's instruction.

2.2.2.2 Determination of DNA concentration

DNA concentration was determent through separation on 1.0 % agarose gel and comparison with a DNA ladder. Several dilution steps of the sample were separated and stained with ethidium bromide along with a DNA ladder with predefined DNA amounts. The intensity of the sample band was compared to the intensity of the ladder band.

2.2.2.3 DNA agarose gel electrophoresis

DNA agarose gel electrophoresis was used for size dependent separation of DNA samples. The DNA was supplemented with loading dye (6x) to reach a final 1x concentration of dye. The DNA sample was applied to an agarose gel (1.0 % agarose dissolved in 1xTAE) and separated in an electric field (120 V, 20 - 40 min.). The gel was stained in ethidium bromide bath (10 mg/L; 15 min.). For removal of unbound ethidium bromide the gel was washed for 10 min in water. DNA bands were detected with a gel documentation system.

2.2.2.4 Restriction of DNA

DNA was cleaved with the aid of restriction enzymes. The enzymes recognise specific sequences and produce sticky or blunt ends. The following conditions were used for 50 µl samples:

Component	Volume	Final concentration
DNA sample	X µl	1 - 5 µg
Reaction buffer (10 x)	5 µl	1x
BSA (100x), if required	0.5 µl	1x
Restriction enzyme	Y µl (up to 5 µl)	10 - 20 U
dH_2O	44.5 µl - X µl - Y µl	

The sample was incubated (1.5 – 3 h) at the optimum temperature of the used enzyme and inactivated at 65 – 85°C for 20 min if possible. The DNA was purified using the 'NucleoSpin Extract II' kit.

2.2.2.5 Amplification of DNA

For amplification of DNA fragments the polymerase chain reaction (PCR) was used. DNA is denatured at high temperature and oligonucleotides, the primers, which are flanking the region that should be amplified, are binding to the template DNA. A DNA polymerase elongates the primers producing the amplified DNA. A qualitative PCR was used for the amplification of DNA regions for cloning. The colony –PCR was used for rapid identification of correct clones after cloning. The following conditions and temperature programs were used:

1. Qualitative PCR (50 µl)

Component	Volume	Final concentration
DNA template	X µl	20 – 100 ng
Phusion HF Buffer (10x)	5 µl	1x
Phusion DNA polymerase	0.5 µl	1 U
dNTP mix (each 10 mM)	1 µl	0.2 mM each
Primer 1 and 2 (10 µM)	2.5 µl	500 nM
dH_2O	33.5 µl - X µl	

Temperature program: 1. 98°C: 30 s
2. 98°C: 10 s, 3. X °C: 20 s, 4. 72°C: 10 s/kb (2. – 4. 25x)
5. 72°C: 5 min
(3. Annealing temperature X is primer dependent)

2. Colony-PCR (25 µl)

Component	Volume	Final concentration
Colony in 150µl water	19.5 µl	
Phusion HF Buffer (10x)	2.5 µl	1x
Phusion DNA polymerase	0.25 µl	1 U
dNTP mix (each 10 mM)	0.5 µl	0.2 mM each
Primer 1 and 2 (10 µM)	0.5 µl	200 nM each
DMSO	1.25 µl	5%

Temperature program: 1. 98°C: 2 min
2. 98°C: 10 s, 3. X °C: 20 s, 4. 72°C: 10 s/kb (2. – 4. 25x)
5. 72°C: 5 min
(3. Annealing temperature X is primer dependent)

2.2.2.6 Cosmix-plexing

Cosmix-plexing is a technique to increase diversity through DNA recombination and can be used to further increase the diversity of a peptide library. Restriction enzyme sites located at defined positions allow shuffling of DNA cassettes. Cosmix-plexing was used for recombination of the peptide library CPL19YS-2. In the first restriction reaction 5 µg of the library phagemid DNA is cleaved at a type IIs restriction enzyme site located inside the library peptide. The restriction sites of the enzymes BceAI, BsrDI and BpmI can be used. After the first cleavage the DNA is ligated with the Quick Ligation Kit at a concentration of about 2 µg/µl to form concatemers. The ligase is inactivated for 20 min at 65°C and the DNA is diluted 1:8 with water and the concatemers are cleaved with the restriction enzyme BglI at a site located outside of the library sequence. After the second restriction the phagemid DNA is ligated at a concentration < 20 ng/µl to favor intramolecular ligation. The ligated DNA can be used for transformation.

2.2.2.7 Site directed mutagenesis

For the integration of point mutations into plasmids site directed mutagenesis was used. Two complementary oligonucleotides that contain the point mutation in the middle of the DNA sequence were used for the linear amplification of the plasmid and thereby integrating the mutation in the amplified linear vector. The following conditions were used for 50 µl samples:

Component	Volume	Final concentration
DNA vector template	X µl	~25 ng
Phusion HF Buffer (10x)	5 µl	1x
Phusion DNA polymerase	0.5 µl	1 U
dNTP mix (each 10 mM)	1 µl	0.2 mM each
Primer 1 and 2 (10 µM)	2.5 µl	500 nM each
dH_2O	41 µl - X µl	

Temperature program: 1. 98°C: 30 s
2. 98°C: 10 s, 3. 60°C: 30 s, 4. 72°C: 3 min and 40 s (2. – 4. 18x)
5. 72°C: 5 min

The methylated template vector was digested by DpnI, a restriction enzyme that recognises a methylated recognition sequence. 20 U DpnI were directly added to the amplified DNA and incubated for 2 h at 37°C. The restriction enzyme was inactivated at 80°C for 20 min and the DNA was purified using the 'NucleoSpin Extract II' kit.

2.2.2.8 Creating blunt ends

For the removal of 3´ overhanging DNA the T4 DNA polymerase was used to form blunt ends. The 3´ overhang is removed by the 3´→ 5´ exonuclease activity of the polymerase. The following conditions were used for 50 µl samples:

Component	Volume	Final concentration
DNA sample	X µl	1 - 2 µg
NEBuffer 1 (10 x)	5 µl	1x
T4 DNA Polymerase	0.5 µl	10 U
dH_2O	44.5 µl - X µl	

The sample was incubated for 15 min at 12°C and the polymerase was inactivated at 75°C for 20 min. The DNA was purified using the 'NucleoSpin Extract II' kit.

2.2.2.9 Dephosporylation of DNA

To avoid religation of DNA fragments the 5´ phosphate groups from DNA was removed with the help of the Antarctic phosphatase (AP). The DNA was incubated with 5 U of AP for 1 hr at 37°C in 1x AP reaction buffer. The phosphatase was inactivated at 65°C for 20 min and the sample was purified using the 'NucleoSpin Extract II' kit.

2.2.2.10 Phosporylation of DNA

For the ligation of DNA fragments 5´ phosphate groups are necessary. The transfer of a phosphate from ATP to the 5' end of DNA is catalysed by the polynucleotide kinase (PNK). For the phosphorylation up to 10 µM DNA in a 50 µl reaction containing 1x T4 DNA ligase buffer and 10 units of T4 polynucleotide kinase were mixed and the sample was incubated at 37°C for 60 min. The enzyme was inactivated at 65°C for 20 min.

2.2.2.11 Hybridisation of oligonucleotides

For the hybridisation of complementary DNA the single stranded oligonucleotides were mixed at a concentration of 2 µM. The sample was heated for 10 min to 98°C and cooled down to room temperature.

2.2.2.12 DNA ligation

The ligation of linear DNA fragments was done with the T4 DNA ligase or with the help of the Quick Ligation Kit. The T4 ligase was used for liagtion of an insert into a vector. A vector DNA and insert DNA molar ratio of 1:3 was usually used. The Quick Ligation Kit was used for the ligation reactions during cosmix-plexing. The ligation time and temperature varied between 2 h at 16°C for the T4 DNA ligase and 16 h at 4°C for the Quick Ligation Kit. The following conditions were used for 20 µl samples:

1. T4 DNA Ligase

Component	Volume	Final concentration
Vector	X µl	50 -100 ng
Insert	Y µl	
T4 ligase buffer (10x)	2 µl	1x
T4 DNA ligase	1 µl	400 U
dH_2O	17 µl - X µl – Y µl	

2. Quick ligase

Component	Volume	Final concentration
DNA sample	X µl	< 400 ng
Quick Ligase Buffer (2x)	10 µl	1x
Quick Ligase	1 µl	
dH_2O	9 µl - X µl	

2.2.3 Phage-Display methods

2.2.3.1 Packaging of peptide phage display library

The peptide phage display library CPL19YS-2 was existent in *E. coli* Top 10 F` λ^+ cells. For packaging into phagemid particles an infection with M13K07 helper phage was necessary. 200 ml 2xYT medium containing tetracycline and ampicillin were inoculated from a glycerol stock to an OD_{600} of about 0.1. The culture was grown at 37°C and 180 rpm to an OD_{600} of 0.5 and the cells were infected with 2.5 x 10^{11} cfu of M13K07. The culture was incubated at 37°C for 30 min without agitation and was then grown over night at 37°C and 180 rpm. The culture was cooled on ice and centrifuged for 20 min at 8000 rpm and 4°C. The supernatant was decanted mixed with 0.2 volume of PEG/NaCl and incubated on ice for at least 2 h. The phage were precipitated by centrifugation for 60 min at 8000 rpm and 4°C. The supernatant was carefully decanted and remaining liquid removed. The pellet was resuspended in 1 ml of appropriate buffer and cleared by 10 min centrifugation at 13000 rpm at room temperature. NaN_3 was added to the phage solution to a final concentration of 0.02%. The phage titer was determined (see section 2.2.3.2).

2.2.3.2 Determination of phage titer

The phage titer was determined by infection of *E. coli* cells and subsequent cultivation on selective agar plates. For titer measurement 20 ml 2xYT medium containing tetracycline were inoculated from a *E. coli* Top 10 F` λ^+ overnight culture to an $OD_{600} < 0.1$ and incubated at 37°C and 180 rpm to an OD_{600} of about 0.5. The phage solution was used for a dilution series in PBS ($10^6 – 10^{12}$). 10 µl of each dilution were mixed with 50 µl *E. coli* culture and incubated at 37°C for 1 h. The infected culture was plated or spotted on an agar plate with appropriate antibiotic and incubated at 37°C over night. To calculate the phage titer the grown colonies (cfu) were counted and multiplied with the respective dilution factors.

2.2.3.3 Affinity selection of peptide phage particles against MBP-fusion proteins

2.2.3.3.1 Panning with magnetic beads

For an affinity selection using magnetic beads 300 – 500 µg of amylose-magnetic beads or anti-MBP magnetic beads that can bind 1.5 – 2-5 µg of MBP-fusion protein were washed twice with the appropriate buffer. To block unspecific binding sites the beads were incubated for 1 h with 500 µl 2% milk powder in panning buffer with 0.05% Tween 20. The wells were washed twice with 250 µl of appropriate buffer and an excess of fusion protein was immobilised for 30 min at 4°C in an overhead shaker Prior to selection 200 µl peptide phagemid particles in panning buffer with 2% milk powder and 0.05% Tween 20 were incubated with immobilised MBP to reduce unspecific binding and specific binding to either the MBP or the magnetic beads. The beads with the immobilised fusion protein were washed three times with panning buffer and pre-incubated peptide phage particles were added to the beads. The affinity selection was done for 2.5 h at room temperature in an overhead shaker. The supernatant containing the unbound phage was removed and the beads were washed 10 times with 500 µl panning buffer containing 0.05% Tween 20. Bound phage were eluted with acidic elution or competitive elution. For acidic elution 200 µl of elution buffer were added to the beads and incubated for 10 min in the overhead shaker. The elution buffer containing eluted phage particles was removed and immediately mixed with 45 µl neutralisation buffer. For competitive elution 200 µl competitor were added to the beads and incubated for 15 min in the overhead shaker. The eluted phage solution was used for titer determination and reinfection of *E. coli* cells (see section 2.2.3.4).

2.2.3.3.2 Panning in MTPs

For an affinity selection in microtiter plates (Nunc, Maxisorp) 200 ng of anti-MBP IgG in PBS was immobilised for 1 h at room temperature. The wells were washed twice with 250 µl PBS with 0.05% Tween 20 (PBST) and unspecific binding sites were blocked by incubation with 350 µl 2% milk powder in panning buffer with 0.05% Tween 20 for 1 h at room temperature. The wells were washed twice with 250 µl PBST and an excess of fusion protein (1 µg) was immobilised for 1.5 h at 4°C. Prior to selection 200 µl peptide phagemid particles in panning buffer with 2% milk powder and 0.05% Tween 20 were incubated with immobilised MBP to reduce unspecific binding and specific binding to either the MBP or the anti-MBP IgG. The wells with the immobilised fusion protein were washed three times with panning buffer and pre-incubated peptide phage particles were added. The affinity selection was done for 2.5 h at room temperature on a shaker. The supernatant containing the unbound phage was removed and the wells were washed 10 – 20 times with 250 µl panning buffer

containing 0.05 % Tween 20. Bound phage were eluted with acidic elution or competitive elution. For acidic elution 200 µl of elution buffer were added into the wells and incubated for 10 min on a shaker. The elution buffer containing eluted phage particles was removed and immediately mixed with 45 µl neutralisation buffer. For competitive elution 200 µl competitor were added and incubated for 15 min on a shaker. The eluted phage solution was used for titer determination and reinfection of *E. coli* cells (see section 2.2.3.4).

2.2.3.4 Reinfection of *E. coli* cells with eluted phage

To determine the titer of eluted phage 10 µl of eluted phage solution were used (see section 2.2.3.2). The remaining amount was used for infection of 20 ml of a freshly grown *E. coli* Top 10 F` λ^+ culture with an OD_{600} of 0.5. The culture was incubated at 37°C for 30 min without and for 30 min with agitation at 180 rpm. After incubation the cells were pelleted by centrifugation for 10 min at 4000 rpm and resuspended in 300 µl 2xYT medium containing ampicillin and tetracycline. The cell suspension was plated onto a 140/20 mm 2xYT agar plate containing ampicillin and tetracycline and incubated overnight at 37°C. The grown cells were washed from the plate with 5ml 2xYT medium containing antibiotics and used for packaging into phagemid particles (see section 2.2.3.1). From the rest of the cell suspension glycerol stocks were prepared.

2.2.3.5 Characterisation of single clones after reinfection

Single colonies of clones from the titer determination were picked and resuspended in 150 µl dH_2O. The suspension was used for colony-PCR. The PCR sample was afterwards 1:20 diluted with dH_2O and used for sequence analysis with the sequencing primers FSQJCO or RSQJCO.

2.2.3.6 Packaging of single clones

For packaging of single clones into phagemid particles an infection with M13K07 helper phage was necessary. 50 ml 2xYT medium containing tetracycline and ampicillin were inoculated from an overnight culture of the single clone to an OD_{600} of about 0.1. The culture was grown at 37°C and 180 rpm to an OD_{600} of 0.5 and the cells were infected with 0.5 x 10^{10} pfu of M13K07. The culture was incubated at 37°C for 30 min without agitation and was then grown over night at 37°C and 180 rpm. The culture was cooled on ice and centrifuged for 20 min at 4000 rpm and 4°C. The supernatant was decanted mixed with 0.2 volume of PEG/NaCl and incubated on ice for at least 2 h. The phage were precipitated by centrifugation for 60 min at 4000 rpm and 4°C. The supernatant was carefully decanted and remaining liquid removed. The pellet was resuspended in 0.5 ml of appropriate buffer and cleared by 10 min centrifugation at 13000 rpm at room temperature. NaN_3 was added to the phage solution to a final concentration of 0.02%. The phage titer was determined (see section 2.2.3.2).

2.2.4 Proteinbiochemical methods

2.2.4.1 Phage ELISA with MBP-fusion protein

For binding of the MBP-fusion protein 200 ng/well of anti-MBP IgG were immobilised in a microtiter plate (Nunc, Maxisorp) for 1 h at room temperature. The wells were washed 3 times with PBST and unspecific binding sites were blocked by incubation with 350 µl 2% milk powder in PBST for 1 h at room temperature. The wells were washed twice with 250 µl of appropriate buffer and an excess of fusion protein (1 µg) was immobilised for 1.5 h. The wells were washed three times with 250 µl of appropriate buffer and 200 µl peptide phagemid particles in buffer with 2% milk powder and 0.05 % Tween 20 were added and incubated for 1.5 h at room temperature. For a competitive phage ELISA the competitor was added during binding of phage particles. Unbound phage were removed by washing 3 – 10 times with 250 µl buffer with 0.05 % Tween 20. Bound phage were detected with 100 µl anti-M13 IgG (1:5000 in appropriate buffer with 2% milk powder and 0.05 % Tween 20) for 1.5 h at room temperature. For detection 200 µl ABTS substrate solution was added and the absorption at 410 nm was measured every minute for half an hour in an MTP-reader (Tecan Sunrise).

2.2.4.2 Cell disruption

2.2.4.2.1 BugBuster

E. coli pellets were thawed on ice and resuspended in 50 µl / OD_{600} unit BugBuster solution (Novagen). The cells were lysed for 20 min at 20°C under agitation. The insoluble protein fraction was pelleted at 15,000 rpm and 4°C for 20 min. The supernatant containing the soluble cytosolic proteins was stored and the pellet was resuspended in 50 µl / OD_{600} unit PBS. The soluble and insoluble protein fractions were used for analysis of the protein production.

2.2.4.2.2 Lysozym lysis buffer

The *E. coli* cell pellet from the protein production was thawed on ice and resuspended in ‘lysozym lysis buffer’. For resuspension the tenth part of the volume of the production culture was used. The cells were lysed for 30 min at 4°C under agitation in an overhead shaker. Insoluble material was removed by centrifugation at 14,000 rpm and 4°C for 20 min. The supernatant containing the soluble cytosolic proteins was used for protein purification.

2.2.4.2.3 Homogeniser

The *E. coli* cell pellet from the protein production was thawed on ice and resuspended in ‘homogeniser lysis buffer’. For resuspension the tenth part of the volume of the production culture was used. The homogeniser was cooled to 4°C and equilibrated with 40 ml lysis buffer at 10 kpsi. The cells were lysed twice at 20 kpsi and insoluble material was removed twice by centrifugation at 16,000 rpm and 4°C for 20 min. The supernatant containing the soluble cytosolic proteins was used for protein purification.

2.2.4.2.4 ‘Inclusion bodies’ solubilisation

The *E. coli* cell pellet from the protein production was thawed on ice and resuspended in ‘inclusion bodies lysis buffer’. For resuspension the tenth part of the volume of the production culture was used. The cells were lysed for 60 min at room temperature under agitation in an overhead shaker. Insoluble

material was removed by centrifugation at 14,000 rpm and 4°C for 20 min. The supernatant containing the solubilised 'inclusion bodies' was used for protein purification.

2.2.4.3 IMAC protein purification

For IMAC purification His Select nickel affinity gel was washed with 10 volumes buffer (MBP-NS3/4A or MBP-peptides: buffer A; MBP-NS2-3: inclusion bodies lysis buffer) and centrifuged for 5 min at 5000 g and 4°C. 10 ml cell extract was added to 200 µl HIS Select gel and incubated for 30 min at 4°C in an overhead shaker. The gel was separated by centrifugation for 5 min at 5000 g and 4°C. The HIS Select gel was washed 3 times with 10 volumes wash buffer (buffer + 10 mM imidazole) and bound protein was eluted with two volumes of elution buffer (buffer + 300 mM imidazole) for 15 min at 4°C in an overhead shaker. The gel was removed by centrifugation and the elution fraction was used for dialysis or buffer exchange with centrifugal filter units and stored at -80°C afterwards.

2.2.4.4 Protein purification using the Profinia system

For IMAC purification with the Profinia protein purification instrument (BioRad) the 'Native IMAC purification and desalting' program for 1 ml IMAC cartridge and 10 ml desalting cartridge or 5 ml IMAC cartridge and 50 ml desalting cartridge was used, respectively. The cell extract was loaded onto the equilibrated IMAC cartridge which was than washed with the 'Profinia native IMAC wash buffer' 1 and 2. The bound protein was eluted with the elution buffer. The buffer was exchanged with the help of the desalting cartridge. After a first purification with the 5 ml IMAC cartridge and 50 ml desalting cartridge the protein was eluted in the 'Profinia desalting buffer 1'. Imidazole was added to the elution fraction to a concentration of 5 mM and used for second purification with the 1 ml IMAC cartridge and 10 ml desalting cartridge. The protein was eluted in the 'Profinia desalting buffer 2' and stored at -80°C.

2.2.4.5 Precipitation of protein samples

Ethanol precipitation was used to concentrate protein solutions or for removal of buffer components. The sample was cooled on ice and cold ethanol was added to a final concentration of 90%. The sample was mixed thoroughly and incubated for at least 30 min at -20°C. The protein was collected by centrifugation at 15,000 rpm and 4°C for 20 min. The pellet was air dried and resuspended in an appropriate amount of buffer.

2.2.4.6 SDS Page

For separation of protein samples with a size range of 20 – 100 kDa the discontinued Glycine-SDS-polyacrylamide gel electrophoresis (SDS-PAGE) was used. It consists of a stacking and separation gel. The separation gel was casted between two glass slides (Bio-Rad Mini-Protean) and polymerised with a layer of water on top. The water was removed; the stacking gel casted on top and a comp was inserted. After polymerisation the gel was put into the gel chamber which was filled with SDS running buffer. The comb was removed and the samples and a protein ladder were loaded onto the

gel. Samples were mixed with an appropriate amount of 6x Laemmli-buffer and incubated at 95°C for 5 – 10 min. The samples were separated at 20 mA for about 45 min. The following formulations were used for stacking and separation gels:

Component	Volume			
	Separating gel			Stacking gel
	10%	12%	15%	4.5%
40% acrylamide mix	2.5 ml	3 ml	3.75 ml	0.55 ml
1 M TrisHCl pH 6.8	-	-	-	0.625 ml
1 M TrisHCl pH 8.8	2.5 ml	2.5 ml	2.5 ml	-
10% SDS	100 µl	100 µl	100 µl	50 µl
APS	80 µl	80 µl	80 µl	40 µl
TEMED	8 µl	8 µl	8 µl	4 µl
dH_2O	4.8	4.3 ml	3.55 ml	3.75

2.2.4.7 Tricine Page

For separation of protein samples with a size range of 5 – 100 kDa the discontinued Tricine-SDS-polyacrylamide gel electrophoresis (Tricine-PAGE) was used. It consists of a stacking and separation gel. The separation gel was casted between two glass slides (Bio-Rad Mini-Protean) and a stacking gel was casted on top and a comp was inserted. After polymerisation the gel was put into the gel chamber which was filled with Tricine-PAGE anode and cathode buffer. The comb was removed and the samples and a protein ladder were loaded onto the gel. Samples were mixed with an appropriate amount of 4x Tricine-PAGE sample buffer and incubated at 95°C for 5 min. Electrophoresis was started with an initial voltage of 30 V and maintained at this voltage until the sample has completely entered the stacking gel. Samples were separated at 80 V for about 90 min. The following formulations were used for stacking and separation gels:

Component	Volume	
	Separating gel 10%	Stacking gel 4%
40% acrylamide mix (19:1)	2.5 ml	0.6 ml
Gel buffer (3x)	3.333 ml	1.5
Glycerol (87%)	1.16 ml	-
APS	50 µl	45 µl
TEMED	5 µl	4.5 µl
dH_2O	2.95 ml	3.85 ml

2.2.4.8 Staining methods

2.2.4.8.1 Coomassie staining

Polyacrylamide gels were stained for at least 1 h in coomassie staining solution on a shaker. The gels were washed with water and transferred into discoloration solution until destaining was complete. The gels were stored in water.

2.2.4.8.2 Silver staining

For silver staining of proteins in polyacrylamide gels the ‘Roti-Black P’ silver staining kit was used. The staining was done according to manufacturer’s instruction.

2.2.4.9 Concentration determination of protein solutions

2.2.4.9.1 Bradford assay

One method for protein concentration measurement is the Bradford assay. This assay is based on complexing of proteins with Brilliant Blue G. Various BSA concentrations were used to create a standard curve. Standard and samples were diluted in a 96 well plate. The protein samples were mixed with Bradford reagent (Sigma-Aldrich) according to manufacturer’s instruction, incubated at room temperature for 30 min and the absorption was measured at 595 nm.

2.2.4.9.2 Densitometric measurement

For protein concentration determination the intensity of protein bands was measured. The protein samples and various concentrations of a standard protein (MBP4 or BSA) in the same buffer were separated on an acrylamid gel and coomassie stained. The stained gel was scanned and the intensity of the protein bands was determined using the software *Image J*. The standard protein was used to create a standard curve which was used for calculation of the unknown protein concentration.

2.2.4.9.3 UV spectroscopy

The protein concentration was measured at 280 nm with the NanoDrop spectrophotometer. The photometer was calibrated to zero absorbance with buffer solution and the absorbance of the protein solution was measured. To calculate the molar concentration the absorbance coefficient was used.

2.2.4.10 Dialysis of protein solutions

For dialysis of protein solutions a dialysis membrane with a 14 kDa molecular weight cut off was used. The membrane was cleaned according to manufacturer’s instruction prior to use. The protein solution was filled into the membrane which was sealed with dialysis membrane clamps. The dialysis was done for 4 h at 4°C under agitation in dialysis buffer. The volume of the lysis buffer was at least 100-fold the volume of the protein solution. After dialysis the protein solution was stored at -80°C.

2.2.4.11 Western blot

2.2.4.11.1 Transfer to membrane

By SDS-PAGE separated proteins were transferred to a nitrocellulose membrane using a semi-dry blotter (BioRad). The acrylamide gel was equilibrated in blotting buffer for 20 min. The membrane and blot paper ‘Protean XL’ in the size of the gel was wetted in blotting buffer. A filter was put on the anode of the semi-dry blotter and the membrane was put on top. The equilibrated gel and another filter paper were added on the membrane and air bubbles were rolled out with a spatula. The blotter was closed and the proteins were transferred at 15 V for 30 min.

2.2.4.11.2 Immunostaining

The proteins transferred to a nitrocellulose membrane were detected using antibodies specific to the target protein. The membrane was blocked with 2% milk powder in PBS for 1 h at room temperature to saturate all free binding sites. The membrane was washed shortly and for 5 min with PBST. A protein specific antibody conjugated with HRP was diluted in PBS with 2% milk powder and added for 1.5 h to the membrane. Unbound antibody was removed by washing shortly and for 5 min with PBST. The immune staining was started by adding the DAB substrate solution and stopped by washing of the membrane with water.

2.2.4.12 NS2-3 protease activity assay

The NS2-3 protease was diluted in 'cleavage buffer' for activation. Refolded protease was diluted 1:5 in cleavage buffer and denatured protease was diluted 1:50 in cleavage buffer. The diluted protease was incubated for 5 min on ice and then incubated at 23°C. The protein was precipitated using ethanol, dissolved in laemmli buffer and loaded onto a Glycine- or Tricine-SDS PAGE gel. After electrophoresis and staining of the gel the amount of cleaved protease was determined by densitometric measurement of the protein bands.

2.2.4.13 NS3/4A protease activity assay

The activity of the NS3/4A protease was tested with a fluorescence resonance energy transfer (FRET) assay (Taliani *et al.*, 1996). The substrate M-2235 (Ac-Asp-Glu-Asp(EDANS)-Glu-Glu-Abu-y-[COO]Ala-Ser-Lys(DABCYL)-NH2, Bachem) is derived from the HCV 4A/4B cleavage site. An ester bond is incorporated between residues P1 and P1´. The donor chromophore DABCYL and the acceptor chromophore EDANS are incorporated into the substrate. The absorbance maximum and emission maximum are ~355 nm and ~500 nm, respectively. In the uncut substrate the donor and acceptor are in proximity and the emission wavelength of the donor overlaps with the absorbance wavelength of the acceptor. For a NS3/4A activity assay in MTPs (µclear non-binding, Greiner bio-one) normally 0.5 – 1 nM protease were diluted in buffer M2235 (Misialek *et al.*, 2009) and 5 µM substrate were added. Substances that have been tested for an inhibitory effect on the NS3/4A protease were incubated with the protease 10 – 15 min at room temperature before adding of the substrate. The final volume was 200 µl. Fluorescence increase was measured every minute for 30 – 60 min at 30°C in a MTP reader (Excitation filter: 360/40 nm, emission filter: 460/40 nm, Biotek Synergy 2). Velocity of fluorescence increase over one hour was compared to that of a control peptide and percent inhibition at each inhibitor concentration was calculated.

Curve fitting was done with *GraphPad Prism* using a nonlinear regression model with variable slope and normalised response: Y=100/(1+10^((LogIC$_{50}$-X)*slope)) or using a nonlinear regression model with variable slope : Y=Bottom+(Top-Bottom)/ (1+10^((LogIC$_{50}$-X)*slope)). Obtained IC$_{50}$ values in these experiments were converted to apparent K_i values using the equation $K_i = IC_{50}/(1 + [S]/K_m)$ for competitive inhibitors (Cheng and Prusoff, 1973).

2.2.4.14 Encapsulation of peptides into polymersomes

The encapsulation of peptides into polymersomes was done at the laboratory of Dr Giuseppe Battaglia (Department of Biomedical Science, University Sheffield, UK). 10 mg of PMPC25-PDPA70 copolymer were dissolved in a glass vial in 1 ml PBS pH 2. The pH was gradually increased to pH 6 and 1 mg peptide was added to the solution and dissolved. The suspension was sonicated for 20 min (Sonicor Instruments Corporation) and sterilised using a 0.22 µm filter. The pH of the solution was raised to 7.3 and again sonicated for 15 – 30 min. The polymersomes solution was then purified by gel permeation chromatography using a sepharose 4B size exclusion column to extract the fraction containing polymersomes. In all cases the polymersomes size distribution was determined by dynamic light scattering (DLS) and the concentration of the polymer and peptide was measured by HPLC. Polymersomes were stored at 4°C until use.

2.2.5 Crystallisation methods

2.2.5.1 Preparation of protease-peptide complex

To 40 – 90 µM purified NS3/4A protease at least two fold molar excess of peptide was added in 'Profinia Desalting buffer 2' and incubated on ice for at least 2 h. The solution was centrifuged at 15,000 rpm and 4°C for 20 min and concentrated to about 220 µM (~5 mg/ml) using an Amicon Ultra 4 ml centrifugal filter (10 kDa). The peptide (dissolved in 100 % (v/v) DMSO) was added to a final concentration of 500 µM resulting in a final DMSO concentration of 5% (v/v). The solution was centrifuged at 15,000 rpm and 4°C for 20 min and used for crystal screens. Unused complex was stored at -80°C.

2.2.5.2 Initial crystallisation screen

Initial screening was performed at 19°C with commercial screening suites from QIAGEN (Anions, Cations, pHClear II, AmSO4 and JCSG$^+$) using sitting drop, vapor-diffusion technique.

The reservoir solution and the drops of crystallisation experiments were set up on a Cartesian Honeybee crystallisation robot (Zinsser Analytic) in 96-3 well Intelli plates (Hampton Research). The reservoir was filled with 65 µl and equal amounts (200 nl) of two different NS3/4A protease complexes (~5 mg/ml) and precipitant were dispensed in two of the three sitting wells. In the remaining well a control with buffer lacking protein was used to identify likely salt crystals. The plates were sealed with tape and incubated at 19°C. Initial crystal formation was observed after several days. A total of 480 crystallisation conditions were tested.

2.2.5.3 Optimisation of crystallisation conditions

Conditions which yielded initial crystals had to be optimised to obtain a suitable size for x-ray diffraction measurements. For optimisation of NS3/4A protease and inhibitory peptide co-complex crystals hanging drop, vapor-diffusion technique in 24-6 well or 15-6 well plates (EasyXtal from QIAGEN) at 19°C was used. The primary method of optimisation was to screen around the initial hit, varying the precipitant concentration, the pH or the salt concentration. Grid screens were designed with the web-based application 'MakeTray' (Hampton Research, Aliso Viejo, USA). The reservoir

volume was 500 µl and 1 µl of protein complex with 1 µl reservoir solution were mixed. For each condition 100 – 230 µM (2 – 5 mg/ml) of protein complex was used for crystallisation. In the last optimisation step dilutions of 100 µM (2 mg/ml) and 120 µM (2.5 mg/ml) NS3/4A protease with 0.1 M buffer of the crystallisation condition (e.g. 0.1 M MES pH 6.0 or 0.1 M Na-citrate pH 5.1) were used. The plates were incubated for up to four weeks and crystal formation was checked as in the screening process.

2.2.5.4 X-ray diffraction measurement

X-ray diffraction measurements and model building was done by Dr. Stefan Schmelz (Department Molecular Structural Biology, HZI). Crystals in buffer with 30% glycerol were flash-frozen in liquid nitrogen and mounted in a 100K cryostream. X-ray diffraction data were collected at the European Synchrotron Radiation Facility (ESRF, Grenoble, ID-29) and at Berliner Elektronenspeicherring-Gesellschaft für Synchrotronstrahlung (BESSY, MX-15.1). Diffraction intensities of the complexes were indexed, integrated and scaled in HKL2000 (Otwinowski and Minor, 1997) or XDS and XSCALE (Kabsch, 2010).

The structure was solved by molecular replacement with *Phaser* (McCoy *et al.*, 2007), using NS3/4A coordinates (Protein Databank code 1DXP) as search a model. The resulting model was refined with *Phenix.refine* (Adams *et al.*, 2004) or *Refmac5* (Murshudov *et al.*, 1997) and manually checked with *COOT* (Emsley and Cowtan, 2004). The inhibitory peptides were manually built with *COOT* (Emsley and Cowtan, 2004). Figures and structure alignments were prepared using PyMOL (DeLano, 2002).

2.2.6 Intracellular delivery of inhibitory peptides

2.2.6.1 Cell culture replicon assay

The cell culture replicon assay was done by Juliane Gentzsch (Department of Experimental Virology, Twincore, Hannover). The replicon assay was used for analysis of intracellular inhibition of viral replication. For the assay 4 x 10^6 cells (Lunet N#3 hCD81_G-Luc_BLR) were transfected by electroporation (270 V, 975 µF, 4 mm cuvette) with 5 µg in vitro-transcribed replicon RNA. The cells were seeded on a 96 well plate (20000 cells/well in 200 µl medium) and incubated at 37°C for 4 – 5 h. After incubation the inhibitory peptides were added in different concentrations (or dilutions for polymersomes). Before addition the cells of a few wells were lysed for normalisation to transfection efficiency and stored at -20°C. Addition of water or buffer was used as a negative control and 1 ng/ml IFN was used as positive control. The medium of the cells was changed to the medium containing the inhibitors in different concentrations (duplicates) or the controls. The cells were incubated for 48 h with the inhibitors and then used for a luciferase assay. The cells were washed once with PBS and lysed. After substrate addition the firefly luciferase activity was detected with a plate luminometer. Luciferase levels are tightly correlated to the replication of the replicon. For analysis of cell viability the gaussia luciferase activity was measured.

Curve fitting was done with *GraphPad Prism* using a nonlinear regression model with variable slope and normalised response: Y=100/(1+10^((LogEC_{50}-X)*slope)) or using a nonlinear regression model with variable slope: Y=Bottom+(Top-Bottom)/ (1+10^((LogEC_{50}-X)*slope)).

3. Results

3.1 NS2-3 protease

3.1.1 Production, refolding and activity of recombinant NS2-3 protease

The HCV NS2-3 protease was produced with the pMAL expression system (New England BioLabs). The DNA encoding the NS2-3 protease was inserted into the pMAL-c4E vector down-stream from the *malE* gene, which encodes the maltose-binding protein (MBP). This results in the expression of a MBP-NS2-3 fusion protein with a 23 aa linker between MBP and protease (see Figure 3-1). A truncated form of the NS2-3 protease that is still capable of autoprocessing was produced according to Pallaoro and co-workers. It consists of the residues 907 – 1206 of the HCV polyprotein, encompassing the cytoplasmic catalytic domain of NS2 and the NS3 serine protease domain with the Zn^{2+} binding site (Thibeault *et al.*, 2001; Pallaoro *et al.*, 2001). For PCR amplification the HCV replicon 'I389/NS2-3'UTR' which was constructed from the consensus sequence of genotype 1b isolate cDNA served as a template (Lohmann *et al.*, 1999). The primer primNS2-3 and primNS2-3-rev, which introduced a KpnI and PstI restriction site and a C-terminal His-Tag with a short linker, were used. It was intended to use the MBP protein for immobilisation of the protease during affinity enrichment and the His-Tag for IMAC purification after production in *E. coli*. The NS2-3 insert was ligated into the dephosphorylated pMAL-c4E vector which was also cut with the restriction enzymes KpnI and PstI and transformed into *E. coli* Top10 F´cells.

Figure 3-1: Schematic picture of the expression vector pMAL-c4E with NS2-3 insert. The protease insert was ligated into the KpnI and PstI cut vector. malE: maltose-binding protein gene, lacZ alpha: ß-galactosidase alpha fragment gene, bla: ß-lactamase gene, M13 ori: M13 phage origin of replication, pMB1 ori: E. coli origin of replication from plasmid pMB1, lacIq: lac repressor gene.

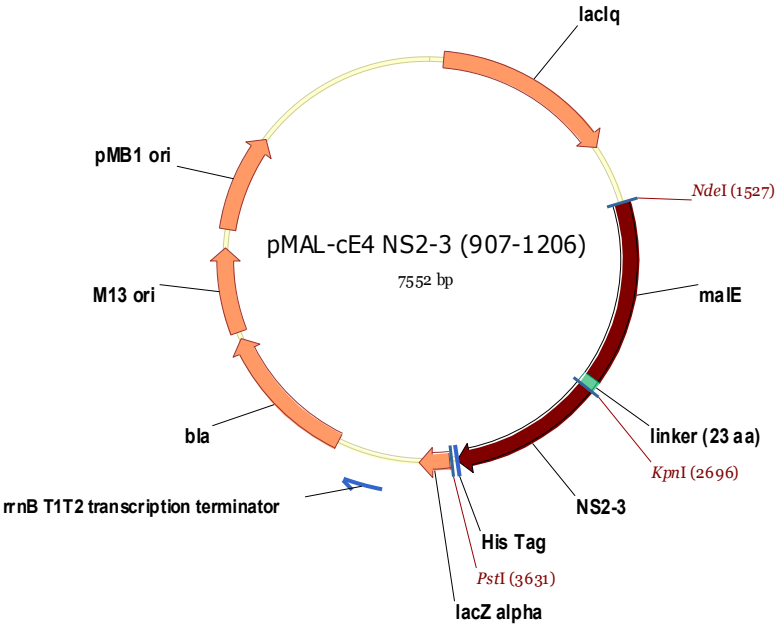

Soluble expression of NS2-3 protease results in autocleavage during production. Since the enzyme requires zinc for activity the MBP-NS2-3 protease fusion protein was expressed in M9 minimal medium without zinc, under which condition most of the material was found as insoluble 'inclusion bodies'. It has previously been reported that the NS3 protease domain requires Zn^{2+} for correct

folding and without zinc the misfolded protease accumulates in inclusion bodies (Pallaoro *et al.*, 2001). The inclusion bodies were solubilised in 6 M guanidine HCl and purified by IMAC. Figure 3-2 shows the results of the production and purification of the MBP-NS2-3 protein. The protease could be produced and purified in suitable amounts and purity.

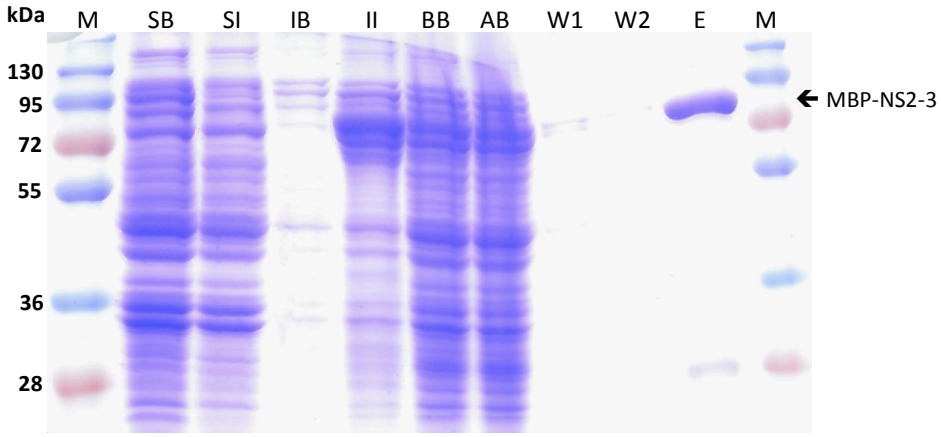

Figure 3-2: Production and purification of MBP-NS2-3. 12% SDS-gel, M: molecular weight marker, SB: soluble fraction before induction, SI: soluble fraction 5 h after induction, IB: insoluble fraction before induction, II: insoluble fraction 5 h after induction, BB: before binding, AB: after binding; W1 and W2: washing fractions, E: elution fraction. 3 µl of each fraction were loaded onto the gel.

The purified MBP-NS2-3 protease solubilised in 6 M guanidine HCl was dialysed against 0.75 M guanidine HCl supplemented with Zn^{2+}. Under these conditions the NS2-3 protease refolds but undergoes no self-processing (Pallaoro *et al.*, 2001). The dialysed protease was stored at -80°C until use. The concentration of purified MBP-NS2-3 was determined by densitometric measurement of the coomassie stained protein bands and comparison to a BSA standard. To initiate the auto-cleavage reaction the NS2-3 protease was diluted in cleavage buffer and incubated at 23°C. The samples were analysed on a SDS-gel and by western blot (see Figure 3-3 A and B). A significant fraction of the MBP-NS2-3 protease undergoes self-cleavage. It is assumed that this ensues following correct refolding and represents the normal autocatalytic activity of the protein.

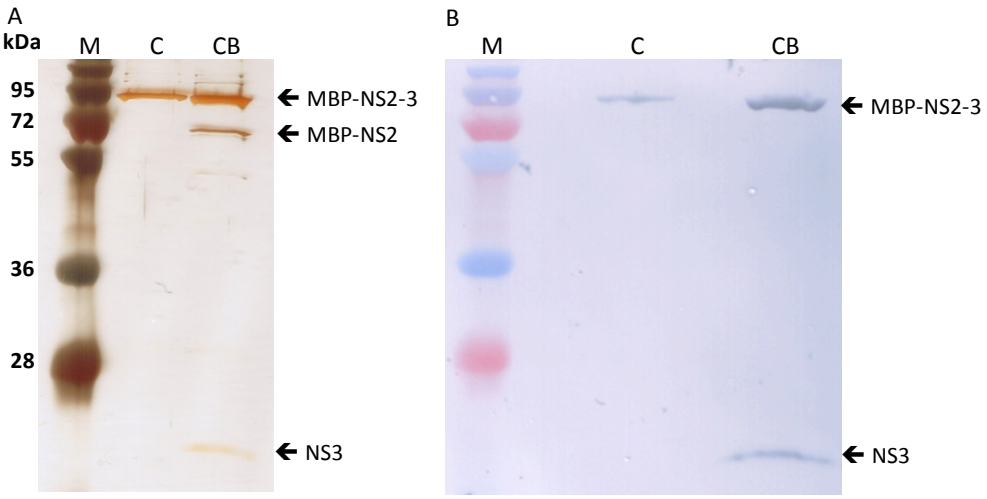

Figure 3-3: Activity assay with refolded MBP-NS2-3 protease. M: molecular weight marker, C: control, CB: cleavage buffer. The protease was diluted 1:5 with cleavage buffer 1 (CB) or water (control) and incubated over night at 23°C. Samples were separated on 12% SDS gels and silver stained (A) or used for a western blot with detection of the His-Tag with a anti-polyHistidine IgG HRP linked (B).

To optimise the auto-processing reaction of the NS2-3 protease four different cleavage buffers (see Table 3-1), three different protease concentrations and two dilution protocols were analysed. Concentrations of 50, 100 and 700 nM NS2-3 protease were tested and the protease was diluted 1:5 or 1:10 in cleavage buffer.

Table 3-1: Formulation of different cleavage buffers for NS2-3 protease self-processing.

Cleavage Buffer	Detergent	Glycerol v/v [%]	NaCl [mM]	Additive
1	1% TritonX	50	250	3mM cysteine
2	1% CHAPS	50	250	3mM cysteine
3	0.2% CHAPS	30	0	
4	0.05% Tween 20	10	150	
Common components	50 mM TrisHCl (pH 7.5)		3 mM DTT	50 µM $ZnCl_2$

After the auto-cleavage reaction the samples were separated on a SDS-gel and the amount of cleaved protease determined by densitometric measurement of the coomassie stained protein bands (see Figure 3-4 and Table 3-2).

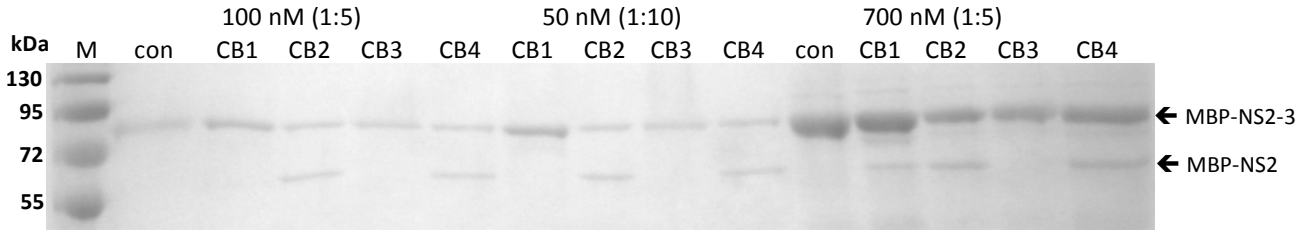

Figure 3-4: Cleavage of MBP-NS2-3 at different protease concentrations and diluted in various cleavage buffers. 12% SDS-gel, M: molecular weight marker, con: NS2-3 diluted in water, CB: cleavage buffer.

The highest self-processing of the NS2-3 protease could be achieved by dilution in cleavage buffer 2 (CB2) or CB4 (see Table 3-2). A 1:5 or 1:10 dilution to 100 nM or 50 nM NS2-3 protease resulted in about 50% of protease cleavage. Dilution of the protease in cleavage buffer 2 or 4 to 700 nM resulted only in cleavage of 25% of the protease. The CB4 was chosen for later experiments because of its simpler formulation with less detergent, glycerol and additives that could interfere during the affinity selection step of subsequent panning experiments.

Table 3-2: Amount of cleaved NS2-3 protease after dilution in various cleavage buffers and at different concentrations.

	50 nM (1:10 dilution)		100 nM (1:5 dilution)		700 nM (1:5 dilution)	
	NS2-3 [%]	NS2 [%]	NS2-3 [%]	NS2 [%]	NS2-3 [%]	NS2 [%]
Cleavage buffer 1	100	0	100	0	92	8
Cleavage buffer 2	53	47	48	52	75	25
Cleavage buffer 3	100	0	100	0	100	0
Cleavage buffer 4	48	52	51	49	75	25

The correct refolding of the maltose-binding protein was analysed by binding to magnetic beads on which amylose is covalently coupled. The MBP needs to be in a functional native conformation to bind amylose. As seen in Figure 3-5 the MBP is completely refolded and binds to the amylose beads. MBP-NS2-3 protease was detectable neither in the supernatant after binding to the beads nor in the washing fraction.

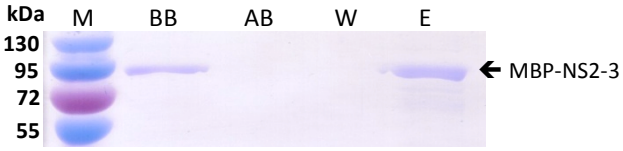

Figure 3-5: Binding of refolded MBP-NS2-3 to amylose magnetic beads. 12% SDS-gel, M: molecular weight marker, BB: before binding, AB: after binding, W: washing fraction, E: eluted protein from amylose beads.

3.1.2 Panning against NS2-3 protease

For an affinity selection with the peptide phage display library CPL19YS-2 the NS2-3 protease was immobilised on anti-MBP magnetic beads. The beads are coupled with monoclonal anti-MBP IgG which binds the MBP of the fusion protein. For each panning round 2 µg MBP-NS2-3 protease diluted in cleavage buffer 4 were immobilised at 4°C to prevent cleavage (Pallaoro *et al.*, 2001). About 1 x 10^{11} peptide-displaying phagemid particles in PBS were used for selection at RT. To reduce unspecific binding and specific binding to either the MBP or the anti-MBP IgG, the peptide phagemid were incubated on immobilised MBP prior to selection on the NS2-3 protease. After selection on the immobilised protease unbound phagmid were removed by washing 10 times with PBS (0.05% Tween 20) and subsequent acidic elution of bound peptide phage. Figure 3-6 shows the ratio of eluted and added phage for each panning round. The ratio increases after the second and fifth selection round, but is constant after the second and third selection round.

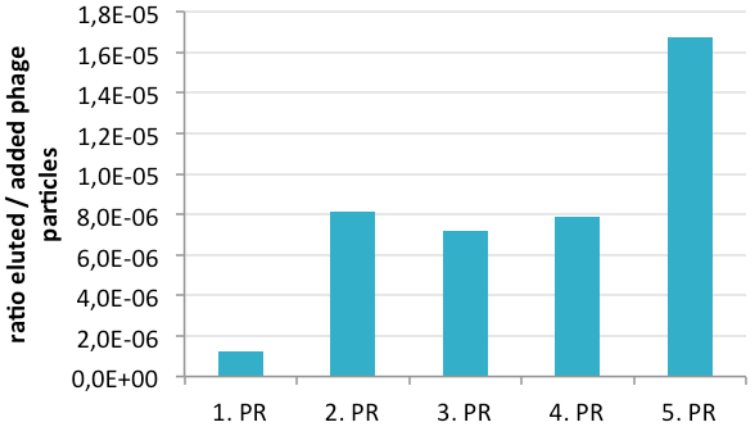

Figure 3-6: Ratio of eluted/added phage particles. The ratio of five panning rounds on immobilised MBP-NS2-3 with phage display peptide library CPL19YS-2 is shown.

After the 3rd panning round 24 single clones and after the 4th and 5th panning round 36 single clones were selected for sequencing. In Figure 3-7 the sequences of the peptides after the 5th panning round are shown.

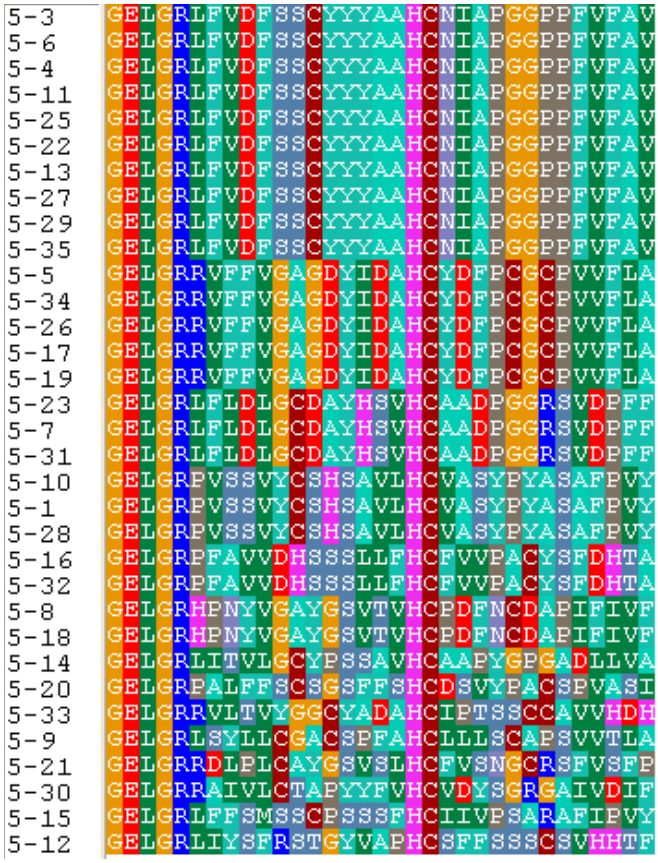

Figure 3-7: Amino acid sequences of 33 single clones after the 5th panning round on the NS2-3 protease with phage display peptide library CPL19YS-2.

Four peptides showed an enrichment with three or more clones from the sequenced 33 clones (see Table 3-3) after the 5th panning round. Three of these peptides (K5-10, K5-11 and K5-17) were also seen after the 4th panning round and the clone K5-11 was already present after the 3rd selection round. The clone K5-11 showed the highest enrichment of 30% of all sequenced clones after the 5th panning round. The peptide sequences do not show a definite homology in their sequence. Only the peptide K5-11 and K5-31 have a similar hydrophobic motive in the N-terminal part of the peptide that is interrupted by an aspartic acid: L-F-V/L-D-F/L.

Table 3-3: Peptides enriched in panning against MBP-NS2-3 protease. PR: panning round. Constant sequence parts are coloured in blue and homologies are coloured in orange.

Clone name	Sequence	Number of clones		
		3. PR	4. PR	5. PR
K5-11	GELGRLFVDFSSCYYYAAHCNIAPGGPPFVFAV	2 (10 %)	5 (16 %)	10 (30%)
K5-17	GELGRRVFFVGAGDYIDAHCYDFPCGCPVVFLA	-	3 (9 %)	5 (15%)
K5-31	GELGRLFLDLGCDAYHSVHCAADPGGRSVDPFF	-	-	3 (9%)
K5-10	GELGRPVSSVYCSHSAVLHCVASYPYASAFPVY	-	1 (3 %)	3 (9%)

Specific binding of the enriched peptides of the 5th panning round to the NS2-3 protease was analysed by phage ELISA. MBP-NS2-3 was immobilised over anti-MBP IgG and incubated with peptide presenting phage. Bound phage were detected by an anti-M13 IgG HRP conjugate. Immobilised MBP and helper phage M13K07 were used as controls. In Figure 3-8 A and B the results for the peptides K11 and K17 are shown. Both peptides show specific binding to the NS2-3 protease in a concentration dependent manner and only a low unspecific binding to the MBP control.

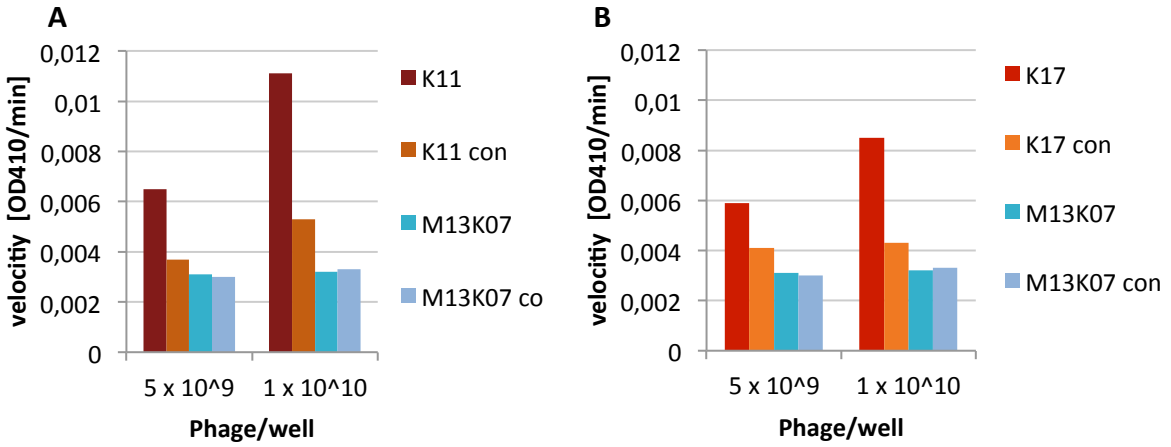

Figure 3-8: Phage ELISA with enriched clones K11 and K17. Binding of peptide presenting phage particles to NS2-3 protease was analysed. 0.6 µg MBP-NS2-3 was immobilised over anti-MBP IgG (100 ng), detection of bound phage by anti-M13 IgG HRP conjugate, 10 washing steps before and after addition of detection antibody. Con: MBP control, negative control with M13K07 helper phage. **A:** Phage ELISA with clone K11, **B:** Phage ELISA with clone K17 (see Table 3-3).

In Figure 3-9 the results for the peptides K10 and K31 are shown. The peptide phage of the clones K10 and K31 do not show specific binding to the NS2-3 protease. The binding to the MBP control is as high as to the protease or in the case of clone K31 even higher. K10 and K31 are probably specific binders of the MBP or the anti-MBP IgG.

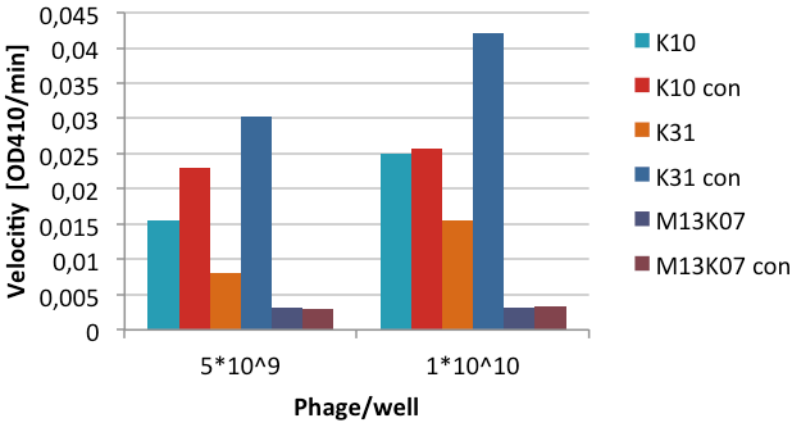

Figure 3-9: Phage ELISA with enriched clones K10 and K31 (see Table 3-3). Binding of peptide presenting phage particles to NS2-3 protease was analysed. 0.6 µg MBP-NS2-3 was immobilised over anti-MBP IgG (100 ng), detection of bound phage by anti-M13 IgG HRP conjugate, 10 washing steps before and after addition of detection antibody. Con: MBP control, negative control with M13K07 helper phage.

3.1.3 Production of peptides

To test if the peptides K11 and K17 inhibit the NS2-3 cleavage reaction the peptides should be produced without fusion to the M13 phage. Because of the relative long and hydrophobic sequence of the peptides a chemical synthesis would have been difficult. Therefore it was proposed to produce the peptides in *E. coli* and purify them by IMAC. The peptides were produced with an N-terminal fusion to the Antennapedia peptide (Antp). The Antp should increase the solubility of the peptides and could be used for later cellular delivery of the peptides.

For production of the peptides the pET expression system (Novagen) was used. In pET vectors the cloned DNA is under the control of the bacteriophage T7 transcription and translation signals for strong expression. The Antp DNA sequence was inserted into the pET28c expression vector at the NcoI restriction site with the oligonucleotids ‘Ant-pET 5`’ and ‘Ant-pET 3`’. The Antp oligonuleotides were designed to leave only one NcoI restriction site at the 3` end. The oligonuleotides were hybridised and ligated into the pET28c vector which was cut with the restriction enzyme NcoI. The insertion of the Antp was checked by sequencing. For cloning of the peptide insert into the vector the NcoI and XhoI restriction sites should be used. This results in a ‘SM’ linker between the Antennapedia peptide and cloned DNA and an N-terminal His-Tag that can be used for IMAC purification. The sequences coding the enriched peptides were amplified by PCR with the primer ‘Pep-pET uni 5`’ and ‘Pep-pET uni 3`’ introducing an NcoI and XhoI restriction site. The corresponding peptide phagemid served as a template. The peptide insert was ligated into the dephosphorylated pET28c-Antp vector which was also cut with the restriction enzymes NcoI and XhoI and transformed into *E. coli* Rosetta 2 cells. Rosetta 2 cells supply tRNAs for 7 rare codons in *E. coli* and carry a chromosomal copy of the T7 RNA polymerase gene.

After expression of the peptides most of the material was found as insoluble ‘inclusion bodies’. The inclusion bodies were solubilised in 6 M guanidine HCl and purified by IMAC. Figure 3-10 shows the results of the expression and purification of the K11 and K17 Antennapedia fusion peptides (Ant-K11 and Ant-K17).

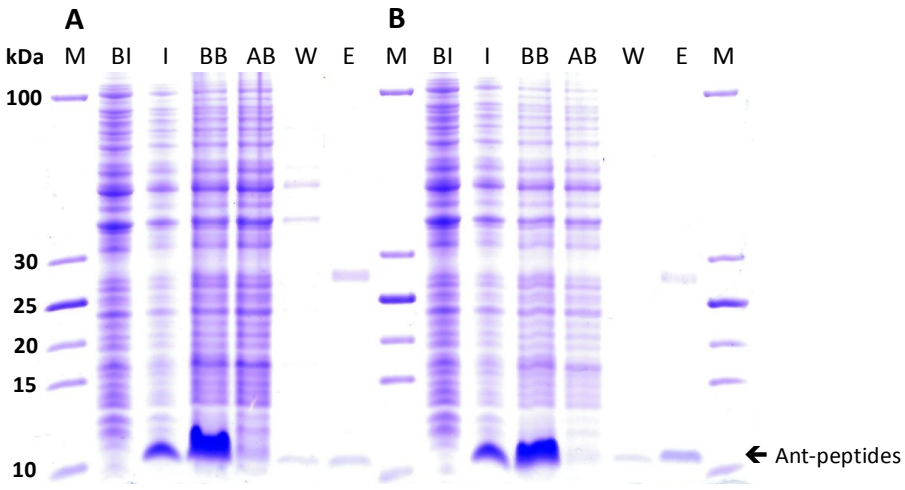

Figure 3-10: Production and purification of Ant-K17 and Ant-K11 peptides. 10% Tricine PAGE gel, M: molecular weight marker, BI: before induction, I: 5 h after induction, BB: before binding, AB: after binding; W: washing fractions, E: elution fraction. 3 µl of each fraction were loaded onto the gel. A: Ant-K17, B: Ant-K11.

The peptides could be produced and purified in suitable amounts. The purity of the peptides was about 55% for the Ant-K17 peptide and 80% for the Ant-K11 peptide. The concentration of the

purified Antennapedia fusion peptides was determined by Bradford protein assay taking the purity of the eluted protein into consideration. The concentration of the K11-peptide was about 80 µM and for the K17-peptide 18 µM.

3.1.4 Inhibition of NS2-3 protease activity

The inhibitory effect of the peptides on NS2-3 protease cleavage was tested in an activity assay. MBP-NS2-3 protease solubilised in 6 M guanidine HCl was mixed with peptide also solubilised in 6 M guanidine HCl and diluted 1:50 in cleavage buffer 4 and incubated for 5 minutes on ice for refolding of the protease. The cleavage reaction was initiated by increasing the temperature to 23°C (Pallaoro *et al.*, 2001). During dialysis refolded NS2-3 protease was not used for the activity assay because it is known that the protease has formed dimers after refolding (Pallaoro *et al.*, 2001). Therefore inhibition of dimer formation would not be detectable.

To identify the optimal incubation time the cleavage kinetics of the NS2-3 protease were first determined without added peptide. The cleavage kinetics of the NS2-3 protease showed the maximum of the cleavage reaction after about 1.5 hours of incubation in cleavage buffer at 23°C (see Figure 3-11). After 1.5 hours of incubation no significant increase in protease cleavage was measurable. The amount of cleaved NS2-3 protease was about 20%.

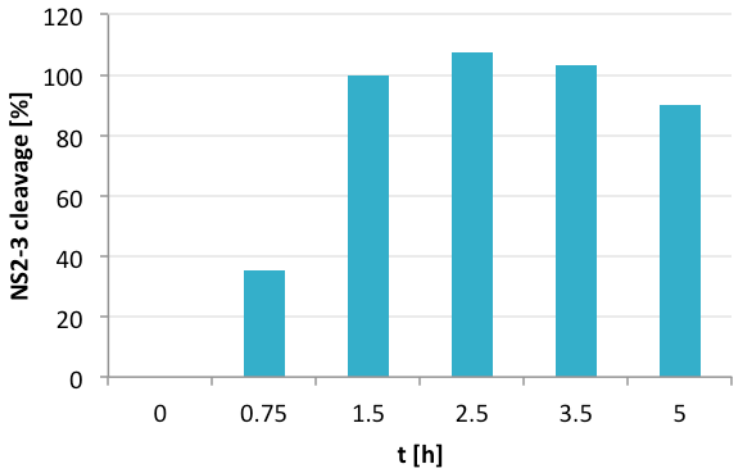

Figure 3-11: Cleavage kinetics of the MBP-NS2-3 protease. NS2-3 protease was diluted 1:50 in cleavage buffer 4 to 50 nM and incubated at 23°C for different durations. Samples were separeated on a SDS-gel and the amount of cleaved protease determined by densitometric measurement of the coomassie stained protein bands. The amount of cleaved protease after 1.5 h was set to 100%.

NS2-3 activity assay samples were incubated for 1.5 hours at 23°C. The sample was concentrated by ethanol precipitation and loaded onto a 10% Tricine-page gel. The amount of cleaved protease was determined by densitometric measurement of the coomassie stained protein bands (see Figure 3-12). To exclude that the added peptides only interfere with the refolding of the MBP-NS2-3 protease the peptide Ant-K5-66 was chosen as a control (see appendix

Figure 7-1). The peptide binds specific to the NS3 protease domain. The peptides were added to the protease to a final concentration of 270 nM.

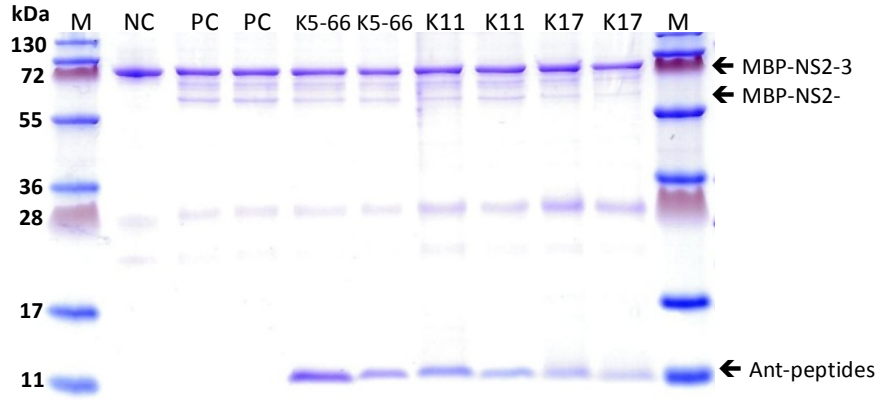

Figure 3-12: NS2-3 protease activity assay with peptides Ant-K11 and Ant-K17. NS2-3 protease with or without peptide was diluted 1:50 in cleavage buffer 4 to 50 nM protease and 270 nM peptide and incubated at 23°C for 1.5 h. Samples were separated on a 10% Tricine-page gel. M: molecular weight marker, NC: negative control (1:50 dilution of NS2-3 protease with water), PC: positive control without peptide, 5-66: control with peptide Ant-K5-66, K11: sample with peptide Ant-K11, K17: sample with peptide Ant-K17.

The results of the NS2-3 activity assay with the peptides K11 and K17 are shown in Figure 3-13. The control peptide K5-66 reduced the cleavage of the protease to about 75% compared to the control without peptide. The peptide K11 showed a reduction of the protease cleavage to about 90%. The peptide K17 showed the highest inhibitory effect on NS2-3 cleavage. After incubation with peptide K17 only about 55% of NS2-3 were processed.

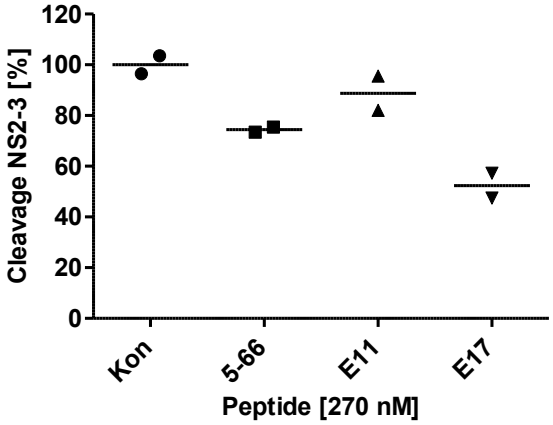

Figure 3-13: Inhibitory effect of peptides on NS2-3 protease cleavage. Con: positive control without peptide, K5-66: control with peptide Ant-K5-66, K11: sample with peptide Ant-K11, K17: sample with peptide Ant-K17. Protease 50 nM, peptide 270 nM. The amount of cleaved protease of the control without peptide was set to 100%.

Since the peptide K11 showed no inhibitory effect on protease cleavage compared to the control peptide the activity assay was only repeated with peptide K17 to confirm the results. In Figure 3-14 the combined results of different experiments are shown.

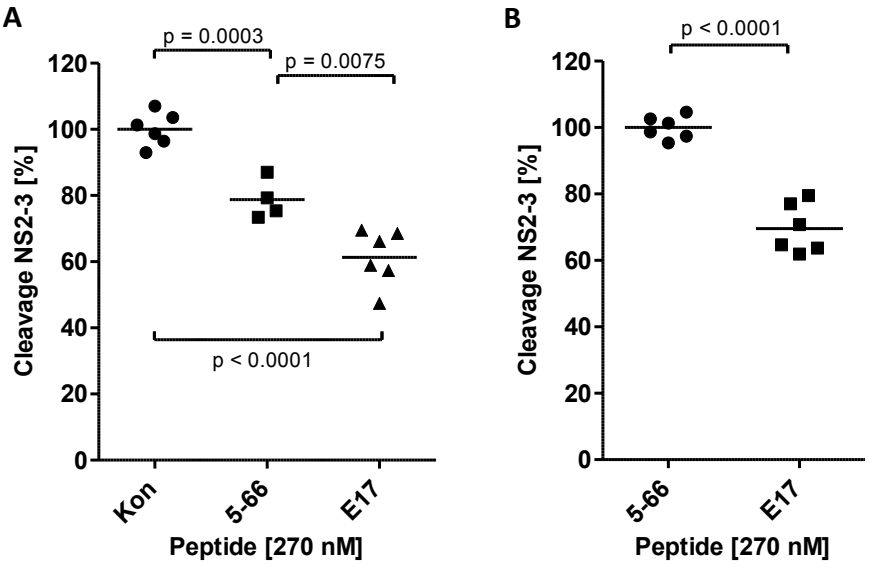

Figure 3-14: Inhibitory effect of peptides on NS2-3 protease cleavage. Con: positive control without peptide, K5-66: control with peptide Ant-K5-66, K17: sample with peptide Ant-K17. Protease 50nM, peptide 270 nM. **A:** the amount of cleaved protease of the control without peptide was set to 100%, **B:** the amount of cleaved protease with the control peptide K5-66 was set to 100%. P-values were calculated with *GraphPad Prism* (unpaired t-test with two-tailed p-value and 95% confidence interval).

The control peptide K5-66 reduced the protease cleavage to about 80% compared to the control without peptide. This is statistically significant with a p-value below 0.05. The peptide K17 showed reduction of protease cleavage to about 60% which is statistically significant (p-value below 0.05) also in comparison to the control peptide K5-66. In direct comparison to the peptide K5-66 the protease processing is reduced to about 70% for peptide K17 at 270 nM.

The concentration dependency of the inhibitory effect of peptide K17 was tested at three different concentrations. The results are shown in Figure 3-15.

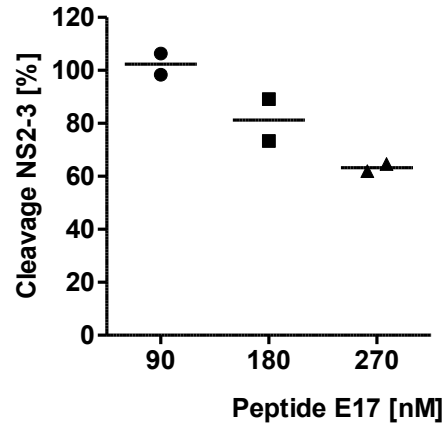

Figure 3-15: Concentration dependence of inhibitory effect of peptide Ant-K17 on NS2-3 protease cleavage. Mean value of NS2-3 cleavage of control peptide Ant-K5-66 was set to 100% for each concentration.

The inhibition of protease cleavage is concentration dependent for the peptide K17. At a peptide concentration of 90 nM no inhibition was detectable compared to the control peptide K5-66.

NS2-3 protease dialysed against 0.75 M guanidine HCl supplemented with Zn^{2+} refolds and forms protease dimers but undergoes no self-processing under these conditions (Pallaoro *et al.*, 2001). To analyse the effect of the peptide K17 on refolded protease the assay was done with dialysed protease. In Figure 3-16 the results of two experiments are shown.

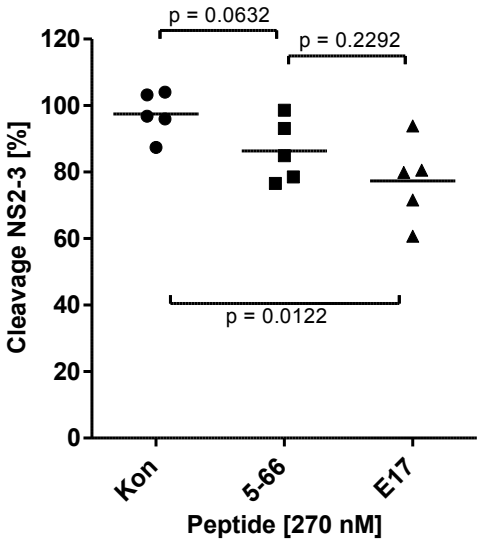

Figure 3-16: Inhibitory effect of peptides on NS2-3 cleavage with prior refolded MBP-NS2-3 protease. Con: positive control without peptide, K5-66: control with peptide Ant-K5-66, K17: sample with peptide Ant-K17. Protease 50 nM, peptide 270 nM. The cleaved protease of the control was set to 100%. P-values were calculated with *GraphPad Prism* (unpaired t-test with two-tailed p-value and 95% confidence interval).

The inhibitory effect of the peptide K17 is reduced in the activity assay when measured with refolded protease. 77% of the NS2-3 protease is cleaved compared to the control without peptide. With the control peptide K5-66 the processing of the protease is reduced to about 87%. The inhibitory effect of the peptide K17 is statistically significant (p-value below 0.05) when compared to the control without peptide but the values show a high fluctuation around the mean value.

3.2 NS3/4A protease

3.2.1 Production and activity of recombinant NS3/4A protease

The HCV NS3/4A protease was produced with the pMAL expression system (New England BioLabs) similar to the NS2-3 protease. The DNA encoding the NS3/4A protease was inserted into the pMAL-c4E vector down-stream from the *malE* gene, which encodes the maltose-binding protein (MBP). This results in the expression of a MBP-NS3/4A fusion protein with a 23 aa linker between MBP and protease. A single chain form of the NS3 protease domain linked to the NS4A cofactor peptide was produced according to Dimasi and co-workers. It consists of the residues 21 – 34 of the NS4A peptide and the residues 2 – 180 of the NS3 serine protease domain which are connected by a GG linker (see Figure 3-17 A and B). For PCR amplification the HCV replicon 'I389/NS3-3'UTR' which was constructed from the consensus sequence of genotype 1b isolate cDNA served as a template (Lohmann *et al.*, 1999). The primer 'primNS3/4A' and 'primNS3/4a-rev' which introduced a KpnI and PstI restriction site, the N-terminal NS4A peptide with the GG-linker and a C-terminal His-Tag with a short linker were used. It was intended to use the MBP protein for immobilisation of the protease during affinity enrichment and the His-Tag for IMAC purification of the protein after production in *E. coli*. The NS3/4A insert was ligated into the dephosphorylated pMAL-c4E vector which was also cut with the restriction enzymes KpnI and PstI and transformed into *E. coli* Top10 F´cells.

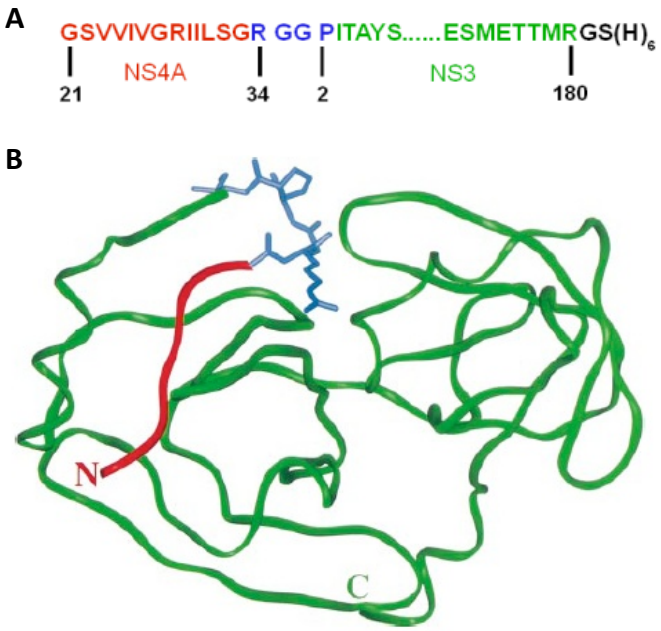

Figure 3-17: Single chain NS3/4A. A: Sequence of the single-chain NS3/4A. Residues 21 – 34 of NS4A and residues 2 – 180 of NS3 were connected by a GG linker. The C-terminal His-Tag with linker is shown. **B:** Model of single chain NS3/4A, NS4A: red, NS3: green, linker with neighboring amino acid of NS3 and NS4A is shown in blue (RGGP) (modified from Dimasi *et al.*, 1998).

The MBP-NS3/4A fusion protein was produced in soluble form at 30°C. The protease was purified by IMAC and the elution fraction dialysed against buffer D. The dialysed protease was stored at -80°C until usage. In Figure 3-18 A the results of the production and purification of the MBP-NS3/4A protein are shown. The protease could be produced and purified in suitable amounts and purity. The

full-length of the protease and the purification of the correct protein was confirmed by InVision His-tag In-gel staining (see Figure 3-18 B).

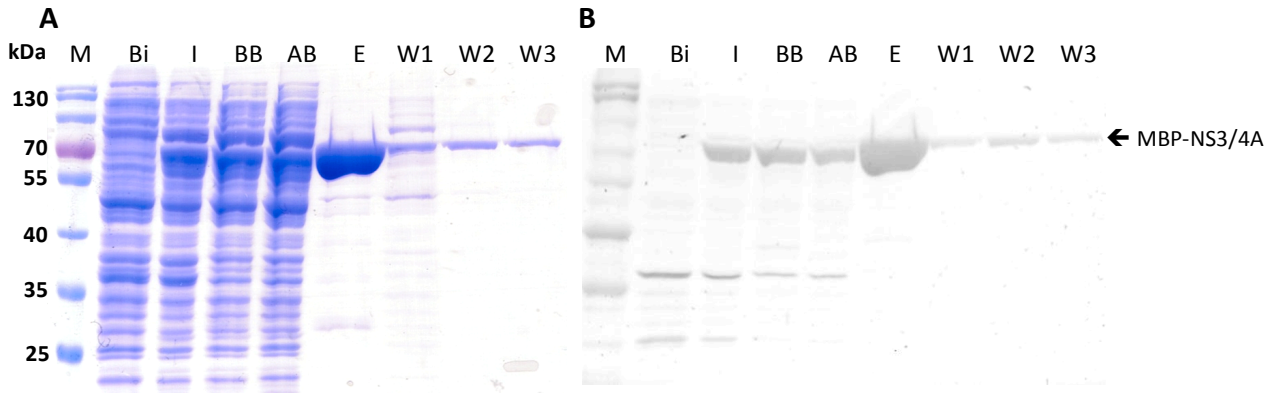

Figure 3-18: Production and purification of MBP-NS3/4A. 12% SDS-gel, M: molecular weight marker, BI: before induction, I: 3 h after induction, BB: before binding, AB: after binding; W1-3: washing fractions, E: elution fraction. 3 µl of each fraction were loaded onto the gel, except for the elution fraction: 1 µl. **A:** Coomassie stained SDS-page, **B:** 'InVision His-tag In-gel Stain' stained SDS-gel.

The concentration of purified MBP-NS3/4A was determined by densitometric measurement of the Coomassie stained protein bands and comparison to a MBP standard. Concentrations of up to 7 mg/ml of MBP-NS3/4A could be obtained.

The activity of the purified NS3/4A protease was tested with a fluorescence resonance energy transfer (FRET) assay (Taliani *et al.*, 1996; Misialek *et al.*, 2009). Figure 3-19 shows the results for various protease concentrations. The NS3/4A protease was active and therefore in a native active conformation and could be used for an affinity enrichment. The correct folding of the NS3/4A single-chain construct was later confirmed by structure determination (see 3.2.7.2).

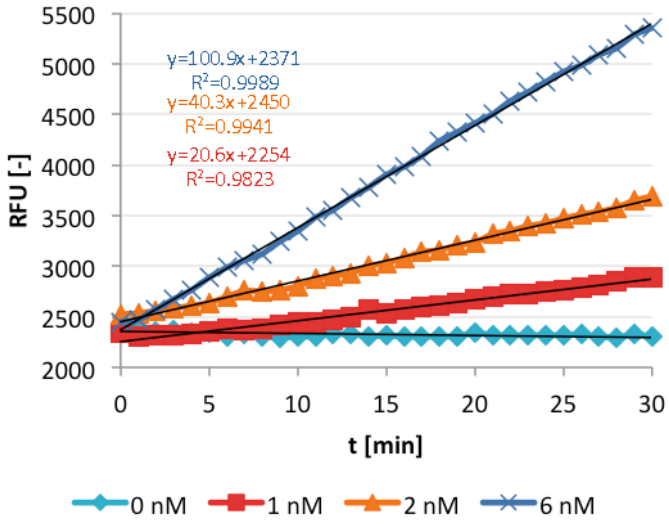

Figure 3-19: Activity assay with MBP-NS3/4A protease. Assay was done in buffer M2235 with 5 µM substrate M-2235 (Bachem) and 0, 1, 2 or 6 nM NS3/4A. Excitation filter: 360/40 nm, emission filter: 460/40 nm, RFU: Relative Fluorescence Units. Equation of trend lines are shown.

3.2.2 Panning against NS3/4A protease

For affinity selection of inhibitory peptides against the NS3/4A protease with the peptide phage display library CPL19YS-2 various panning conditions were used (see Table 3-4). The protease was immobilised in microtiter plates (MTPs) or on magnetic beads. In MTPs the protease was bound via immobilised anti-MBP IgG which binds the MBP of the fusion protein. The magnetic beads have covalently bound amylose or anti-MBP IgG on their surface for binding of the MBP. For the affinity selections two different panning buffers were used: one buffer with a high salt concentration of about 140 mM (1xPBS) and one buffer with no salt (buffer H). For the binding of the NS3/4A substrates or for the binding of known peptide inhibitors ionic interactions are important (Ingallinella *et al.*, 1998). For an initial enrichment a buffer with a low ionic strength was used to strengthen the possible ionic interactions of peptides and protease. Bound phage were eluted by acidic and competitive elution. Acidic elution is a nonspecific elution which elutes all bound phage by denaturing the target protein through change of the pH. For competitive elution a known NS3/4A inhibitor N-1725 (Bachem) was used which binds at the subsites S1 – S6 of the protease and has an IC_{50} value of 40 nM at 150 nM NaCl (Ingallinella *et al.*, 1998).

Table 3-4: Panning conditions of affinity selections on NS3/4A protease. MTP: microtiter plate, PR: panning round.

Immobilisation method	Salt [mM]	Elution method	Enrichment of peptides
Amylose and anti-MBP Beads	140	acidic competitive	no
MTP	140	acidic competitive	no
Anti-MBP Beads	0	acidic competitive	no
MTP	0	acidic competitive	yes

Only the panning in MTPs with a low ionic strength buffer led to the enrichment of peptides with acidic and competitive elution. For each panning round 1 µg MBP-NS3/4 protease was immobilised on 200 ng anti-MBP IgG and about 1 – 4 x 10^{11} peptide phages in buffer H were used for selection. To reduce unspecific binding and specific binding to either the MBP or the anti-MBP IgG, the peptide phagemid were incubated on immobilised MBP prior to selection on the NS3/4A protease. After selection unbound phage were removed by 10-fold washing with buffer H (0.05% Tween 20). The panning was performed by Juliane Lindner. In Figure 3-20 the sequences of peptides after the 5th panning round of acidic elution and after the 6th panning round of competitive elution are shown.

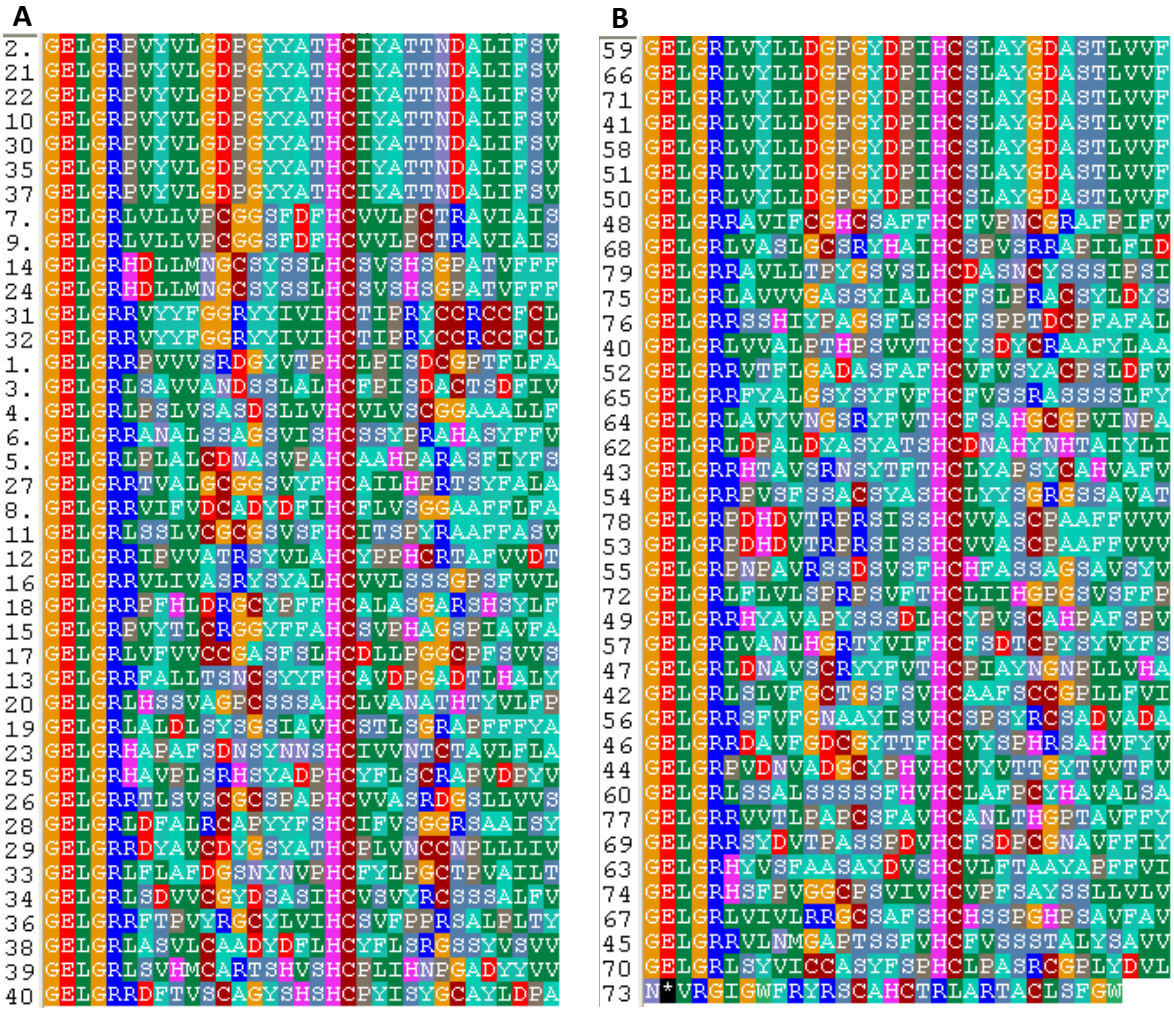

Figure 3-20: Amino acid sequences of single clones after the 5th or 6th panning round on NS3/4A protease with phage display peptide library CPL19YS-2. A: Sequences of 40 single clones after the 6th panning round with competitive elution, B: Sequences of 39 single clones after the 5th panning round with acidic elution.

Both elution conditions led to the enrichment of one clone. Clone K5-66 for the acidic elution after the 5th panning round and clone K6-10 for the competitive elution after the 6th panning round. Also two clones, K5-78 and K6-7, were identified which were found in a previous panning round (see Table 3-5). The clone K5-66 showed the highest enrichment being present as 70% of all sequenced clones after the 6th panning round. The peptide sequences of clones K5-66 and K6-10 show a homology in their sequence. They have a similar quite hydrophobic 9 aa long motiv in the N-terminal part of the peptide that is interrupted by an aspartic acid: V-Y-L/V-L-D/G-G/D-P-G-Y (see Table 3-5).

Table 3-5: Peptides enriched in 'low salt panning' against MBP-NS3/4A protease in MTP. Results of acidic and competitive elution. PR: panning round. Constant sequence parts are coloured in blue and homologies are coloured in orange.

Elution method	Clone name	Sequence	Number of clones	
			5. PR	6. PR
acidic	K5-78	GELGRPDHDVTRPRSISSHCVVASCPAAFFVVV	2 (5%)	1 (2.5%)
acidic	K5-66	GELGRLVYLLDGPGYDPIHCSLAYGDASTLVVF	7 (17%)	29 (72.5%)
competitive	K6-10	GELGRPVYVLGDPGYYATHCIYATTNDALIFSV	-	7 (17.5%)
competitive	K6-7	GELGRLVLLVPCGGSFDFHCVVLPCTRAVIAIS	2 (5%)	2 (5%)

Specific binding of the enriched peptides to the NS3/4A protease was analysed by phage ELISA. MBP-NS3/4A was immobilised over anti-MBP IgG and incubated with peptide-presenting phagemid particles. Bound phage were detected by an anti-M13 IgG HRP conjugate. Immobilised MBP, anti-MBP IgG alone and helper phage M13K07 were used as controls. In Figure 3-21 the results for the clones K6-10, K6-7, K5-66 and K5-78 are shown.

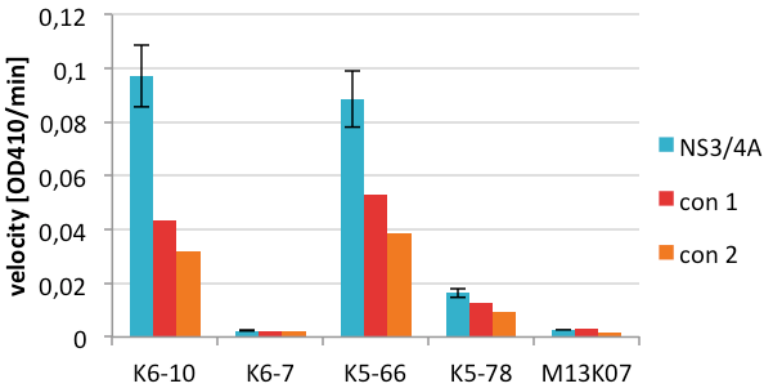

Figure 3-21: Phage ELISA with enriched clones K6-10, K6-7, K5-66 and K5-78. Binding of peptide presenting phage particles to NS3/4A protease was analysed. 1 µg MBP-NS3/4A was immobilised over anti-MBP IgG (200 ng), 1 x 10^9 phage/well in buffer H, detection of bound phage by anti-M13 IgG HRP conjugate, 3 washing steps before and after addition of detection antibody. Con 1: immobilised MBP control, con 2: immobilised anti-MBP IgG control, negative control with M13K07 helper phage. Measurements with NS3/4A protease were done in duplicate.

The peptides K6-10 and K5-66 show specific binding to the NS3/4A protease but also a high background binding to the controls. The peptide phage of the clones K6-7 and K5-78 do not show specific binding to the NS3/4A protease. The binding to the MBP control is as high as to the protease. The phage ELISA with the peptides K6-10 and K5-66 was optimised by variation of the amount of peptide phage and by increasing the washing steps before and after addition of the detection antibody to reduce the amount of unspecific bound phage. Also the inhibitor used for competitive elution was added to the peptide phage to analyse if the peptides bind at the same epitope as the inhibitor. If the peptides bind at the same epitope the ELISA signal would be reduced because the inhibitor would block the binding site of the NS3/4A protease. In Figure 3-22 A and B the results of the phage ELISA are shown.

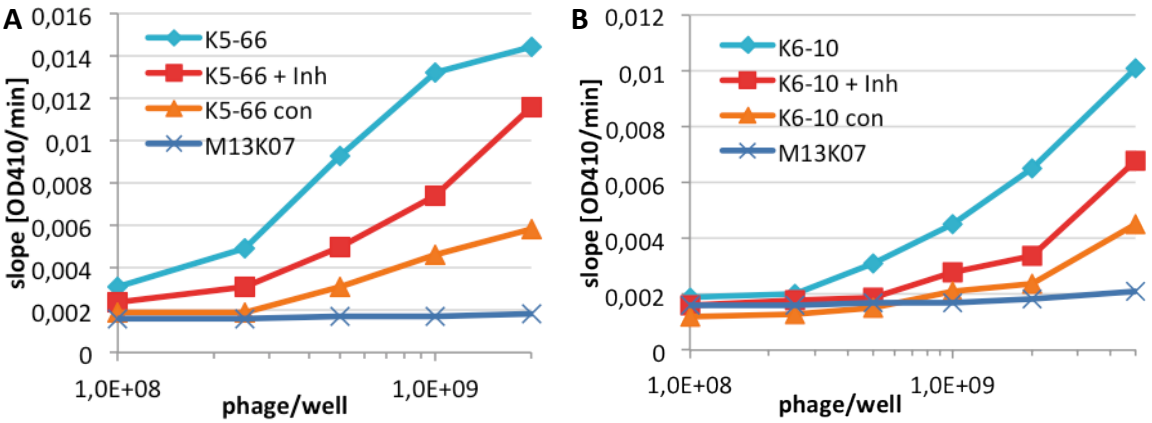

Figure 3-22: Phage ELISA with clone K5-66 (A) and K6-10 (B). Binding of peptide presenting phage particles to NS3/4A protease was analysed. Buffer: buffer H, 1 µg MBP-NS3/4A was immobilised over anti-MBP IgG (200 ng), detection of bound phage by anti-M13 IgG HRP conjugate, 6 washing steps before and after addition of detection antibody. Con: immobilised MBP control, + Inh: 1 µM NS3/4A inhibitor N-1725 (Bachem) added as competitor (Ingallinella *et al.*, 1998), negative control with M13K07 helper phage incubated on NS3/4A protease.

Both peptides show specific binding to the NS3/4A protease in a concentration dependent manner and only a low unspecific binding to the MBP control at lower phage concentrations. Also the peptides show a reduced ELISA signal when protease inhibitor was added during binding to the protease. This implies a competitive binding of the peptides K6-10 and K5-66 with the inhibitor and a binding at the same epitope of the NS3/4A protease.

3.2.3 Production of MBP fusion peptides

To test if the peptides K5-66 and K6-10 inhibit the NS3/4A protease activity the peptides should be produced without fusion to the M13 phage. Because of the length and the partly hydrophobic sequence of the peptides a chemical synthesis failed. Therefore it was attempted to produce the peptides in *E. coli* and purify them by IMAC. The peptides were produced with a N-terminal fusion to the maltose-binding protein to increase the solubility and molecular weight of the peptides.

The inhibitory peptides were produced with the pMAL expression system (New England BioLabs) similar to the NS3/4A protease. The DNA encoding the peptide was inserted into the pMAL-c4E vector down-stream from the *malE* gene, which encodes the maltose-binding protein (MBP). For PCR amplification the corresponding peptide phagemid DNA served as a template. The primer ‘pep-pMAL uni 5`’ and ‘pep-pMAL uni 3`’ which introduced a 3` PstI restriction site and a C-terminal His-Tag with a short linker were used. A 5` KpnI restriction site could not be used because of a KpnI site located at the C-terminal constant region of the library peptide (see also Figure 3-26). Therefore the pMAL-c4E vector was first cut with KpnI and the overhanging 3`end was removed using the T4 polymerase exonuclease activity. The blunt ended vector was cut with PstI and dephosphorylated. The phosphorylated peptide insert with 5` blunt end was ligated into the pMAL-c4E vector and transformed into *E. coli* Top10 F´cells. The MBP fusion peptides were produced in soluble form at 30°C. The MBP-peptides were purified by IMAC and the buffer of the elution fraction was exchanged with the use of centrifugal filter units with 10 kDa cut off. The peptides in buffer M2235 were stored at -80°C until usage. In Figure 3-23 the results of the production and purification of one peptide is shown as an example (see also appendix 7.2). The peptides could be produced and purified in suitable amounts and purity.

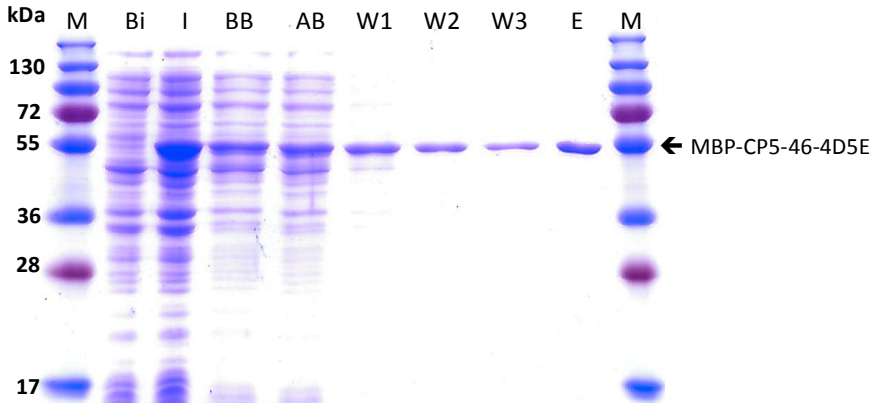

Figure 3-23: Production and purification of MBP-CP5-46-4D5E peptide. 12% SDS-gel, M: molecular weight marker, BI: before induction, I: 3 h after induction, BB: before binding, AB: after binding; W1-3: washing fractions, E: elution fraction. 3 µl of each fraction were loaded onto the gel, except elution fraction: 1 µl 1:5 dilution.

The concentration of purified MBP-peptide was determined by densitometric measurement of the coomassie stained protein bands and comparison to a MBP standard. Concentrations of up to 4.4 mg/ml of MBP-fusion peptides could be obtained.

3.2.4 Inhibition of NS3/4A activity

The MBP fusion proteins of the peptides K5-66 and K6-10 were tested in the NS3/4A activity assay if they have an inhibitory effect on protease activity. Various peptide concentrations were tested and the IC_{50} value was calculated with *GraphPad Prism* using a nonlinear regression model. In Figure 3-24 the results for both peptides are shown.

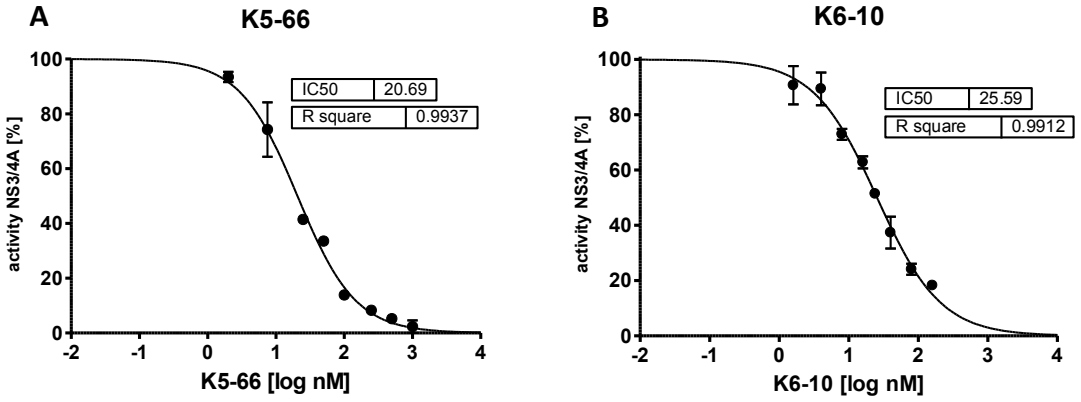

Figure 3-24: Determination of the IC_{50} of peptide K5-66 (A) and K6-10 (B) using the NS3/4A activity assay. Assay was done in buffer M2235 with 5 µM substrate M-2235 (Bachem) and 1 nM NS3/4A. Peptides produced as MBP fusion proteins with His-Tag. Excitation filter: 360/40 nm, emission filter: 460/40 nm. Velocity of fluorescence increase over one hour was compared to that of the NS2-K11 control peptide (K5-66) or MBP control (K6-10). Each measurement was done in duplicate, IC_{50} in nM. The curve was fitted with *GraphPad Prism* using a nonlinear regression model with variable slope and normalised response: $Y=100/(1+10^{((LogIC_{50}-X)*slope)})$.

Both peptides have an inhibitory effect on protease activity. Peptide K5-66 has an IC_{50} value of about 21 nM and peptide K6-10 of about 26 nM.

To analyse if the MBP or His-Tag have an inhibitory effect on the protease the peptide NS2-K11 that was not enriched in the panning against the NS3/4A protease was used as a control (see Figure 3-25). The peptide shows no inhibition of protease activity.

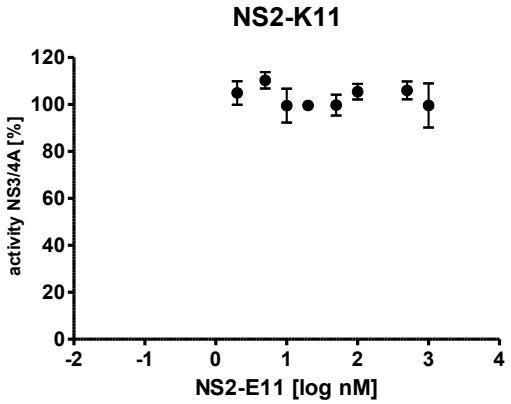

Figure 3-25: NS3/4A activity assay with control peptide MBP-NS2-K11. Assay was done in buffer M2235 with 5 µM substrate M-2235 (Bachem) and 1 nM NS3/4A. Peptide NS2-K11 produced as MBP fusion protein with His-Tag. Excitation filter: 360/40 nm, emission filter: 460/40 nm. Velocity of fluorescence increase over one hour was compared to that of a MBP control. Each measurement was done in duplicate

Also the N-terminal and C-terminal part of the peptides were tested separately to see which sequence is important for NS3/4A protease inhibition. These peptides were synthesised chemically. See Table 3-6 for results. In both cases the N-terminal part of the peptides, which comprises the homolog sequence motive, is important for inhibition of the protease and binds presumably to the active site. The inhibitory effect is reduced compared to that of the full length peptide, about 6-fold for peptide K5-66 and 9-fold for peptide K6-10. The C-terminal parts have no inhibitory effect at the tested concentrations but seem to work synergistically with the N-terminal parts.

Table 3-6: Inhibitory effect of peptides K5-66, K6-10 and their N- and C-terminal parts on NS3/4A activity. IC_{50} values were calculated with *GraphPad Prism* using a nonlinear regression model with variable slope and normalised response: Y=100/(1+10^((LogIC_{50}-X)*slope)). Constant sequence parts are coloured in blue and homologies are coloured in orange.

Peptide	Sequence	IC_{50} [nM]	K_i [nM]
K5-66	GELGRLVYLLDGPGYDPIHCSLAYGDASTLVVF	**20.7 ± 3.6**	**9.6 ± 1.7**
K5-66-A	GELGRLVYLLDGPGYDPI	125.4	58
K5-66-B	HCSLAYGDASTLVVF	>> 1µM	-
K6-10	GELGRPVYVLGDPGYYATHCIYATTNDALIFSV	**25.6 ± 3.5**	**11.8 ± 1.7**
K6-10-A	GELGRPVYVLGDPGYYAT	227.6	105
K6-10-B	HCIYATTNDALIFSV	>> 1µM	-
NS2-K11	GELGRLFVDFSSCYYYAAHCNIAPGGPPFVFAV	>> 1 µM	-
K5-66-R	GELGRIPSDTYDLAVGALHCPFYLVSGLVYLDG	>> 1 µM	-

3.2.5 Cosmix-plexing of inhibitory peptides K5-66 and K6-10

After initial selection rounds with the peptide phage display library CPL19YS-2 which yielded the inhibitory peptides K5-66 and K6-10 a recombination was done using the cosmix-plexing technique (Collins *et al.*, 2001) to further improve the affinity of the peptides. The pre-selected populations, after the 5th panning round with acidic elution, and after the 6th panning round with competitive elution were chosen for recombination. Both populations contain about 20% of the clone K5-66 or K6-10, respectively. The N-terminal parts of these peptides, which show sequence homology, bind presumably to the active site of the protease and seem to work synergistically with the C-terminal parts (see Table 3-6). It was intended to recombine the N- and C-terminal parts of the peptides with pre-selected peptides showing weak affinity to form novel ligands that exhibit stronger binding to the NS3/4A protease. Isolated phagemid DNA was recombined using the BsrDI restriction site. Recombination at this site shuffles the cassettes that are separated by the constant 'HC' motive in the middle of the library peptide (see Figure 3-26).

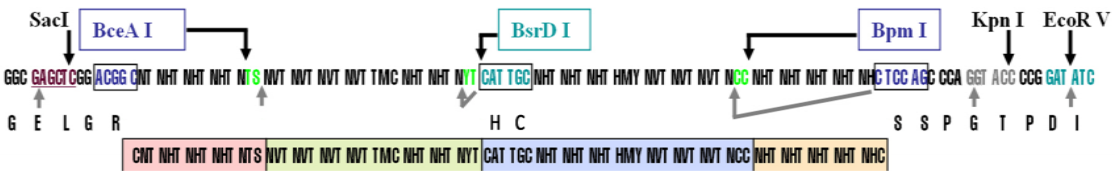

Figure 3-26: CPL19YS-2 library sequence. The four coloured boxes indicate the four cassettes of the library, constant aa are written beneath the nucleotide sequence. The recognition sequences and restriction sites of restriction enzymes are labeled, the three type IIs restriction enzyme sites are marked with a box (modified from Pollmann, 2010).

After cosmix-plexing of the pre-selected population after the 5th panning round with acidic elution and 6th panning round with competitive elution the number of single clones was 8.9 x 10^7 and 9.6 x 10^7, respectively. The effective recombination at the BsrDI site was confirmed by sequencing. The results from both recombinations are shown in Figure 3-27 A and B.

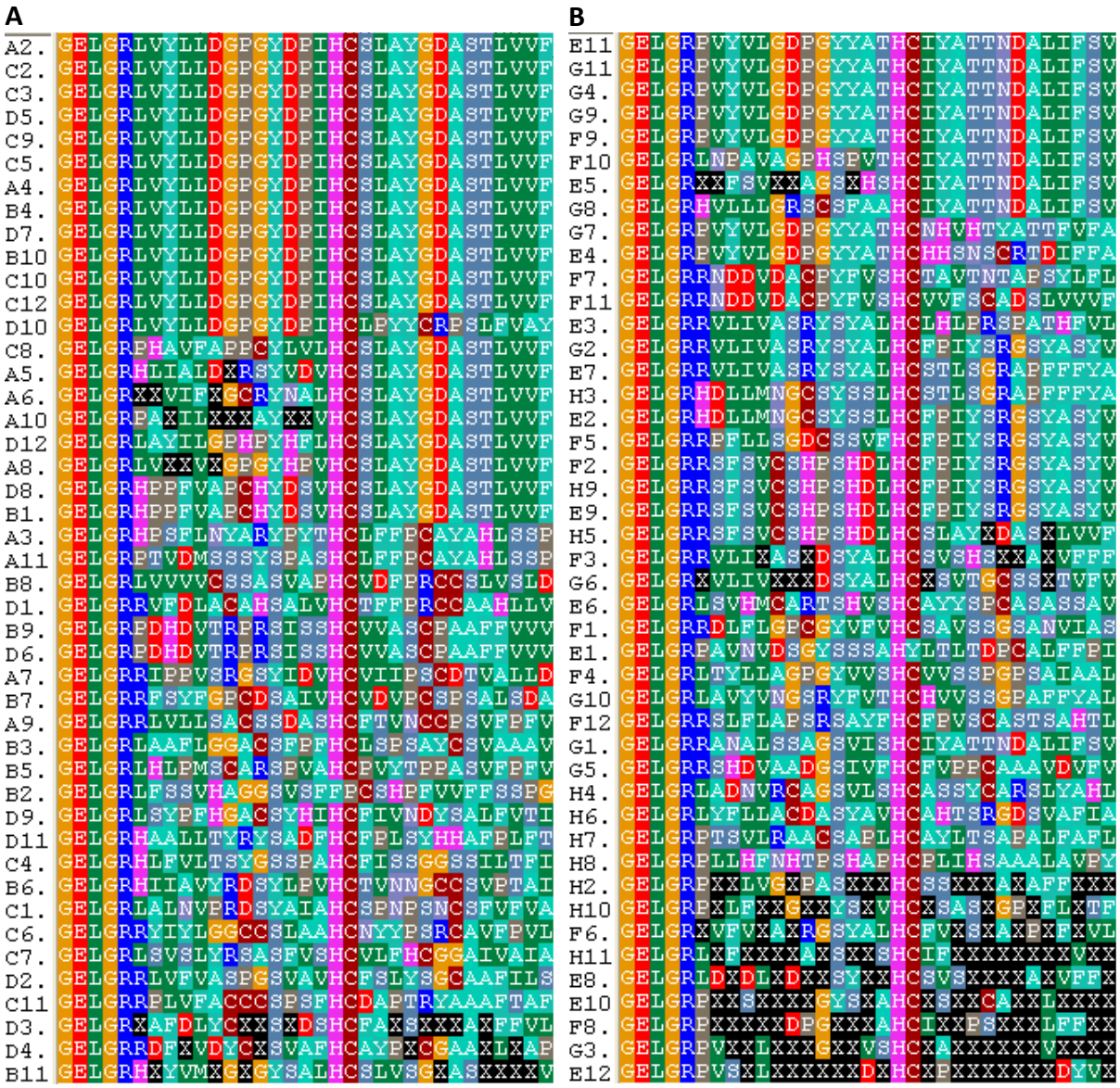

Figure 3-27: Amino acid sequences of 45 single clones after recombination with the cosmix-plexing method using the BsrDI restriction site. The eluted clones of the 5th panning round with acidic elution or 6th panning round with competitive elution were recombined. **A:** Sequences of single clones after the recombination of the 5th panning round with acidic elution, **B:** Sequences of single clones after the 6th panning round with competitive elution.

After cosmix-plexing several peptides with recognisable recombined sequences were found, e.g. A-D10, A-C8, A-A3, A-A11, B-F10 and B-G7. There was still a high proportion of 'original' or 'parental' peptides, e.g. K5-66 (25%, A-A2) and K6-10 (12%, B-E11). Notably for the peptide K5-66 most new variants have an 'original' C-terminus (A-C8 – A-B1). Also after recombination of the clones from the competitive elution 6th PR, an additional peptide (B-F2) was found that appears to have already been enriched and which had previously escaped identification.

The recombined variants of the acidic and competitive elution were packed in phagemid particles and submitted to further affinity selection. The panning was performed in a buffer with a salt

concentration of about 70 nM (0.5xPBS) to increase the stringency through weakening of ionic interactions. Bound phagemid particles were eluted by acidic elution. For each panning round 1 µg MBP-NS3/4 protease was immobilised on 200 ng anti-MBP IgG in MTPs and about 2 – 5 x 10^{11} peptide phage in 0.5xPBS were used for selection. To reduce unspecific binding and specific binding to either the MBP or the anti-MBP IgG, the peptide phagemid were incubated on immobilised MBP prior to selection on the NS3/4A protease. After selection unbound phage were removed by 16-fold washing (1. PR) or 20-fold washing (2. PR) with 0.5xPBS (0.05% Tween 20). In Figure 3-28 the sequences of peptides after the 2nd panning round are shown.

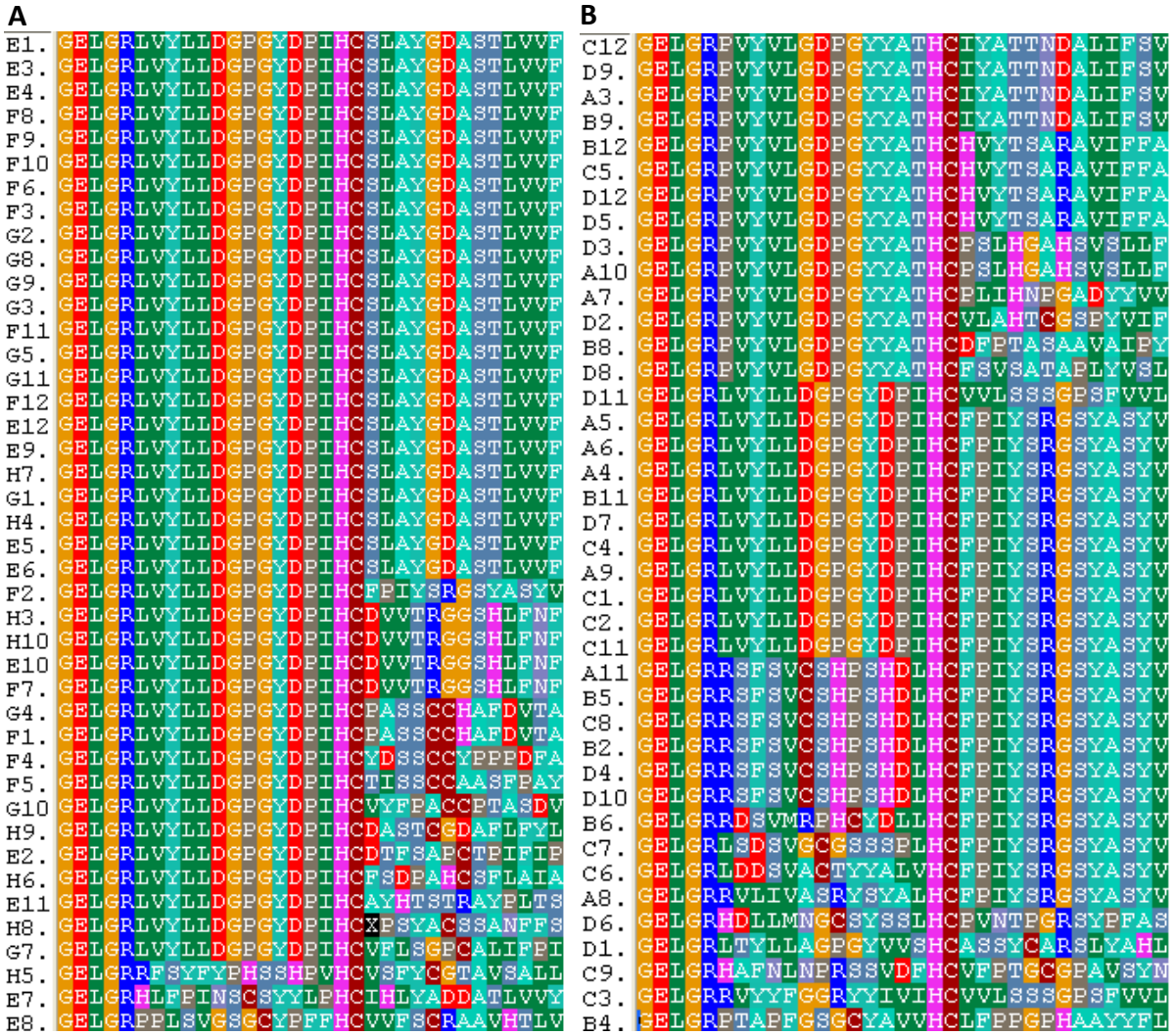

Figure 3-28: Amino acid sequences of single clones after the 2nd panning round after cosmix-plexing. A: Sequences of 42 single clones from panning with recombined sequences of the 5th panning round with acidic elution, **B:** Sequences of 40 single clones from panning with recombined sequences of the 6th panning round with competitive elution.

After two rounds of affinity selection with the recombined peptides of the 5th panning round with acidic elution an enrichment of the 'original' clone K5-66 (A-E1, about 55%) was seen. Also the N-terminal part of the clone K5-66 (A-F2 – A-G7, about 93%) was highly enriched. Some of the peptides with a different C-terminal sequence shared sequence homology. Two motives were enriched: S/T-R-G-G/(-)-S (clones A-F2 and A-H3) and S-S-C-C (clones A-G4 and A-F4). From the clones with a different C-terminal part the clone A-H3 showed the highest enrichment (about 10%).

After affinity selection with the recombined peptides of the 6th panning round with competitive elution an enrichment of various peptides was seen. The 'original' clone K6-10 (B-C12) was not enriched during panning (before: 12%, after: 10%), however, the N-terminal part did show an enrichment (35%). The enriched peptide that was first identified after recombination (B-A11) was also enriched during panning (before: 7.5%, after: 15%). Notably the C-terminal part of this peptide showed a strong enrichment (50%). Most interestingly a new variant with the N-terminal part of peptide K5-66 and the C-terminal part of clone B-A11 showed a high enrichment (25%) and was also found after affinity selection with the recombined peptides of the 5th panning round with acidic elution (clone A-F2). The clone K5-66 had not previously been identified in the panning with competitive elution.

Several clones were chosen for a phage ELISA (see Table 3-7).

Table 3-7: Peptides enriched in against MBP-NS3/4A protease after cosmix-plexing. PR: panning round. Constant sequence parts are coloured in blue and homologies are coloured in orange or green.

Peptide	Sequence
K5-66	GELGRLVYLLDGPGYDPIHCSLAYGDASTLVVF
CP5-46 (A-H3)	GELGRLVYLLDGPGYDPIHCDVVTRGGSHLFNF
CP5-11 (A-G4)	GELGRLVYLLDGPGYDPIHCPASSCCHAFDVTA
CP6-4 (A-F2, B-A5)	GELGRLVYLLDGPGYDPIHCFPIYSRGSYASYV
CP6-11 (B-A11)	GELGRRSFSVCSHPSHDLHCFPIYSRGSYASYV

An increase of the affinity of the enriched peptides to the NS3/4A protease was analysed by phage ELISA and comparison to the peptide K5-66. MBP-NS3/4A was immobilised on anti-MBP IgG coated MTPs and incubated with peptide presenting phagemid particles. Bound phage were detected by an anti-M13 IgG HRP conjugate. Immobilised MBP and helper phage M13K07 were used as controls. In Figure 3-29 the results with the clones CP5-46 (A-H3), CP5-11 (A-G4), CP6-4 (B-A5) and CP6-11 (B-A11) are shown.

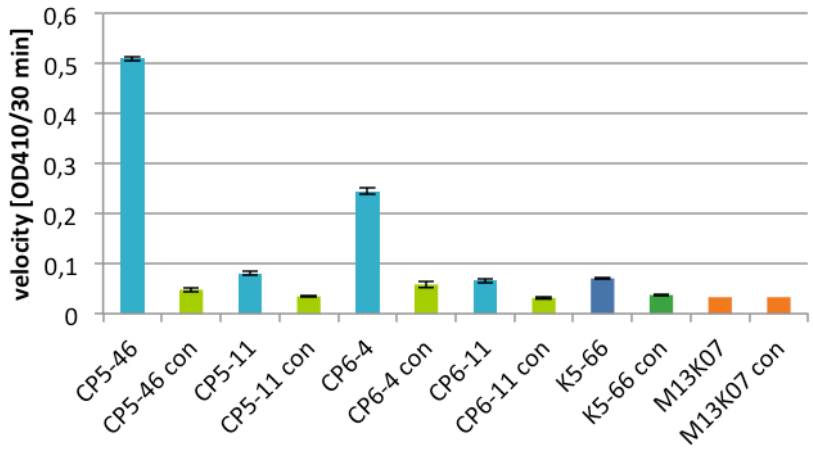

Figure 3-29: Phage ELISA with enriched clones after cosmix-plexing. Binding of peptide presenting phage particles to NS3/4A protease. 1 µg MBP-NS3/4A was immobilised over anti-MBP IgG (200 ng), 5 x 10^8 phages/well in 1xPBS, detection of bound phage by anti-M13 IgG HRP conjugate, 10 washing steps with 1xPBS before and after addition of detection antibody. con: immobilised MBP control, negative control with M13K07 helper phage. Measurements were done in duplicate.

The peptides CP5-46 and CP6-4 show an increased ELISA signal than the peptide K5-66 and should have a higher affinity to NS3/4A protease. The peptide phage of the clones CP5-11 and CP6-11 do not show show an increased ELISA signal compared to the peptide K5-66.

The peptides CP5-46, CP6-4 and CP6-11 were produced as MBP fusion proteins and tested in the NS3/4A activity assay if they have an increased inhibitory effect on protease activity compared to the peptide K5-66. Various peptide concentrations were tested and the IC_{50} value was calculated with *GraphPad Prism* using a nonlinear regression model. In Figure 3-30 the results for the peptides CP5-46 and CP6-4 are shown.

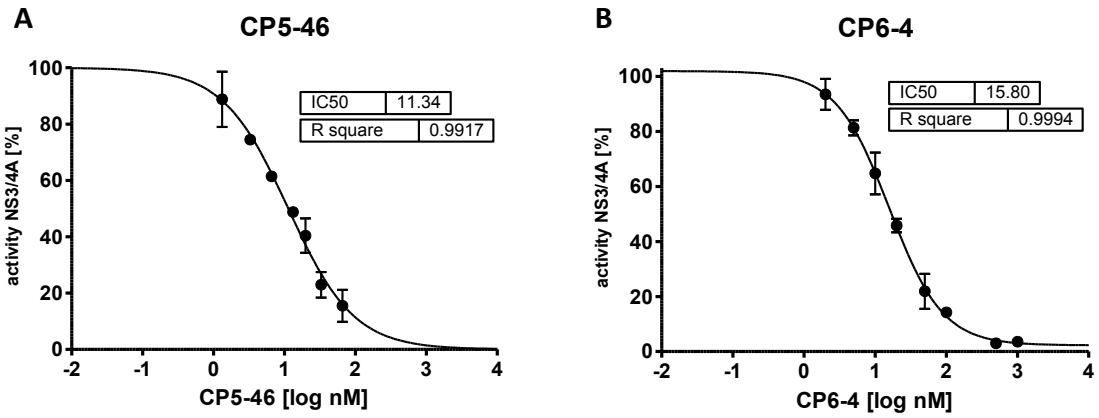

Figure 3-30: Determination of the IC_{50} of peptide CP5-46 (A) and CP-6-4 (B) using the NS3/4A activity assay. Assay was done in buffer M2235 with 5 µM substrate M-2235 (Bachem) and 1 nM NS3/4A. Peptides produced as MBP fusion proteins with His-Tag. Excitation filter: 360/40 nm, emission filter: 460/40 nm. Velocity of fluorescence increase over one hour was compared to that of the NS2-K11 control peptide. Each measurement was done in duplicate, IC_{50} in nM. The curve was fitted with *GraphPad Prism* using (A) a nonlinear regression model with variable slope and normalised response: Y=100/(1+10^((LogIC$_{50}$-X)*slope)) or (B) a nonlinear regression model with variable slope : Y=Bottom+(Top-Bottom)/(1+10^((LogIC$_{50}$-X)*slope)).

The peptide CP5-46 has an increased inhibitory effect on protease activity with an IC_{50} value of about 11.3 nM, i.e. the cosmix-plexing strategy had rapidly yielded two-fold improvement compared to the best peptide, K5-66, isolated before the recombination. The peptide CP6-11 (see appendix Figure 7-6 B) showed only a low inhibitory effect on NS3/4A protease activity with an IC_{50} value of about 2.4 µM (see Table 3-8). The peptide CP6-4 with the N-terminal part of K5-66 and the C-terminal part of CP6-11 showed an increase in the inhibitory effect with an IC_{50} value of about 15.8 nM. The recombination of pre-selected peptides using the cosmix-plexing technique resulted in novel ligands that exhibit stronger inhibition of the NS3/4A protease.

Table 3-8: Inhibitory effect of peptides enriched after cosmix-plexing on NS3/4A activity. IC_{50} values were calculated with *GraphPad Prism* using a nonlinear regression model with variable slope and normalised response. Constant sequence parts are coloured in blue and homologies are coloured in orange or green.

Peptide	Sequence	IC_{50} [nM]	K_i [nM]
K5-66	GELGRLVYLLDGPGYDPIHCSLAYGDASTLVVF	20,7 ± 3,6	9.6 ± 1.7
CP5-46	GELGRLVYLLDGPGYDPIHCDVVTRGGSHLFNF	11.3 ± 1.6	5.2 ± 0.75
CP6-4	GELGRLVYLLDGPGYDPIHCFPIYSRGSYASYV	15.8 ± 2.4	7.3 ± 1.1
CP6-11	GELGRRSFSVCSHPSHDLHCFPIYSRGSYASYV	~2.38 µM	~1.08 µM

All peptides that were tested in the NS3/4A activity assay were produced as MBP fusion proteins with an N-terminal MBP with a 23 aa linker and a C-terminal His-Tag. To analyse if the extensions have

an impact on the inhibitory effect the peptide CP5-46 was produced by chemical synthesis and tested in the NS3/4A activity assay. The synthetic peptide without N- or C-terminal fusions shows no significant difference in the IC_{50} value (see Table 3-9 and appendix Figure 7-6 A).

Table 3-9: Comparison of IC_{50} value of MBP-fusion peptide and synthetic peptide.

Peptide	IC_{50} [nM]
MBP-CP5-46	11.3 ± 1.6
CP5-46	13.3 ± 2.7

To more narrowly identify the most important inhibitory sequence motive of peptide CP5-46 that is important for inhibition of the NS3/4A protease, or rather to identify regions which contribute little or nothing to the inhibitory effect, several truncated peptides were tested in the activity assay. The results are shown in Table 3-10 (see also appendix Figure 7-7).

Table 3-10: Identification of the binding motive necessary for NS3/4A inhibition of peptide CP5-46. IC_{50} values were calculated with *GraphPad Prism* using a nonlinear regression model with variable slope and normalised response: Y=100/(1+10^((LogIC_{50}-X)*slope)). Constant sequence parts are coloured in blue.

Peptide name	Sequence	IC_{50} [nM]
CP5-46	GELGRLVYLLDGPGYDPIHCDVVTRGGSHLFNF	13.3
CP5-46-A	GELGRLVYLLDGPGYDPIHCD	124.0
K5-66-A	GELGRLVYLLDGPGYDPI	125.4
CP5-46-P1	RLVYLLDGPGYDPI	157.1
CP5-46-P3	DGPGYDPIHCD	>> 1µM
CP5-46-P4	DGPGYDPIHCDVVTRGGS	>> 1µM
CP5-46-R (control)	GELGRDIGGPLDLYPVDLHCY	>> 1µM

As seen before for inhibition of NS3/4A protease activity the N-terminal part of the peptide is important. Especially a part of the N-terminal constant region and the following hydrophobic amino acids are necessary for inhibition of the protease. Without the N-terminal hydrophobic amino acids (aa 6 – 10) the inhibitory effect is completely abolished (see Table 3-10 peptides CP5-46-P3 and P4). A synergy between the N-terminal and the C-proximal region is also implied.

3.2.6 Peptide cleavage and specificity

3.2.6.1 Specificity of the peptide CP5-46

The specificity of peptide CP5-46 for the NS3/4A protease was tested with three other serine proteases: chymotrypsin, trypsin and elastase. The reduction of the protease activity was measured in the presence of 50 µM peptide CP5-46. The known serine protease inhibitor aprotinin was used as a positive control at the same concentration. The results are shown in Figure 3-31. The peptide CP5-46 showed no inhibition of the tested serine proteases at a concentration of 50 µM.

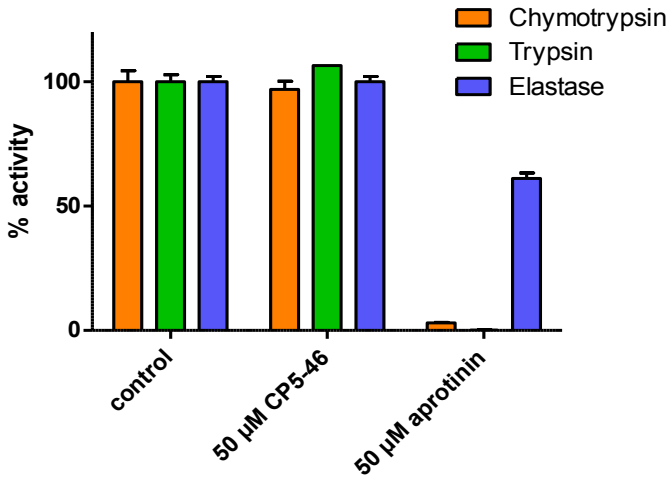

Figure 3-31: Specificity of the peptide CP5-46 for the NS3/4A protease. The inhibition of the serine proteases trypsin, chymotrypsin and elastase was tested. Trypsin: 5 µM protease, 800 µM substrate N-α-benzoyl-DL-Arg-pNA in 100 mM TrisHCl pH 8, 20 mM $CaCl_2$. Chymotrypsin: 300 nM protease, 200 µM substrate Succinyl-Ala-Ala-Pro-Phe-pNA in 40 mM Hepes pH 7.5, 15 mM $CaCl_2$. Elastase: 20 nM protease, 200 µM substrate Succinyl-Ala-Ala-Ala-pNA in 100 mM TrisHCl pH 8, 20 mM $CaCl_2$. Concentration of peptide CP5-46 and positive control aprotinin was 50 µM, control: enzyme without inhibitor. Absorbance increase at 405 nm was measured every 30 s for 20 min in a microplate reader. The slope of the absorbance increase of the control was set to 100%. Each measurement was done in duplicate.

3.2.6.2 Cleavage of peptide CP5-46 by the NS3/4A protease

To analyse if the peptide CP5-46 is cleaved by the NS3/4A protease 10 µM peptide was incubated with 1 µM protease for 16 hours at 30°C and the samples were analysed by LC/MS. LC/MS analysis was done by Dr. Raimo Franke (Department of Chemical Biology, HZI). The results are shown in Table 3-11. Almost no reduction of the peptide concentration was measurable after incubation with the protease and no cleavage fragments were found in the LC/MS spectra (data not shown). Therefore it can be assumed that the peptide is not cleaved by the NS3/4A protease.

Table 3-11: Cleavage of peptide CP5-46 by the NS3/4A protease. 10 µM peptide in buffer M2235 were incubated with 1 µM NS3/4A for 16 h at 30°C and analysed by LC/MS. Control: peptide without protease, NS3/4A: peptide with protease.

	Area CP5-46 [mAU x min]	%
control	8.187	100
NS3/4A	7.838	95.7

3.2.7 Structure-based optimisation

To further optimise the inhibitory peptide CP5-46 crystallisation of the NS3/4A protease in complex with the peptide was attempted. The structure of the peptide-protease complex which can be obtained by X-ray defraction of such crystals should show the exact site and geometry of binding and allow identification of the atoms involved in the interaction. Molecular modelling can then be applied to identify potential amino acids exchanges that might improve the potency of the peptide as an inhibitor.

3.2.7.1 Production of NS3/4A for crystallisation

For crystallisation experiments the HCV NS3/4A protease was produced as a single chain construct similar to the MBP-NS3/4A protease. The NS3/4A protease needed to be produced without MBP fusion because the flexible linker region would hamper crystal formation due to the conformational heterogeneity (Smyth *et al.*, 2003).

For production of the protease the pET expression system (Novagen) was used. In pET vectors the cloned DNA is under the control of the bacteriophage T7 transcription and translation signals for strong expression. For PCR amplification the HCV replicon 'I389/NS3-3'UTR' which was constructed from the consensus sequence of genotype 1b isolate cDNA served as a template (Lohmann *et al.*, 1999). The primer 'primNS3/4A-pET' and 'primNS3/4a-pET-rev', which introduced NcoI and XhoI restriction sites, the N-terminal NS4A peptide with the GG-linker and a C-terminal His-Tag with a short linker were used. The protease insert was ligated into the dephosphorylated pET28c vector, which was had also been cut with the restriction enzymes NcoI and XhoI and transformed into *E. coli* Rosetta 2 cells. The NS3/4A protease was produced in soluble form at 18°C. IMAC purification was carried out with the Profinia protein purification system (Bio-Rad). For the first purification step a 5 ml IMAC affinity cartridge and a 50 ml desalting cartridge and for the second purification step a 1 ml / 10 ml cartridges were used. The protease in 'Profinia Desalting Buffer 2' was stored at -80 °C until usage. In Figure 3-32 the results of the production and purification are shown.

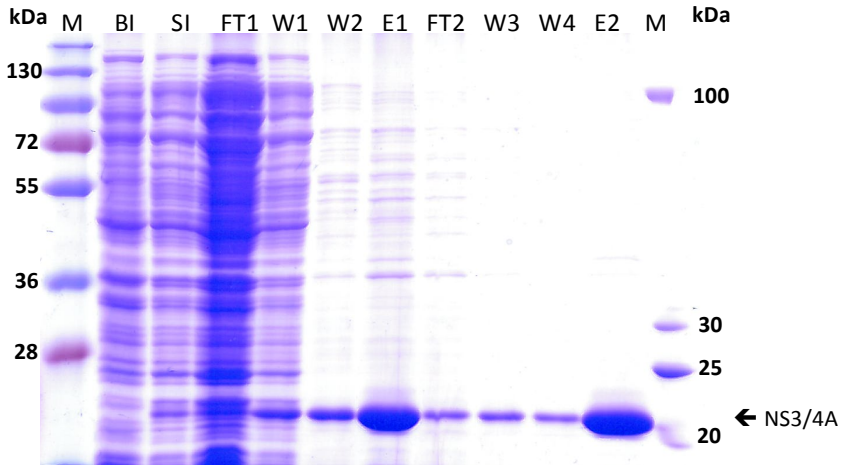

Figure 3-32: Production and purification of NS3/4A. 12% SDS-gel, M: molecular weight marker, BI: before induction, SI: soluble fraction after cell lysis (1:70), FT1: flow through 5 ml IMAC cartridge (1:10), W1-2: washing fractions 5 ml IMAC cartridge, E1: elution fraction 50 ml desalting cartridge, FT2: flow through 1 ml IMAC cartridge, W3-4: washing fractions 1 ml IMAC cartridge, E-2: elution fraction 10 ml desalting cartridge, 3 µl of each fraction were loaded onto the gel, except for the elution fractions: 1 µl.

Up to 8 mg NS3/4A protease could be purified from 2 L culture with a purity of > 90% as estimated from a SDS gel (see Figure 3-32). The concentration of purified NS3/4A was determined by UV spectroscopy at 280 nm and calculated with a theoretical molar absorption coefficient of ε_{280} = 18,450 $M^{-1}cm^{-1}$ (Calculated with ProtParam, Gasteiger *et al.*, 2005). Concentrations of about 90 µM (~2 mg/ml) of NS3/4A could be obtained.

The activity of the purified NS3/4A protease was tested with a fluorescence resonance energy transfer (FRET) assay (Taliani *et al.*, 1996; Misialek *et al.*, 2009). Figure 3-19 shows the results of both elution fractions. The NS3/4A protease of both fractions had the same specific activity as the MBP-NS3/4A protease produced for affinity enrichment (see Figure 3-19: 1 nM wild type protease 20.6 RFU/min). It was concluded that the protease is in a native active conformation and thus suitable for crystallisation studies.

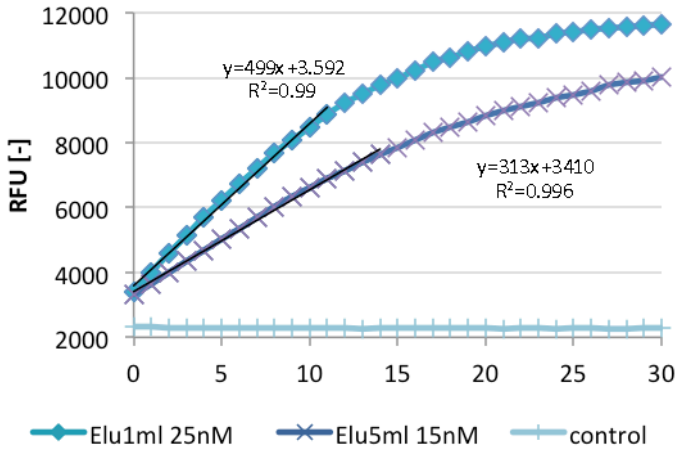

Figure 3-33: Activity assay with NS3/4A protease. Assay was done in buffer M2235 with 5 µM substrate M-2235 (Bachem) and 15 or 25 nM NS3/4A. Excitation filter: 360/40 nm, emission filter: 460/40 nm. Elu1ml: Elution fraction after IMAC purification with 1 ml affinity cartridge, Elu5ml: Elution fraction after IMAC purification with 5 ml affinity cartridge, control: 5 µM substrate M-2235 without NS3/4A protease, RFU: Relative Fluorescence Units. Equation of trend lines of the linear parts of the graphs are shown.

3.2.7.2 Co-crystallisation of NS3/4A with CP5-46 and CP5-46-A

Co-crystallisation experiments were done with the peptide CP5-46 and a truncated form CP5-46-A (see Table 3-12).

Table 3-12: Peptides used for co-crystallisation experiments.

Peptide name	Sequence	K_i[nM]
CP5-46	GELGRLVYLLDGPGYDPIHCDVVTRGGSHLFNF	5.2
CP5-46-A	GELGRLVYLLDGPGYDPIHCD	57.3

The peptides were co-crystallised with NS3-4A in several screening conditions containing high salt such as NaCl, KCl or $(NH_4)_2SO_4$. Crystals were obtained under several conditions although these were initially too small for X-ray diffraction measurement (see Figure 3-34 A). The conditions were optimised by stochastic optimisation and grid screening to a final condition with 0.1 M MES pH 6.0,

2.2 M KCl, 5% isopropanol (~100 µM NS3/4A, diluted with 0.1 M buffer, and ~500 µM peptide with a final molar ratio of protease and peptide of 1:5). Crystals for diffraction measurement could only be obtained for peptide CP5-46-A (see Figure 3-34 B).

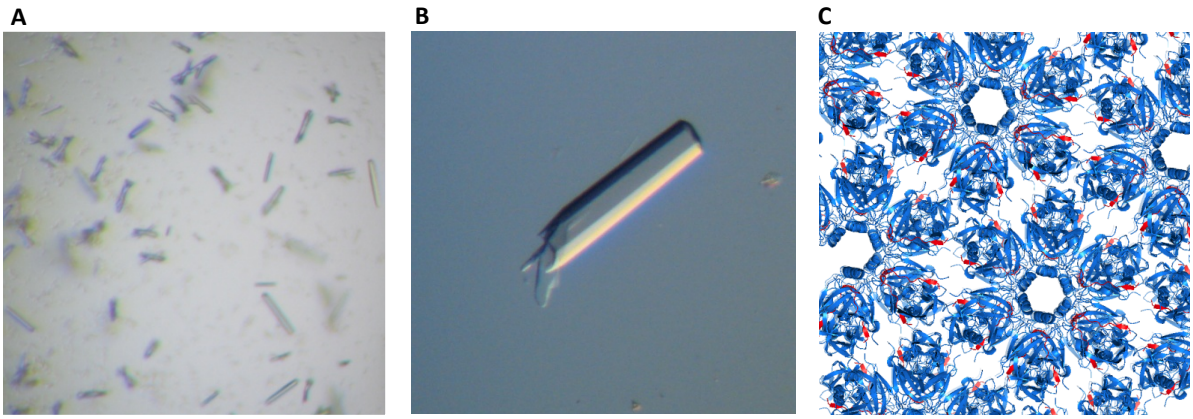

Figure 3-34: A: initial crystals of CP5-46-A / NS3/4A complex. **B:** optimised crystal of CP5-46-A / NS3/4A complex. **C:** crystal packing of CP5-46-A / NS3/4A complex. Space group P61. NS3/4A: blue, CP5-46-A: red.

The crystals diffracted to 2.1 Å and belonged to the hexagonal space group $P6_1$ with cell dimensions of a = b = 93.2 Å and c = 120 Å (see appendix Figure 7-9). The crystal packing of the complex is shown in Figure 3-34 C. X-ray diffraction measurements and model building was done by Dr. Stefan Schmelz (Department Molecular Structural Biology, HZI).

In Figure 3-35 A and B the resolved structure of the NS3/4A single chain construct is shown.

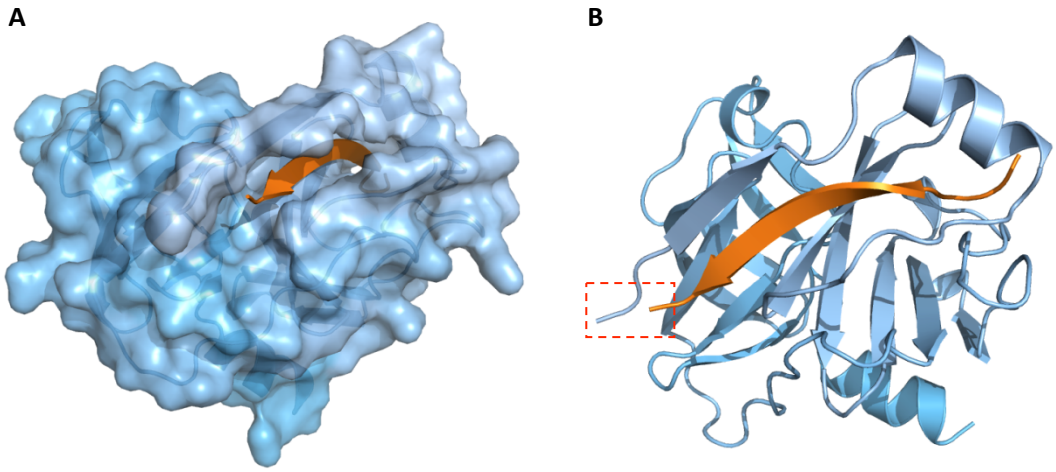

Figure 3-35: Structure of the single chain NS3/4A protease. The NS3 protease domain (blue) is shown with modeled surface (A) or as ribbon structure (B). The NS4 peptide is shown as ribbon structure (orange). The red square (B) shows the linker region between NS4A and NS3 (Figures A and B made by Dr. Stefan Schmelz).

Comparing to a previous crystal structure (Protein Databank code 1DXP) it was concluded that the NS3/4A protease was correctly folded. The N- and C-terminal sub-domains of NS3 formed two ß-barrel structures with the NS4 peptide contributing an additional ß-strand to the N-terminal sub-domain (Lin 2006). No electron density was observed for the flexible 'GG' linker between NS4A and NS3 (Figure 3-35 B, red square).

In Figure 3-36 A – D various views of the resolved structure of the peptide CP5-46-A bound to the NS3/4A protease are shown.

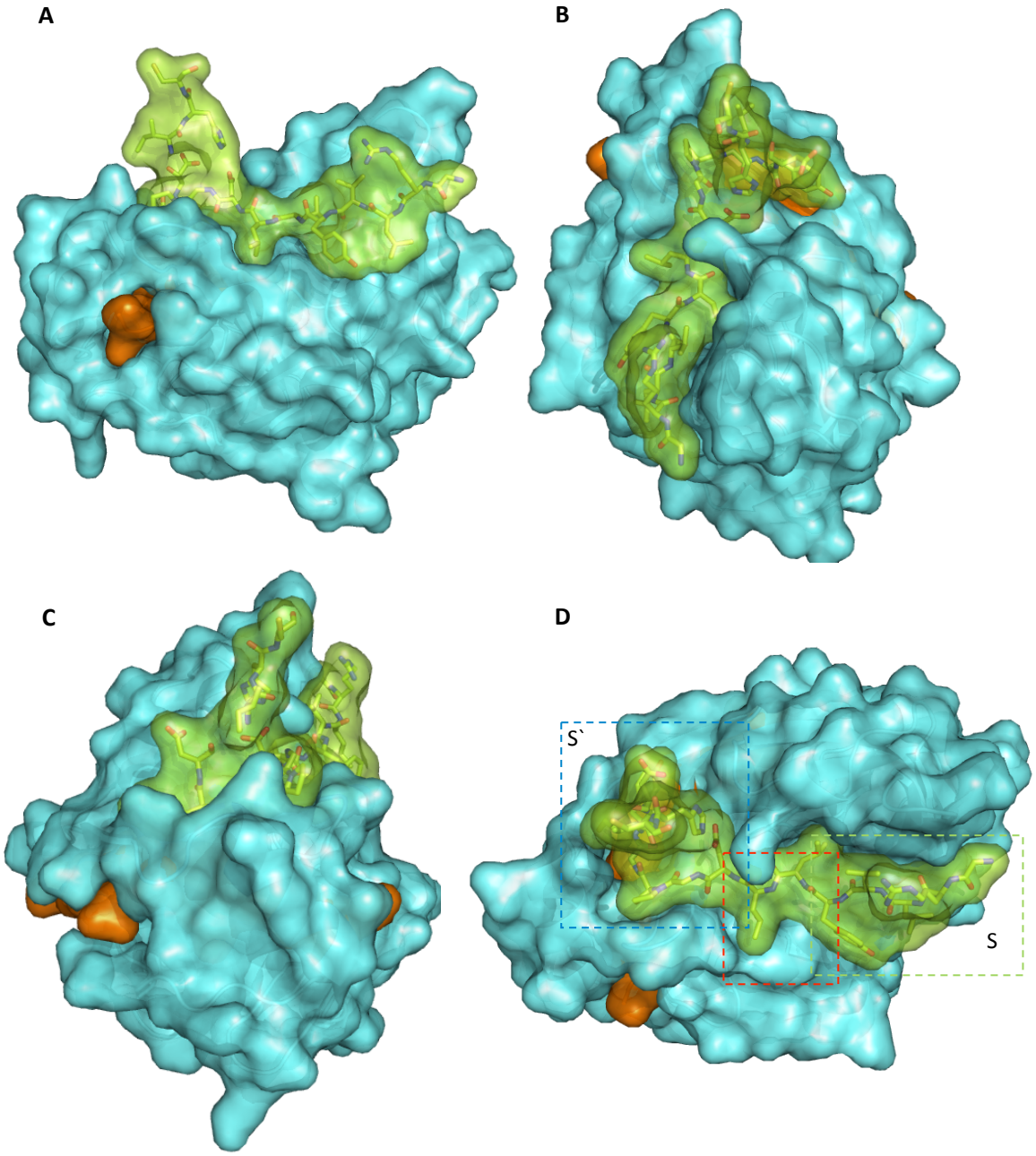

Figure 3-36: Structure of the bound peptide CP5-46-A (green) to the NS3 protease domain (blue) with NS4A cofactor (orange). The peptide is shown as stick structure with modeled surface and the NS3/4A protease is shown as ribbon structure with modeled surface. A – D: Views from different angles. (D) blue square: primed-site of the protease (S`), red square: active site region of the protease, green square: non-primed-site of the protease (S).

Electron density for the amino acids 4 – 20 of the peptide could be measured. CP5-46-A binds to NS3/4A covering a large part of the protease surface. The active site is covered (see Figure 3-36 D, red square) and the peptide is coordinated at several positions on the non-primed and primed site of the protease (see Figure 3-36 D, green and blue square).

In Figure 3-37 A – C the coordination of the peptide at the non-primed and primed site of the protease and the blocking of the active site are shown in detail.

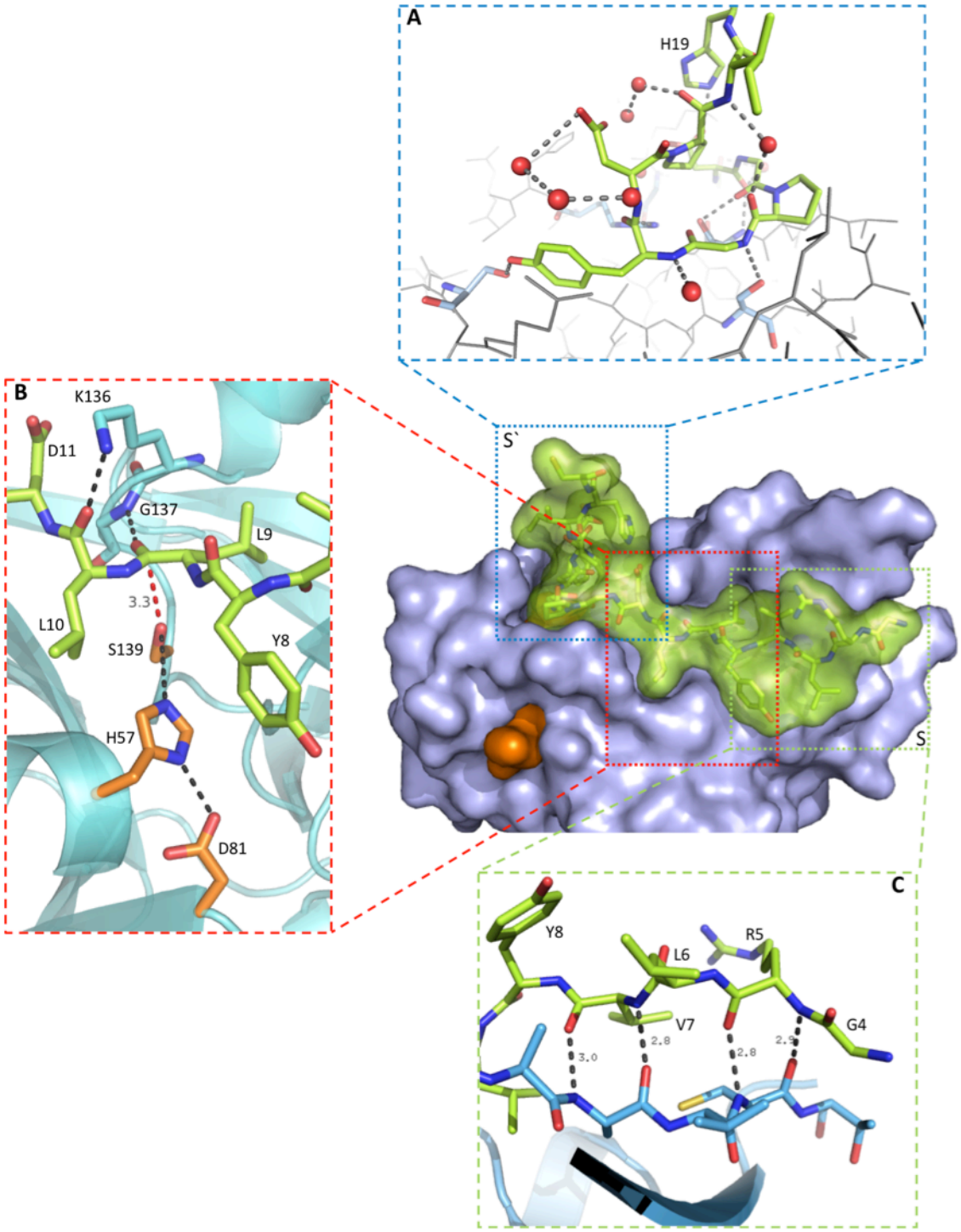

Figure 3-37: Detailed views on the interactions of peptide CP5-46-A (green) with NS3/4A (blue). A: primed site of the protease with bound 'proline'-finger motive, coordinated water molecules are shown as red dots. **B:** View on the active site of NS3/4A (blue) with bound peptide CP5-46-A (green). The side chains of the amino acids of the catalytic triad: S139, H57, D81 are shown as orange sticks. The distance between the S139 of the catalytic triad and the nearest peptide backbone (L9-L10) is shown in Å (red dashed line). H-bonds are indicated as grey dashed lines. **C:** non-primed site of the protease, peptide (green) forms ß-strand with backbone of the NS3/4A protease (blue) (Figures A and C made by Dr. Stefan Schmelz).

The substrate binding pockets of proteases are termed subsites. Non-primed subsites are numbered Sn – S1 from the N terminus of the substrate to the scissile bond and primed sites S1` – Sn` towards

the C terminus. The substrate residues binding to the pockets are numbered P1 – Pn and P1` – Pn`, respectively (see section 1.1.4). The C-terminal part of the peptide CP5-46-A, which is located at the primed site of the protease, forms a 'proline'-finger motive that binds to a pocket located next to the NS4A peptide (see Figure 3-37 A and Figure 3-39). The finger motive is coordinated by several hydrogen bonds and water molecules. His19 forms an intramolecular salt bridge with Asp11 stabilizing the structure, but removal of Cys20 and His19 from the peptide has no influence on the IC_{50} value (see Table 3-10).

The bound peptide covers the active site of the protease and the hydroxyl group of the Ser139 of the catalytic triad is over 3.3 Å away from the nearest peptide carbonyl carbon of Leu9 or Leu10 and therefore too far away for a nucleophilic attack (see Figure 3-37 B). The residues of the catalytic triad, namely Ser139, His57 and D81, are not directly affected by the binding of the peptide. The positioning of the side chain of His57 by D81 and the abstraction of a proton from Ser139 by His57 are not disturbed. Protease residues Lys136 and Gly137 are forming two hydrogen bonds with the peptide residues Leu9 and Leu10 moving the peptide backbone away from the active site residues. Notably the backbone amide of Gly137 is part of the oxyanion hole (Kim *et al.*, 1996). The S1` pocket can also bind larger side chains than that of the natural P1` residue Ser (Urbani *et al.*, 1997). The larger side chain of peptide P1` residue Leu10 has an auxiliary effect on moving the peptide backbone away from the active site residues.

The N-terminal part of the peptide, which binds to the non-primed site of the protease, forms an anti-parallel ß-strand with the backbone of the NS3/4A protease (see Figure 3-37 C). Four hydrogen bonds are formed between the backbone amide and carbonyl group of protease residues Cys159 and Ala157 and peptide residues Lys5 and Val7, respectively. Notably the same anti-parallel ß-strand is conserved between all protease substrates (Romano *et al.*, 2010). In Figure 3-38 the comparison of binding of peptide CP5-46-A and substrate 4B5A is shown. In the region of the anti-parallel ß-strand the binding of the peptide and substrate backbone (Gly4 – Leu6) is similar. In the region of the active site the peptide backbone is shifted away from the active site residues as described above.

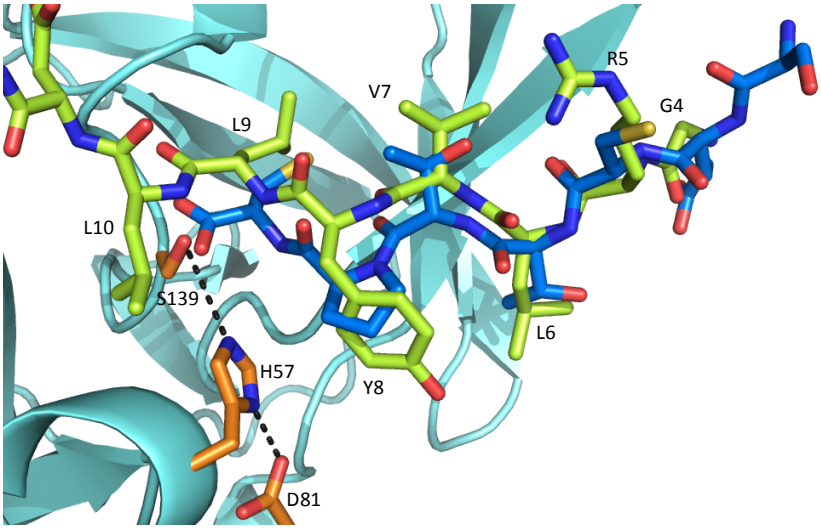

Figure 3-38: Comparison of binding of peptide CP5-46-A (green stick model) and substrate 4B5A (blue stick model). NS3 protease domain is shown as blue ribbon structure. The side chains of active site residues: S139, H57, D81 are shown as orange sticks. Substrate 4B5A (SECTTPC, PDB ID 3M5N, Romano *et al.*, 2010) was aligned with *Pymol*.

Notably the peptide CP5-46-A binds to regions of the substrate subsites S6 – S4` at the non-prime and prime region of the protease (see Figure 3-39). The anti-parallel ß-strand (R5 – V7) binds in the region of S5 – S3. In comparison to the natural substrate a negative charged amino acid at position P6 is missing that could interact with Lys165 or Arg163. Amino acids Tyr7 – Pro13 bind to the regions of the subsites S2 – S4`. The 'proline'-finger motive extends the binding of the peptide at the S` site of the protease to a region probably not occupied by the natural substrate.

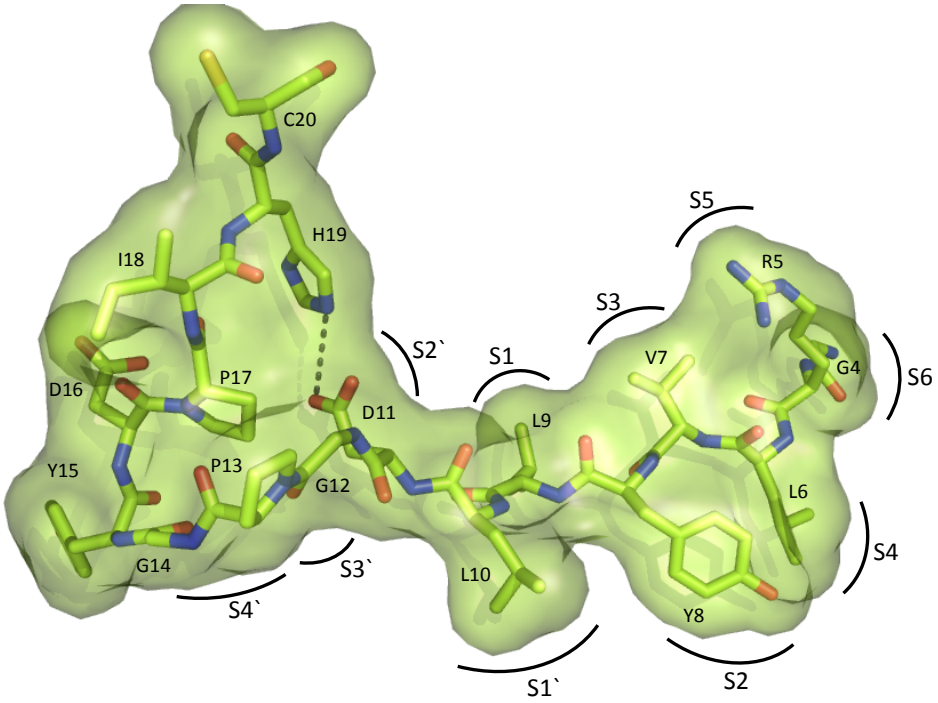

Figure 3-39: Structure of peptide CP5-46-A bound to the NS3/4A protease. The peptide is shown in stick representation with modelled surface. H-bond between H19 and D11 is indicated as grey dashed line. Location of the protease subsites are labelled with semi circles (positions from Ingallinella *et al.*, 2000 and Ingallinella *et al.*, 2002).

In Figure 3-40 the comparison of binding of peptide CP5-46-A and the peptidomimetic small molecule inhibitors boceprevir, TMC435 and ITMN-191 are shown.

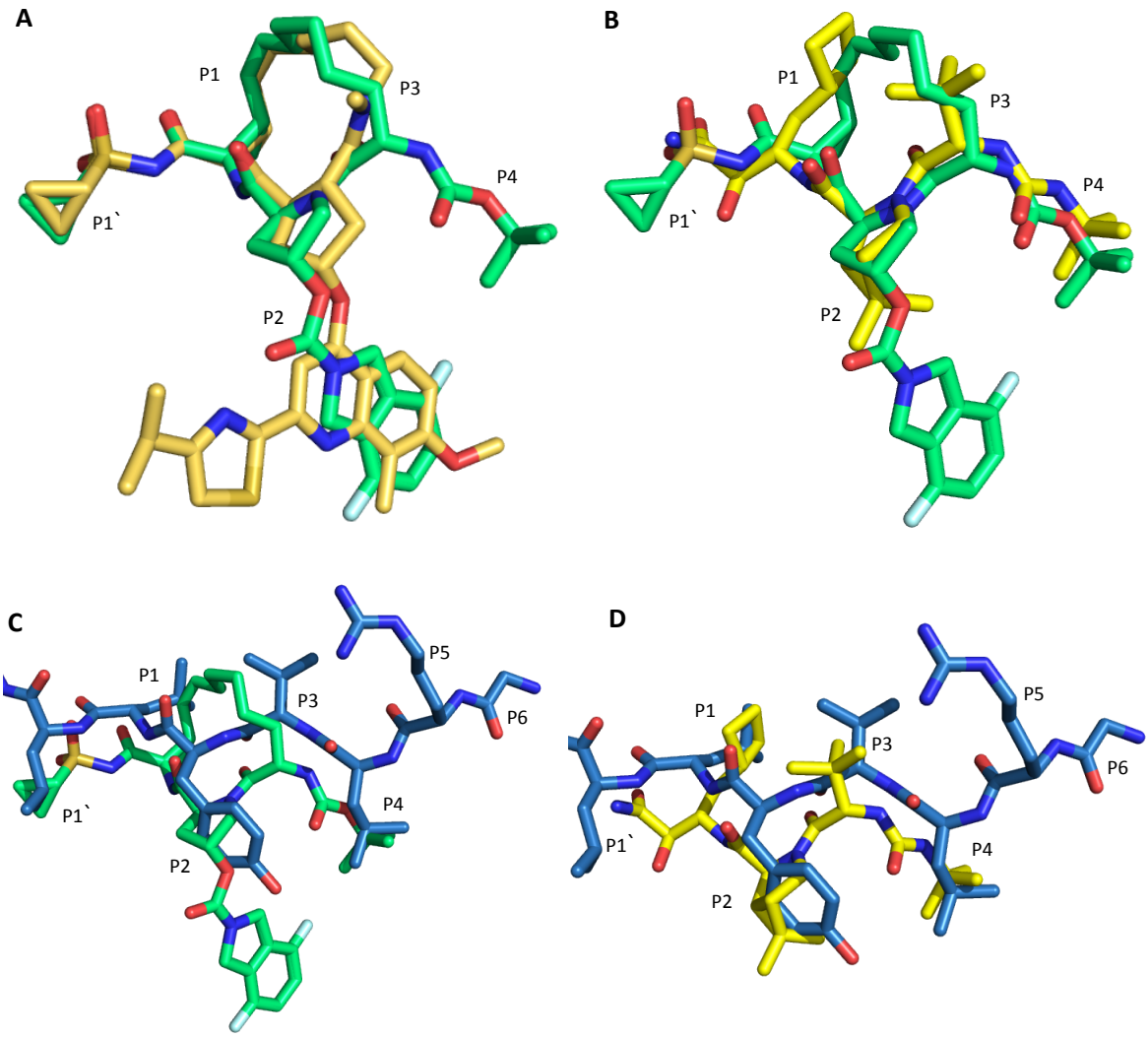

Figure 3-40: Comparison of binding of peptide CP5-46-A (blue stick model) and small molecule inhibitors boceprevir (yellow stick model, PDB ID 2OC8), TMC435 (brown stick model, PDB ID 3KEE) and ITMN-191 (green stick model, PDB ID 3M5L). A: Comparison of binding of TMC435 (brown stick model) and ITMN-191 (green stick model). **B:** Comparison of binding of boceprevir (yellow stick model) and ITMN-191 (green stick model). **C:** Comparison of binding of peptide CP5-46-A (blue stick model) and ITMN-191 (green stick model). **D:** Comparison of binding of peptide CP5-46-A (blue stick model) and boceprevir (yellow stick model). The residues binding to the protease subsites are indicated (P1` - P6). Structures were aligned with *Pymol*.

The two macrocyclic inhibitors TMC435 and ITMN-191, which are both developed from BILN-2061, have a similar structure with an almost identical binding pattern to the NS3/4A protease (Figure 3-40 A). Both inhibitors are bound at the active site, spanning the S3 – S1` subsites. A P1` cyclopropyl group binds to the S1` subsite of the NS3/4A protease. The P1 to P3 side chains are connected to a macrocycle. Both inhibitors have a large P2 substituent that binds to an extended S2 subsite. Additionally ITMN-191 has a P4 tert-butyl group that fits into the S4 subsite of NS3/4A (Cummings *et al.*, 2010; Romano *et al.*, 2010). The linear α-ketoamide inhibitor boceprevir binds to the S4–S1 subsites of the NS3/4A protease and shows almost the same binding of the backbone compared to the macrocyclic inhibitors (Figure 3-40 B). The functional groups are positioned similar and the binding to the S1 and S3 subsites is achieved with similar atom types. The P4 tert-butyl group of boceprevir is identical to that of ITMN-191 and shows the same binding at the S4 subsite (Romano *et al.*, 2010).

The peptide CP5-46-A has a different mode of binding than the small molecule inhibitors (Figure 3-40 C and D). The peptide backbone has a similar geometric structure but is shifted away from the active side residues of the NS3/4A protease compared to the small molecule inhibitors. The side chains of the peptide residues P1` – P4 are similar to the functional groups of TMC435, ITMN-191 and boceprevir. The P1` cyclopropyl group of TMC435 and ITMN-191 (see Figure 3-40 C) and the P1 cyclobutyl group of boceprevir (see Figure 3-40 D) are similar to the isopropyl side chains of Leu10 and Leu9, respectively. The functional groups are hydrophobic and the positioning in the protease subsites is very similar. The P3 functional groups of the small molecule inhibitors overlap closely with the P3 residue Tyr8 of the peptide and are also hydrophobic. The P4 tert-butyl group of the small molecule inhibitors is similar to the isopropyl side chain of the Leu6 residue of the peptide and is positioned similar in the S4 pocket. The same similarity is also seen for the functional group of the P3 residues of the peptide and boceprevir but the position of the bound side chains is different.

3.2.7.3 Structure-based optimisation of peptide CP5-46-A

Examination of the crystal structure of the complex, allowed a prognosis that exchanges at four positions for potential amino acid exchanges, might improve binding geometry and charge interaction between the peptide and the enzyme. It was envisaged that these could improve the inhibitory effect with respect to the peptide CP5-46-A:

Leu10 binds in the S1` pocket of the NS3/4A protease; modelling of the surface area of the side chain showed that the pocket is not completely occupied by the amino acid side chain (see Figure 3-41 A). Leu10 was exchanged to Asp, Glu or Gln for potential interaction with the side chains of protease residues Gln41, His57 or with the backbone of Gly58.

The S4 pocket is not fully occupied by the Leu6 residue (see Figure 3-41 B). An exchange of this Leu by Glu or Gln was suggested, which should allow a better potential interaction with the residues Arg155 or Arg123 of the NS3/4A protease.

Comparison of the bound peptide to the bound substrate residues P1 – P6 of the cleavage site 4A4B (PDB ID 3M5M, Romano *et al.*, 2010) revealed a similar binding of the peptide backbone and the substrate backbone of amino acids R5 and G6 of the peptide and P5-Glu and P6-Asp of the substrate 4A4B (see Figure 3-41 C). Positions P5 and P6 are important for the binding of the substrate 4A4B because of electrostatic interactions with basic amino acids especially interaction of P6-Asp with Lys165 of the NS3/4A protease (Steinkühler *et al.*, 1998; Koch *et al.*, 2001; Romano *et al.*, 2010). In order to imitate this binding it was proposed to exchange Gly4 to Asp4 and Arg5 to Glu5 mimicking the substrate 4A4B.

In order to facilitate the chemical synthesis and later handling of the peptide, Cys20 which is not important for binding of the peptide, was changed to a Ser20 (see Figure 3-41 D).

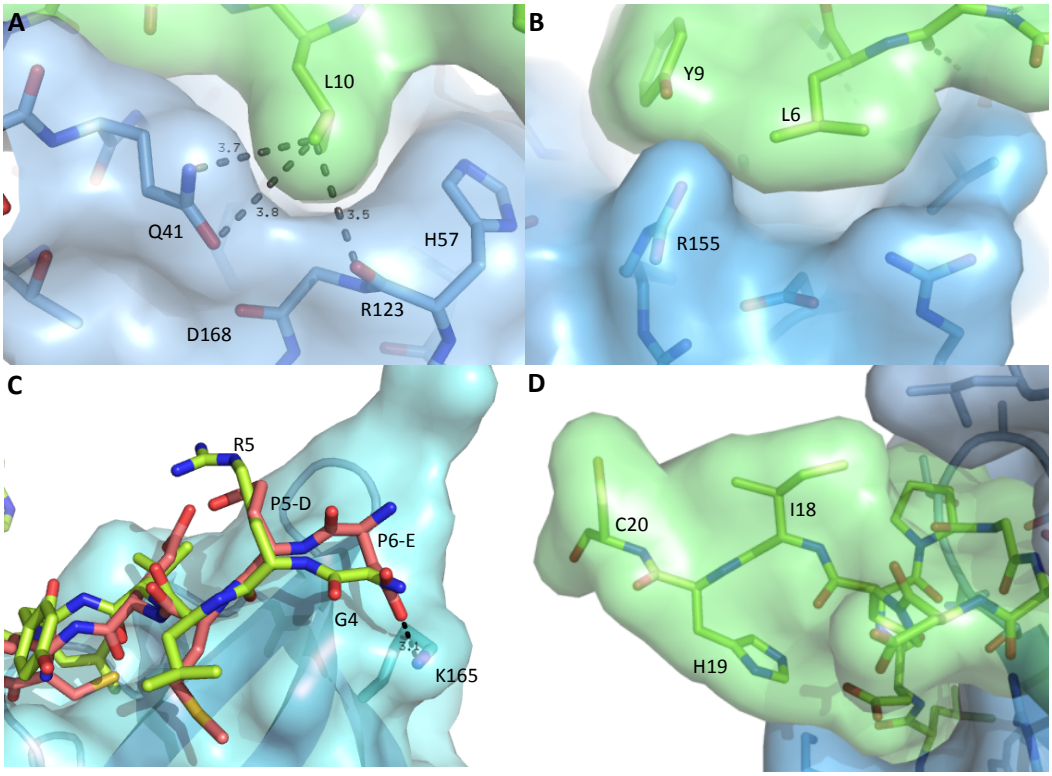

Figure 3-41: Potential sites of peptide CP5-46-A (green) for improvement. A: Leu10 binds in the S1` pocket of the NS3/4A protease (blue). **B:** S4 pocket is not fully occupied by the Leu6 residue. **C:** similar binding of the peptide and the substrate 4A4B (red) of amino acids R5 and G6 of the peptide and P5-D and P6-E of the substrate. **D:** Cys20 is not important for binding of the peptide (Figures A, B and D made by Dr. Stefan Schmelz).

All peptides with suggested amino acid exchanges were produced chemically and tested in the NS3/4A activity assay. The results of are summarised in Table 3-13 (see Figure 7-8).

Table 3-13: Comparison of IC_{50} values of the CP5-46-A variants.

Peptide	Sequence	IC_{50} [nM]
CP5-46-A	GELGRLVYLLDGPGYDPIHCD	124.0
CP5-46-A-4D5E	GELDELVYLLDGPGYDPIHS	**22.8**
CP5-46-A-6D	GELGRDVYLLDGPGYDPIHS	2.7 µM
CP5-46-A-6E	GELGREVYLLDGPGYDPIHS	>> 1µM
CP5-46-A-6Q	GELGRQVYLLDGPGYDPIHS	>> 1µM
CP5-46-A-10Q	GELGRLVYLQDGPGYDPIHS	>> 1µM
CP5-46-A-10E	GELGRLVYLEDGPGYDPIHS	>> 1µM

Amino acid exchanges at position 10 totally abrogated the inhibitory effect of the protease. At position 6 exchanges to amino acids with longer side chains (Glu and Gln) diminished or abolished the inhibitory effect. An exchange to Asp at position 6 decreased the IC_{50} 20-fold. Only the change at position 4 and 5 to the negative charged amino acids Asp and Glu increased the potency of the peptide about 6-fold to an IC_{50} of about 23 nM.

The peptides with the amino acid changes 6E, 10Q and 10E were examined with respect to cleavage by the NS3/4A protease. 10 µM peptide was incubated with 1 µM protease for 16 hours and the

samples were analysed by LC/MS. LC/MS analysis was done by Dr. Raimo Franke (Department of Chemical Biology, HZI). Almost no reduction of peptide concentration was measurable after incubation with the protease and no cleavage fragments were found in the LC/MS spectra (data not shown). Therefore it can be assumed that the peptides are not cleaved by the NS3/4A protease.

The optimised peptide CP5-46A-4D5E was co-crystallised with NS3-4A. One important question was whether or not the proposed ionic interactions between the peptide residues Glu5 and Asp4, especially the interaction between Asp4 and Lys165 of the NS3/4A protease, had in fact contributed to the observed increase of the inhibitory effect. The crystallisation conditions were optimised and crystals could be obtained with 0.1 M Na-citrate pH 5.1, 2.2M KCl, 5% isopropanol (~100 µM NS3/4A, diluted with 0.1 M buffer, and ~500 µM peptide with a final molar ratio of protease and peptide of 1:5). The crystals diffracted to 2.8 Å and belonged to the space group $P6_1$. Diffraction measurements and model building was done by Dr. Stefan Schmelz (Department Molecular Structural Biology, HZI).

In Figure 3-42 A and B the alignment of the structures of the peptides CP5-46-A (green) and CP5-46A-4D5E (blue) bound to the NS3/4A protease are shown.

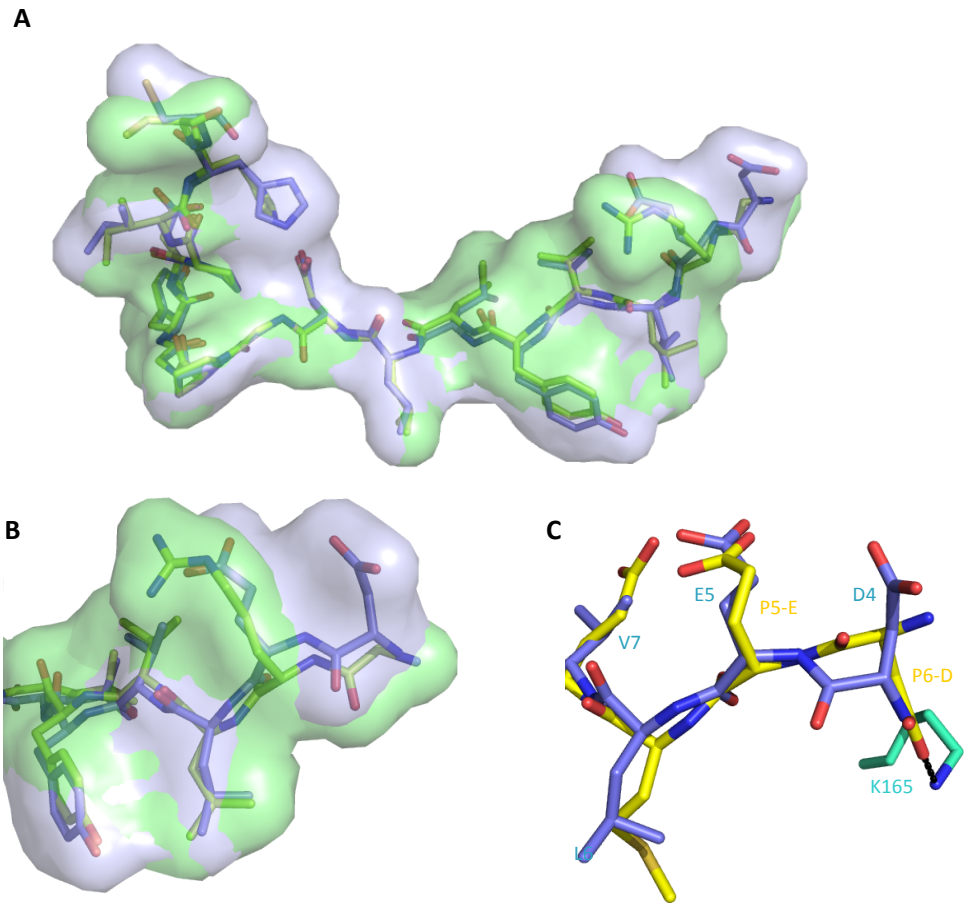

Figure 3-42: Comparison of structure of peptide CP5-46-A (green) and CP5-46A-4D5E (blue) bound to the NS3/4A protease. A: Alignment of structures of the peptides CP5-46-A (green) and CP5-46A-4D5E (blue) bound to the NS3/4A protease; the peptides are shown in stick representation with modelled surface. **B:** Zoom on the non-prime sites of the peptides CP5-46-A (green) and CP5-46A-4D5E (blue) bound to the NS3/4A protease. **C:** Comparison of binding of N-terminal part of the peptide CP5-46A-4D5E (blue) and the substrate 4A4B (yellow, PDB ID 3M5M). K165 of the NS3/4A protease is shown.

The alignment of the structures of peptides CP5-46-A and CP5-46A-4D5E bound to the NS3/4A protease shows that the binding of the optimised peptide is not altered by the change of the amino acids Gly4 to Asp4 and Arg5 to Glu5. The N-terminal part of the peptide still forms an anti-parallel ß-strand with the backbone of the NS3/4A protease at the non-primed site of the protease and the C-terminal part of the peptide forms a 'proline'-finger motive at the primed site of the protease.

The suggested ionic interactions between Asp4 of the peptide CP5-46A-4D5E and Lys165 of the NS3/4A protease have apparently not formed. The side chain of Asp4 points in the opposite direction away from Lys165 of the NS3/4A protease (see Figure 3-42 C). Notably the position of the backbone and side chain of Glu5 is similar to the binding of P5-Glu of the substrate 4A4B (PDB ID 3M5M, Romano *et al.*, 2010) mimicking the binding of the substrate.

The full-length peptide CP5-46 was produced as an MBP fusion protein with the acidic amino acid exchanges at position 4 and 5. The mutations were introduced with the primer 'primCP5-46-4D5E 5'' and the peptide produced as mentioned in section 3.2.3. The purified peptide was tested in the NS3/4A activity assay. The results are shown in Table 3-14 (see also Figure 3-47 A).

Table 3-14: Comparison of IC_{50} values and K_i values of the peptides CP5-46 and CP5-46-4D5E.

Peptide	Sequence	IC_{50} [nM]	K_i [nM]
CP5-46	GELGRLVYLLDGPGYDPIHCDVVTRGGSHLFNF	11.3 ± 1.6	5.2 ± 0.75
CP5-46-4D5E	GELDELVYLLDGPGYDPIHCDVVTRGGSHLFNF	1.14 ± 0.053	0.53 ± 0.02

The introduction of the amino acid exchanges Asp4 and Glu5 improved the IC_{50} value of the full-length peptide 10-fold to 1.14 nM with a K_i of about 530 pM.

3.2.8 NS3/4A protease resistance mutation A156V

An important problem of new protease inhibitors in development is the rapid emergence of resistant variants. Because of the low viral polymerase fidelity and the high viral yield, huge numbers of novel variants are produced constantly (Gaudieri *et al*., 2009). Monotherapy with different protease inhibitors leads to the rapid selection of resistant protease variants. Amino acids associated with resistance mutations against protease inhibitors are shown in Figure 3-43.

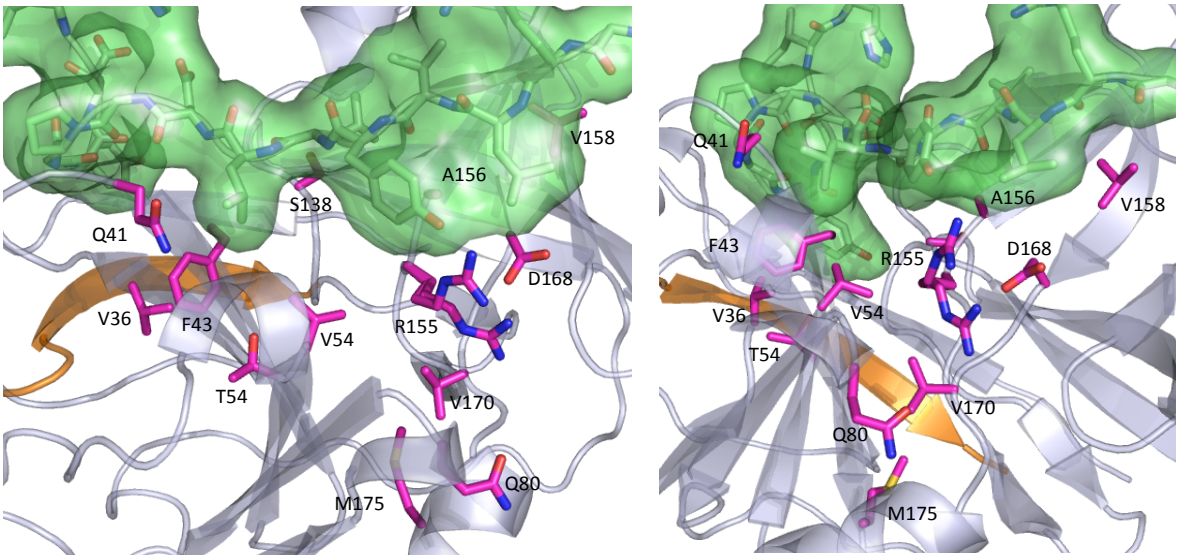

Figure 3-43: Resistant mutations of the NS3/4A protease. The peptide CP5-46-A is shown as stick structure with modeled surface (green), the NS3 domain (grey) and NS4A (orange) are shown as ribbon structure. Amino acids of NS3 that are known to be involved in resistance mutations against protease inhibitors are shown as purple sticks. For R155 two possible rotamers are shown.

Several amino acids of NS3 that are involved in resistance mutations against protease inhibitors are in proximity of the bound peptide CP5-46-A: Q41, F43, A156, V158 and D168 (see Figure 3-44).

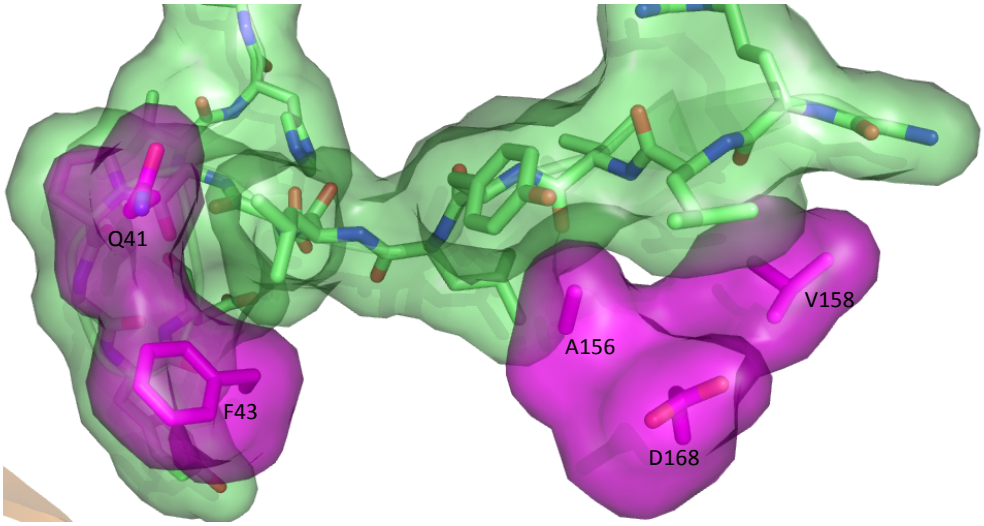

Figure 3-44: Resistance mutations in proximity to the peptide CP5-46-A (green). Amino acids of NS3 that are known to be involved in resistance mutations against protease inhibitors and are in proximity to the peptide CP5-46-A are shown in purple. Stick presentation with modeled surface.

Especially A156 is totally covered by the modelled surface of the peptide and in direct contact. A mutation at this position could have the highest impact on the inhibitory potency of the peptide.

Chemically related inhibitors share a similar resistance profile with resistance mutations at the same positions. The resistance mutation A156V has the greatest impact on the activity of both compound groups, the linear α-ketoamide inhibitors and the macrocyclic inhibitors (see Table 3-15, Lenz *et al.*, 2010).

Table 3-15: Effect of NS3 mutation A156V. Fold change in the EC_{50} for the mutant replicon compared to that for the wild-type replicon (Lenz *et al.*, 2010).

Inhibitor	Fold change
TMC435	2149
BILN-2061	2085
ITMN-191	63
Boceprevir	75
Telaprevir	112

It was thus of primary interest to investigate the effect of the peptide CP5-46-4D5E on known resistant HCV NS3/4A mutations, in particular A156V. It is noted again here that it had been a primary intention in developing longer peptides as inhibitors to have inhibitors which might provide an alternative binding mechanism to the small molecular weight inhibitors in development. In Figure 3-45 the A156V mutation was modelled and the three possible rotamers are shown.

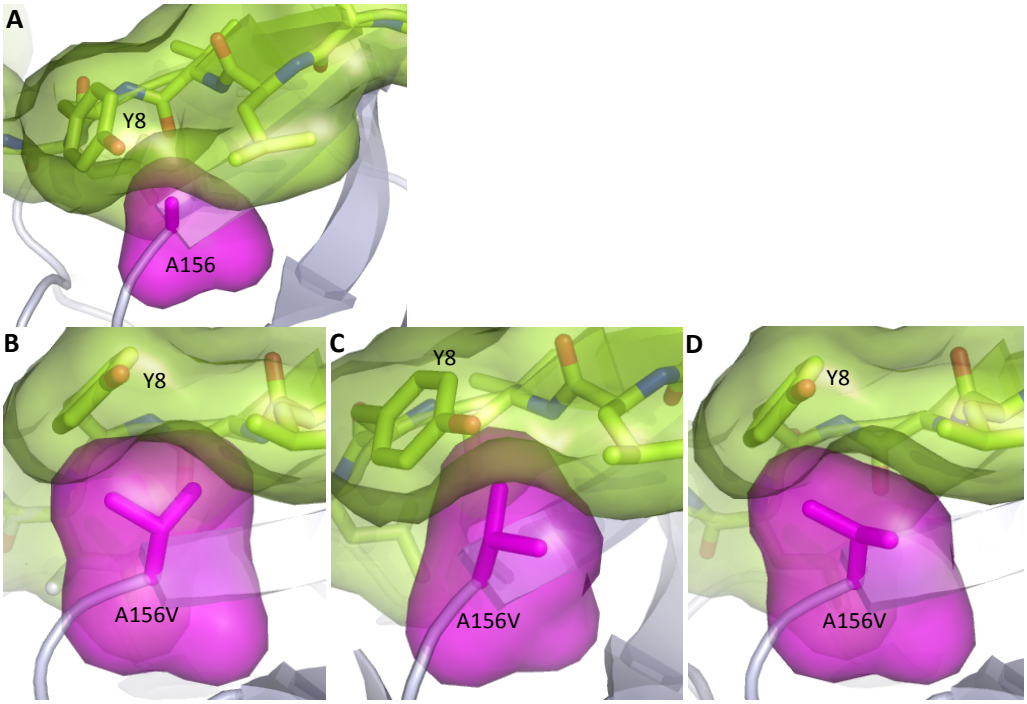

Figure 3-45: Model of the resistance mutation A156V. The peptide is shown as stick structure with modeled surface (green) and the protease is shown as ribbon structure (grey). **A:** the aa A156 in stick presentation with modeled surface is shown in purple. **B**, **C** and **D**: modeled mutation of A156 to V, the three possible rotamers are shown.

The Val occupies much more space then the previous Ala and should interfere with the binding of the peptide because of a steric clash between Y8 (of the peptide inhibitor) and V156.

The point mutation for mutation of Ala156 to Val was inserted by site directed mutagenesis. The complementary primer 'mutA156V' and 'mutA156V-rev' with the point mutation were used for

linear amplification of the pMAL-c4E vector with NS3/4A single chain construct (see 3.2.1). After amplification the methylated template DNA was digested with DpnI and the amplified vector was transformed into *E. coli* Top10 F´cells.

A number of isolated clones were sequenced and the presence of NS3/4A genes with the A156V confirmed. The MBP-NS3/4A A156V fusion protein was produced in soluble form at 30°C. The protease was purified by IMAC and the buffer of the elution fraction was exchanged with the use of centrifugal filter units with 10 kDa cut off. The protease was stored at -80°C until usage. The protease could be produced and purified in suitable amounts and purity (see appendix Figure 7-10).

The concentration of purified NS3/4A A156V was determined by densitometric measurement of the coomassie stained protein bands and comparison to a MBP standard. A concentration of about 3 mg/ml of MBP-NS3/4A A156V could be obtained.

The activity of the purified NS3/4A protease was tested with the NS3/4A activity assay (Taliani *et al.*, 1996; Misialek *et al.*, 2009). Figure 3-46 shows the results for two protease concentrations. The NS3/4A A156V protease had the same specific activity as the wild type protease (see Figure 3-19: 1 nM wild type protease 20.6 RFU/min).

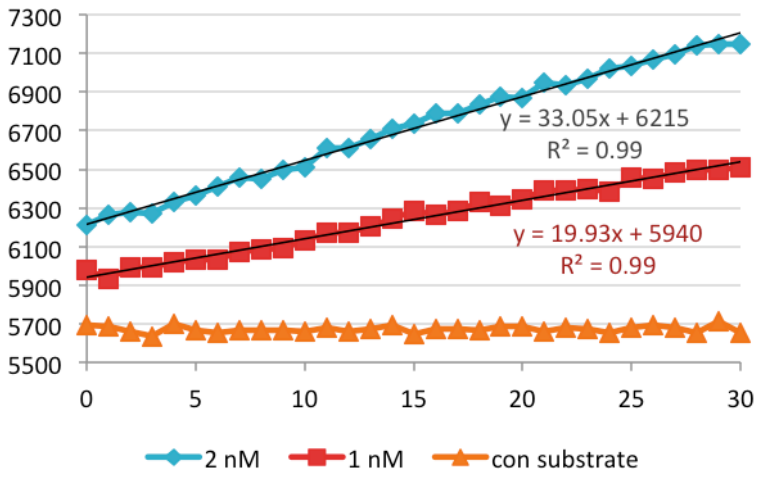

Figure 3-46: Activity assay with mutant MBP-NS3/4A protease A156V. Assay was done in buffer M2235 with 5 µM substrate M-2235 (Bachem) and 1 nM or 2 nM NS3/4A A156V. con: control without protease. Excitation filter: 360/40 nm, emission filter: 460/40 nm, RFU: Relative Fluorescence Units. Equation of trend lines are shown.

The optimised peptide CP5-46-4D5E was tested with the NS3/4A protease with the resistance mutation A156V. The results of the activity assay are shown in Figure 3-47 B.

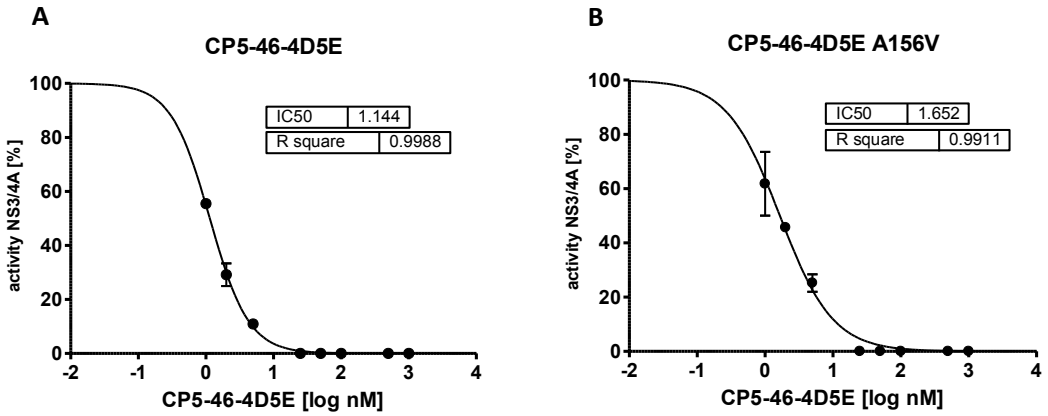

Figure 3-47: Determination of the IC_{50} of peptide CP5-46-4D5E using the wild type NS3/4A (A) or NS3/4A mutant A156V. Activity assay was done in buffer M2235 with 5 µM substrate M-2235 (Bachem) and 0.5 nM NS3/4A. Peptide CP5-46-4D5E produced as MBP fusion protein with His-Tag. Excitation filter: 360/40 nm, emission filter: 460/40 nm. Velocity of fluorescence increase over one hour was compared to that of the NS2-K11 control peptide. Each measurement was done in duplicate, IC_{50} in nM. The curve was fitted with *GraphPad Prism* using a nonlinear regression model with variable slope and normalised response: Y=100/(1+10^((LogIC_{50}-X)*slope)).

Compared to the wild type protease (Figure 3-47 A) the IC_{50} value changes from 1.14 nM to about 1.65 nM. This corresponds to a 1.5-fold increase (see Table 3-16). Compared to the other NS3/4A inhibitors (see Table 3-15) the peptide shows negligible susceptibility to the A156V mutation.

Table 3-16: Effect of NS3 mutation A156V on peptide CP5-46-4D5E. Fold change (FC) in the IC_{50} for the mutant NS3/4A protease compared to that for the wild-type (wt) protease.

Protease	IC_{50} [nM]	FC
NS3/4A wt	1.14 ± 0.047	
NS3/4A A156V	1.65 ± 0.248	**1.5**

3.3 Intracellular delivery of inhibitory peptides

The inhibitory peptides against the NS3/4A protease target an intracellular enzyme. Therefore they have to cross the plasma membrane to reach their site of action. Because of the highly selective permeability of cell membranes to macromolecules, methods designed for membrane permeability were assayed for their suitability for cell delivery of the peptide inhibitors described above. The intracellular delivery of inhibitory peptides was attempted using fusion of the peptide to cell penetrating peptides (CPP) and via encapsulation into polymersomes.

3.3.1 Intracellular delivery of peptides using cell penetrating peptides

CPPs are short peptides that can traverse the cell membrane and thereby deliver a cargo into eukaryotic cells (Schwarze *et al.*, 2000). For peptide delivery several CPPs have been described in the literature and were tested for their suitability to transfer the inhibitors described. These include cationic CPPs: HIV-Tat peptide (Green and Loewenstein, 1988), the Antennapedia peptide (Joliot *et al.*, 1991) and the nona-arg peptide. Also an amphipathic peptide, the PTD-5 peptide, was tested (see Table 3-17).

Table 3-17: Peptides (black) fused to cell penetrating peptides (blue) used for cell delivery.

Peptide name	Sequence
Ant-K5-66-A	RQIKIWFQNRRMKWKKGELGRLVYLLDGPGYDPI
Tat-K5-66-A	GRKKRRQRRRPPQGELGRLVYLLDGPGYDPI
Nona-arg-K5-66-A	RRRRRRRRRGELGRLVYLLDGPGYDPI
PTD-5-K5-66-A	RRQRRTSKLMKRGELGRLVYLLDGPGYDPI
Ant-CP5-46	RQIKIWFQNRRMKWKKGELGRLVYLLDGPGYDPIHCDVVTRGGSHLFNF
Ant-CP6-4	RQIKIWFQNRRMKWKKGELGRLVYLLDGPGYDPIHCFPIYSRGSYASYV
CPP-Control 1	RLIFAGKQLEDGRGELGRVYLLDGPGYDPI
CPP-Control 2	RQIKIWFQNRRMKWKKYVGIPRDLGLDGYEPLG

All CPP-peptide fusions were chemically synthesised and inhibition of viral replication in cell culture was tested with the replicon assay using the HCV Con1 replicon ‘i341 PiLuc/3-3´/ET’ (Lohmann *et al.*, 2003) which was constructed from the consensus sequence of genotype 1b isolate cDNA. For measurement of HCV replication a fire-fly luciferase gene was inserted in the replicon. The luciferase activity reflects the HCV RNA level in the cells and is therefore a measure of viral replication. The assay was done in Huh7-Lunet cells which have a gaussia luciferase gene in their genome that can be used for a cell viability assay. The cell culture replicon assay was performed by Juliane Gentzsch (Department of Experimental Virology, Twincore, Hannover) with the synthetic peptides described in Table 3-17. The peptide K5-66-A was chosen for initial tests with different CPPs. The results of the replicon cell culture assay are shown in Figure 3-48 A – F.

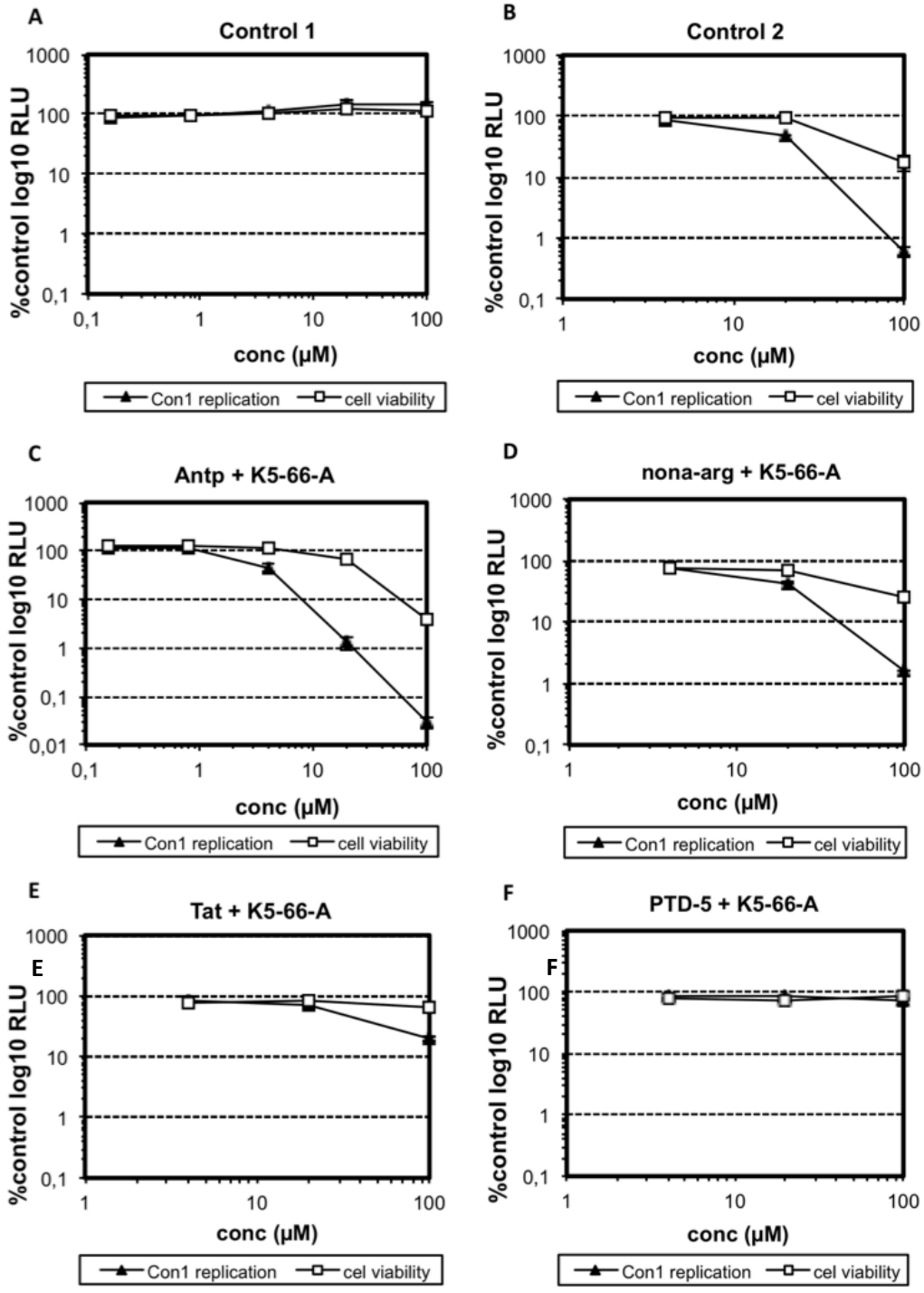

Figure 3-48: Inhibition of viral replication in cell culture using various peptides. Replicon pFK i341 PiLuc/3-3′/ET (Lohmann et al, 2003). Luciferase assay after 48h, luciferase activity compared to water control. Black triangle: Firefly luciferase activity that reflects replication of Con1 replicon, white square: Gaussia luciferase activity that reflects cell viability. A: Control 1: peptide K5-66-A with 13 aa N-terminal ubiquitin fusion, B: Control 2: scrambled peptide K5-66-A sequence with Antennapedia-peptide fusion. Each measurement was done in duplicate.

The first control peptide K5-66-A with an N-terminal ubiquitin fusion showed no inhibition of the viral replication. Also no decrease in the cell viability was detectable (Figure 3-48 A). Interestingly the scrambled control peptide with Antennapedia peptide fusion showed an inhibitory effect at 20 µM. A peptide concentration of 100 µM started to be toxic for the cells (Figure 3-48 B). A fusion of K5-66-A to the Tat peptide or nona-arg peptide showed only a low inhibition of viral replication at 20

µM and started to be toxic at higher concentration (Figure 3-48 D and E). A PTD-5-K5-66-A fusion showed no inhibitory effect or toxicity (Figure 3-48 F). The highest inhibition of replication was exhibited by the N-terminal fusion of the Antennapedia peptide. At a concentration of 20 µM an almost two log reduction of viral replication was detectable but the peptide fusion started to become slightly toxic (70% cell viability compared to control) (Figure 3-48 C). The EC_{50} value of the Antp-K5-66-A peptide is about 3.4 µM (see Figure 3-49). Compared to the IC_{50} value of the NS3/4A in vitro assay (125 nM) this corresponds to a 27-fold increase.

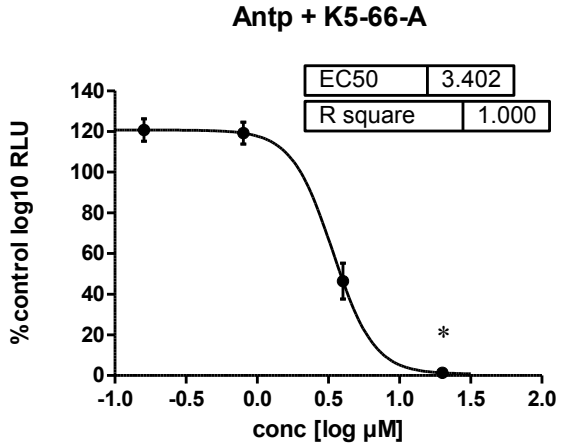

Figure 3-49: Inhibition of viral replication in cell culture using peptide Antp-K5-66-A. Determination of the IC_{50} of peptide Antp-K5-66-A. Replicon pFK i341 PiLuc/3-3´/ET (Lohmann et al, 2003) luciferase assay after 48 h, luciferase activity compared to water control. Each measurement was done in duplicate, EC_{50} in µM. The curve was fitted with *GraphPad Prism* using a nonlinear regression model with variable slope: Y=Bottom+(Top-Bottom)/ (1+10^((LogEC_{50}-X)*slope)). *: cell viability decreased to 70%.

The Antennapedia peptide seems to be the most promising CPP for intracellular delivery. Therefore it was fused to the full length peptides CP5-46 and CP6-4 and the fusion peptides were tested in the replicon cell culture assay. The results are shown in Figure 3-50 A and B.

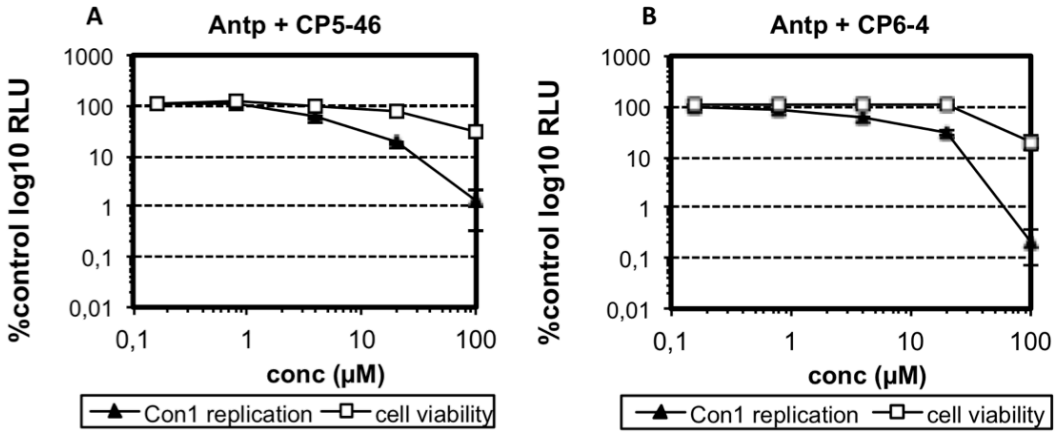

Figure 3-50: Inhibition of viral replication in cell culture using peptides Antp-CP5-46 and Antp-CP6-4. Replicon pFK i341 PiLuc/3-3´/ET (Lohmann et al, 2003). Luciferase assay after 48 h, luciferase activity compared to water control. Black triangle: Firefly luciferase activity that reflects replication of Con1 replicon, white square: Gaussia luciferase activity that reflects cell viability. **A:** Antennapedia-peptide CP5-46-peptide fusion. **B:** Antennapedia-peptide CP6-4-peptide fusion.

The Antennapedia peptide CP5-46 and CP6-4 fusions have a lower inhibitory effect than the K5-66-A peptide in the replicon cell culture model. At a concentration of 20 µM a reduction of viral replication

to about 20 to 30% was detectable compared to a reduction to about 1% of the K5-66-A peptide. At 100 µM both fusion peptides started to become toxic

3.3.2 Intracellular delivery of peptides using polymersomes

Polymersomes are nanoparticles that consist of a pH-sensitive copolymer which self assembles and forms vesicles in nanometer size at a pH higher than 6.5. They are internalised by cells via endocytosis. Acidification of the early endosomes leads to disaggregation of the polymersomes. Because of the abrupt local change in osmotic pressure caused by this, pores are formed in the endosomal membrane and the cargo is released into the cytosol (Massignani *et al.*, 2009; Massignani *et al.*, 2010).

The peptide CP5-46-A and a scrambled control peptide were packaged into polymersomes for intracellular delivery (see Table 3-18).

Table 3-18: Peptides used for packaging into polymersomes.

Peptide name	Sequence
CP5-46-A	GELGRLVYLLDGPGYDPIHCD
Control	GELGRDIGGPLDLYPVDLHCY

The packaging was done at the laboratory of Dr. Giuseppe Battaglia (Department of Biomedical Science, University Sheffield, UK) who kindly assented for me to learn this novel technology in his lab. Both peptides could be encapsulated into polymersomes with a final concentration of about 6.3 µM and a polymer concentration of about 2 mg/ml as quantified by HPLC. The polymersome size distribution determined by dynamic light scattering ranged from 50 – 600 nm with an average size of 200 nm (see Figure 3-51 A and B).

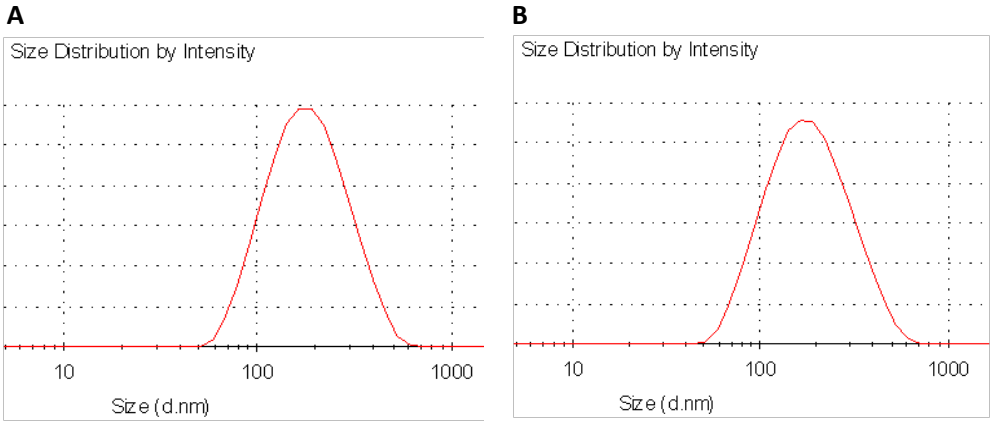

Figure 3-51: Size distribution of polymersomes determined by dynamic light scattering in nm. A: Size distribution of polymersomes with encapsulated peptide CP5-46. **B:** Size distribution of polymersomes with encapsulated control peptide.

Inhibition of viral replication in cell culture by the polymersomes was tested with the replicon assay assay using the HCV Con1 replicon 'i341 PiLuc/3-3'/ET'. For quantification of HCV replication a firefly luciferase gene was inserted in the replicon. The luciferase activity reflects the HCV RNA amount in the cells. The assay was done in Huh7-Lunet cells which have a gaussia luciferase gene in

their genome for measurement of cell viability. The cell culture replicon assay was done by Juliane Gentzsch (Department of Experimental Virology, Twincore, Hannover). The polymersomes were added to the cells at three different peptide concentrations: 3, 1.5 and 0.3 µM (1:2, 1:4 and 1:10 dilution, respectively). In Figure 3-52 the results of the replicon cell culture assay are shown.

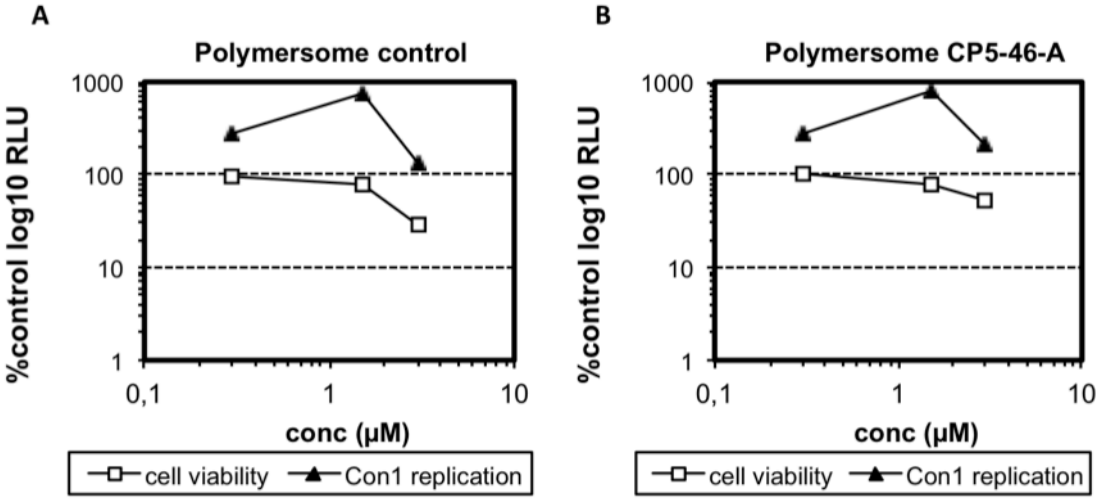

Figure 3-52: Inhibition of viral replication in cell culture using polymersomes. Replicon pFK i341 PiLuc/3-3´/ET (Lohmann et al, 2003). Luciferase assay after 48 h, luciferase activity compared to water control. Black triangle: Firefly luciferase activity that reflects replication of Con1 replicon, white square: Gaussia luciferase activity that reflects cell viability. A: control peptide encapsulated in polymersomes. B: peptide CP5-46-A encapsulated in polymersomes.

No inhibition of the viral replication was measurable for the peptide CP5-46-A and the control peptide. Notably an increase of the viral replication was detectable upon addition of polymersomes that was concentration dependent. At the highest polymersome concentration and dilution of the cell culture medium (2 mg/ml and 1:2 dilution) the polymersomes started to become toxic (Figure 3-52 A and B). It is assumed that the intracellular peptide delivery was not very efficient.

4. Discussion

It is estimated that worldwide up to 170 million people are chronically infected with HCV (Yu and Chiang, 2010). The standard of care achieves a sustained viral response in only about half of the patients treated and is associated with considerable severe side effects (Manns *et al*, 2001; Fried, 2002). HCV infection is the leading cause of liver cirrhosis and hepatocellular carcinoma (Shepard, 2005). Thus there is a huge unmet need for direct anti-HCV drugs for more effective treatments with fewer side effects. The viral proteases, the NS2-3 and NS3/4A proteases, essential for the viral life cycle, are interesting targets for new specific HCV drugs. A combinatorial phage display peptide library displaying large peptides is described in this thesis and how it was used for iterative affinity enrichment on these immobilised HCV proteases for development of inhibitory peptides against the HCV proteases. In the latter stages of optimisation of the peptides as inhibitors, X-ray crystallography and structural modelling were successfully implemented. This endeavour was undertaken with the intention that the products developed, or their derivatives can either be confectioned to be of use for future treatment of HCV, especially in combatting development of spontaneous viral resistance to drugs or at the very least to deliver novel lead structures for further structure-based drug design which are not simply based on geometric fit into the active site of the enzymes.

4.1 NS2-3 protease

The NS2-3 protease is responsible for the intramolecular cleavage between the non structural proteins NS2 and NS3. It is a cysteine autoprotease with the active site residues entirely located in the NS2 protein (Grakoui, 1993; Lorenz *et al.*, 2006). Two NS2 monomers form a dimeric cysteine autoprotease with two composite active sites. After intramolecular cleavage between NS2 and NS3 the protease is inactivated. For the full activity of NS2-3 protease not only the C-terminal part of NS2 but also the N-terminal part of the NS3 protein that encompasses the NS3 serine protease domain with the Zn^{2+} binding site is necessary (Thibeault *et al.*, 2001; Pallaoro *et al.*, 2001). Although there are few NS2-3 protease inhibitors the only ones known act indirectly by disrupting the conformation of the uncleaved NS2-3 protease. Because of the essential role of the NS2 protein for the viral life cycle peptides that directly inhibit NS2-3 protease cleavage and/or dimer formation would be interesting for the development of new specific HCV drugs.

4.1.1 Affinity selection against NS2-3 protease

The NS2-3 protease was produced by recombinant expression in *E. coli* to be applied for affinity enrichment of ligands, which were then to be screened for their inhibitor activity. It was produced with an N-terminal MBP fusion for later immobilisation. The protease could not be produced in a native active form because soluble expression of NS2-3 protease results in auto-cleavage during production (data not shown and Pallaoro *et al.*, 2001). Therefore, it was necessary to produce the NS2-3 protease in an insoluble form and to refold it to a native active state. For refolding known buffer conditions were used under which the protease refolds but undergoes no self-processing (Pallaoro *et al.*, 2001). After refolding of the protease the intramolecular cleavage was induced by dilution into a cleavage buffer. After optimisation of the cleavage buffer processing of about 50% of

the NS2-3 protease was detectable. The cleavage buffer could be optimised to a simpler formulation with less detergent, glycerol and additives that could interfere during the affinity selection. Interestingly cleavage buffer formulations described in the literature all contain detergent concentrations above the critical micelle concentration (CMC) for optimal cleavage of NS2-3 (Thibeault *et al.*, 2001; Pallaoro *et al.*, 2001). The detergent concentration used in the optimised cleavage buffer (0.05% Tween 20) is below the CMC (0.1%). It is proposed that the NS2-3 protease is associated with cellular membranes (Lorenz *et al.*, 2006) and aggregation of the protease is avoided by binding of the detergent to the transmembrane segments. At detergent concentrations below the CMC most membrane proteins tend to be insoluble (Le Maire *et al.*, 2000). The maltose binding protein is known to increase the solubility of the fusion partner by prevention of aggregation (Kapust and Waugh, 1999). Therefore the lower detergent concentration that was necessary for efficient cleavage of the NS2-3 protease could be due to additional stabilisation and solubilisation effects of the MBP fusion. The less efficient processing of NS2-3 protease at higher protease concentrations is correlated with aggregation observed at protein concentrations above 200 nM (Pallaoro *et al.*, 2001).

About 50% of the NS2-3 protease remained unprocessed after incubation in cleavage buffer. This may be a natural phenomenon characteristic of the enzyme, although processing of up to 70% of refolded protease is described (Pallaoro *et al.*, 2001). However, it can be assumed that some of the protease is not correctly refolded perhaps due to impurities after purification that interfere with the refolding process or due to sub-optimal refolding and cleavage conditions. Binding tests of the refolded MBP showed that the refolding of the MBP is almost complete. Therefore, if there is also incorrectly refolded NS2-3 it will also be immobilised, which could lead to unspecific binding of peptides.

Pallaoro and coworkers showed that after refolding under mildly denaturating conditions the NS2-3 protease is not active, but can however, already form dimers. It is thus concluded that the refolded NS2-3 protease used for the affinity enrichment could also contain refolded NS2-3 dimers. An NS2 monomer consists of two subdomains connected by an extended linker and has probably a very flexible structure, which is stabilised after dimer formation. The active site is formed after dimer formation of two NS2 monomers (Lorenz *et al.*, 2006). NS2 monomers are targets for peptides that interfere with dimer formation and NS2 dimers are targets for peptides that bind to the composite active site and prevent cleavage. Also the NS3 serine protease part, which is important for correct folding of the NS2 protein and positioning of the NS2 active site, can be a target for peptides that interfere with intramolecular coordination. These various targets are showing the lack of a confined dominant binding site.

During the panning with the peptide phage display library CPL19YS-2 the amount of immobilised NS2-3 protease was kept constant and the stringency of the washing conditions was not increased over five panning rounds. If peptides are enriched during panning an increased ratio of eluted and added phage after each panning round would be expected. For the panning against the NS2-3 protease the ratio increased from the first to fifth panning round which is a sign of enrichment of peptides. Sequencing of several peptide coding sequences after the 3rd, 4th and 5th panning round confirmed the enrichment of peptides. Four peptides showed an enrichment after the 5th panning round, of which three were also identified after the 4th panning round and one also after the 3rd panning round. A significant enrichment of peptides was first seen after the 4th panning round with six enriched peptides. A comparison of their sequences did not reveal any obvious homology or common structural

consensus motif. This variety of different peptides indicates the lack of a confined dominant binding site. This may be due to the actual nature of the protease which can bind peptides on various parts of its surface with similar affinity or it could additionally or solely be due to the heterogeneity of the NS2-3 protease species created by partial refolding, misfolding or dimer formation offering many different possible binding sites for peptides. After the 5th panning round two peptides were more strongly enriched. Also no 'junk' clones with deletions or frame shifts within the peptide-coding region were observed. Such 'junk' clones would be a sign for unspecific enrichment of clones with faster propagation which are often observed accumulating in the absence of specific enrichment of truly affine specific clones (Collins, 1997).

Specific binding of the enriched peptides of the 5th panning round to the NS2-3 protease was analysed by phage ELISA and showed that only two of the four peptides bind specifically to the NS2-3 protease. The peptides with the highest enrichment in the 5th panning round both bind specifically to the NS2-3 protease but it is unclear whether or not the peptides bind to the NS2-3 monomer or NS2-3 dimer. The other two peptides bind strongly to the MBP or the anti-MBP IgG thus partly explaining the lack of similarity between the enriched sequences.

The enriched peptides do not show a definite homology in their sequence. Both sequences are hydrophobic at the N-terminal and C-terminal ends. Hydrophobic amino acids are over represented in these variable regions (Pollmann, 2010). Interestingly both peptides could form potential disulfide bridges with a loop length of six amino acids (peptide E11) or four to six amino acids (peptide E17). These disulfide bridges could stabilise a secondary structure of the peptides.

To test if the peptides that bind to the NS2-3 protease also inhibit cleavage of the protease the peptides were produced without fusion to the M13 phage. An N-terminal fusion to the Antp peptide was used to both increase the solubility of the peptides and could potentially serve for cellular delivery of the peptides. An increase in the molecular weight of the peptide can be important for protection of the peptides from proteolytic degradation in serum (Li, 2009). Despite the fusion to the hydrophilic Antp the peptides aggregated after expression forming insoluble 'inclusion bodies'. Aggregation of the peptides occurred presumably because of the hydrophobicity of the peptides. The peptides were purified under denaturing and reducing conditions disrupting the secondary structure and possible disulfide bridges of the peptides. The yield of purified peptide fluctuated from one preparation to the next. It was observed that an unwanted *E. coli* protein was co-purified, in the case of the Ant-K17 peptide reducing the purity to 55% of total protein.

4.1.2 Inhibition of NS2-3 activity

The inhibitory effect of the peptides on NS2-3 protease cleavage was tested in a protease activity assay. For the activity assay denatured NS2-3 protease was refolded in cleavage buffer in the presence of the peptide. Prior refolding of the NS2-3 protease was not used for the activity assay because it is known that the protease can form dimers after refolding (Pallaoro *et al.*, 2001). Therefore inhibition of dimer formation would not have been detectable. The peptide Ant-K5-66 which is known to bind to the NS3/4A protease was used as a control to see if there is an effect on the refolding of the NS2-3 protease. The control peptide reduced the cleavage of NS2-3 protease to about 80% compared to the control without peptide, i.e. a reduction of 20%. This could be due to interference in the refolding process, possibly leading to misfolded protease that is not active. The peptide E11 has less of an effect

on the protease activity indicating no impact of the peptide on dimer formation or protease cleavage. The peptide E17 showed a higher reduction of the protease activity to 60% compared to the control without peptide. This could be due to inhibition of the NS2-3 dimer formation or to blocking of the active site. In direct comparison to the peptide K5-66 the protease processing is reduced to about 70% and the inhibition is concentration dependent with an inhibitory effect at concentrations higher than 90 nM. The inhibitory effect of the peptide E17 is quite low with an IC_{50} higher than 300 nM. However, the peptide could be a starting point for the development of peptides with a higher inhibitory effect, e.g. with the cosmix plexing technology.

The inhibition of protease cleavage diminishes for the peptide K17 when refolded NS2-3 protease was used for the activity assay. These results could indicate that the peptide K17 inhibits the dimer formation of the NS2-3 protease. Little is known about the kinetics of dimer formation and cleavage velocity of the NS2-3 protease. If the cleavage occurs directly after dimer formation, the addition of the peptide after refolding of the protease could be too late for the binding of the peptide to the active site and inhibition of cleavage. It should be noticed that the peptide E17 prep contained the highest level of contamination by unwanted protein. These impurities could also have an effect on NS2-3 refolding and could account for some of the inhibitory effect of the peptide. This does not appear to be the case since the same impurities do not increase the inhibitory effect of the peptide E11 peptide (about twice as much protein contaminants compared to the purified control peptide Antp-K5-66). The assay was performed under reducing conditions which prevent formation of disulfide bridges that could be important for the peptide structure and possibly compromise the inhibitory effect of the peptide.

Besides the essential role in HCV polyprotein processing, the NS2 protein is a key organiser for viral assembly (Jirasko *et al.*, 2010), is important for evasion of the immune system (Kaukinen *et al.*, 2006) and inhibition of apoptosis (Machida *et al.*, 2001). This opens the possibility that peptides binding to the NS2 protein could interfere with the viral life cycle at one of these other steps without inhibiting the protease function. If the cell delivery of the peptides is accomplished they could be tested in the cell-based infectious HCV assay which is decisive in evaluating the effect of the peptides E11 and E17 on the NS2 protein. This would be a valuable extension to purely *in vitro* enzyme assays performed to date.

4.2 NS3/4A protease

The HCV NS3 protein is a bifunctional enzyme that consists of two domains, an N-terminal serine protease domain and a C-terminal helicase/ATPase domain. The NS3 protease is essential for polyprotein processing (Yao *et al.*, 1999). It is a chymotrypsin-like serine protease and forms a heterodimeric complex with the NS4A protein which is a cofactor of the NS3 protease domain enhancing the proteolytic activity (Lin *et al.*, 1995). The shallow and solvent exposed substrate binding pocket made it difficult to identify specific inhibitors of HCV NS3/4A protease (Kim *et al.*, 1996). The finding that the protease is inhibited by peptides corresponding to the C-terminus of the cleavage products led to the development of first protease inhibitors (Ingallinella *et al.*, 1998; Lamarre *et al.*, 2003). This product-based drug design was used for the development of the two α-ketoamide inhibitors, telaprevir (Vertex Pharmaceuticals) and boceprevir (Merck) which were approved in 2011 (Poordad, 2011). Most of the new protease inhibitors are bound at the active site of

the NS3/4A protease, spanning only the S4–S1` subsites and thus showing a similar binding pattern and resistance profile. The newly developed drugs can only be used as supplement to the current treatment because of the high mutation rate during HCV replication which leads to rapid development of resistance to the drugs. Treated patients will be exposed to the same side effects as before (Gentile *et al.*, 2010). Large peptides might provide an alternative binding mechanism to the small molecular weight inhibitors in development. These might be *a priori* binding at alternative sites and/or because of their larger interactive surface be less affected by HCV resistance mutations at the substrate binding site (see below for indications that this seems to be the case for the NS3/4A peptide protease inhibitors developed here).

4.2.1 Affinity selection against NS3/4A protease

For affinity enrichment the NS3/4A protease was produced by recombinant expression in *E. coli*. A single chain form of the NS3 protease domain linked to the NS4A cofactor peptide was produced according to Dimasi and co-workers. The correct folding of the NS3/4A single chain protein was later confirmed by solving the crystal structure of the protease. The MBP fusion showed no effect on the activity of the protease compared to a NS3/4A construct without fusion. Interestingly the MBP protein strongly increased the solubility of the NS3/4A single chain construct. The MBP-NS3/4A could be produced at 30°C in high amounts and in soluble form whereas the NS3/4A protease without fusion was mostly found in insoluble form even when produced in cells grown at 18°C (data not shown).

For affinity enrichment the peptide phage display library CPL19YS-2 was used. The N-terminal and C-terminal parts of the library peptides are separated by the constant 'HC' motive in the middle of the library peptide. Various immobilisation strategies for the NS3/4A protease and a number of panning conditions were used. To avoid enrichment of peptides that bind to the immobilisation matrix it was tried in the first panning series to change the immobilisation strategy after each panning round. Anti-MBP magnetic beads and amylose magnetic beads were used in alteration for immobilisation but due to the low binding affinity of the MBP to the amylose in the micromolar range (Miller *et al.*, 1983) the fusion protein started to 'bleed out' from the amylose beads during the incubation with the peptide phage (data not shown). Therefore for later pannings only anti-MBP magnetic beads or immobilisation in MTPs over anti-MBP IgG were used. Panning experiments with panning buffers with physiological salt concentration (~140 mM) did not lead to the enrichment of peptides. For the binding of the NS3/4A substrates or for the binding of known peptide inhibitors ionic interactions are important. A high ionic strength in the buffer weakens these interactions, especially the P5 and P6 interactions, which leads to an increase of the K_m of the substrates or IC_{50} of inhibitors (Ingallinella *et al.*, 1998). Therefore, the affinity enrichment was done in a buffer with a low ionic strength to strengthen the possible ionic interactions of peptides and protease. Interestingly only the panning in MTPs with low ionic strength buffer led to enrichment of peptides demonstrating the importance of both immobilisation method *and* panning condition for the outcome of the affinity enrichment. The reduction of the ionic strength led to the strong enrichment of two peptides, one with acidic elution (K5-66) and one with competitive elution (K6-10).

4.2.2 Inhibition of NS3/4A activity

To test the inhibitory effect of these peptides in the *in vitro* NS3/4A activity assay the peptides were produced with an N-terminal MBP fusion and C-terminal His-Tag. Therefore the peptides had no free N- and C-terminus. The peptides could be produced in soluble form and in high amounts with the MBP fusion. The comparison with a chemically synthesised peptide showed that the N- and C-terminal extensions had no influence on the inhibitory effect of the peptide.

The peptides, K5-66 and K6-10, showed competitive binding with the NS3/4A inhibitor N-1725 (Bachem) in a phage-ELISA experiment. This result gave a first hint that the peptides could bind at the same epitope of the NS3/4A protease as the inhibitor which binds at the subsites S1 – S6 of the protease (Ingallinella *et al.*, 1998). Both peptides have a homology in their sequence. They have a similar quite hydrophobic 9 aa long motiv in the N-terminal part of the peptide that is interrupted by an aspartic acid: V-Y-L/V-L-D/G-G/D-P-G-Y. Later co-crystallisation of the N-terminal part of peptide K5-66 confirmed the assumption that this region is important for binding at the substrate binding region of the NS3/4A protease. Because of the homology in their sequence the peptides K5-66 and K6-10 probably bind similar to the NS3/4A protease in this region. Both peptides have an inhibitory effect on protease activity. Peptide K5-66 has an IC_{50} value of about 21 nM and peptide K6-10 of about 26 nM. Also the N-terminal and C-terminal part of the peptides were tested separately in the activity assay. In both cases the N-terminal part of the peptides shows inhibition of the protease without the C-terminal part, but the inhibitory effect is reduced compared to that of the full length peptide. The C-terminal parts have no inhibitory effect at the tested concentrations. This finding is consistent with the results of the co-crystallisation studies. The crystal structure revealed that the N-terminal part of K5-66 covers the active site of the protease. The C-terminal parts seem to work synergistically with the N-terminal parts increasing the inhibitory effect of the peptides presumably by additionally interactions with the protease surface and/or by stabilizing the peptide structure.

4.2.3 Cosmix-plexing of inhibitory peptides K5-66 and K6-10

To further improve the affinity of the peptides a recombination of the N-terminal and C-terminal parts was carried out with pre-selected populations using the cosmix-plexing technique (Collins *et al.*, 2001). Populations, containing about 20% of the clone K5-66 or K6-10, respectively, were chosen for recombination. It was intended to recombine the parts of the peptides with pre-selected peptides showing weak affinity to form novel ligands that exhibit stronger binding to the NS3/4A protease. It also automatically leads to identification of the region containing the most dominant motifs which contribute to the binding.

The cosmix-plexing recombination yields N^2 variants from the pre-selected population of N clones. The lowest number of eluted phages during the ‘low salt panning’ against MBP-NS3/4A protease in MTP was 2.06×10^4 phages for the acidic elution and 1.64×10^4 phages for the competitive elution after the 2nd panning round (PR). If it is assumed that these are all single clones and that at least two-fold enrichment of binding clones over non-binders in each panning round occurred (Clackson and Lowman, 2004), the theoretical number of variants after recombination is about 1.6×10^7 for acidic elution 5th PR (clone K5-66) and 7.6×10^6 for competitive elution 6th PR (clone K6-10). After cosmix-plexing of the pre-selected population after the 5th panning round with acidic elution containing the peptide K5-66 (termed ‘peptides of K5-66’) and 6th panning round with competitive

elution containing the peptide K6-10 (termed 'peptides of K6-10') the number of single clones was 8.9 x 10^7 and 9.6 x 10^7, respectively. This corresponds to 6 to 12-fold coverage of all possible variants after recombination. After cosmix-plexing several peptides with recognisable recombined sequences were found, but there were still a high proportion of 'original' or 'parental' peptides K5-66 and K6-10. This could ensue where there is incomplete recombination or recombination between two identical clones.

The recombined variants were submitted to further affinity selection under more stringent panning conditions with a panning buffer with a higher salt concentration to increase the stringency through weakening of ionic interactions and increased washing steps to identify peptides with higher affinity to the NS3/4A protease. Two separate pannings with the recombined peptides of K5-66 and K6-10, respectively, were performed. In both cases an enrichment of the N-terminal parts of the 'original' peptide with new C-terminal parts was seen. The enrichment shows that N-terminal parts of the peptides contribute the most to the binding to the protease and that the C-terminal parts could have a low affinity or act synergistically by stabilizing the peptide structure as noted above.

From the panning with the peptides of K6-10 one peptide, CP6-4, with increased affinity to the NS3/4A protease could be identified. The peptide CP6-4 consists of the N-terminal part of peptide K5-66 and the C-terminal part of a peptide, CP6-11, that was first identified after recombination of the pre-selected population. The peptide CP6-11 and dominantly the C-terminal part of this peptide were enriched during panning. Therefore the C-terminal part could contribute the most to the binding of the peptide to the NS3/4A protease. The peptide CP6-11 showed the same affinity in the phage-ELISA as the peptide K5-66 and has only a low inhibitory effect on the protease (~2.4 µM) under reducing conditions that prevented possible disulfide bond formation. The peptide K5-66 was not identified in panning with competitive elution before. The occurrence of the N-terminal part of this peptide in the panning with the peptides of K6-10 shows that the peptide was also enriched with the competitive elution method. The emergence of the N-terminal part could be due to high affinity of the peptide resulting in less efficient elution with the competitor. The acidic elution after recombination presumably led to a higher enrichment of this peptide. The recombination of the N-terminal part of peptide K5-66 and the C-terminal part of peptide CP6-11 resulted in the formation of a new inhibitor (CP6-4) with higher affinity to the NS3/4A protease. The peptide showed a ca. 4-fold increase of the phage-ELISA signal compared to the peptide K5-66 which corresponded to a decrease of the IC_{50} value to 16 nM.

Notably the peptide CP6-4 was also found in the elution of the panning of peptides of K5-66. This shows that the peptide CP6-11 was also enriched during panning with acidic elution and that the same recombined variant was enrichment. The low enrichment of the peptide CP6-4 could be due to the high amount of peptide K5-66 after recombination which favours the enrichment of the 'original' peptide. From the panning with the peptides of K5-66 also one additionally peptide, CP5-46, with increased affinity to the NS3/4A protease could be identified. The peptide consists of the N-terminal part of peptide K5-66 with new C-terminal part and showed an about 8-fold increase of the phage-ELISA signal compared to the peptide K5-66 which corresponded to a decrease of the IC_{50} value to about 11 nM. Both peptides, CP5-46 and CP6-4, have the N-terminal part of peptide K5-66 and share sequence homology in their C-terminal part: namely S/T-R-G-G/(-)-S.

The identification of two peptides with recombined sequences of inhibitory peptides that have an increased inhibitory effect and affinity to the NS3/4A protease shows that the cosmix-plexing was an efficient method to form novel ligands that exhibit stronger binding to the NS3/4A protease.

4.2.4 Co-crystallisation of NS3/4A with CP5-46 and CP5-46-A

To further optimise the peptide with the highest inhibitory effect, namely CP5-46, crystallisation of the NS3/4A protease in complex with the peptide was attempted. Co-crystallisation experiments were done with the peptide CP5-46 and a truncated form CP5-46-A that comprises the N-terminal part of the peptide. Crystals for diffraction measurement could only be obtained for peptide CP5-46-A and not for the full length peptide CP5-46. The crystal packing of the peptide CP5-46-A and NS3/4A complex showed that the peptide is located at the outside of the hexagonal unit cell. The bound full-length peptide could interfere with the stacking of the unit cells and preclude the crystal formation. It could also be possible that the C-terminal part of the peptide is not fully bound to the protease and the emerging conformational heterogeneity hinders crystal growth.

The resolved structure of the peptide-protease complex revealed that the peptide CP5-46-A is coordinated over a large part of the protease surface covering the active site of NS3/4A. Electron density for the amino acids 4 – 20 of the peptide could be measured. The first three amino acids, which are part of the N-terminal constant region, are not bound to the protease and therefore no electron density could be observed.

The C-terminal part of the peptide, Pro13 – His19, forms a ‘proline’-finger motive that binds to a pocket at the primed site of the protease. The shallow depression extends the S4` subsite of the protease and the bottom of the pocket is formed by the NS4A cofactor. The ‘proline’-finger motive fits nicely into the pocket, thus also interacting with the surface of the NS4A cofactor. It also forms several hydrogen bonds with NS3 residues and coordinated water molecules. His19 forms an intramolecular salt bridge with Asp11 stabilizing the structure of the ‘proline’-finger motive, however, removal of this interaction by deletion of Cys20 and His19 from peptide CP5-46-A had no influence on the inhibitory effect of the peptide. The intramolecular salt bridge could be important for the folding and structure of the full-length peptide. The ‘proline’-finger motive extends the binding of the peptide at the primed site of the protease to a region probably not occupied by the natural substrate and, therefore, displaying interactions with the protease differing from the substrate or product-based inhibitors.

The N-terminal part of the peptide, Gly4 – Pro13, binds in the region of the protease with the designated subsites S6 – S4`, essentially mimicking the binding of a natural substrate and covering the active site of the NS3/4A protease. Arg5 – Val7 bind in the region of the subsites S5 – S3 forming an anti-parallel ß-strand with the backbone of the NS3/4A protease. The formation of an anti-parallel ß-sheet is conserved between all protease substrates (Romano *et al.*, 2010). In the region of the ß-strand, Gly4 – Leu6, the peptide is positioned similarly to the way the enzyme binds the natural substrates, but the peptide backbone is shifted away in the region of the subsites S3 – S1 compared to the binding of the substrates. Most of the product-based inhibitors are bound at the active site of the NS3/4A protease, spanning the S4 – S1` subsites and thus showing a similar binding pattern of the backbone compared to the natural substrates. It is emphasised here that the novel peptide inhibitors differ in this respect from product-based inhibitors developed to mimic the natural substrate.

Compared to product-based small molecules the peptide backbone of CP5-46-A that binds in the region of the subsites S1` to S4 has a similar geometric structure but is shifted away from the active side residues of the NS3/4A protease. Most interestingly the side chains of the peptide in this region have similar functional groups and they are positioned similarly compared to the functional groups of the small molecule inhibitors (see Figure 3-40 C and D). The peptide residues P1` – P4 show similar hydrophobic interactions with the protease surface and some side chains show the same occupation of the protease subsites compared to the functional groups of the small molecule inhibitors. This shows that using the phage display method an inhibitor could be found that revealed a similar optimised binding to the S1` – S4 subsites like the small molecule inhibitors but differing in exhibiting a different binding of the peptide backbone. This could be important in the case of resistance development as discussed further below.

The shift of the peptide backbone away from the active side residues of the NS3/4A protease is important for preventing cleavage of the peptide. The peptide is coordinated at both sides of the catalytic triad of the protease but it was shown that it is not processed by the protease. Several parameters preclude the nucleophilic attack on the peptide backbone. The large side chain of Leu10 that binds to the subsite S1` moves the peptide backbone away from the active site residues. Also two hydrogen bonds are formed that have an additive effect on the geometrically constraint. They are formed by the peptide residues that could be attacked by the hydroxyl group of the catalytic triad keeping the peptide backbone away from the active site residues. One hydrogen bond is formed with a backbone amide that is part of the oxyanion hole presumably diminishing the charge redistribution function of the oxyanion hole disturbing the stabilisation of the tetrahedral intermediate and therefore increasing the activation energy of the reaction. The prevention of peptide cleavage is a sum of geometrically constraints and inhibition of the function of the oxyanion hole.

The co-crystallisation of peptide CP5-46-A showed that large peptides have the potential for additive binding interactions at different sites of the protease. The exact class of binding differs from the binding of the natural substrates and product based small molecule inhibitors. Therefore the newly developed inhibitory peptide defines new areas of binding which could open new channels of drug development or new derivatives.

The C-terminal part of the peptide CP5-46 could have additionally interactions with the protease surface or it could stabilise the peptide structure by intramolecular interactions. The peptide could form a native-like secondary structure already in solution (Fersht, 1999) before binding that has a higher affinity for the protease, increasing the rate of association (k_a).

4.2.5 Structure-based optimisation of peptide CP5-46-A

Examination of the crystal structure of the complex, allowed a prognosis for potential amino acid exchanges which might improve binding geometry and charge interaction between the peptide and the enzyme and could improve the inhibitory effect with respect to the peptide CP5-46-A. Exchanges for the amino acids were suggested that bind to the S1` and S4 subsites of the protease that could have a better potential interaction with residues of the NS3/4A protease. It was also attempted to mimic the electrostatic interactions of a natural substrate at positions P5 and P6.

The amino acid exchanges proposed at the positions P1` and P4 did not enhance the inhibitory effect of the peptide; in fact quite to the contrary, the inhibition of the protease was totally abolished or

substantially decreased. The amino acid exchanges did not lead to a cleavage of the peptides suggesting that the binding of the peptide to the protease is perturbed. In contrast, an exchange at position P4 to Asp, which has a different functional group but a side chain of the same length as the 'original' Leu, decreased the IC_{50} 20-fold. The exchange to Glu, which has the same functional group but a longer side chain than Asp, abolished the inhibitory effect. This shows that the subsites could not accommodate the binding of a larger side chain and that a negative charge is not preferred for binding at these subsites.

The change at amino acid positions 4 and 5 of peptide CP5-46-A to the negative charged amino acids Asp and Glu increased the potency of the peptide about 6-fold. To solve the question whether or not the proposed ionic interactions between the new peptide residues had in fact contributed to the observed increase of the inhibitory effect, the optimised peptide was co-crystallised with NS3/4A. The structure of the complex showed that the overall binding of the peptide to the protease is not influenced by these amino acid exchanges. Notably the position of the backbone and side chain of Glu5 is similar to the binding of the mimicked substrate. It was shown for short peptide inhibitors that a change of Glu5 to a positively charged amino acid resulted in a 3 to 10-fold decrease in the inhibitory effect (Ingallinella *et al.*, 1998). The suggested ionic interactions between Asp4 of the peptide CP5-46-A-4D5E and Lys165 of the NS3/4A protease have apparently not formed. Therefore, it was concluded that the amino acid exchange at position P5 could be solely responsible for the increase in the inhibitory effect. However, it could also be possible that the high ionic strength during crystal formation (~1.1 M KCl) destabilised the ionic interactions between Asp4 and Lys165 and that the flexible N-terminal end led to a dislocation of the side chain. Peptides with only one amino acid exchange could be used to test if both changes have an influence on the increase of the inhibitory effect of the optimised peptide.

The introduction of the amino acid exchanges Asp4 and Glu5 into the full length peptide CP5-46 improved the inhibitory potency about 10-fold to a K_i of about 530 pM. This shows that it was possible to develop a potent long peptide inhibitor using various methods including phage-display, cosmix-plexing and structure based optimisation, leading finally to the identification of an inhibitor with a binding affinity in the picomolar range.

4.2.6 NS3/4A protease resistance mutation A156V

In 2011 two NS3/4A protease inhibitors received approval for clinical use (Klein and Struble, 2011; Poordad, 2011). Monotherapy with these protease inhibitors leads to the rapid selection of resistant variants. The newly developed drugs can therefore only be used in combination therapy with state of the art therapy regimes. Thus patients will be exposed to the same side effects as before (Sarrazin and Zeuzem, 2010; Gentile *et al.*, 2010). Most of the new protease inhibitors are bound at the active site of the NS3/4A protease, spanning only the S4–S1` subsites and thus showing a similar binding pattern and resistance profile (Sarrazin and Zeuzem, 2010; He *et al.*, 2008). It was suggested that resistance mutations occur at positions where the inhibitors have part of their structure extending outside the consensus volume modelled to be occupied by the normal substrates, the 'substrate envelope' thus the binding of the inhibitors is weakened without severe influence on substrate binding (Romano *et al.*, 2010). Notably the residues R155 and A156 interact with the inhibitors where they extend most

extensively beyond the 'substrate envelope'. Mutation at these positions confer high-level resistance against nearly all drugs reported in the literature (Romano *et al.*, 2010; Lenz *et al.*, 2010).

It was thus of primary interest to investigate the effect of known resistant HCV NS3/4A mutations on the inhibitory effect of the optimised peptide CP5-46-4D5E. The primary intention in developing longer peptides as inhibitors was to have inhibitors which might provide an alternative binding mechanism to the small molecular weight inhibitors. These might be *a priori* binding at alternative sites and/or because of their larger interactive surface be less affected by HCV resistance mutations. Several amino acids of NS3 that are involved in resistance mutations against protease inhibitors are in the proximity of the bound peptide. Especially A156 is totally covered by the modelled surface of the peptide and is in direct contact with the surface of the peptide. Modelling showed that a mutation to Val could have the highest impact on the inhibitory potency of the peptide and therefore the NS3/4A protease with the point mutation A156V was produced in recombinant form and used for activity measurements. The peptide CP5-46-4D4E was tested with the NS3/4A protease with the resistance mutation A156V. The peptide shows *negligible* susceptibility to the A156V mutation (1.5-fold increase of IC_{50} value). This shows for one of the most important resistance mutations that the peptide inhibitor is far less affected than small molecule inhibitors. The resistance mutation A156V has the greatest impact on the activity of both alternative compound groups, namely the linear α-ketoamide inhibitors and the macrocyclic inhibitors (Lenz *et al.*, 2010). Many other resistance mutations against NS3/4A inhibitors are known and it still remains to be tested with the peptide inhibitor to maintain the assumption that the peptide inhibitor has a higher barrier for resistance development. It is not unlikely that resistance mutation can also occur against the peptide inhibitors, however, because of the alternative binding mechanism and because of their larger interactive surface single HCV resistance mutations should be less effective. Such mutations could occur at yet unknown sites many likely remote from the binding site for the small molecule inhibitors. The larger interactive surface and more flexible binding of the peptide inhibitors should also allow binding even if one resistance mutation occurs, making it likely that more than one amino acid mutation would be needed to completely prevent binding of the inhibitor (McKeage *et al*., 2009; Ghany *et al*., 2009).

Because of the heterogeneity between genotypes and subgenotypes, inhibitors will not have the same activity in all HCV variants. The new small molecule protease inhibitors show a varying activity in different genotypes. The optimised peptide inhibitor was developed with a HCV genotype 1b protease from one of the clinically most relevant subgroups. It remains to be tested if it shows such a strong inhibitory effect on proteases of the different genotypes. Because of the large interactive surface and more flexible binding of the peptide inhibitors they could also exhibit the same efficacy for NS3/4A proteases of other genotypes. Even if this were not the case the method demonstrated here for the development of peptide inhibitors could be rapidly utilised, initially using the immobilised protease from the desired resistant genotype as affinity target.

4.3 Intracellular peptide delivery

Sufficient bioavailability and *in vivo* distribution is a major requirement for new drug candidates in development. The pharmaceutical industry was challenged in the 1990s by high drug candidate attrition, at least partly due to adverse pharmacokinetics and bioavailability (Kola and Landis, 2004). A comparison of successful small molecule drugs with failed drug candidates led to the development

of the ‘rule of five’ to evaluate the drug-likeness of lead candidates (Lipinski *et al.*, 2001). In summary this highly empirical rule postulates that drug candidates must be not highly lipophilic, should be low molecular weight molecules with no more than five hydrogen bond donors and no more than 10 hydrogen bond acceptors. These demands on the compound properties constrict the number of possible lead candidates for drug development. Also the ‘druggable genome study’ revealed for the human genome a much smaller number of possible targets than originally thought (Hopkins and Groom, 2002). Many biological targets are not ‘druggable’ because of the lack of suitable ('addressable') binding pockets. Peptides in contrast can have a larger surface area that is involved in binding and a synergistic binding effect of many interactions at various sites on the target protein. Therefore peptides have the potential to extend the number of ‘druggable’ targets (Groner, 2009). On the other hand peptides have a low oral bioavailability because they are degraded by proteolytic enzymes and they cannot cross the membrane of the intestinal tract. Also peptide drugs that target intracellular proteins have to cross the plasma membrane. Because of the highly selective permeability of cell membranes to macromolecules, methods for cell delivery of peptides are necessary.

The sufficient bioavailability of small molecule drugs is dearly purchased at the cost of diversity of compounds that are located within the available chemical space. Especially proteases have often similar catalytic mechanism requiring relatively large peptidic or peptidomimetic inhibitors to achieve selective inhibition (Drag and Salvesen, 2010). Decreasing the diversity of compounds reduces presumably the specificity of drug candidates. Also the number of ‘druggable’ targets is constricted because of the constraints of small molecule drugs. Biologic drugs, including peptides, in contrast, have the positive attributes of high activity, target specificity, low side-effects and lower potential toxicity but, on the negative side, low bioavailability (Sato *et al.*, 2006). Therefore novel application and cell delivery methods would not only enhance the development of biological drugs but also expand the development possibilities of small molecule drugs.

For the intracellular delivery of the inhibitory peptides against the NS3/4A protease two different delivery methods were explored: cell penetrating peptides (CPP) and pH sensitive polymersomes. CPPs are short peptides that can cross cellular membranes and thereby deliver a cargo into cells (Schwarze *et al.*, 2000). Polymersomes are nanoparticles that consist of a pH-sensitive copolymer which self assembles and forms vesicles that disrupt after acidification in the endosomes releasing the cargo into the cytosol because of a massive osmotic shock (Massignani *et al.*, 2009; Massignani *et al.*, 2010).

4.3.1 Intracellular delivery of peptides using polymersomes

The encapsulation of the inhibitory peptides into polymersomes seemed the most promising method for intracellular delivery because of the efficient endosomal escape that was described in literature (Massignani *et al.*, 2010) and because of a protection of the peptide from peptidases inside the polymersomes. Also targeting of hepatocytes with specific ligands on the surface of the polymersomes could have been possible. Unfortunately the polymersomes with encapsulated inhibitory peptide showed no inhibition of viral replication in the cell culture replicon assay compared to the control. Interestingly an increase in viral replication was seen at increased polymersome concentration. This effect cannot be explained. Because of the preparation and testing of the

polymersomes in different laboratories the polymersomes containing the peptides were stored for over four weeks until usage. Degradation of the polymersomes or peptide could be possible. Also the encapsulation of peptide was not very efficient in the experiments and needs to be further optimised. Even though the intracellular delivery of inhibitory peptides with polymersomes was not very efficient in the first experiments it is still an interesting method for intracellular delivery of peptides and should be further explored.

4.3.2 Intracellular delivery of peptides using cell penetrating peptides

It has been shown that cell penetrating peptides (CPP) were able to deliver various biological cargos into cells and also some *in vivo* animal studies were done that demonstrated intracellular delivery using CPPs and demonstrating biological activity of the cargo (Sawant and Torchilin, 2010; Chen and Harrison, 2007). To test the intracellular delivery of the inhibitory peptides different CPPs were fused to the peptides and tested in the cell culture replicon assay. As controls the inhibitory peptide fused to a non-CPP peptide and a fusion of a CPP to a scramble peptide were used. The inhibitory peptide fused to a non-CPP peptide had neither influence on the viral replication nor on the cell viability even at high peptide concentrations. Interestingly the CPP fused to the scramble peptide showed a low inhibitory effect at 20 µM and started to become toxic for the cells at a peptide concentration of 100 µM. This could be due to cell stress because of accumulation of peptide inside the cell that leads also to degradation of viral proteins. Only the fusion of the inhibitory peptide to the Antennapedia peptide showed an inhibitory effect in the replicon assay. The other peptide-CPP fusions tested showed no inhibitory effect at all or only a low inhibitory effect comparable to the control. This shows that the successful delivery using CPPs strongly depends on the delivered cargo, the concentration of the CPP and the cell type. No systematic pattern has been discerned to date, leaving only empirical trial and error (Richard *et al.*, 2005; Duchardt *et al*., 2007; Patel *et al.*, 2007; Van den Berg and Dowdy, 2011). The EC_{50} value of the Antp-K5-66-A peptide is about 3.4 µM which is a 27-fold increase compared to the IC_{50} value of the NS3/4A assay (125 nM). This increase could be due to low endosomal escape of the CPP-peptide fusion, which leads to degradation of the peptide in the lysosomes (Heitz *et al.*, 2009; Patel *et al.*, 2007). Another possibility could be degradation of the peptide by any of several cellular pathways for protein degradation leading to the apparent increase in the IC_{50} value. The N-terminal fusion of the Antp peptide to an inhibitory peptide had no influence on the inhibitory effect of the peptide (data not shown). In this case it appears that the decrease of the inhibitory effect is due to inefficient cell delivery and/or due to low stability of the peptide in cell culture. The fusion of the Antp peptide with the full length peptides CP5-46 and CP6-4, that have an higher potency *in vitro* than the peptide K5-66-A, showed a reduced inhibitory effect in the replicon cell culture model compared to the peptide K5-66-A. There maybe a negative correlation between the length of the fusion peptide fusion and uptake into the cell. Also the localisation of the peptide fusion in the cell could have been altered. Fluorescence labeled peptides could be used to see if there are differences in the cell localisation of the full-length peptide and N-terminal part (K5-66-A).

The inhibition of the viral replication by the Antp-K5-66-A fusion in the replicon cell culture model is an encouraging initial indication of an *in vivo* effect of the peptide showing that it is possible to inhibit the HCV virus also with large inhibitors that are unable to cross the cell membrane on their own. Further studies have to be made to increase the efficacy of intracellular delivery but the feasibility of HCV inhibition by large peptide in cell culture has been shown.

4.4 Perspectives

With the use of peptide phage display inhibitory peptides against both HCV proteases were isolated. For a clinical application these peptides need further development.

Against the NS2-3 protease one peptide was found that presumably inhibits protease cleavage on dimer formation. This initial indication of a direct effect on NS2-3 cleavage needs further corroborative evidence. Besides the essential role in HCV polyprotein processing, the NS2 protein has other essential functions in the viral life cycle. A second peptide that showed specific affinity for the NS2-3 protease might therefore interfere with other NS2 functions without inhibiting the protease function. If the cell delivery efficacy is improved the cell-based infectious HCV assay could be used to evaluate the effect of both peptides on the NS2 protein. This would be a valuable extension to the *in vitro* enzyme assay performed to date.

Affinity selection against the NS3/4A protease resulted in the identification of inhibitory peptides in the low nanomolar range. Recombination, using the cosmix-plexing technique, and structure based optimisation was shown to be applicable to improve the affinity of the peptide inhibitor to a K_i down to the pM range. To further improve the affinity additional amino acid exchanges could be tested. For instance an exchange of Glu5 of the optimised peptide to D-Glu5 could improve the inhibitory effect 3-fold (Ingallinella *et al.*, 1998). D-amino acid exchanges could also be used to increase the stability of the peptide for cell delivery to avoid degradation by cellular proteases. This would in all likelihood also reduce the immunogenicity of the peptides due to a limitation in MHC presentation which requires porteolytic trimming of the antigen before presentation in the MHC complex (Lien and Lowman, 2003; Sato *et al.*, 2006). For the Antp peptide it has been shown that the D-amino acid enantiomer is internalised as efficiently as the L-amino acid form (Derossi *et al.*, 1996) and could also increase the stability of the peptide fusion.

Several CPP-conjugated drugs are in clinical development with promising results (Johnson *et al.*, 2011) and fusion to a CPP could serve for clinical application of the peptides. Nevertheless, for a therapeutic use the efficacy of the cell delivery must be increased.

Another possibility for improvement lies in the area of cell-specific targeting, i.e. cell type specific delivery should be tried, e.g., by coupling hepatocyte specific ligands to nano particles, to boost the cell delivery. Should these issues remain unsolved in the immediate future the peptides can still serve as lead structures for the development of peptide mimetics, e.g., in a fashion following the development of the clinically relevant small molecules discussed above which were originally modelled on the normal substrate peptides.

5. Abstract

At the outset it was planned to develop inhibitory peptides against the NS2-3 and NS3/4A proteases of the Hepatitis C Virus (HCV) as leads for drugs for HCV treatment. These proteases are essential for the viral life cycle and therefore present interesting targets for the development of new specific antiviral HCV drugs. Worldwide up to 170 million people are chronically infected with HCV (Yu and Chiang, 2010). HCV infections are the leading cause of chronic hepatitis, liver cirrhosis and hepatocellular carcinoma (Shepard, 2005). The standard of care achieves a sustained viral response in only about half of the patients treated and is associated with considerable severe side effects (Manns *et al*, 2001).

In 2011, two new HCV drugs, NS3/4A protease inhibitors, were approved by the FDA (Klein and Struble, 2011; Poordad, 2011). Because of rapid resistance development the drugs can only be used in combination with the current treatment. Thus there remains an unmet need for HCV drugs for an effective treatment that can replace the standard of care with its severe side effects.

Large peptides might provide an alternative binding mechanism to the small molecular weight inhibitors in development. These might be binding at alternative sites and/or because of their larger interactive surface peptides are less affected by HCV resistance mutations. In this work the combinatorial phage display peptide library CPL19YS-2 displaying large peptides was used for iterative affinity enrichment on these HCV proteases.

The NS2-3 protease was produced in a form that exhibited 50% self-cleavage activity. Affinity enrichment against the NS2-3 protease led to the identification of two peptides that showed specific affinity for the NS2-3 protease. One peptide showed low inhibition of NS2-3 protease cleavage to about 70% at a concentration of 270 nM presumably due to inhibition of protease dimer formation. This is an initial indication of a direct effect on protease cleavage requiring further corroborative evidence.

The NS3/4A protease was produced as a single chain construct connecting the NS3 protease domain with the NS4A co-factor (Dimasi *et al.*, 1998). An MBP fusion increased the solubility of the protease considerably. Affinity enrichment against NS3/4A protease led to the identification of two peptides that inhibited the NS3/4A protease in the low nanomolar range. Recombination of the peptides with pre-selected populations led to the identification of peptides with increased affinity to the protease. One showing a two-fold increase in the K_i value to 5.2 nM. For optimisation of the inhibitory peptide X-ray crystallography and structural modelling were successfully implemented for the N-terminal region of the peptide. The co-crystallisation showed that the peptide covers the active site and that peptide cleavage is prevented by a sum of geometrical constraints and inhibition of the function of the oxyanion hole. Protein modelling was applied to make predictions for structural optimisation by mimicking ionic interactions of a natural substrate. One such designed variant increased affinity 10-fold to a K_i value of about 530 pM. The optimised peptide showed a negligible susceptibility to the important A156V resistance mutation of the NS3/4A protease, which is highly resistant to the small molecular weight inhibitors. This gives an initial indication that large peptides are less affected by resistance mutations. Inhibition of viral replication in cell culture was demonstrated by fusion of an inhibitory peptide to the Antp cell penetrating peptide. The efficacy of the peptide was reduced about 30-fold but it is an encouraging initial indication of intracellular inhibition of viral replication.

5.1 Zusammenfassung

Ziel dieser Arbeit war die Entwicklung inhibitorischer Peptide gegen die NS2-3 und NS3/4A Proteasen des Hepatitis C Virus (HCV), die als Ausgangspunkt für die Entwicklung von Medikamenten dienen können. Die HCV Proteasen sind essentiell für den Lebenszyklus des Virus und daher interessante Ziele für die Entwicklung neuer spezifischer Medikamente. Weltweit sind bis 170 Millionen Menschen chronisch mit HCV infiziert (Yu und Chiang, 2010). HCV Infektionen sind der Hauptgrund für chronische Hepatitis, Leberzirrhose und Leberzellkarzinom (Shepard, 2005). Die Standardbehandlung erreicht nur in ungefähr der Hälfte der behandelten Patienten eine dauerhafte Eliminierung des Virus und ist verbunden mit zahlreichen Nebenwirkungen(Manns *et al*, 2001).

2011 wurden zwei NS3/4A Protease-Inhibitoren zur Behandlung von HCV zugelassen (Klein und Struble, 2011; Poordad, 2011). Da der Virus schnell Resistenzen gegen diese Inhibitoren entwickelt, ist nur eine Anwendung mit der ursprünglichen Therapie möglich, die starke Nebenwirkungen hat. Daher besteht noch immer ein großer Bedarf an neuen Medikamenten für eine Behandlung, die die Standardbehandlung ersetzen können. Große Peptide könnten alternative Bindungsmechanismen bieten, verglichen mit den Kleinmolekül-Inhibitoren in Entwicklung. Dies könnte Bindung an alternative Stellen sein und/oder Peptide werden möglicherweise wegen ihrer großen Bindungsoberfläche weniger stark von HCV Resistenzmutationen beeinträchtigt. In dieser Arbeit wurde die Phagen Display Peptid Bibliothek CPL19YS-2, die große Peptide präsentiert, für iterative Affinitätsanreicherungen verwendet.

Die NS2-3 Protease konnte in einer Form produziert werden, die 50% Selbstspaltungs-Aktivität aufwies. Mittels Affinitätsanreicherung konnten zwei Peptide identifiziert werden, die spezifische Affinität für die NS2-3 Protease zeigen. Ein Peptid reduziert bei einer Konzentration von 270 nM die Aktivität der Protease auf 70%, wahrscheinlich durch Verhinderung der Dimer-Bildung. Dies ist ein erster Hinweis auf eine direkte Wirkung auf die Aktivität der Protease, die aber noch weitergehend untersucht werden muss.

Die NS3/4A Protease wurde als Fusionsprotein produziert, bei dem die NS3 Protease Domäne mit dem NS4A Kofaktor verbunden wurde (Dimasi *et al.*, 1998). Eine zusätzliche Fusion mit dem MBP Protein verbesserte die Löslichkeit der Protease erheblich. Mittels Affinitätsanreicherung konnten zwei Peptide identifiziert werden, die die NS3/4A Protease bei Konzentrationen im unteren nanomolaren Bereich inhibieren. Rekombination der Peptide mit pre-selektierten Peptiden führte zu Varianten mit verbesserter Affinität. Eine Variante zeigte eine zweifache Verbesserung des K_i Wertes auf 5,2 nM. Für die weitere Verbesserung des N-terminalen Bereichs des Peptids wurden Röntgenkristallographie und Strukturmodellierung erfolgreich eingesetzt. Die Ko-Kristallisation zeigte, dass das Peptid das aktive Zentrum der Protease verdeckt und das die Spaltung des Peptids durch geometrische Beschränkungen und Inhibierung des „oxyanion hole“ verhindert wird. Anhand des Modells vorgeschlagene ionische Interaktionen, die denen des natürlichen Substrats ähneln, konnten die Affinität des Peptids 10-fach auf einen K_i Wert von 530 pM verbessern. Das optimierte Peptid zeigte nur eine geringe Anfälligkeit für die A156V Resistenzmutation der NS3/4A Protease, die starke Resistenz gegen Kleinmolekül-Inhibitoren bewirkt. Dies ist ein erster Anhaltspunkt dafür, dass große Peptide weniger stark von Resistenzmutationen beeinträchtigt sind. Inhibition von viraler Replikation in Zellkultur konnte mittels Fusion an das zellpenetrierende Peptid Antp gezeigt werden. Die Wirksamkeit des Peptids war ca. 30-fach verringert, aber es ist ein erster viel versprechender Befund für eine intrazelluläre inhibitorische Wirkung.

6. References:

Adams, P. D., Gopal, K., Grosse-Kunstleve, R. W., Hung, L. W., Ioerger, T. R., McCoy, A. J., Moriarty, N. W., Pai, R. K., Read, R. J., Romo, T. D., Sacchettini, J. C., Sauter, N. K., Storoni, L. C., and Terwilliger, T. C. (2004). Recent developments in the PHENIX software for automated crystallographic structure determination. *J Synchrotron Radiat* **11**(Pt 1)**,** 53-5.

Adey, N. B., Mataragnon, A. H., Rider, J. E., Carter, J. M., and Kay, B. K. (1995). Characterization of phage that bind plastic from phage-displayed random peptide libraries. *Gene* **156**(1)**,** 27-31.

Alberti, A., Chemello, L., and Benvegnu, L. (1999). Natural history of hepatitis C. *J Hepatol* **31 Suppl 1,** 17-24.

Alter, M. J. (1997). Epidemiology of hepatitis C. *Hepatology* **26**(3 Suppl 1)**,** 62S-65S.

Arap, M. (2005). Phage display technology - Applications and innovations. *Genetics and Molecular Biology* **28**(1)**,** 1-9.

Bae, A., Sun, S. C., Qi, X., Chen, X., Ku, K., Worth, A., Wong, K. A., Harris, J., Miller, M. D., and Mo, H. (2010). Susceptibility of treatment-naive hepatitis C virus (HCV) clinical isolates to HCV protease inhibitors. *Antimicrob Agents Chemother* **54**(12)**,** 5288-97.

Barbas, C. F., 3rd, Kang, A. S., Lerner, R. A., and Benkovic, S. J. (1991). Assembly of combinatorial antibody libraries on phage surfaces: the gene III site. *Proc Natl Acad Sci U S A* **88**(18)**,** 7978-82.

Barbato, G., Cicero, D. O., Cordier, F., Narjes, F., Gerlach, B., Sambucini, S., Grzesiek, S., Matassa, V. G., De Francesco, R., and Bazzo, R. (2000). Inhibitor binding induces active site stabilization of the HCV NS3 protein serine protease domain. *EMBO J* **19**(6)**,** 1195-206.

Bartenschlager, R., Frese, M., and Pietschmann, T. (2004). Novel insights into hepatitis C virus replication and persistence. *Adv Virus Res* **63,** 71-180.

Bartenschlager, R., and Lohmann, V. (2000). Replication of the hepatitis C virus. *Baillieres Best Pract Res Clin Gastroenterol* **14**(2)**,** 241-54.

Barth, H., Schafer, C., Adah, M. I., Zhang, F., Linhardt, R. J., Toyoda, H., Kinoshita-Toyoda, A., Toida, T., Van Kuppevelt, T. H., Depla, E., Von Weizsacker, F., Blum, H. E., and Baumert, T. F. (2003). Cellular binding of hepatitis C virus envelope glycoprotein E2 requires cell surface heparan sulfate. *J Biol Chem* **278**(42)**,** 41003-12.

Bartosch, B., and Cosset, F. L. (2006). Cell entry of hepatitis C virus. *Virology* **348**(1)**,** 1-12.

Beran, R. K., and Pyle, A. M. (2008). Hepatitis C viral NS3-4A protease activity is enhanced by the NS3 helicase. *J Biol Chem* **283**(44)**,** 29929-37.

Bird, G. H., Madani, N., Perry, A. F., Princiotto, A. M., Supko, J. G., He, X., Gavathiotis, E., Sodroski, J. G., and Walensky, L. D. (2010). Hydrocarbon double-stapling remedies the proteolytic instability of a lengthy peptide therapeutic. *Proc Natl Acad Sci U S A* **107**(32)**,** 14093-8.

Bissig, K. D., Wieland, S. F., Tran, P., Isogawa, M., Le, T. T., Chisari, F. V., and Verma, I. M. (2010). Human liver chimeric mice provide a model for hepatitis B and C virus infection and treatment. *J Clin Invest* **120**(3)**,** 924-30.

Bitzegeio, J., Bankwitz, D., Hueging, K., Haid, S., Brohm, C., Zeisel, M. B., Herrmann, E., Iken, M., Ott, M., Baumert, T. F., and Pietschmann, T. (2010). Adaptation of hepatitis C virus to mouse CD81 permits infection of mouse cells in the absence of human entry factors. *PLoS Pathog* **6,** e1000978.

Blanchard, E., Belouzard, S., Goueslain, L., Wakita, T., Dubuisson, J., Wychowski, C., and Rouille, Y. (2006). Hepatitis C virus entry depends on clathrin-mediated endocytosis. *J Virol* **80**(14)**,** 6964-72.

Blight, K. J., McKeating, J. A., Marcotrigiano, J., and Rice, C. M. (2003). Efficient replication of hepatitis C virus genotype 1a RNAs in cell culture. *J Virol* **77**(5)**,** 3181-90.

Boonstra, A., van der Laan, L. J., Vanwolleghem, T., and Janssen, H. L. (2009). Experimental models for hepatitis C viral infection. *Hepatology* **50**(5)**,** 1646-55.

Bratkovic, T. (2010). Progress in phage display: evolution of the technique and its application. *Cell Mol Life Sci* **67**(5)**,** 749-67.

Breitling, F., and Dübel, S. (1997). "Rekombinante Antikörper." Spektrum Akadem Verlag, Heidelberg.

Breitling, F., Dubel, S., Seehaus, T., Klewinghaus, I., and Little, M. (1991). A surface expression vector for antibody screening. *Gene* **104**(2)**,** 147-53.

Buchholz, K., and Collins, J. (2011). "Concepts in Biotechnology: History, science and business." Wiley-VCH Verlag GmbH & Co. KGaA, Weinheim.

Bukh, J. (2004). A critical role for the chimpanzee model in the study of hepatitis C. *Hepatology* **39**(6)**,** 1469-75.

Burlone, M. E., and Budkowska, A. (2009). Hepatitis C virus cell entry: role of lipoproteins and cellular receptors. *J Gen Virol* **90**(Pt 5)**,** 1055-70.

Chen, C. H., and Yu, M. L. (2010). Evolution of interferon-based therapy for chronic hepatitis C. *Hepat Res Treat* **2010,** 140953.

Chen, L., and Harrison, S. D. (2007). Cell-penetrating peptides in drug development: enabling intracellular targets. *Biochem Soc Trans* **35**(Pt 4)**,** 821-5.

Cheng, Y., and Prusoff, W. H. (1973). Relationship between the inhibition constant (K1) and the concentration of inhibitor which causes 50 per cent inhibition (I50) of an enzymatic reaction. *Biochem Pharmacol* **22**(23)**,** 3099-108.

Choo, Q. L., Kuo, G., Weiner, A. J., Overby, L. R., Bradley, D. W., and Houghton, M. (1989). Isolation of a cDNA clone derived from a blood-borne non-A, non-B viral hepatitis genome. *Science* **244**(4902)**,** 359-62.

Ciesek, S., Steinmann, E., Wedemeyer, H., Manns, M. P., Neyts, J., Tautz, N., Madan, V., Bartenschlager, R., von Hahn, T., and Pietschmann, T. (2009). Cyclosporine A inhibits hepatitis C virus nonstructural protein 2 through cyclophilin A. *Hepatology* **50**(5)**,** 1638-45.

Cohen, J. (1999). The scientific challenge of hepatitis C. *Science* **285**(5424)**,** 26-30.

Collins, J. (1997). Phage display. *In* "Annual reports in combinatorial chemistry and molecular diversity" (W. H. Moos, M. R. Pavia, A. D. Ellington, and B. K. Kay, Eds.), Vol. 1, pp. 210-262. ESCOM Science publ., Leiden.

Collins, J., Horn, N., Wadenback, J., and Szardenings, M. (2001). Cosmix-plexing: a novel recombinatorial approach for evolutionary selection from combinatorial libraries. *J Biotechnol* **74**(4)**,** 317-38.

Contreras, A. M., Ochoa-Jimenez, R. J., Celis, A., Mendez, C., Olivares, L., Rebolledo, C. E., Hernandez-Lugo, I., Aguirre-Zavala, A. I., Jimenez-Mendez, R., and Chung, R. T. (2010). High antibody level: an accurate serologic marker of viremia in asymptomatic people with hepatitis C infection. *Transfusion* **50**(6)**,** 1335-43.

Cormier, E. G., Durso, R. J., Tsamis, F., Boussemart, L., Manix, C., Olson, W. C., Gardner, J. P., and Dragic, T. (2004). L-SIGN (CD209L) and DC-SIGN (CD209) mediate transinfection of liver cells by hepatitis C virus. *Proc Natl Acad Sci U S A* **101**(39)**,** 14067-72.

Cummings, M. D., Lindberg, J., Lin, T. I., de Kock, H., Lenz, O., Lilja, E., Fellander, S., Baraznenok, V., Nystrom, S., Nilsson, M., Vrang, L., Edlund, M., Rosenquist, A., Samuelsson, B., Raboisson, P., and Simmen, K. (2010). Induced-fit binding of the macrocyclic noncovalent inhibitor TMC435 to its HCV NS3/NS4A protease target. *Angew Chem Int Ed Engl* **49**(9)**,** 1652-5.

de Bruijne, J., Weegink, C. J., Jansen, P. L., and Reesink, H. W. (2009). New developments in the antiviral treatment of hepatitis C. *Vox Sang* **97**(1)**,** 1-12.

DeLano, W. L. (2002). The PyMOL Molecular Graphics System. *DeLano Scientific LLC***,** San Carlos, CA.

Dentzer, T. G., Lorenz, I. C., Evans, M. J., and Rice, C. M. (2009). Determinants of the hepatitis C virus nonstructural protein 2 protease domain required for production of infectious virus. *J Virol* **83**(24)**,** 12702-13.

Derossi, D., Calvet, S., Trembleau, A., Brunissen, A., Chassaing, G., and Prochiantz, A. (1996). Cell internalization of the third helix of the Antennapedia homeodomain is receptor-independent. *J Biol Chem* **271**(30)**,** 18188-93.

Devlin, J. J., Panganiban, L. C., and Devlin, P. E. (1990). Random peptide libraries: a source of specific protein binding molecules. *Science* **249**(4967)**,** 404-6.

Dimasi, N., Pasquo, A., Martin, F., Di Marco, S., Steinkuhler, C., Cortese, R., and Sollazzo, M. (1998). Engineering, characterization and phage display of hepatitis C virus NS3 protease and NS4A cofactor peptide as a single-chain protein. *Protein Eng* **11**(12)**,** 1257-65.

Drag, M., and Salvesen, G. S. (2010). Emerging principles in protease-based drug discovery. *Nat Rev Drug Discov* **9**(9)**,** 690-701.

Duchardt, F., Fotin-Mleczek, M., Schwarz, H., Fischer, R., and Brock, R. (2007). A comprehensive model for the cellular uptake of cationic cell-penetrating peptides. *Traffic* **8**(7)**,** 848-66.

Empfield, J. R., and Leeson, P. D. (2010). Lessons learned from candidate drug attrition. *IDrugs* **13**(12)**,** 869-73.

Emsley, P., and Cowtan, K. (2004). Coot: model-building tools for molecular graphics. *Acta Crystallogr D Biol Crystallogr* **60**(Pt 12 Pt 1)**,** 2126-32.

Farci, P., Shimoda, A., Coiana, A., Diaz, G., Peddis, G., Melpolder, J. C., Strazzera, A., Chien, D. Y., Munoz, S. J., Balestrieri, A., Purcell, R. H., and Alter, H. J. (2000). The outcome of acute hepatitis C predicted by the evolution of the viral quasispecies. *Science* **288**(5464)**,** 339-44.

Feinstone, S. M., Kapikian, A. Z., Purcell, R. H., Alter, H. J., and Holland, P. V. (1975). Transfusion-associated hepatitis not due to viral hepatitis type A or B. *N Engl J Med* **292**(15)**,** 767-70.

Feld, J. J., and Hoofnagle, J. H. (2005). Mechanism of action of interferon and ribavirin in treatment of hepatitis C. *Nature* **436**(7053)**,** 967-72.

Fersht, A. (1999). "Structure and mechanism in protein science: a guide to enzyme catalysis and protein folding." W.H. Freeman.

Fischer, R., Kohler, K., Fotin-Mleczek, M., and Brock, R. (2004). A stepwise dissection of the intracellular fate of cationic cell-penetrating peptides. *J Biol Chem* **279**(13)**,** 12625-35.

Flamm, S. L. (2003). Chronic hepatitis C virus infection. *JAMA* **289**(18)**,** 2413-7.

Freeman, A. J., Dore, G. J., Law, M. G., Thorpe, M., Von Overbeck, J., Lloyd, A. R., Marinos, G., and Kaldor, J. M. (2001). Estimating progression to cirrhosis in chronic hepatitis C virus infection. *Hepatology* **34**(4 Pt 1)**,** 809-16.

Friebe, P., Lohmann, V., Krieger, N., and Bartenschlager, R. (2001). Sequences in the 5' nontranslated region of hepatitis C virus required for RNA replication. *J Virol* **75**(24)**,** 12047-57.

Fried, M. W. (2002). Side effects of therapy of hepatitis C and their management. *Hepatology* **36**(5 Suppl 1)**,** S237-44.

Fried, M. W., Shiffman, M. L., Reddy, K. R., Smith, C., Marinos, G., Goncales, F. L., Jr., Haussinger, D., Diago, M., Carosi, G., Dhumeaux, D., Craxi, A., Lin, A., Hoffman, J., and Yu, J. (2002). Peginterferon alfa-2a plus ribavirin for chronic hepatitis C virus infection. *N Engl J Med* **347**(13)**,** 975-82.

Garber, K. (2007). Hepatitis C: staying the course. *Nat Biotechnol* **25**(12)**,** 1379-81.

Garrett, R., and Grisham, C. M. (2010). "Biochemistry." Brooks/Cole Pub Co.

Gasteiger, E., Hoogland, C., Gattiker, A., Duvaud, S., Wilkins, M. R., Appel, R. D., and Bairoch, A. (2005). Protein Identification and Analysis Tools on the ExPASy Server. *In* "The Proteomics Protocols Handbook" (J. M. Walker, Ed.), pp. 571-607 Humana Press, New York.

Gaudieri, S., Rauch, A., Pfafferott, K., Barnes, E., Cheng, W., McCaughan, G., Shackel, N., Jeffrey, G. P., Mollison, L., Baker, R., Furrer, H., Gunthard, H. F., Freitas, E., Humphreys, I., Klenerman, P., Mallal, S., James, I., Roberts, S., Nolan, D., and Lucas, M. (2009). Hepatitis C virus drug resistance and immune-driven adaptations: relevance to new antiviral therapy. *Hepatology* **49**(4)**,** 1069-82.

Gentile, I., Carleo, M. A., Borgia, F., Castaldo, G., and Borgia, G. (2010). The efficacy and safety of telaprevir - a new protease inhibitor against hepatitis C virus. *Expert Opin Investig Drugs* **19**(1)**,** 151-9.

Gentzsch, J., Hinkelmann, B., Kaderali, L., Irschik, H., Jansen, R., Sasse, F., Frank, R., and Pietschmann, T. (2011). Hepatitis C virus complete life cycle screen for identification of small molecules with pro- or antiviral activity. *Antiviral Res* **89**(2)**,** 136-48.

Georgel, P., Schuster, C., Zeisel, M. B., Stoll-Keller, F., Berg, T., Bahram, S., and Baumert, T. F. (2010). Virus-host interactions in hepatitis C virus infection: implications for molecular pathogenesis and antiviral strategies. *Trends Mol Med* **16**(6)**,** 277-86.

Ghany, M. G., and Doo, E. C. (2009). Antiviral resistance and hepatitis B therapy. *Hepatology* **49**(5 Suppl)**,** S174-84.

Grakoui, A., McCourt, D. W., Wychowski, C., Feinstone, S. M., and Rice, C. M. (1993). Characterization of the hepatitis C virus-encoded serine proteinase: determination of proteinase-dependent polyprotein cleavage sites. *J Virol* **67**(5)**,** 2832-43.

Grakoui, A., McCourt, D. W., Wychowski, C., Feinstone, S. M., and Rice, C. M. (1993). A second hepatitis C virus-encoded proteinase. *Proc Natl Acad Sci U S A* **90**(22)**,** 10583-7.

Grammatikos, G., and Sarrazin, C. (2010). Chronic hepatitis C. *Dtsch Med Wochenschr* **135**(50)**,** 2525-34; quiz 2535-8.

Green, M., and Loewenstein, P. M. (1988). Autonomous functional domains of chemically synthesized human immunodeficiency virus tat trans-activator protein. *Cell* **55**(6)**,** 1179-88.

Gripon, P., Cannie, I., and Urban, S. (2005). Efficient inhibition of hepatitis B virus infection by acylated peptides derived from the large viral surface protein. *J Virol* **79**(3)**,** 1613-22.

Groner, B. (2009). Peptides as drugs: Discovery and development. *In* "Peptides as drugs: Discovery and development" (B. Groner, Ed.), Vol. 1, pp. 1-9. Wiley-VCH Verlag GmbH & Co. KGaA, Weinheim.

He, Y., King, M. S., Kempf, D. J., Lu, L., Lim, H. B., Krishnan, P., Kati, W., Middleton, T., and Molla, A. (2008). Relative replication capacity and selective advantage profiles of protease inhibitor-resistant hepatitis C virus (HCV) NS3 protease mutants in the HCV genotype 1b replicon system. *Antimicrob Agents Chemother* **52**(3)**,** 1101-10.

Heitz, F., Morris, M. C., and Divita, G. (2009). Twenty years of cell-penetrating peptides: from molecular mechanisms to therapeutics. *Br J Pharmacol* **157**(2)**,** 195-206.

Helle, F., and Dubuisson, J. (2008). Hepatitis C virus entry into host cells. *Cell Mol Life Sci* **65**(1)**,** 100-12.

Herrmann, E., Neumann, A. U., Schmidt, J. M., and Zeuzem, S. (2000). Hepatitis C virus kinetics. *Antivir Ther* **5**(2)**,** 85-90.

Hoofnagle, J. H. (1997). Hepatitis C: the clinical spectrum of disease. *Hepatology* **26**(3 Suppl 1)**,** 15S-20S.

Hoofnagle, J. H., Mullen, K. D., Jones, D. B., Rustgi, V., Di Bisceglie, A., Peters, M., Waggoner, J. G., Park, Y., and Jones, E. A. (1986). Treatment of chronic non-A,non-B hepatitis with recombinant human alpha interferon. A preliminary report. *N Engl J Med* **315**(25)**,** 1575-8.

Hopkins, A. L., and Groom, C. R. (2002). The druggable genome. *Nat Rev Drug Discov* **1**(9)**,** 727-30.

Iacovacci, S., Sargiacomo, M., Parolini, I., Ponzetto, A., Peschle, C., and Carloni, G. (1993). Replication and multiplication of hepatitis C virus genome in human foetal liver cells. *Res Virol* **144**(4)**,** 275-9.

Ikeda, M., Yi, M., Li, K., and Lemon, S. M. (2002). Selectable subgenomic and genome-length dicistronic RNAs derived from an infectious molecular clone of the HCV-N strain of hepatitis C virus replicate efficiently in cultured Huh7 cells. *J Virol* **76**(6)**,** 2997-3006.

Ingallinella, P., Altamura, S., Bianchi, E., Taliani, M., Ingenito, R., Cortese, R., De Francesco, R., Steinkuhler, C., and Pessi, A. (1998). Potent peptide inhibitors of human hepatitis C virus NS3 protease are obtained by optimizing the cleavage products. *Biochemistry* **37**(25)**,** 8906-14.

Ingallinella, P., Bianchi, E., Ingenito, R., Koch, U., Steinkuhler, C., Altamura, S., and Pessi, A. (2000). Optimization of the P'-region of peptide inhibitors of hepatitis C virus NS3/4A protease. *Biochemistry* **39**(42)**,** 12898-906.

Ingallinella, P., Fattori, D., Altamura, S., Steinkuhler, C., Koch, U., Cicero, D., Bazzo, R., Cortese, R., Bianchi, E., and Pessi, A. (2002). Prime site binding inhibitors of a serine protease: NS3/4A of hepatitis C virus. *Biochemistry* **41**(17)**,** 5483-92.

Jirasko, V., Montserret, R., Lee, J. Y., Gouttenoire, J., Moradpour, D., Penin, F., and Bartenschlager, R. (2010). Structural and functional studies of nonstructural protein 2 of the hepatitis C virus reveal its key role as organizer of virion assembly. *PLoS Pathog* **6**(12)**,** e1001233.

Johnson, R. M., Harrison, S. D., and Maclean, D. (2011). Therapeutic applications of cell-penetrating peptides. *Methods Mol Biol* **683,** 535-51.

Joliot, A., Pernelle, C., Deagostini-Bazin, H., and Prochiantz, A. (1991). Antennapedia homeobox peptide regulates neural morphogenesis. *Proc Natl Acad Sci U S A* **88**(5)**,** 1864-8.

Jones, D. M., and McLauchlan, J. (2010). Hepatitis C virus: assembly and release of virus particles. *J Biol Chem* **285**(30)**,** 22733-9.

Kabsch, W. (2010). Xds. *Acta Crystallogr D Biol Crystallogr* **66**(Pt 2)**,** 125-32.

Kapust, R. B., and Waugh, D. S. (1999). Escherichia coli maltose-binding protein is uncommonly effective at promoting the solubility of polypeptides to which it is fused. *Protein Sci* **8**(8)**,** 1668-74.

Kasai, N., Tsumoto, K., Niwa, S., Misawa, S., Ueno, T., Hayashi, H., and Kumagai, I. (2001). Inhibition of the hepatitis C virus NS3 protease activity by Fv fragment of antibody 8D4. *Biochem Biophys Res Commun* **281**(2)**,** 416-24.

Kato, T., Date, T., Miyamoto, M., Furusaka, A., Tokushige, K., Mizokami, M., and Wakita, T. (2003). Efficient replication of the genotype 2a hepatitis C virus subgenomic replicon. *Gastroenterology* **125**(6)**,** 1808-17.

Kaukinen, P., Sillanpaa, M., Kotenko, S., Lin, R., Hiscott, J., Melen, K., and Julkunen, I. (2006). Hepatitis C virus NS2 and NS3/4A proteins are potent inhibitors of host cell cytokine/chemokine gene expression. *Virol J* **3,** 66.

Kay, B. K., Kurakin, A. V., and Hyde-DeRuyscher, R. (1998). From peptides to drugs via phage display. *Drug Discovery Today* **3**(8)**,** 370-378.

Kazmierski, W. M., Kenakin, T. P., and Gudmundsson, K. S. (2006). Peptide, peptidomimetic and small-molecule drug discovery targeting HIV-1 host-cell attachment and entry through gp120, gp41, CCR5 and CXCR4. *Chem Biol Drug Des* **67**(1)**,** 13-26.

Kim, J. L., Morgenstern, K. A., Lin, C., Fox, T., Dwyer, M. D., Landro, J. A., Chambers, S. P., Markland, W., Lepre, C. A., O'Malley, E. T., Harbeson, S. L., Rice, C. M., Murcko, M. A., Caron, P. R., and Thomson, J. A. (1996). Crystal structure of the hepatitis C virus NS3 protease domain complexed with a synthetic NS4A cofactor peptide. *Cell* **87**(2)**,** 343-55.

Klein, R., and Struble, K. (2011). FDA briefing on boceprevir and telaprevir. U. S. Food and Drug Administration.

Koch, U., Biasiol, G., Brunetti, M., Fattori, D., Pallaoro, M., and Steinkuhler, C. (2001). Role of charged residues in the catalytic mechanism of hepatitis C virus NS3 protease: electrostatic precollision guidance and transition-state stabilization. *Biochemistry* **40**(3)**,** 631-40.

Kola, I., and Landis, J. (2004). Can the pharmaceutical industry reduce attrition rates? *Nat Rev Drug Discov* **3**(8)**,** 711-5.

Krieger, N., Lohmann, V., and Bartenschlager, R. (2001). Enhancement of hepatitis C virus RNA replication by cell culture-adaptive mutations. *J Virol* **75**(10)**,** 4614-24.

Kuiken, C., and Simmonds, P. (2009). Nomenclature and numbering of the hepatitis C virus. *Methods Mol Biol* **510,** 33-53.

Kumar, P. K., Machida, K., Urvil, P. T., Kakiuchi, N., Vishnuvardhan, D., Shimotohno, K., Taira, K., and Nishikawa, S. (1997). Isolation of RNA aptamers specific to the NS3 protein of hepatitis C virus from a pool of completely random RNA. *Virology* **237**(2)**,** 270-82.

Lamarre, D., Anderson, P. C., Bailey, M., Beaulieu, P., Bolger, G., Bonneau, P., Bos, M., Cameron, D. R., Cartier, M., Cordingley, M. G., Faucher, A. M., Goudreau, N., Kawai, S. H., Kukolj, G., Lagace, L., LaPlante, S. R., Narjes, H., Poupart, M. A., Rancourt, J., Sentjens, R. E., St George, R., Simoneau, B., Steinmann, G., Thibeault, D., Tsantrizos, Y. S., Weldon, S. M., Yong, C. L., and Llinas-Brunet, M. (2003). An NS3 protease inhibitor with antiviral effects in humans infected with hepatitis C virus. *Nature* **426**(6963)**,** 186-9.

Landro, J. A., Raybuck, S. A., Luong, Y. P., O'Malley, E. T., Harbeson, S. L., Morgenstern, K. A., Rao, G., and Livingston, D. J. (1997). Mechanistic role of an NS4A peptide cofactor with the truncated NS3 protease of hepatitis C virus: elucidation of the NS4A stimulatory effect via kinetic analysis and inhibitor mapping. *Biochemistry* **36**(31)**,** 9340-8.

Lanford, R. E., Sureau, C., Jacob, J. R., White, R., and Fuerst, T. R. (1994). Demonstration of in vitro infection of chimpanzee hepatocytes with hepatitis C virus using strand-specific RT/PCR. *Virology* **202**(2)**,** 606-14.

Lange, C. M., Sarrazin, C., and Zeuzem, S. (2010). Review article: specifically targeted anti-viral therapy for hepatitis C - a new era in therapy. *Aliment Pharmacol Ther* **32**(1)**,** 14-28.

Lauer, G. M., and Walker, B. D. (2001). Hepatitis C virus infection. *N Engl J Med* **345**(1)**,** 41-52.

Lavillette, D., Pecheur, E. I., Donot, P., Fresquet, J., Molle, J., Corbau, R., Dreux, M., Penin, F., and Cosset, F. L. (2007). Characterization of fusion determinants points to the involvement of three discrete regions of both E1 and E2 glycoproteins in the membrane fusion process of hepatitis C virus. *J Virol* **81**(16)**,** 8752-65.

le Maire, M., Champeil, P., and Moller, J. V. (2000). Interaction of membrane proteins and lipids with solubilizing detergents. *Biochim Biophys Acta* **1508**(1-2)**,** 86-111.

Lemon, S. M. (2010). Induction and evasion of innate antiviral responses by hepatitis C virus. *J Biol Chem* **285**(30)**,** 22741-7.

Lenz, O., Verbinnen, T., Lin, T. I., Vijgen, L., Cummings, M. D., Lindberg, J., Berke, J. M., Dehertogh, P., Fransen, E., Scholliers, A., Vermeiren, K., Ivens, T., Raboisson, P., Edlund, M., Storm, S., Vrang, L., de Kock, H., Fanning, G. C., and Simmen, K. A. (2010). In vitro resistance profile of the hepatitis C virus NS3/4A protease inhibitor TMC435. *Antimicrob Agents Chemother* **54**(5)**,** 1878-87.

Li, X. D., Sun, L., Seth, R. B., Pineda, G., and Chen, Z. J. (2005). Hepatitis C virus protease NS3/4A cleaves mitochondrial antiviral signaling protein off the mitochondria to evade innate immunity. *Proc Natl Acad Sci U S A* **102**(49)**,** 17717-22.

Li, Y. (2009). Carrier proteins for fusion expression of antimicrobial peptides in Escherichia coli. *Biotechnol Appl Biochem* **54**(1)**,** 1-9.

Lien, S., and Lowman, H. B. (2003). Therapeutic peptides. *Trends Biotechnol* **21**(12)**,** 556-62.

Lin, C. (2006). HCV NS3-4A Serine Protease.

Lin, C., Kwong, A. D., and Perni, R. B. (2006). Discovery and development of VX-950, a novel, covalent, and reversible inhibitor of hepatitis C virus NS3.4A serine protease. *Infect Disord Drug Targets* **6**(1)**,** 3-16.

Lin, C., Thomson, J. A., and Rice, C. M. (1995). A central region in the hepatitis C virus NS4A protein allows formation of an active NS3-NS4A serine proteinase complex in vivo and in vitro. *J Virol* **69**(7)**,** 4373-80.

Lin, R., Lacoste, J., Nakhaei, P., Sun, Q., Yang, L., Paz, S., Wilkinson, P., Julkunen, I., Vitour, D., Meurs, E., and Hiscott, J. (2006). Dissociation of a MAVS/IPS-1/VISA/Cardif-IKKepsilon molecular complex from the mitochondrial outer membrane by hepatitis C virus NS3-4A proteolytic cleavage. *J Virol* **80**(12)**,** 6072-83.

Lindenbach, B. D., Evans, M. J., Syder, A. J., Wolk, B., Tellinghuisen, T. L., Liu, C. C., Maruyama, T., Hynes, R. O., Burton, D. R., McKeating, J. A., and Rice, C. M. (2005). Complete replication of hepatitis C virus in cell culture. *Science* **309**(5734)**,** 623-6.

Lindenbach, B. D., Meuleman, P., Ploss, A., Vanwolleghem, T., Syder, A. J., McKeating, J. A., Lanford, R. E., Feinstone, S. M., Major, M. E., Leroux-Roels, G., and Rice, C. M. (2006). Cell culture-grown hepatitis C virus is infectious in vivo and can be recultured in vitro. *Proc Natl Acad Sci U S A* **103**(10)**,** 3805-9.

Lindenbach, B. D., and Rice, C. M. (2003). Molecular biology of flaviviruses. *Adv Virus Res* **59,** 23-61.

Lipinski, C. A., Lombardo, F., Dominy, B. W., and Feeney, P. J. (2001). Experimental and computational approaches to estimate solubility and permeability in drug discovery and development settings. *Adv Drug Deliv Rev* **46**(1-3)**,** 3-26.

Lohmann, V., Hoffmann, S., Herian, U., Penin, F., and Bartenschlager, R. (2003). Viral and cellular determinants of hepatitis C virus RNA replication in cell culture. *J Virol* **77**(5)**,** 3007-19.

Lohmann, V., Korner, F., Koch, J., Herian, U., Theilmann, L., and Bartenschlager, R. (1999). Replication of subgenomic hepatitis C virus RNAs in a hepatoma cell line. *Science* **285**(5424)**,** 110-3.

Lorenz, I. C., Marcotrigiano, J., Dentzer, T. G., and Rice, C. M. (2006). Structure of the catalytic domain of the hepatitis C virus NS2-3 protease. *Nature* **442**(7104)**,** 831-5.

Lowman, H. B. (1997). Bacteriophage display and discovery of peptide leads for drug development. *Annu Rev Biophys Biomol Struct* **26,** 401-24.

Machida, K., Kondo, Y., Huang, J. Y., Chen, Y. C., Cheng, K. T., Keck, Z., Foung, S., Dubuisson, J., Sung, V. M., and Lai, M. M. (2008). Hepatitis C virus (HCV)-induced immunoglobulin hypermutation reduces the affinity and neutralizing activities of antibodies against HCV envelope protein. *J Virol* **82**(13)**,** 6711-20.

Machida, K., Tsukiyama-Kohara, K., Seike, E., Tone, S., Shibasaki, F., Shimizu, M., Takahashi, H., Hayashi, Y., Funata, N., Taya, C., Yonekawa, H., and Kohara, M. (2001). Inhibition of cytochrome c release in Fas-mediated signaling pathway in transgenic mice induced to express hepatitis C viral proteins. *J Biol Chem* **276**(15)**,** 12140-6.

Manns, M. P., McHutchison, J. G., Gordon, S. C., Rustgi, V. K., Shiffman, M., Reindollar, R., Goodman, Z. D., Koury, K., Ling, M., and Albrecht, J. K. (2001). Peginterferon alfa-2b plus ribavirin compared with interferon alfa-2b plus ribavirin for initial treatment of chronic hepatitis C: a randomised trial. *Lancet* **358**(9286)**,** 958-65.

Mao, S., Cun, D., and Kawashima, Y. (2009). Novel Non Injectable Formulation Approaches of Peptides Proteins. *In* "Delivery Technologies for Biopharmaceuticals: Peptides, Proteins, Nucleic Acids and Vaccines" (L. Jorgensen, and H. M. Nielson, Eds.), Vol. 1, pp. 29-69. Wiley-VCH Verlag GmbH & Co. KGaA, Weinheim.

Martin, F., Volpari, C., Steinkuhler, C., Dimasi, N., Brunetti, M., Biasiol, G., Altamura, S., Cortese, R., De Francesco, R., and Sollazzo, M. (1997). Affinity selection of a camelized V(H) domain antibody inhibitor of hepatitis C virus NS3 protease. *Protein Eng* **10**(5)**,** 607-14.

Martinot-Peignoux, M., Boyer, N., Pouteau, M., Castelnau, C., Giuily, N., Duchatelle, V., Auperin, A., Degott, C., Benhamou, J. P., Erlinger, S., and Marcellin, P. (1998). Predictors of sustained response to alpha interferon therapy in chronic hepatitis C. *J Hepatol* **29**(2)**,** 214-23.

Massignani, M., Canton, I., Patikarnmonthon, N., Warren, N. J., Armes, S. P., Lewis, A. L., and Battaglia, G. (2010). Cellular delivery of antibodies: effective targeted subcellular imaging and new therapeutic tool. *Available from Nature Precedings* (http://hdl.handle.net/10101/npre.2010.4427.1).

Massignani, M., LoPresti, C., Blanazs, A., Madsen, J., Armes, S. P., Lewis, A. L., and Battaglia, G. (2009). Controlling cellular uptake by surface chemistry, size, and surface topology at the nanoscale. *Small* **5**(21)**,** 2424-32.

McCoy, A. J., Grosse-Kunstleve, R. W., Adams, P. D., Winn, M. D., Storoni, L. C., and Read, R. J. (2007). Phaser crystallographic software. *J Appl Crystallogr* **40**(Pt 4)**,** 658-674.

McKeage, K., Perry, C. M., and Keam, S. J. (2009). Darunavir: a review of its use in the management of HIV infection in adults. *Drugs* **69**(4)**,** 477-503.

Meuleman, P., and Leroux-Roels, G. (2008). The human liver-uPA-SCID mouse: a model for the evaluation of antiviral compounds against HBV and HCV. *Antiviral Res* **80**(3)**,** 231-8.

Mihm, S. (2010). Hepatitis C virus, diabetes and steatosis: clinical evidence in favor of a linkage and role of genotypes. *Dig Dis* **28**(1)**,** 280-4.

Miller, D. M., 3rd, Olson, J. S., Pflugrath, J. W., and Quiocho, F. A. (1983). Rates of ligand binding to periplasmic proteins involved in bacterial transport and chemotaxis. *J Biol Chem* **258**(22)**,** 13665-72.

Misialek, S., Rajagopalan, R., Stevens, S. K., Beigelman, L., Seiwert, S. D., and Kossen, K. (2009). Optimization of the multiple enzymatic activities of the hepatitis C virus NS3 protein. *Anal Biochem* **394**(1)**,** 138-40.

Model, P., and Russel, M. (1988). Filamentous bacteriophage. *In* "The bacteriophages" (R. Calendar, Ed.), Vol. 2, pp. 375–456. Plenum Publishers, New York.

Molek, P., Strukelj, B., and Bratkovic, T. (2011). Peptide phage display as a tool for drug discovery: targeting membrane receptors. *Molecules* **16**(1)**,** 857-87.

Moradpour, D., Penin, F., and Rice, C. M. (2007). Replication of hepatitis C virus. *Nat Rev Microbiol* **5**(6)**,** 453-63.

Cloëtta Foundation (2008). Hepatitis C: Molecular virology and antiviral targets. Moradpour, M.

Morris, M. C., Depollier, J., Mery, J., Heitz, F., and Divita, G. (2001). A peptide carrier for the delivery of biologically active proteins into mammalian cells. *Nat Biotechnol* **19**(12)**,** 1173-6.

Mullard, A. (2011). 2010 FDA drug approvals. *Nat Rev Drug Discov* **10**(2)**,** 82-5.

Murshudov, G. N., Vagin, A. A., and Dodson, E. J. (1997). Refinement of macromolecular structures by the maximum-likelihood method. *Acta Crystallogr D Biol Crystallogr* **53**(Pt 3)**,** 240-55.

Nakamura, G. R., Reynolds, M. E., Chen, Y. M., Starovasnik, M. A., and Lowman, H. B. (2002). Stable "zeta" peptides that act as potent antagonists of the high-affinity IgE receptor. *Proc Natl Acad Sci U S A* **99**(3)**,** 1303-8.

Nakamura, M., Saito, H., and Hibi, T. (2008). Advances in genomic research on hepatitis C virus with a useful tool, replicon system. *Keio J Med* **57**(2)**,** 75-83.

Nalam, M. N., Ali, A., Altman, M. D., Reddy, G. S., Chellappan, S., Kairys, V., Ozen, A., Cao, H., Gilson, M. K., Tidor, B., Rana, T. M., and Schiffer, C. A. (2010). Evaluating the substrate-envelope hypothesis: structural analysis of novel HIV-1 protease inhibitors designed to be robust against drug resistance. *J Virol* **84**(10)**,** 5368-78.

Negro, F. (2010). Hepatitis C virus-induced steatosis: an overview. *Dig Dis* **28**(1)**,** 294-9.

Nielsen, S. U., Bassendine, M. F., Burt, A. D., Martin, C., Pumeechockchai, W., and Toms, G. L. (2006). Association between hepatitis C virus and very-low-density lipoprotein (VLDL)/LDL analysed in iodixanol density gradients. *J Virol* **80**(5)**,** 2418-28.

Nielson, H. M., and Jorgensen, L. (2009). Challenges in Delivery of Biopharmaceuticals; the Need for Advanced Delivery Systems. *In* "Delivery Technologies for Biopharmaceuticals: Peptides, Proteins, Nucleic Acids and Vaccines" (L. Jorgensen, and H. M. Nielson, Eds.), Vol. 1, pp. 1-9. Wiley-VCH Verlag GmbH & Co. KGaA, Weinheim.

Ortqvist, P., Gising, J., Ehrenberg, A. E., Vema, A., Borg, A., Karlen, A., Larhed, M., Danielson, U. H., and Sandstrom, A. (2010). Discovery of achiral inhibitors of the hepatitis C virus NS3 protease based on 2(1H)-pyrazinones. *Bioorg Med Chem* **18**(17)**,** 6512-25.

Otto, H. H., and Schirmeister, T. (1997). Cysteine Proteases and Their Inhibitors. *Chem Rev* **97**(1)**,** 133-172.

Otvos, L., Jr. (2008). Peptide-based drug design: here and now. *Methods Mol Biol* **494,** 1-8.

Otwinowski, Z., and Minor, W. (1997). Processing of X-ray diffraction data collected in oscillation mode. *In* "Methods in Enzymology" (Charles W. Carter, Jr., Ed.), Vol. Volume 276, pp. 307-326. Academic Press.

Pallaoro, M., Lahm, A., Biasiol, G., Brunetti, M., Nardella, C., Orsatti, L., Bonelli, F., Orru, S., Narjes, F., and Steinkuhler, C. (2001). Characterization of the hepatitis C virus NS2/3 processing reaction by using a purified precursor protein. *J Virol* **75**(20)**,** 9939-46.

Parmley, S. F., and Smith, G. P. (1988). Antibody-selectable filamentous fd phage vectors: affinity purification of target genes. *Gene* **73**(2)**,** 305-18.

Patel, K., Muir, A. J., and McHutchison, J. G. (2006). Diagnosis and treatment of chronic hepatitis C infection. *BMJ* **332**(7548)**,** 1013-7.

Patel, L. N., Zaro, J. L., and Shen, W. C. (2007). Cell penetrating peptides: intracellular pathways and pharmaceutical perspectives. *Pharm Res* **24**(11)**,** 1977-92.

Pawlotsky, J. M. (2006). Therapy of hepatitis C: from empiricism to eradication. *Hepatology* **43**(2 Suppl 1)**,** S207-20.

Perni, R. B., Almquist, S. J., Byrn, R. A., Chandorkar, G., Chaturvedi, P. R., Courtney, L. F., Decker, C. J., Dinehart, K., Gates, C. A., Harbeson, S. L., Heiser, A., Kalkeri, G., Kolaczkowski, E., Lin, K., Luong, Y. P., Rao, B. G., Taylor, W. P., Thomson, J. A., Tung, R. D., Wei, Y., Kwong, A. D., and Lin, C. (2006). Preclinical profile of VX-950, a potent, selective, and orally bioavailable inhibitor of hepatitis C virus NS3-4A serine protease. *Antimicrob Agents Chemother* **50**(3)**,** 899-909.

Perz, J. F., Armstrong, G. L., Farrington, L. A., Hutin, Y. J., and Bell, B. P. (2006). The contributions of hepatitis B virus and hepatitis C virus infections to cirrhosis and primary liver cancer worldwide. *J Hepatol* **45**(4)**,** 529-38.

Pietschmann, T., Kaul, A., Koutsoudakis, G., Shavinskaya, A., Kallis, S., Steinmann, E., Abid, K., Negro, F., Dreux, M., Cosset, F. L., and Bartenschlager, R. (2006). Construction and characterization of infectious intragenotypic and intergenotypic hepatitis C virus chimeras. *Proc Natl Acad Sci U S A* **103**(19)**,** 7408-13.

Pietschmann, T., Lohmann, V., Kaul, A., Krieger, N., Rinck, G., Rutter, G., Strand, D., and Bartenschlager, R. (2002). Persistent and transient replication of full-length hepatitis C virus genomes in cell culture. *J Virol* **76**(8)**,** 4008-21.

Polaina, J., and MacCabe, A. P. (2007). "Industrial enzymes: structure, function and applications." Springer.

Pollmann, E. (2010). TU Braunschweig, Braunschweig.

Pooga, M., Hallbrink, M., Zorko, M., and Langel, U. (1998). Cell penetration by transportan. *FASEB J* **12**(1)**,** 67-77.

Poordad, F. (2011). Big changes are coming in hepatitis C. *Curr Gastroenterol Rep* **13**(1)**,** 72-7.

Potocky, T. B., Menon, A. K., and Gellman, S. H. (2003). Cytoplasmic and nuclear delivery of a TAT-derived peptide and a beta-peptide after endocytic uptake into HeLa cells. *J Biol Chem* **278**(50)**,** 50188-94.

Pujals, S., Fernandez-Carneado, J., Lopez-Iglesias, C., Kogan, M. J., and Giralt, E. (2006). Mechanistic aspects of CPP-mediated intracellular drug delivery: relevance of CPP self-assembly. *Biochim Biophys Acta* **1758**(3)**,** 264-79.

Raney, K. D., Sharma, S. D., Moustafa, I. M., and Cameron, C. E. (2010). Hepatitis C virus non-structural protein 3 (HCV NS3): a multifunctional antiviral target. *J Biol Chem* **285**(30)**,** 22725-31.

Rehermann, B. (2009). Hepatitis C virus versus innate and adaptive immune responses: a tale of coevolution and coexistence. *J Clin Invest* **119**(7)**,** 1745-54.

Reichard, O., Andersson, J., Schvarcz, R., and Weiland, O. (1991). Ribavirin treatment for chronic hepatitis C. *Lancet* **337**(8749)**,** 1058-61.

Peptide Therapeutics Foundation (2010). 2010 Report Summary. Reichert, J., Pechon, P., Tartar, A., and Dunn, M. K.

Reiser, M., Hinrichsen, H., Benhamou, Y., Reesink, H. W., Wedemeyer, H., Avendano, C., Riba, N., Yong, C. L., Nehmiz, G., and Steinmann, G. G. (2005). Antiviral efficacy of NS3-serine protease inhibitor BILN-2061 in patients with chronic genotype 2 and 3 hepatitis C. *Hepatology* **41**(4)**,** 832-5.

Richard, J. P., Melikov, K., Brooks, H., Prevot, P., Lebleu, B., and Chernomordik, L. V. (2005). Cellular uptake of unconjugated TAT peptide involves clathrin-dependent endocytosis and heparan sulfate receptors. *J Biol Chem* **280**(15)**,** 15300-6.

Romano, K. P., Ali, A., Royer, W. E., and Schiffer, C. A. (2010). Drug resistance against HCV NS3/4A inhibitors is defined by the balance of substrate recognition versus inhibitor binding. *Proc Natl Acad Sci U S A* **107**(49)**,** 20986-91.

Rottgen, P., and Collins, J. (1995). A human pancreatic secretory trypsin inhibitor presenting a hypervariable highly constrained epitope via monovalent phagemid display. *Gene* **164**(2)**,** 243-50.

Russel, M., Clackson, T., and Lowman, H. (2004). Introduction to phage biology and phage display. *In* "Phage display" (T. Clackson, and H. Lowman, Eds.), pp. 1-26. Oxford University Press, Oxford.

Sarrazin, C., and Zeuzem, S. (2010). Resistance to direct antiviral agents in patients with hepatitis C virus infection. *Gastroenterology* **138**(2)**,** 447-62.

Sato, A. K., Viswanathan, M., Kent, R. B., and Wood, C. R. (2006). Therapeutic peptides: technological advances driving peptides into development. *Curr Opin Biotechnol* **17**(6)**,** 638-42.

Sawant, R., and Torchilin, V. (2010). Intracellular transduction using cell-penetrating peptides. *Mol Biosyst* **6**(4)**,** 628-40.

Schmidt, J., Thimme, R., and Neumann-Haefelin, C. (2011). Host genetics in immune-mediated hepatitis C virus clearance. *Biomark Med* **5**(2)**,** 155-69.

Schregel, V., Jacobi, S., Penin, F., and Tautz, N. (2009). Hepatitis C virus NS2 is a protease stimulated by cofactor domains in NS3. *Proc Natl Acad Sci U S A* **106**(13)**,** 5342-7.

Schwarze, S. R., Hruska, K. A., and Dowdy, S. F. (2000). Protein transduction: unrestricted delivery into all cells? *Trends Cell Biol* **10**(7)**,** 290-5.

Shepard, C. W., Finelli, L., and Alter, M. J. (2005). Global epidemiology of hepatitis C virus infection. *Lancet Infect Dis* **5**(9)**,** 558-67.

Sillerud, L. O., and Larson, R. S. (2005). Design and structure of peptide and peptidomimetic antagonists of protein-protein interaction. *Curr Protein Pept Sci* **6**(2)**,** 151-69.

Simmonds, P., Bukh, J., Combet, C., Deleage, G., Enomoto, N., Feinstone, S., Halfon, P., Inchauspe, G., Kuiken, C., Maertens, G., Mizokami, M., Murphy, D. G., Okamoto, H., Pawlotsky, J. M., Penin, F., Sablon, E., Shin, I. T., Stuyver, L. J., Thiel, H. J., Viazov, S., Weiner, A. J., and Widell, A. (2005). Consensus proposals for a unified system of nomenclature of hepatitis C virus genotypes. *Hepatology* **42**(4)**,** 962-73.

Smith, G. P. (1985). Filamentous fusion phage: novel expression vectors that display cloned antigens on the virion surface. *Science* **228**(4705)**,** 1315-7.

Smyth, D. R., Mrozkiewicz, M. K., McGrath, W. J., Listwan, P., and Kobe, B. (2003). Crystal structures of fusion proteins with large-affinity tags. *Protein Sci* **12**(7)**,** 1313-22.

Steinkuhler, C., Biasiol, G., Brunetti, M., Urbani, A., Koch, U., Cortese, R., Pessi, A., and De Francesco, R. (1998). Product inhibition of the hepatitis C virus NS3 protease. *Biochemistry* **37**(25)**,** 8899-905.

Steinkühler, C., Urbani, A., and De Francesco, R. (1999). Proteases of the Hepatitis C Virus. *In* "Proteases of Infectious Agents" (B. Dunn, Ed.), Vol. 1, pp. 61-91. Academic Press, Burlington.

Sudo, K., Yamaji, K., Kawamura, K., Nishijima, T., Kojima, N., Aibe, K., Shimotohno, K., and Shimizu, Y. (2005). High-throughput screening of low molecular weight NS3-NS4A protease inhibitors using a fluorescence resonance energy transfer substrate. *Antivir Chem Chemother* **16**(6)**,** 385-92.

Sy, T., and Jamal, M. M. (2006). Epidemiology of hepatitis C virus (HCV) infection. *Int J Med Sci* **3**(2)**,** 41-6.

Taliani, M., Bianchi, E., Narjes, F., Fossatelli, M., Urbani, A., Steinkuhler, C., De Francesco, R., and Pessi, A. (1996). A continuous assay of hepatitis C virus protease based on resonance energy transfer depsipeptide substrates. *Anal Biochem* **240**(1)**,** 60-7.

Tang, H., and Grise, H. (2009). Cellular and molecular biology of HCV infection and hepatitis. *Clin Sci (Lond)* **117**(2)**,** 49-65.

Taremi, S. S., Beyer, B., Maher, M., Yao, N., Prosise, W., Weber, P. C., and Malcolm, B. A. (1998). Construction, expression, and characterization of a novel fully activated recombinant single-chain hepatitis C virus protease. *Protein Sci* **7**(10)**,** 2143-9.

Tedbury, P. R., and Harris, M. (2007). Characterisation of the role of zinc in the hepatitis C virus NS2/3 auto-cleavage and NS3 protease activities. *J Mol Biol* **366**(5)**,** 1652-60.

Terrault, N. A. (2002). Sexual activity as a risk factor for hepatitis C. *Hepatology* **36**(5 Suppl 1)**,** S99-105.

Thibeault, D., Maurice, R., Pilote, L., Lamarre, D., and Pause, A. (2001). In vitro characterization of a purified NS2/3 protease variant of hepatitis C virus. *J Biol Chem* **276**(49)**,** 46678-84.

Tomei, L., Failla, C., Vitale, R. L., Bianchi, E., and De Francesco, R. (1996). A central hydrophobic domain of the hepatitis C virus NS4A protein is necessary and sufficient for the activation of the NS3 protease. *J Gen Virol* **77 (Pt 5),** 1065-70.

Torchilin, V. (2008). Intracellular delivery of protein and peptide therapeutics. *Drug Discovery Today: Technologies* **5**(2-3)**,** 95-103.

Torchilin, V. P., and Lukyanov, A. N. (2003). Peptide and protein drug delivery to and into tumors: challenges and solutions. *Drug Discov Today* **8**(6)**,** 259-66.

Trabi, M., Schirra, H. J., and Craik, D. J. (2001). Three-dimensional structure of RTD-1, a cyclic antimicrobial defensin from Rhesus macaque leukocytes. *Biochemistry* **40**(14)**,** 4211-21.

Tsantrizos, Y. S. (2004). The design of a potent inhibitor of the hepatitis C virus NS3 protease: BILN 2061--from the NMR tube to the clinic. *Biopolymers* **76**(4)**,** 309-23.

Turk, B. (2006). Targeting proteases: successes, failures and future prospects. *Nat Rev Drug Discov* **5**(9)**,** 785-99.

Urbani, A., Bianchi, E., Narjes, F., Tramontano, A., De Francesco, R., Steinkuhler, C., and Pessi, A. (1997). Substrate specificity of the hepatitis C virus serine protease NS3. *J Biol Chem* **272**(14)**,** 9204-9.

van den Berg, A., and Dowdy, S. F. (2011). Protein transduction domain delivery of therapeutic macromolecules. *Curr Opin Biotechnol*.

Vasievich, E. A., and Huang, L. (2009). Chemical Vectors for Delivery of Nucleic Acid-based Drugs. *In* "Delivery Technologies for Biopharmaceuticals: Peptides, Proteins, Nucleic Acids and Vaccines" (L. Jorgensen, and H. M. Nielson, Eds.), Vol. 1, pp. 69-93. Wiley-VCH Verlag GmbH & Co. KGaA, Weinheim.

Velazquez-Campoy, A., Ohtaka, H., Nezami, A., Muzammil, S., and Freire, E. (2004). Isothermal titration calorimetry. *Curr Protoc Cell Biol* **Chapter 17,** Unit 17 8.

Vieira, J., and Messing, J. (1987). Production of single-stranded plasmid DNA. *Methods Enzymol* **153,** 3-11.

Wakita, T., Pietschmann, T., Kato, T., Date, T., Miyamoto, M., Zhao, Z., Murthy, K., Habermann, A., Krausslich, H. G., Mizokami, M., Bartenschlager, R., and Liang, T. J. (2005). Production of infectious hepatitis C virus in tissue culture from a cloned viral genome. *Nat Med* **11**(7)**,** 791-6.

Walker, C. M. (2010). Adaptive immunity to the hepatitis C virus. *Adv Virus Res* **78,** 43-86.

Walters, K. A., Joyce, M. A., Thompson, J. C., Smith, M. W., Yeh, M. M., Proll, S., Zhu, L. F., Gao, T. J., Kneteman, N. M., Tyrrell, D. L., and Katze, M. G. (2006). Host-specific response to HCV infection in the chimeric SCID-beige/Alb-uPA mouse model: role of the innate antiviral immune response. *PLoS Pathog* **2**(6)**,** e59.

Wang, C., Sarnow, P., and Siddiqui, A. (1993). Translation of human hepatitis C virus RNA in cultured cells is mediated by an internal ribosome-binding mechanism. *J Virol* **67**(6)**,** 3338-44.

Washburn, M. L., Bility, M. T., Zhang, L., Kovalev, G. I., Buntzman, A., Frelinger, J. A., Barry, W., Ploss, A., Rice, C. M., and Su, L. (2011). A Humanized Mouse Model to Study Hepatitis C Virus Infection, Immune Response, and Liver Disease. *Gastroenterology*.

Welbourn, S., Green, R., Gamache, I., Dandache, S., Lohmann, V., Bartenschlager, R., Meerovitch, K., and Pause, A. (2005). Hepatitis C virus NS2/3 processing is required for NS3 stability and viral RNA replication. *J Biol Chem* **280**(33)**,** 29604-11.

Wolk, B., Sansonno, D., Krausslich, H. G., Dammacco, F., Rice, C. M., Blum, H. E., and Moradpour, D. (2000). Subcellular localization, stability, and trans-cleavage competence of the hepatitis C virus NS3-NS4A complex expressed in tetracycline-regulated cell lines. *J Virol* **74**(5)**,** 2293-304.

Xu, Z., Choi, J., Yen, T. S., Lu, W., Strohecker, A., Govindarajan, S., Chien, D., Selby, M. J., and Ou, J. (2001). Synthesis of a novel hepatitis C virus protein by ribosomal frameshift. *EMBO J* **20**(14)**,** 3840-8.

Yao, N., Reichert, P., Taremi, S. S., Prosise, W. W., and Weber, P. C. (1999). Molecular views of viral polyprotein processing revealed by the crystal structure of the hepatitis C virus bifunctional protease-helicase. *Structure* **7**(11)**,** 1353-63.

Yu, C. I., and Chiang, B. L. (2010). A new insight into hepatitis C vaccine development. *J Biomed Biotechnol* **2010,** 548280.

Zhou, Y., Muh, U., Hanzelka, B. L., Bartels, D. J., Wei, Y., Rao, B. G., Brennan, D. L., Tigges, A. M., Swenson, L., Kwong, A. D., and Lin, C. (2007). Phenotypic and structural analyses of hepatitis C virus NS3 protease Arg155 variants: sensitivity to telaprevir (VX-950) and interferon alpha. *J Biol Chem* **282**(31)**,** 22619-28.

7. Appendix

7.1 Purification of Antennapedia-peptides

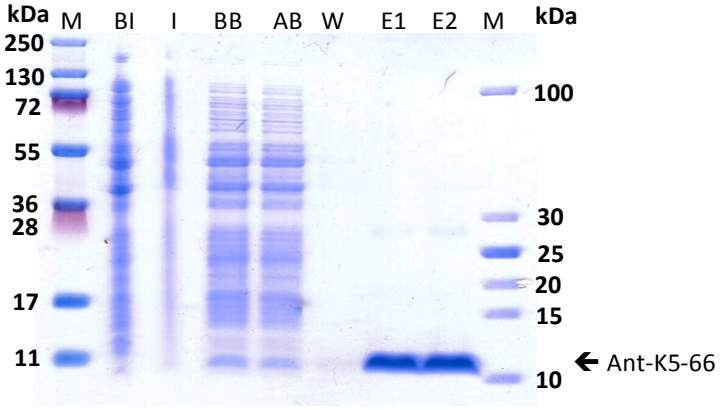

Figure 7-1: Production and purification of Ant-K5-66 peptide. 10% Tricine PAGE gel, M: molecular weight marker, BI: before induction, I: 5h after induction, BB: before binding, AB: after binding; W: washing fractions, E1: elution fraction 1 µl, E2: elution fraction 1.5 µl. 3µl of each other fraction were loaded onto the gel.

7.2 Purification of MBP-peptides

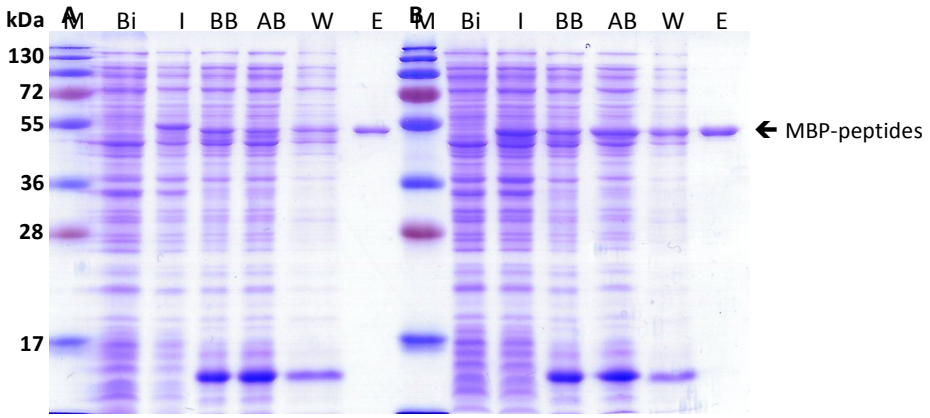

Figure 7-2: Production and purification of MBP-K6-10 (A) and MBP-K5-66 (B) peptide. 12% SDS-gel, M: molecular weight marker, BI: before induction, I: 3 h after induction, BB: before binding, AB: after binding; W: washing fractions, E: elution fraction. 3 µl of each fraction were loaded onto the gel, except elution fraction: A: 2 µl, B: 2 µl.

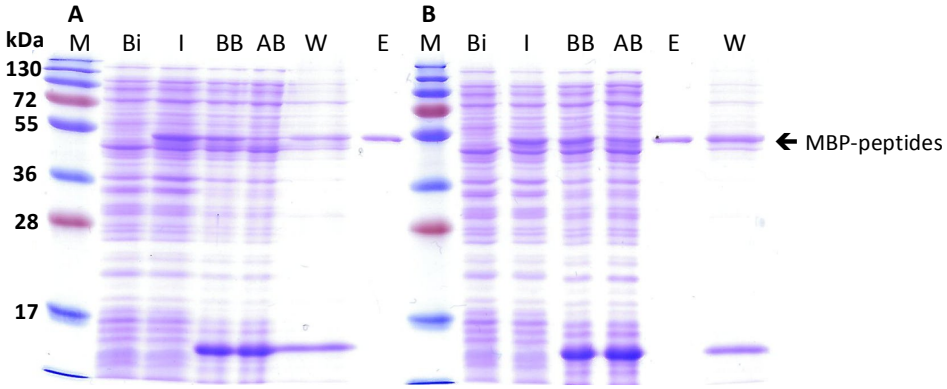

Figure 7-3: Production and purification of MBP-CP5-46 (A) and MBP-CP6-4 (B) peptide. 12% SDS-gel, M: molecular weight marker, BI: before induction, I: 3 h after induction, BB: before binding, AB: after binding; W: washing fractions, E: elution fraction. 3 µl of each fraction were loaded onto the gel, except elution fraction: A: 1 µl, B: 2 µl 1:5 dilution.

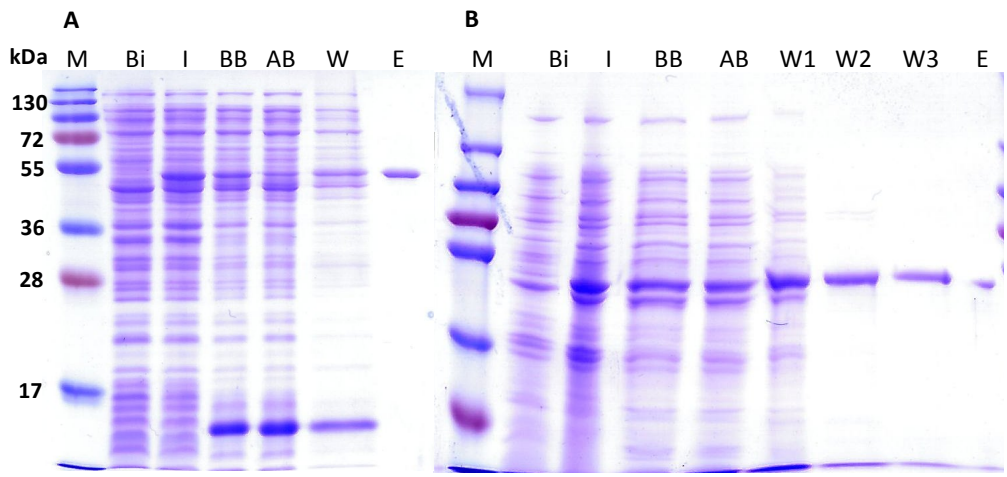

Figure 7-4: Production and purification of MBP-NS2-E11 (A) and MBP-CP6-11 (B) peptide. 12% SDS-gel, M: molecular weight marker, BI: before induction, I: 3 h after induction, BB: before binding, AB: after binding; W: washing fractions, E: elution fraction. 3 µl of each fraction were loaded onto the gel, except elution fraction: A: 1 µl 1:5 dilution, B: 1 µl 1:5 dilution.

7.3 NS3/4A activity assay

7.3.1 Inhibition of NS3/4A activity

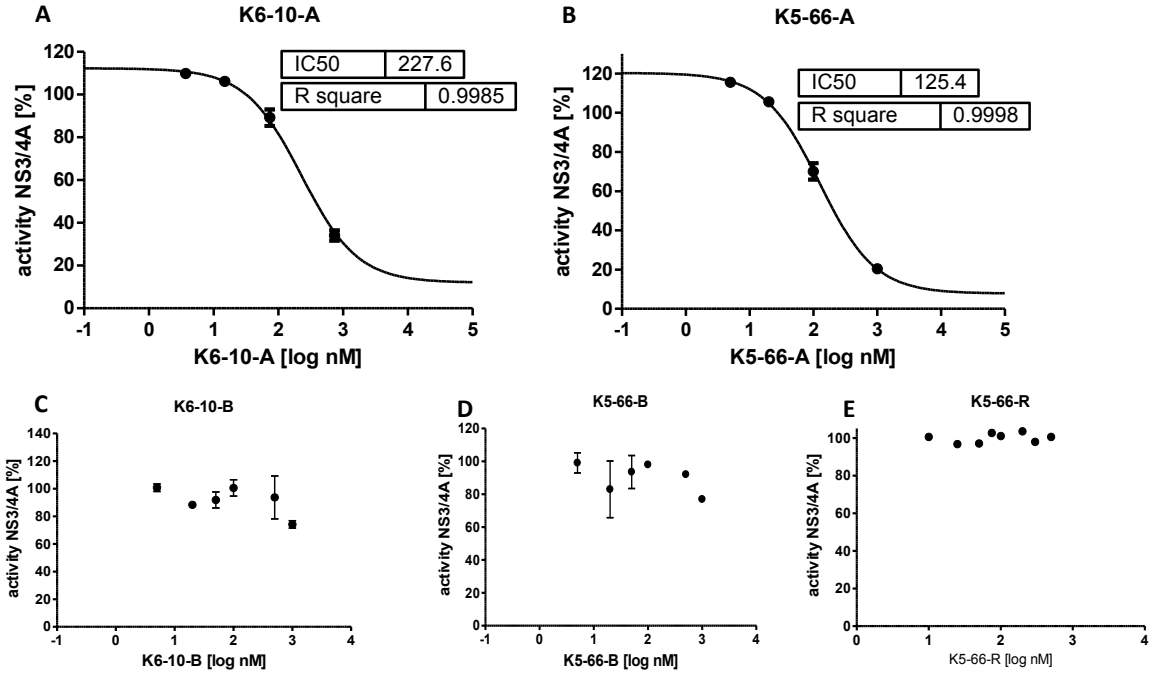

Figure 7-5: Determination of the IC_{50} of peptide K6-10-A (A), K5-66-A (B) K6-10-B (C), and K5-66-B (D) using the NS3/4A activity assay. Assay was done in buffer M2235 with 5 µM substrate M-2235 (Bachem) and 1 nM NS3/4A. All peptides chemically synthesised. Excitation filter: 360/40 nm, emission filter: 460/40 nm. Velocity of fluorescence increase over one hour was compared to that of a scrambled control peptide K5-66-R (E). Each measurement was done in duplicate, IC_{50} in nM. The curve was fitted with *GraphPad Prism* using a nonlinear regression model with variable slope : Y=Bottom+(Top-Bottom)/ (1+10^((LogIC_{50}-X)*slope)).

7.3.2 Cosmix-plexing of inhibitory peptides K5-66 and K6-10

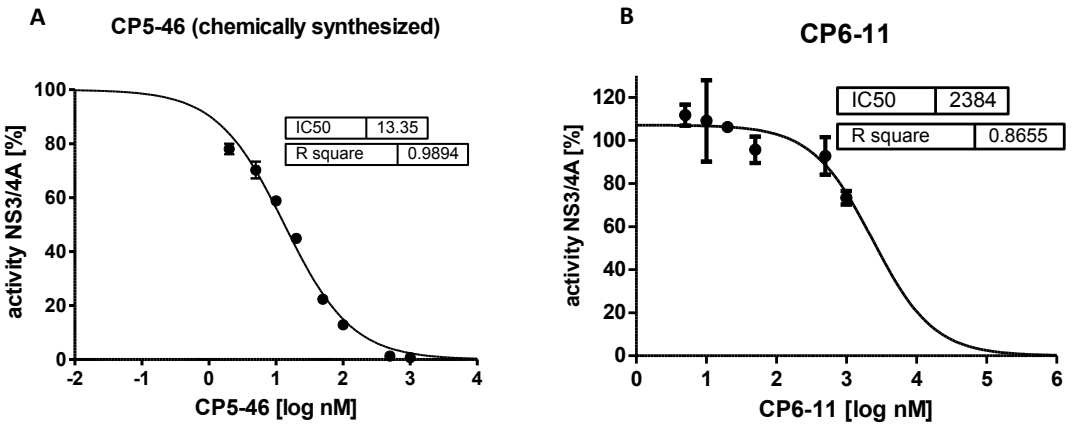

Figure 7-6: Determination of the IC_{50} of peptide CP5-46 (A) and CP6-11 (B) using the NS3/4A activity assay. Assay was done in buffer M2235 with 5 µM substrate M-2235 (Bachem) and 1 nM NS3/4A. Peptide CP5-46 was chemically synthesised. Peptide CP6-11 was produced as MBP fusion protein with His-Tag. Excitation filter: 360/40 nm, emission filter: 460/40 nm. Velocity of fluorescence increase over one hour was compared to that of a scrambled control peptide or the NS2-K11 control peptide. Each measurement was done in duplicate, IC_{50} in nM. The curve was fitted with *GraphPad Prism* using a (A) nonlinear regression model with variable slope and normalised response: Y=100/(1+10^((LogIC$_{50}$-X)*slope)) or a (B) nonlinear regression model with variable slope : Y=Bottom+(Top-Bottom)/ (1+10^((LogIC$_{50}$-X)*slope)).

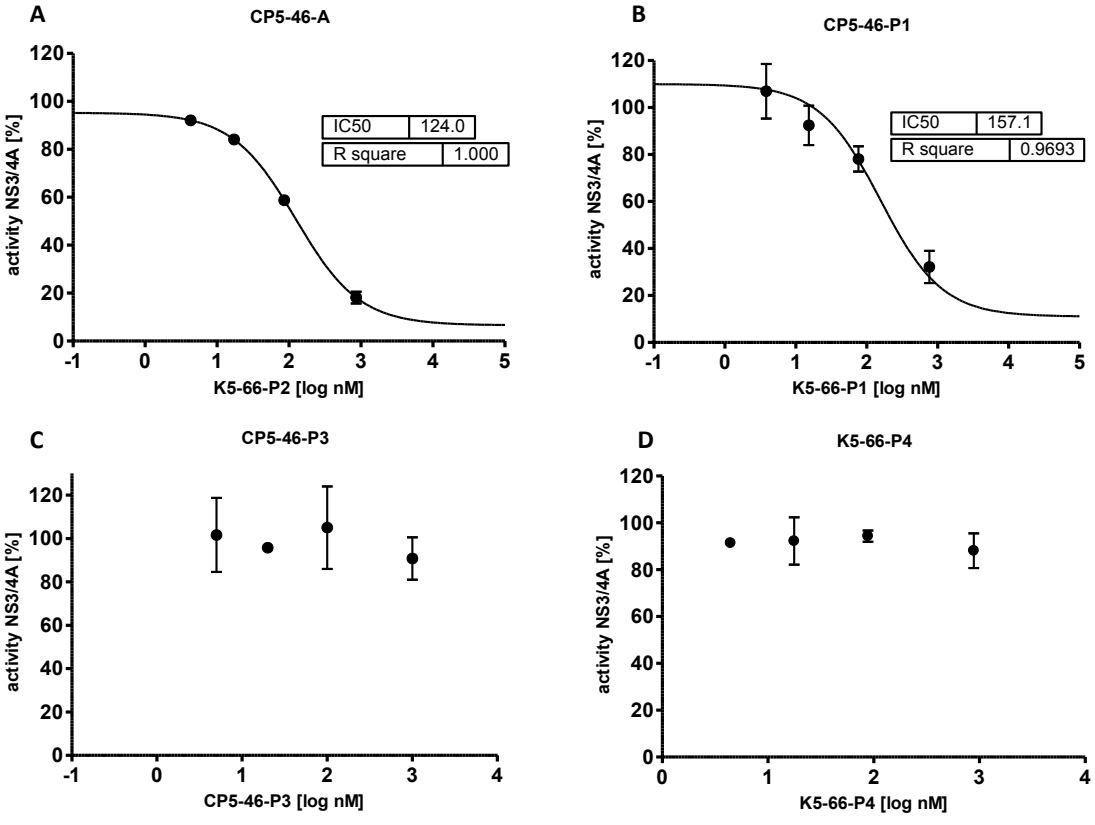

Figure 7-7: Determination of the IC_{50} of peptide CP5-46-A (A), CP5-46-P1 (B), CP5-46-P3(C) and CP5-46-P4 (D) using the NS3/4A activity assay. Assay was done in buffer M2235 with 5 µM substrate M-2235 (Bachem) and 1 nM NS3/4A. All peptides chemically synthesised. Excitation filter: 360/40 nm, emission filter: 460/40 nm. Velocity of fluorescence increase over one hour was compared to that of a scrambled control peptide CP5-46-R. Each measurement was done in duplicate, IC_{50} in nM. The curve was fitted with *GraphPad Prism* using a nonlinear regression model with variable slope: Y=Bottom+(Top-Bottom)/ (1+10^((LogIC$_{50}$-X)*slope)).

7.3.3 Structure-based optimisation of peptide CP5-46-A

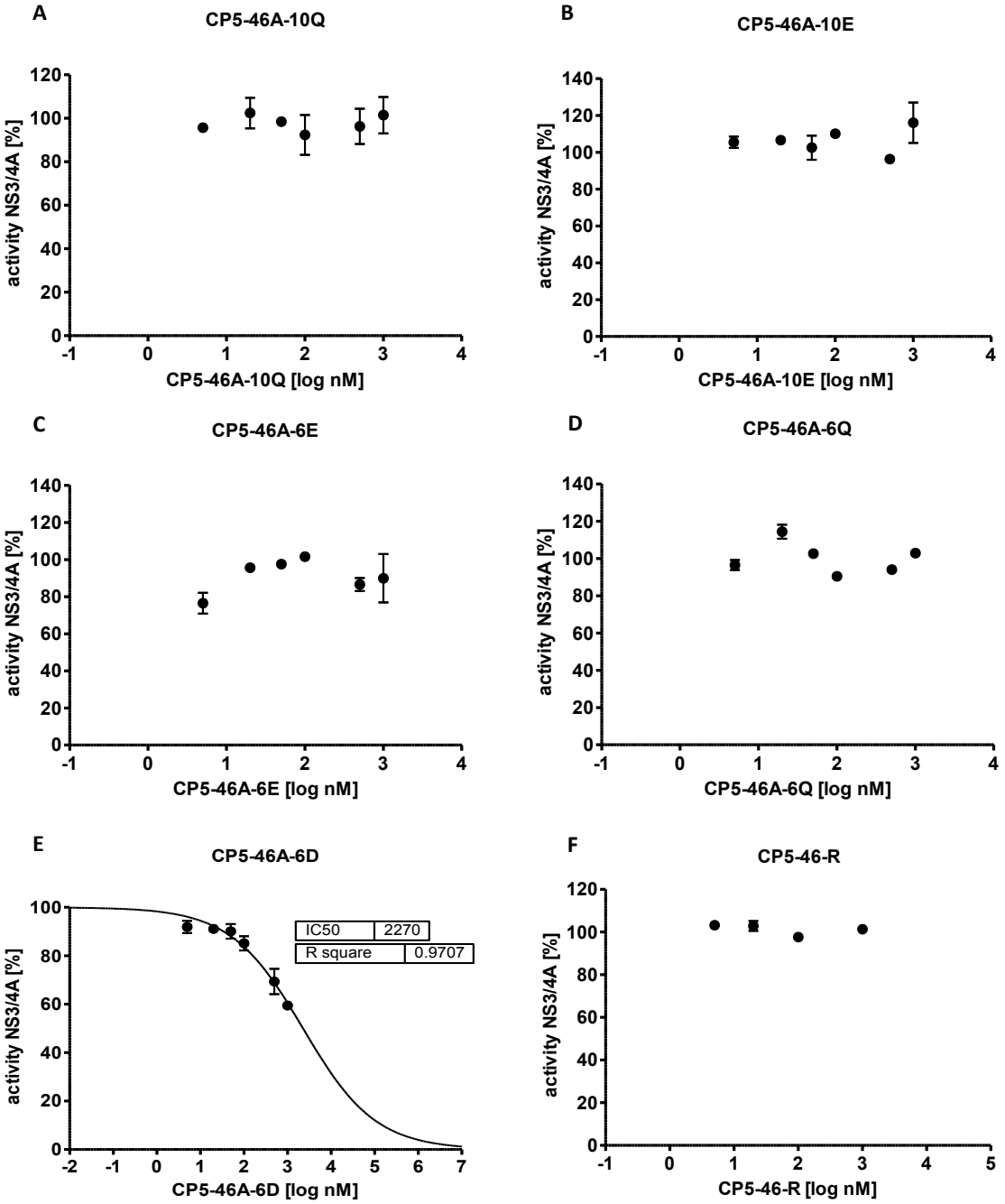

Figure 7-8: Determination of the IC_{50} of peptide CP5-46-A-10Q (A), CP5-46-A-10E (B), CP5-46-A-6E (C) , CP5-46-A-6Q (D) and CP5-46-A-6D (E) using the NS3/4A activity assay. Assay was done in buffer M2235 with 5 µM substrate M-2235 (Bachem) and 1 nM NS3/4A. All peptides chemically synthesised. Excitation filter: 360/40 nm, emission filter: 460/40 nm. Velocity of fluorescence increase over one hour was compared to that of a scrambled control peptide CP5-46-R (F). Each measurement was done in duplicate, IC_{50} in nM. The curve was fitted with *GraphPad Prism* using a nonlinear regression model with variable slope : Y=Bottom+(Top-Bottom)/ (1+10^((LogIC_{50}-X)*slope)).

7.4 Co-crystallisation of NS3/4A with CP5-46 and CP5-46-A

	NS3-4A + CP5-46A peptide
Data collection	
Space group	$P6_1$
Cell dimensions a, b, c (Å) α, β, γ (°)	 a=93.2, b=93.2, c=93.2 α=90, β=90, γ=120
Resolution (Å) (highest shell (Å))	40-2.1 (2.18-2.10)
*R*merge	0.119 (0.441)
$I/\sigma I$	14.3 (4.3)
Completeness (%)	99.8 (100)
Redundancy	6.3 (6.2)
Refinement	
No. reflections	22696
R_{work} / R_{free}	0.211/0.252
No. Atoms in	
- protein	2689
- CP5-46A peptide	264
- water	208
- K	4
- Zn	2
- glycerol	24
B-factors	
- protein	27.1
- CP5-46A peptide	33.9
- water	34.9
- K	29.3
- Zn	39.3
- glycerol	51.2
R.m.s deviations	
Bond lengths (Å)	0.009
Bond angles (°)	1.22
Ramachandran Allowed / forbidden	99.26 /0.0
Molprobity score/percentile	1.52 /97

Figure 7-9: *Refmac5* refinement data.

7.5 NS3/4A protease resistance mutation A156V

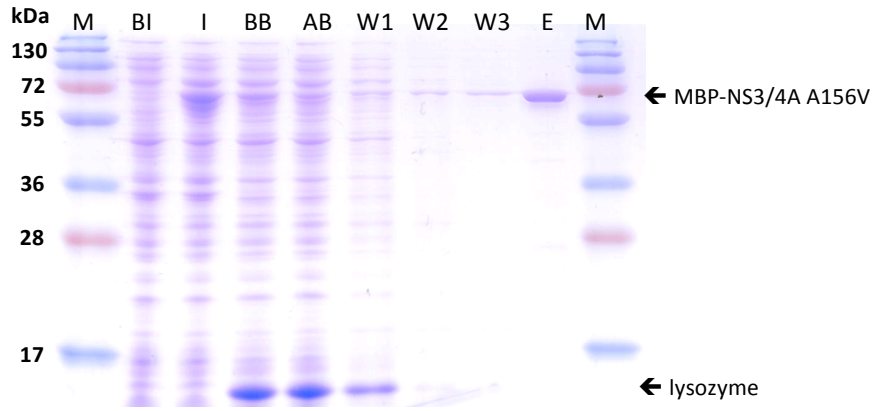

Figure 7-10: Production and purification of MBP-NS3/4A A156V. 14% SDS-gel, M: molecular weight marker, BI: before induction, I: 3 h after induction, BB: before binding, AB: after binding; W1-3: washing fractions, E: elution fraction. 3 µl of each fraction were loaded onto the gel, except elution fraction: 1 µl 1:20 dilution.